

Dynamics of Neutron Stars and Binaries in Globular Clusters

or, Ménages à trois: revitalizing burnt out degenerates through partner swapping

Thesis by

Steinn Sigurdsson

In Partial Fulfillment of the Requirements

for the Degree of

Doctor of Philosophy

California Institute of Technology

Pasadena, California

1992

(Submitted August, 1991)

Dissertation Advisor: E. Sterl Phinney, California Institute of Technology

Acknowledgements

Writing a thesis has been one of the more challenging activities I have come across in life, so far, and numerous thanks are due to people who have made the task doable. In particular I thank Anneliese for her encouragement, timely distractions and endless patience when I felt ready to give up. She has made life at Caltech altogether more enjoyable, and I hope she can continue to put up with me.

For the last couple of years a small printed note has been stuck in the right top corner of my office door. It reads:

'There's this rabbit sitting under a tree, typing, as rabbits do, when along comes this lion and says "whatcha doin', bunny?" as lions do. So, the rabbit says "I'm typing my thesis as it happens." "yeah, what's it about?" "Well, I aim to prove conclusively that rabbits eat lions!" "Never, get away." and other such derogatory remarks. "Yeah, come back to the warren and I'll show you the proof." Anyway, the lion does and is never seen again!

Later a wolf comes along and the script is much the same only with the wolf interchanged for the lion. And the wolf goes back to the warren, goes in and there, inside, is this mighty great bear, surrounded by lion bones, and proceeds to tear the wolf apart limb from limb. The moral of the story is - It's not what you put into your thesis, it's who your supervisor is!'

Without my advisor, Sterl Phinney, this thesis would not have been written; he suggested the topic, corrected many of my numerous errors (any remaining are due to me), answered innumerable stupid questions, kept me focused on the topic at hand, and, most importantly, put up with me when it seemed that everything was going wrong!

Thanks are due to my parents, and my grandmother, who bailed me out when I came to Caltech and supported me at desperate times. I am eternally grateful to Donna, who guided me through Caltech's paperwork, and provided a most useful shoulder to cry on, and to Millý who held off the Icelandic bureaucracy for all these years.

Thanks are also due to Shri Kulkarni, Roger Blandford, Kip Thorne, Peter Goldreich and Tom Prince from whom I learned most of the astrophysics I know, in particular from Ph136 and 236, which I did not appreciate at the time as much as I should have, and Peter's rejuvenating seminar on neutron stars. The many members of TAPIR I thank, especially Paolo "The Decisive" Coppi and Chris "The Squasher" Kochanek for their patient explanations of some of the arcane arts of computing; Cole for reminding me why I gave up on chess; Chuck Evans and the other postdocs for their fascinating Wednesday night expositions of the world of astrophysics; and Lars Hernquist, Frank Verbunt, David Chernoff, Piet Hut and many other visitors, whom I met all too briefly.

Various people at Caltech made life interesting, pre-eminently Steve, my long suffering flatmate, and Leslie. Also Pete; the astronomy gang, especially the soccer team; my past flatmates, Irwin, John, Charles and James, the latter striving to maintain my ideological purity against all odds; the physicists; Gil, Patricia, Brian and others, who were always good for an argument in the Ath; Mark for ensuring a sufficient supply of science fiction, and Stuart and Helen for telling me where the pulsars are. A specific mention must be made of the Tall Texan, Tyler.

A special mention must be made of the USTA Bar oligarchy for providing much needed relief on occasion, bridge games on demand, biker bodyguards, a perspective on life and endless encouragement from a distance, especially Steve "The Mouse" Chapman, Sarah and Dom, as well as the visitors, Roy "The Bruce" Gary, Dave and Chris. I must also thank Gabriel Barton for encouraging me to

stay in physics, David Bailin for suggesting I go to Caltech and John Barrow for telling me who my advisor should be!

Finally my thanks to any and all whose name I may have omitted, through no design, but poor memory and little time.

Abstract

Interaction cross-sections and collision cross-sections for a set of hard multi-mass binary-single star interactions are calculated in order to estimate three-body collision cross-sections in galactic globular clusters. The cross-sections are calculated by direct integration of binary-single star encounters, using Monte Carlo sampling to average over the three-body phase space. A number of mass-ratios physically relevant to the globular cluster environment are used. Differential energy transfer rates due to three-body interactions are calculated. Parametric approximations for the various cross-sections calculated are found.

The results of the cross-sections are used to evaluate various formation scenarios for the pulsars PSR2127+11C (M15C) and PSR1744-24A (TER5A). In addition the contribution of the globular cluster system to the galactic birthrate of PSR1913+16 type systems is estimated.

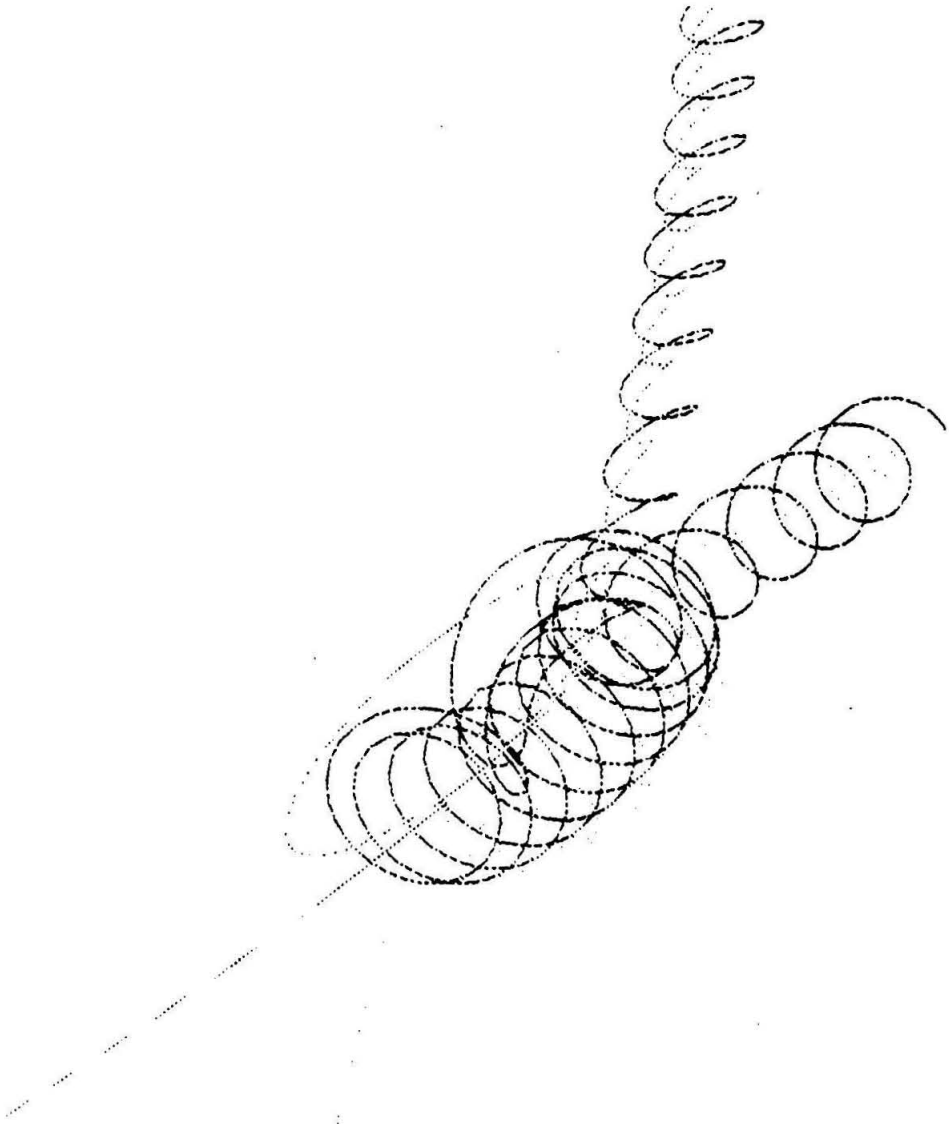
The dynamics and interactions of a test binary population in a number of globular cluster models are calculated in a static background. The cluster method used are isotropic multi-mass King models of varying concentration and density. The model developed is generalisable to an arbitrary cluster distribution function, including one evolving in time. Relative probabilities of different encounters are found for binaries on arbitrary trajectories in the various cluster models. The actual interaction rates of the test population are calculated by direct integration, using Monte Carlo sampling to average over the initial binary parameters. The number of neutron stars expected to be recycled in different concentration clusters is estimated with a particular view to understanding the pulsar population observed in clusters 47Tuc and M15.

Estimates are also made of the binary density profile of the different concentration class clusters, and the final distribution in binary parameters. The

production rate of “blue stragglers” and the interaction rate of (sub)giants and white dwarfs in the various clusters are also estimated.

Table of Contents

Acknowledgements	<i>ii</i>
Abstract	<i>v</i>
Chapter 1: Introduction	1
Chapter 2: Binary–single star interactions in Globular Clusters	36
Chapter 3: Ejection of Pulsars and Binaries to the Outskirts of Globular Clusters	111
Chapter 4: Dynamics of Binaries in Globular Clusters	126



Chapter 1

INTRODUCTION

“Outside the solar system, the problems which demand a practical solution are virtually infinite in number and extent. And these have all arisen and crowded upon our thoughts within less than a hundred years. For sidereal science became a recognised branch of astronomy through Herschel’s discovery of the revolution of double stars in 1802. Yet already it may be, and has been called, ‘the astronomy of the future’, so rapidly has the development of a keen and universal interest attended and stimulated the growth of power to investigate this sublime subject. What has been done is little – is scarcely a beginning; yet it is much in comparison with the total blank of a century past. And our knowledge will, we are easily persuaded, appear in turn the merest ignorance to those who come after us. Yet it is not to be despised, since by it we reach up groping fingers to touch the hem of the garment of the Most High.”

A.M. Clerke, 1902

1. Binaries

The concept of binary stars is a relatively modern one; its genesis may be traced to the observations in antiquity of a small number of variable stars, notably *Algol*, which later was to name a class of close binaries. In the late seventeenth century systematic study of bright variables was started, and the periodicity of *Algol* and *Mira* was noted. Concurrently, the advent of the first telescopes revealed a number of stars to consist of two stars, so close together on the sky as to appear as one when observed with the naked eye. Thus *Mizar* was observed as a double

star by Riccioli in 1650, Hooke found γ *Arietis* to be a double star in 1664 and Huygens observed θ *Orionis* to be a triple in 1656 (Grant, 1852). The possibility that the observed double stars might be physically associated was suggested by Michell (1767, 1784) on the basis of the improbability that such a number of stars should appear so close and not be associated. The theoretical possibility that stars might be bound by Newtonian gravity was readily appreciated, but no evidence for such association was then available. Evidence was forthcoming, as Herschel commenced his cataloguing of the heavens in an effort to establish proper motion and parallax of nearby stars. In the course of his efforts, he observed and catalogued a number of double stars, and found that a number of them move about each other. In particular, combining his observation with those of Bradley fifty years earlier, Herschel found that the aptly named *Castor* formed a **binary** system, with a period of approximately 342 years (Herschel, 1803, 1804). Within a few decades, several thousand visual binaries were found and catalogued, and orbital parameters were deduced for a number of them.

With the invention of spectroscopy a new class of binaries was discovered, when Maury noted line splitting in *Mizar* and β *Aurigæ* on spectrogram plates taken at Harvard, the possibility having been foreseen by Talbot (1871). The spectroscopic binaries consist of close pairs of stars, generally unresolved. *Castor* was found to be a triple, consisting of a spectroscopic binary bound to the already observed visual companion, and *Algol* was discovered to be an eclipsing binary. In the century since, tens of thousands of visual and spectroscopic binaries of all types have been observed, and orbital parameters; of varying quality, have been calculated for thousands of systems. In recent years, the spectrum open to astronomical observations has expanded enormously, and binaries have been observed at frequencies ranging from γ -rays to radio. Of particular interest to our purpose is the discovery of Low Mass X-Ray Binaries (LMXBs) by X-ray

observation by the *Uhuru* satellite in 1971 (Giacconi *et al.*, 1971), on the one hand, and the discovery of binary pulsars (Hulse and Taylor, 1974), through radio observations, on the other hand.

The fundamental physical parameters of binaries, to first order, are the masses of the respective stars, m_1, m_2 , the semi-major axis, a and eccentricity, e . Observationally, it is rare to be able to obtain all the binary parameters, most precise measurements are available for some short period binary radio pulsars, whose parameters can be uniquely determined, assuming General Relativity provides an adequate description of gravity (Taylor and Weisberg, 1989). In the case of optical binaries, one can usually obtain the (projected) semi-major axis, $a \sin i$, the total mass, $m_T = m_1 + m_2$ and the mass function, $f(m)$,

$$\begin{aligned} f(m) &= \frac{4\pi^2(a_1 \sin i)^3}{GP^2} \\ &= \frac{m_2 \sin^3 i}{(1 + q^{-2})}, \end{aligned} \tag{1.1}$$

where i is the inclination of the binary axis to the line of sight, $a_1 = m_2 a / m_T$ and P is the orbital period of the binary. For double line spectroscopic binaries the mass ratio, $q = m_2 / m_1$, may also be obtained. The eccentricity of optical binaries may often be deduced, but determination of the masses is usually model dependent (Batten, 1973), relying on modeling of stellar radii as function of mass for the observed stellar type, the radii being inferred from observations of light profiles during eclipses. The problem is compounded by uncertainties in the line-shift observed, and spurious orbits are often calculated (Morbey and Griffin, 1987). Strong selection effects plague binary observations, in particular optical binaries, with a strong bias towards young bright stars in binaries with mass ratio of approximately unity. For small mass ratios, the amplitude of the velocity modulation of spectroscopic binaries becomes undetectable, and visual binaries become

unobservable as the fainter component is washed out in the glare of its brighter, usually more massive companion. Further, a “period gap” exists between easily detectable, short period, high velocity amplitude, spectroscopic binaries, and the long period visual binaries.

Statistics of parameter distribution for binaries of all types have been calculated extensively (Batten, 1973, Abt, 1983, Latham, 1989, and references therein). The fraction of binary or higher order systems of all types is certainly greater than 20% (counting as fraction of stellar objects on the sky) and may be as high as 100%! (Abt, 1983). We note some evidence for a relative deficiency of giant binaries, and Population II binaries, although the correction for selection effects in those classes is very uncertain (Batten, 1973), the observations being *consistent* with a Population II binarity of 20% (Latham, 1989), and possibly higher. The distribution in semi-major axis and eccentricity is consistent with a uniform distribution in $\log a$ and a “thermal” eccentricity distribution, $P(e) = 2e$ (Harrington, 1975), that is, the binary distribution in phase space depends only on the energy of the binary. There is some evidence for a peaked distribution in semi-major axis (Trimble, 1976), with a peak around $0.2 AU$, and possibly a second peak at around $10 AU$, (Duquennoy and Mayor, 1990), but the uncertainty in the modeling of selection effects is comparable to the confidence in deviation from a uniform log distribution, and we will assume for now that the distribution is uniform in the logarithm. For a given population, the eccentricity distribution is typically found to be cut at some critical semi-major axis, with tidal friction having circularised binaries with semi-major axis less than the critical value; the older the population, the larger the critical semi-major axis, with circularisation time scale, t_c , given by

$$t_c^{-1} = 21 \frac{\lambda_c}{t_f} q(1+q) \left(\frac{R_*}{a} \right)^8, \quad (1.2)$$

where $t_f = (m_f R_*^2 / L_*)^{1/3}$, for a star mass, m_f , radius, R_* , luminosity, L_* , and $\lambda_c \sim 10^{-2}$ (Zahn, 1989, Zahn and Bouchet, 1989, and references therein).

The formation of binaries is not well understood, and it is possible that more than one mechanisms are involved in the genesis of multiple stellar systems (see Bodenheimer *et al.*, 1991, and references therein). In particular, fission of collapsing protostars may bias binary formation towards small mass ratios (Pringle, 1989), particularly for close binaries, which may then undergo mass transfer during the proto-stellar phase changing the calculated mass-ratio, increasing it towards the observed mean value of 0.3. Fragmentation of collapsing molecular clouds may tend to produce wider multiples with more equal mass ratios. The observational evidence is insufficient to discriminate between admittedly poorly developed, possible formation scenarios.

2. Clusters

There are over a hundred globular clusters in the Galaxy, ranging from the massive, metal rich ω Centaurus cluster lying in the plane of the Galaxy, to the tenuous, metal poor Palomar clusters, hovering in the outskirts of the Galactic halo. The globular clusters consist of low mass, metal poor Population II stars, with age estimates ranging from twelve to eighteen thousand million years (VandenBerg, 1983). The origin of the Galactic system of globular clusters is not well understood. Possible scenarios include formation from Jeans instabilities in the early Universe, shortly after recombination, before Galaxy formation (Peebles and Dicke, 1968); during Galaxy formation in shocked, infalling gas (Gunn, 1980, McCrea, 1982); or as a thermal instability during the infall phase (Fall and Rees, 1985). No theory completely accounts for the mass range and metallicity gradients observed in the globular cluster system, nor is it known whether the population observed is a remnant of a larger population most of which is now disrupted, or

whether the current population is more representative of the primordial population (Fall, 1988, Aguilar *et al.*, 1988). There is no current star formation in the Galactic globular clusters, and the stars observed in any one globular cluster are consistent with an equal age population, with a definite turnoff in age from the main-sequence branch. Typical estimates of the turnoff mass are approximately $0.8M_{\odot}$. A small number of stars have been observed in many clusters, apparently on the main-sequence past the turnoff mass, the so called “blue stragglers” (Burbidge and Sandage, 1958). Many explanations to account for the presence of blue stragglers in clusters have been proposed, the most conservative being that they are simply stars whose mass has been increased through mass transfer from a binary companion or by a collision (Mateo *et al.*, 1990, Leonard, 1989).

A typical cluster has a mass of a few hundred thousand solar masses, a central density of few thousand solar masses per cubic parsec, and is of order ten parsecs in radius, the outer radius being determined by the Galactic tidal field at the perigalacton of the cluster orbit. The tidal radius is typically not observed directly, although a lower bound is easily established, and values calculated from models fit the observed lower bounds well. A number of clusters, perhaps as many as one quarter of the population, have surface density profiles observed to increase to a cusp, to the limit of observational resolution (Djorgovski, 1988) (although *HST* observations of M15 show the cusp flattens at a radius of about 0.1 pc (Lauer *et al.*, 1991)), indicative of “core collapse.” Clusters maybe disrupted by both internal and external processes, including evaporation, rapid mass loss, core collapse, tidal shocking and collisions with molecular clouds (Spitzer, 1987, and references therein). Stars in clusters relax on a time scale, t_r , given by

$$t_r = \frac{N}{8 \ln \Lambda} t_{cross}, \quad (2.1)$$

where N is the number of stars in the cluster (core), $\ln \Lambda = \ln(rv^2/Gm_f)$ is the Coulomb logarithm, and $t_{cross} = r/v$ is the time for a star to cross the cluster (core) radius r , for a star mass m_f , speed v . For a cluster (core) mass M , the relaxation time can be conveniently written,

$$t_r = 6.4 \times 10^8 \left(\frac{M}{10^5 M_\odot} \right) \left(\frac{r}{5 \text{ pc}} \right)^{3/7} \left(\frac{m_f}{M_\odot} \right)^{-1} \left(\frac{\ln N}{\ln 10^5} \right)^{-1} \text{ years.} \quad (2.2)$$

Inferred relaxation times of many non-core collapsed globular clusters are short compared to the estimated age of the clusters, suggesting the clusters are on the verge of core collapse (Spitzer and Hart, 1971b, Spitzer and Thuan, 1972, Cohn, 1979, Cohn, 1980, Murphy and Cohn, 1988). Unless we live at a special time in the history of the Galaxy, appeal to *a priori* probabilities forces us to conclude the estimated relaxation times are in error and that core collapse is somehow postponed if not avoided. A major motivation for this thesis is the possible role of primordial binaries in globular clusters in staving off core collapse (Goodman and Hut, 1989).

As noted above, early estimates indicated that there was an apparent deficiency of binaries in globular clusters. An extensive search by Gunn and Griffin (1979) failed to reveal **any** binaries among over a hundred giants observed in M3, suggesting that the fraction of binaries in globular clusters was even smaller than amongst the Galactic Population II stars. Since then, further searches have revealed a number of both binary giants and spectroscopic contact binaries in various globular clusters (Pryor *et al.*, 1985, 1989, Mateo *et al.*, 1990), and, compensating for estimated selection effects, the fraction of binaries in clusters is consistent with 10% or more. As binaries are on average more massive than single stars, mass segregation in the early stages of cluster evolution concentrates the binaries in the cluster core. The binaries interact with single field stars in the clusters (and other binaries), exchanging energy, and occasionally binary membership. We can group

cluster binaries into two classes, *soft* and *hard*, the division being based on the relative magnitude of the binary binding energy, $E_b = -Gm_1m_2/a$ and the mean kinetic energy of a typical field star in the cluster center-of-mass frame, $\frac{1}{2}m_f v^2$. In the next chapter we define the categories more precisely. The time scale for encounters between binaries and field stars, T_X , can be written as

$$T_X = 1.5 \times 10^{10} g(m_i)^{-1} a_{AU}^{-1} n_4^{-1} \left\langle \frac{1}{v_{10}} \right\rangle^{-1} \bar{\sigma}(X)^{-1} \text{ years}, \quad (2.3)$$

where

$$g(m_i) = \frac{m_1 m_2 (m_1 + m_2 + m_f)}{m_f (m_1 + m_2)}, \quad (2.4)$$

a_{AU} is the semi-major axis of the binary in astronomical units, $v_{10} = v/10 \text{ km s}^{-1}$ is the mean relative velocity between the field stars and the binary at infinity, $n_4 = n(t, \mathbf{r})/10^4 \text{ pc}^{-3}$ is the local mean number density of field stars in the cluster, and $\bar{\sigma}(X)$ is a dimensionless cross-section defined in the next chapter. For many events of interest, $\bar{\sigma} \sim 1$. Soft binaries are rapidly disrupted by encounters, although a vestigial population of wide, marginally soft binaries persists in the halo of the cluster, where the timescale for dynamical friction to bring the binary to the core is greater than the age of the cluster, ensuring a small, steady infall of moderately wide binaries to the core at all stages of the cluster evolution. Exchanges tend to eject the least massive star involved from the binary, and thus the mean mass of binaries in the core increases. The star ejected from the binary may be expelled from the cluster core by the recoil of the exchange. For very hard binaries the binary will also be ejected from the core, ensuring that as the core density becomes large the binaries in the core are depleted. In the process, energy is injected into the cluster core, initially holding off core collapse. Later, as harder binaries participate in the interactions, three-body interactions may reverse core collapse (Murphy *et al.*, 1990).

3. Pulsars

The discovery of the first radio pulsar by Jocelyn Bell in 1967 (Hewish *et al.*, 1968) inaugurated a new subfield of astronomy. Over five hundred pulsars have been detected, with periods, P , ranging from a little over 1.5 milliseconds to several seconds, at wavelengths from radio to γ -rays. Baade and Zwicky (1934) had postulated that neutron stars might be formed in some supernovae, and Wheeler (1966) and Pacini (1967) had conjectured that rotating neutron stars might provide energy sources in supernova remnants. It is now generally accepted that pulsars are rotating neutron stars, with surface magnetic fields ranging from 10^8 to 10^{13} gauss. Most radio pulsars are observed to have a positive period derivative, \dot{P} , (where measured), consistent with the picture of a rotating compact object slowing down as it radiates energy. The inferred lifetime of pulsars, $P/2\dot{P}$, ranges from one thousand two hundred and forty years for the Crab pulsar to over six thousand million years for PSR 1553+29.

Neutron stars are believed to have radii of the order of 10 km, and masses of order $1.4M_{\odot}$. A neutron star is supported by neutron degeneracy pressure, having collapsed from an ordinary star when the core mass of the star exceeded the Chandrasekhar limit (Shapiro and Teukolsky, 1983, and references therein) during the final stage of nuclear burning of a massive star, or possibly during accretion onto a heavy white dwarf (Michel, 1987, Grindlay and Bailyn, 1988). The exact mass range of neutron stars is not known, as the equation of state of nuclear matter is only known over a narrow range of densities and pressure. Observed neutron stars have masses in the range $1.3\text{--}1.4M_{\odot}$ (Taylor and Weisberg, 1989, Wolszczan, 1991, Prince *et al.*, 1991); it is thought unlikely that neutron stars would form with a much lower mass. The upper mass limit is uncertain, but probably of the order of $2M_{\odot}$. Due to conservation of angular momentum

the neutron star forms spinning relatively rapidly, and starts spinning down as it radiates energy. It is thought that the neutron stars either form with a high magnetic field, or a magnetic field will be thermoelectrically generated in the hot crust of the neutron star (Blandford *et al.*, 1983); in either case, young neutron stars are observed with a high inferred magnetic field, of order 10^{12} gauss. The magnetic field is inferred from the observed spin down, an estimate of the surface magnetic field dipole, \mathbf{B} , is given by,

$$\begin{aligned} \mathbf{B} &= \sqrt{\frac{3Ic^3P\dot{P}}{8\pi^2R^6}} \\ &= 3.2 \times 10^{19} \sqrt{P\dot{P}} \text{ gauss} \end{aligned}$$

(Manchester and Taylor, 1977, and references therein). There is considerable controversy as to whether the magnetic field decays naturally, or if it is only destroyed by external processes such as accretion, but old neutron stars are observed with low inferred mean dipole magnetic fields of order 10^8 gauss (Kulkarni, 1986). Observations of gamma-ray bursters and high-mass X-ray binaries suggest that at least some old neutron stars may retain patches of high magnetic fields, or the full 10^{12} gauss dipole (Higdon and Lingenfelter, 1990, and references therein), in which case one would infer that recycled pulsars deplete their mean field during the recycling process.

The discovery of the first millisecond pulsar (Backer *et al.*, 1982) demonstrated the possibility of pulsar recycling, whereby an old neutron star may be spun up by accretion, reappearing as a short period, low magnetic field pulsar. It is possible that some of the recycled pulsars are formed from accretion induced collapse instead; in either case considerable mass transfer must have taken place. As noted above, it is not clear whether the low observed magnetic fields of recycled pulsars are due to magnetic field decay or the destruction of the magnetic field

during accretion (Romani, 1990b). A pulsar with magnetic field \mathbf{B} accreting an amount of matter δm , can be spun up to a period P , where P is given by

$$P = 0.2 \left(\frac{M_{NS}}{\delta m} \right)^{3/4} I_{45}^{3/4} \text{ ms}, \quad (3.1)$$

where I_{45} is the moment of inertia of the neutron star in units of 10^{45} gm cm^2 . The spin-up is not sensitive to the exact accretion mechanism, although we note the possibility of transferring the angular momentum of accreting material to the neutron star by coupling to the magnetic field without accreting the matter onto the surface (“a propeller mechanism”) (Illarionov and Sunyaev, 1975). A neutron star accreting at a rate \dot{m} , has equilibrium period

$$\begin{aligned} P &= 2\pi(2GM_{NS})^{-5/7}(\dot{m})^{-3/7}(R)^{18/7}(\mathbf{B})^{6/7} \\ &= 0.83 \left(\frac{\dot{m}}{\dot{m}_{Edd}} \right)^{-3/7} \left(\frac{M_{NS}}{\dot{m}} \right)^{-5/2} \left(\frac{R}{10 \text{ km}} \right)^{18/7} \mathbf{B}_{12}^{6/7} \text{ seconds}, \end{aligned} \quad (3.2)$$

where \mathbf{B}_{12} is the mean dipole field in units of 10^{12} gauss and \dot{m}_{Edd} is the Eddington rate, the maximum accretion rate possible, in the absence of a propeller mechanism,

$$\begin{aligned} \dot{m}_{Edd} &= \frac{4\pi c m_p}{\sigma_T} \left(\frac{\bar{A}}{\bar{Z}} \right) R \\ &= 9.5 \times 10^{17} \left(\frac{R}{10 \text{ km}} \right) \left(\frac{\bar{A}}{\bar{Z}} \right) \text{ gm s}^{-1}, \end{aligned} \quad (3.3)$$

where m_p is the proton mass, σ_T is the Thomson cross-section, \bar{A} is the mean nucleon number and \bar{Z} is the mean proton number of the accreting material (Shapiro and Teukolsky, 1983).

In order to produce millisecond pulsars, high accretion rates are preferred, as up to $0.1M_{\odot}$ must be accreted to produce the short periods observed in some systems. Accreting at the Eddington rate, energy is being released at over $10^{38} \text{ erg s}^{-1}$, mostly in X-rays. The Low Mass X-ray Binaries mentioned above are thought to be neutron stars accreting near or at the Eddington rate from low

mass stellar companions. There are over a hundred LMXBs known in the Galaxy, and another dozen in the globular cluster system. The LMXBs are very bright, and it is thought the count of LMXBs is essentially complete, although we note that *Rosat* is reported to have discovered a number on new soft X-ray sources. It is possible that a number of LMXBs are quiescent for long periods, and thus may not have been observed, but all arguments about relative birthrates scale with the duty cycle of the X-ray source, and thus non-detection of temporarily quiescent sources does not qualitatively change our conclusion. Most of the LMXBs are sub-Eddington luminosity, and to produce a millisecond pulsar need to accrete for 10^8 – 10^9 years, giving a birthrate of order 10^{-6} per year in the Galaxy. About ten millisecond or suspected recycled pulsars are known in the Galaxy, but there the count is very incomplete. Modeling selection effects in surveys indicate of order 10^5 recycled millisecond pulsars in the Galaxy (Kulkarni and Narayan, 1988) with lifetimes of order 10^8 – 10^9 years. Thus the inferred birthrate of millisecond pulsars in the Galaxy exceeds that of their presumptive progenitors by an order of magnitude, or more. Our concern is, however, with a different, but related problem. It was noted (Katz, 1975) that the ratio of LMXBs per unit mass in the globular clusters was two orders of magnitude greater than in the Galaxy. Noting the supposed link between LMXBs and millisecond pulsars, it was suggested that the globular clusters might contain detectable millisecond pulsars (Alpar *et al.*, 1982), and after an intensive search the first cluster pulsar was discovered in M28 (Hamilton *et al.*, 1985, Lyne *et al.*, 1987).

Neutron stars are thought to form as the final stage of the evolution of massive stars. As noted previously, the globular clusters are old systems, with the main-sequence terminating at about $0.8 M_{\odot}$. No current star formation is observed in the Galactic globular clusters; in fact little or no gas is observed in Galactic clusters (Roberts, 1988), so it is clear that no neutron stars are currently forming in the

Galactic globular clusters, ignoring for the moment the possibility of accretion induced collapse.

It would seem, therefore, that the observed neutron stars are primordial neutron stars, that have spun down from their initial birth, and have been recycled as pulsars through accretion. The presence of a disproportionately large number of LMXBs in the globular cluster system supports this hypothesis. However, there are now over thirty pulsars known in Galactic globular clusters, eleven in 47Tuc alone (Phinney and Kulkarni, 1991, van den Heuvel, 1991, Lyne, 1991, Manchester *et al.*, 1991). Modeling the survey selection effects, the inferred cluster pulsar population implies a birthrate at least an order of magnitude larger than the inferred LMXB birthrate, as in the Galaxy (Kulkarni *et al.*, 1990a). Further, the distribution of recycled pulsars is not consistent with the LMXB distribution among the clusters, with many more pulsars found in low density clusters than expected from the LMXB distribution, which is weighed towards the densest clusters (Johnston *et al.*, 1991b, Fruchter and Goss, 1990, Verbunt and Hut, 1987). We must conclude that there is an observed excess of recycled pulsars in the Galactic globular clusters, and that a new formation channel needs to be invoked to account for their presence.

Neutron stars in the Galaxy are observed to have velocities of order 100 km s⁻¹ relative to the local standard of rest (Manchester and Taylor, 1977, Narayan and Ostriker, 1990). It is thought that the neutron stars acquire these velocities at birth, either from the disruption of a binary containing the neutron star progenitor, or from kicks caused by asymmetries in the supernova explosion, or some combination thereof (Bailes, 1989). Most known Galactic pulsars are single, suggesting that if the progenitor is in a binary, the binary is likely to be disrupted by the supernova, although close binaries may survive the explosion if there is significant mass-transfer from the more massive, more evolved star to

the less massive star (van den Heuvel, 1991, and references therein). We also note that pulsar surveys select against finding binary radio pulsars, in particular short period binary radio pulsars (Johnston and Kulkarni, 1991), so the true fraction of neutron stars retained in binaries is not well constrained. Globular clusters typically have low escape velocities, of order 30 km s^{-1} , and one would naively suspect that most neutron stars should be ejected from the clusters at birth (Verbunt and Hut, 1987, Verbunt, 1989). Clearly the number of neutron stars in the Galactic globular clusters can not be **less** than the number of pulsars observed, and is probably much greater. Naively one would then conclude that there must have been a large number of neutron stars generated in the young globular clusters, and we are seeing the few that managed to avoid ejection. However, supernovae, in the absence of mass-transfer to a less massive companion, eject several solar masses at detonation. The main-sequence lifetime of supernova progenitors is short compared to the Hubble time, and the shock from a few supernovae is sufficient to clear most clusters of any gas that might be available for star formation. Thus, shortly after the formation of the first generation of massive stars in the cluster, gas is cleared out of the cluster, precluding further star formation, and there is significant sudden mass loss from cluster by supernovae ejecta. The fact that the cluster survives this process severely constrains the number of supernovae, as the cluster will be disrupted if too large a fraction of its mass is ejected in such an abrupt manner. We thus face a dilemma, as we require a number of neutron stars to be available in the clusters to be recycled in the present epoch, yet only a limited number of neutron stars may be produced, and we expect most of those to be ejected. In the absence of an efficient channel for producing new neutron stars in the present era, such as accretion induced collapse, we must contrive to retain as large a fraction of the neutron stars as possible, and recycle those retained in an efficient manner. It is possible that the

fraction of short period primordial binaries ($a < 0.3 AU$) is higher in the globular cluster population than in the Galaxy, or, conceivably, that the magnitude of the kick the neutron star receives in the supernova explosion is smaller for the low metallicity cluster progenitors.

Accretion induced collapse is another possible channel for forming millisecond pulsars in globular clusters. At certain accretion rates, models indicate that heavy white dwarfs (Nomoto and Kondo, 1991), particularly Carbon–Oxygen (C–O) white dwarfs and Oxygen–Neon–Magnesium (O–Ne–Mg) white dwarfs will grow in mass. They may then collapse to neutron stars upon reaching the Chandrasekhar limit. The accretion presumably spins up the white dwarf, resulting in a rapidly spinning low magnetic field neutron star. The models suggest a very high accretion rate is necessary to avoid burning off the accreted material through repeated nuclear flashing and the associated ejection of matter, or total disruption as a type I supernova instead of collapse to a neutron star, upon reaching the Chandrasekhar limit. The preponderance of C–O or O–Ne–Mg white dwarfs is not well known, and there may not be sufficient numbers in globular clusters to make this a viable channel. We will discuss variations on accretion induced collapse later in this thesis, but for now will assume it is not the dominant formation channel for recycled millisecond pulsars.

A primordial neutron star in a binary with a main–sequence star may start accreting from the star as it evolves off the main–sequence; in particular the pulsars PSR 1310+18 in M53 (Kulkarni *et al.*, 1991) and PSR 1620-26 in M4 (Lyne *et al.*, 1988) are good candidates to be in their primordial binaries and have accreted directly from the evolved companion of their progenitors, or possibly to have exchanged into a binary containing their current companion, before it evolved off the main–sequence. If the binary formed initially with a short period, a main–sequence or white dwarf companion of the neutron star could overflow its Roche.

lobe as the orbit shrank through gravitational radiation, and commence accretion onto the neutron star. The rate of change of a binary of orbital period P_{orb} , \dot{P}_{orb} , due to gravitational radiation is given by

$$\begin{aligned} \frac{\dot{P}_{orb}}{P_{orb}} &= -\frac{96}{5} \frac{G^3}{c^5} \frac{(m_1 + m_2)m_1m_2}{a^4} f(e) \\ &= 5.6 \times 10^{-10} \frac{(m_1 + m_2)m_1m_2 (10^6 \text{ km})^4}{M_{\odot}^3 a^4} f(e) \text{ years}^{-1}, \end{aligned} \quad (3.4)$$

where $f(e) = (1 + \frac{73}{24}e^2 + \frac{37}{96}e^4)(1 - e^2)^{-7/2}$ (Peters, P.C., 1964, Shapiro and Teukolsky, 1983). Undoubtedly some of the observed pulsars evolved naturally from such binaries, but by comparison with the Galactic pulsar frequency this mechanism cannot account for more than one or two of the recycled pulsars; an active channel must exist for recycling pulsars to account for the numbers observed.

We propose that the critical component of the pulsar recycling channel is the presence of hard primordial binaries in the clusters, and that the interaction of multiple star systems with single field stars and other multiple stellar systems is the dominant channel for pulsar recycling. In particular, that resonant interactions and exchanges work to provide large cross-section channels for close encounters between neutron stars (and white dwarfs) and other stars, leading to enhanced tidal capture and collisions. The collisions between neutron stars and other stars, both main-sequence stars, (sub)giants and white dwarfs, can lead to the disruption of the other star and rapid accretion onto the neutron star, reducing some of the discrepancy between the LMXB accretion time and the accretion rate needed (although it may still be necessary to invoke some form of propeller mechanism to eliminate the discrepancy completely).

We also consider, at varying length, the formation of neutron star/white dwarf-neutron star/white dwarf binaries with an orbital period short enough for

merging through gravitational radiation to be possible; the formation of blue stragglers through main-sequence star merging; the ejection of stars and binaries from cluster cores; the energy transfer from binaries to the cluster core and its role in both postponing and reversing core collapse; the exchange and elimination of (sub)giants from moderately hard binaries in medium density clusters; and the mass segregation of binaries in multi-mass cluster models.

4. Three-body interactions

Interactions between multiple stellar systems can substantially enhance the rate of collisions and tidal interactions of degenerate stars in globular clusters. A neutron star passing within a few (~ 3) stellar radii of a main-sequence star, somewhat less for (sub)giants and white dwarfs (Fabian *et al.*, 1975, Press and Teukolsky, 1977, Lee and Ostriker, 1986, McMillan *et al.*, 1990a, Bailyn, 1988), excites tides in the envelope of the star, and may transfer enough energy to become bound to the star, typically on an eccentric orbit with pericenter comparable to the closest approach (Krolik *et al.*, 1984, Kochanek, 1991). Once captured in such an orbit, the neutron star orbit will circularise and shrink by tidal friction, and mass-transfer may take place. A small fraction of neutron stars captured may be ejected by extracting energy from the tidal bulge before it is damped. If immediate mass-transfer does not take place, the neutron star will be in a close enough orbit for mass-transfer to take place as the captor star evolves off the main-sequence. A significant fraction of such encounters will result in a direct or glancing collision between the neutron star and the star, in which case the star may be disrupted and form an accretion disk around the neutron star. The neutron star need only accrete a small fraction of the disk material to unbind the rest of the disk, presumably leaving a single, spun up neutron star behind, a pulsar. Similar scenarios apply to encounters between neutron stars and (sub)giants and neutron

stars and white dwarfs, with the cross section scaling in proportion to the radius of the respective stars. It is thought that most or all of the cluster LMXBs are a consequence of tidal capture (Verbunt and Hut, 1987, Verbunt, 1990). We also note that a similar argument applies to white dwarf–stellar collisions, except the white dwarf is less efficient at unbinding the presumptive accretion disk, in cases where disruption does occur. A white dwarf–main–sequence or (sub)giant merger will probably appear similar to evolved red giants, whereas white dwarf–white dwarf mergers may either form red giants, go supernova, or undergo accretion induced collapse, depending on the composition of the merged components, and the accretion rate achieved (Webbink, 1984, Iben and Tutukov, 1984). White dwarf–white dwarf mergers may form a significant channel for millisecond pulsar formation, if accretion induced collapse is possible. Tidal capture and merging main–sequence stars may account for the presence of some of the contact binaries and the blue stragglers in the clusters respectively (Leonard, 1989, Leonard and Fahlman, 1991, Mateo *et al.*, 1990).

Extensive efforts are currently underway to consider the consequences of tidal interactions and mergers, using hydrodynamical modeling and multipole expansion of tidal excitations (Benz *et al.*, 1987, 1989, 1990, Cleary and Monaghan, 1990, Goodman and Hernquist, 1991, Rasio and Shapiro, 1991, Ruffert and Müller, 1990, Davies *et al.*, 1991, Kochanek, 1991). Results so far suggest that mass loss is 10% or less during mergers, with the largest mass loss occurring from glancing collisions, and little asymmetry in the mass loss. A reasonable approximation to mergers appears to be to assume instantaneous merger with conservation of momentum, and that is the approach we will adapt in our modeling of mergers.

As indicated above, single stellar tidal capture is not consistent with the observed number and distributions of millisecond pulsars in globular clusters, al-

though it may account for the formation of the LMXBs observed. The cross-section for tidal capture, σ_{T2} , can be written

$$\sigma_{T2} = f_t \left(\pi R_*^2 + \frac{2\pi G(m_f + m_1)R_*}{v_\infty^2} \right); \quad (4.1)$$

compare that to the cross-section for a star to approach a binary, σ_{T3} ,

$$\sigma_{T3} = f_t \left(\pi a^2 + \frac{2\pi G(m_f + (m_1 + m_2))a}{v_\infty^2} \right). \quad (4.2)$$

If the binary is hard, the field star may be captured into a resonant orbit with the binary, during which the probability of an encounter between any pair of stars, close enough for tidal dissipation to be effective, is significant. The primary subject of this thesis is the calculation of the encounter probability during resonant interactions for realistic situations. We note that if the local binary fraction is large enough, and the encounter probability is not too small, the single star-binary encounter rate may exceed the single star-single star encounter rate by two orders of magnitude, as typically, $a \gg R_*$. As detailed in subsequent chapters, the density dependence of the consequent pulsar formation rate is less for the binary scenario, and in better accord with observations. Allowing for a time varying binary distribution further improves the predicted rate, and may be sufficient to account for the extraordinary pulsar population in 47Tuc (Manchester *et al.*, 1991).

Three-body calculations have been carried out extensively by a number of people, including Heggie's (1975) thorough analytical analysis, the broad calculations of Hills (1975a,b), and Hut and Bahcall's (1983) comprehensive coverage of the equal mass case. Where our calculations differ is in the concentration on hard binaries, with small but unequal mass-ratios, typical of those expected in globular cluster populations.

Compared to the single star–binary encounter rate, the binary–binary encounter rate is enhanced by a factor of order ten (proportional to the sum of the semi–major axis, and the total mass), and suppressed by a factor of f_b , the local binary fraction. Others have considered binary–binary encounter scenarios (Mikkola, 1983, 1984a,b, Leonard, 1989, Hut, 1990), although a comprehensive calculation over the full phase space remains undone. Preliminary results suggest that the binary–binary encounters do not qualitatively differ from the single star–binary encounters. An untackled problem is the possibility of single star/binary interactions with hierarchical trinearies, in which the interaction cross–section is comparable with marginally hard binaries, and the collision probability is comparable with very hard binaries. Such systems may exist in globular clusters, both as primordial systems and as products of binary–binary encounters, although how common they are is not known.

References

- Abt, H.A., 1983, *Ann. Rev. Astr. Ap.*, **21**, 343.
- Abt, H.A., 1987, *Ap. J.*, **317**, 353.
- Aguilar, L., Hut, P. and Ostriker, J.P., 1988, *Ap. J.*, **335**, 720.
- Alpar, M.A., Cheng, A.F., Ruderman, M.A. and Shaham, J., 1982, *Nature*, **300**, 728.
- Anderson, S.B., Gorham, P.W., Kulkarni, S.R., Prince, T.A. and Wolszczan, A., 1990, *Nature*, **346**, 42.
- Anderson, S.B., Gorham, P.W., Kulkarni, S.R., Prince, T.A. and Wolszczan, A., *Nature*, 1990b, submitted.
- Aurière, M., Ortolani, S. and Lauzeral, C., 1990, *Nature*, **344**, 638.
- Baade, W. and Zwicky, F., 1934, *Proc. Nat. Acad. Sci.*, **20**, 254.
- Backer, D.C., Kulkarni, S.R., Heiles, C., Davis, M.M. and Goss, W.M., 1982, *Nature*, **300**, 615.
- Bailes, M., 1989, *Ap. J.*, **342**, 917.
- Bailyn, C.D. and Grindlay, J.E., 1987, *Ap. J.*, **312**, 748.
- Bailyn, C.D. and Grindlay, J.E., 1987, *Ap. J. (Letters)*, **316**, L25.
- Bailyn, C.D. and Grindlay, J.E., 1990, *Ap. J.*, **353**, 159.
- Bailyn, C.D., 1987, *Ap. J.*, **317**, 737.
- Bailyn, C.D., 1988, *Nature*, **332**, 330.
- Bailyn, C.D., 1989, *Ap. J.*, **341**, 175.
- Bailyn, C.D., 1990, in *Proc. of A.S.P. Conference on Formation and Evolution of Star Clusters*, ed. K. Janes (P.A.S.P. Conference Series).
- Bates, B., Catney, M.G. and Keenan, F.P., 1990, *M.N.R.A.S.*, **245**, 238.

- Batten, A.H., 1973, *Binary and Multiple Systems of Stars* (Pergamon Press, New York).
- Benz, W. and Hills, J.G., 1987, *Ap. J.*, **323**, 614.
- Benz, W., Hills, J.G. and Thielemann, F.-K., 1989, *Ap. J.*, **342**, 986.
- Benz, W., Bowers, R.L., Cameron, A.G.W. and Press, W.H., 1990, *Ap. J.*, **348**, 647.
- Binney, J. and Tremaine, S., 1987, *Galactic Dynamics* (Princeton University Press).
- Birkinshaw, M. and Downies, A.J.B., 1982, *Ap. J.*, **258**, 154.
- Blandford, R.D., Applegate, J.H. and Hernquist, L., 1983, *M.N.R.A.S.*, **204**, 1025.
- Bodenheimer, P., Ruzmaikina, T. and Mathieu, R.D., 1991, *UCSC preprint*.
- Borkowski, K.J. and Harrington, J.P., *Ap. J.*, 1991, submitted.
- Burbidge, E.M. and Sandage, A., 1958, *Ap. J.*, **128**, 174.
- Burrows, A. and Woosley, S., 1986, *Ap. J.*, **308**, 680.
- Canal, R., Isern, J. and Labay, J., 1990, *Ann. Rev. Astr. Ap.*, **28**, 183.
- Chandrasekhar, S., 1943, *Ap. J.*, **97**, 255.
- Charles, P.A. in *Topics in X-ray Astronomy, Proc. 23rd ESLAB Symp.*, ESA SP-296, Vol. 1, 129-137 (1989), eds. J. Hunt & B. Battrock, published Paris.
- Chernoff, D.F. and Shapiro, S.L., 1988, in *The Harlow-Shapley Symposium on Globular Cluster Systems in Galaxies*, eds. J.E. Grindlay and A.G. Davis Philip (Dordrecht, Reidel).
- Chernoff, D.F. and Djorgovski, S., 1989, *Ap. J.*, **339**, 904.

- Chernoff, D.F. and Weinberg, M.D., 1990, *Ap. J.*, **351**, 121.
- Cleary, P.W. and Monaghan, J.J., 1990, *Ap. J.*, **349**, 150.
- Clerke, A.M., 1902, *A Popular History of Astronomy During the Nineteenth Century* (Adam and Charles Black, London).
- Cohn, H., 1979, *Ap. J.*, **234**, 1036.
- Cohn, H., 1980, *Ap. J.*, **242**, 765.
- Cohn, H. and Hut, P., 1984, *Ap. J. (Letters)*, **277**, L45.
- Cohn, H., 1988, in *The Harlow-Shapley Symposium on Globular Cluster Systems in Galaxies*, eds. J.E. Grindlay and A.G. Davis Philip (Dordrecht, Reidel).
- Da Costa, G.S. and Freeman, K.C., 1976, *Ap. J.*, **206**, 128.
- Davies, M.B., Benz, W. and Hills, J.G., *Ap. J.*, 1991, submitted.
- Djorgovski, S., 1988, in *The Harlow-Shapley Symposium on Globular Cluster Systems in Galaxies*, eds. J.E. Grindlay and A.G. Davis Philip, (Dordrecht, Reidel)
- Djorgovski, S., Piotto, G. and King, I.R., 1988, in *Dynamics of Dense Stellar Systems*, ed. D. Merritt (Cambridge University Press) p. 147.
- Djorgovski, S., Piotto, G., Phinney, E.S. and Chernoff, D., *Ap. J. (Letters)*, 1991, submitted.
- Dubath, P., Meylan, G., Mayor, M. and Magain, P., 1990, *Astr. Ap.*, **239**, 142.
- Duquennoy, A. and Mayor, M., 1990, in *New Windows to the Universe*, eds. F. Sanchez and M. Vayquery (Cambridge University Press), p. 253.
- Elson, R. and Hut, P., 1987, *Ann. Rev. Astr. Ap.*, **25**, 565.
- Fabian, A.C., Pringle, J.E. and Rees, M.J., 1975, *M.N.R.A.S.*, **172**, 15P.
- Fabian, A.C., Eggleton, P.P., Hut, P. and Pringle, J.E., 1986, *Ap. J.*, **305**, 333.

- Fahlman, G.G., Richer, H.B. and Vandenberg, D.A., 1985, *Ap. J. Suppl.*, **58**, 225.
- Fall, S.M., 1988, in *The Harlow-Shapley Symposium on Globular Cluster Systems in Galaxies*, eds. J.E. Grindlay and A.G. Davis Philip (Dordrecht, Reidel).
- Fall, S.M. and Rees, M.J., 1985, *Ap. J.*, **298**, 18.
- Finzi, A., 1978, *Astr. Ap.*, **62**, 149.
- Fruchter, A.S. and Goss, W.M., 1990, *Ap. J. (Letters)*, **365**, L63.
- Fullerton, L.W. and Hills, J.G., 1982, *A.J.*, **87**, 175.
- Gao, B., Goodman, J., Cohn, H. and Murphy, B.W., 1991, *Ap. J.*, **370**, 567.
- Garcia, M.R., Bailyn, C.D., Grindlay, J.E. and Molnar, L.A., 1989, *Ap. J. (Letters)*, **341**, L75.
- Giacconi, R., Gursky, H., Kellogg, E., Schreier, E. and Tananbaum, H., 1971, *Ap. J. (Letters)*, **167**, L67.
- Goodman, J. and Hut, P., 1989, *Nature*, **339**, 40.
- Goodman, J. and Hernquist, L., *Ap. J.*, 1991, in the press.
- Grant, R., 1852, *History of Physical Astronomy From the Earliest Ages to the Middle of the Nineteenth Century* (Henry G. Bohn, London).
- Grindlay, J.E., Hertz, P., Steiner, J.E., Murray, S.S. and Lightman, A.P., 1984, *Ap. J. (Letters)*, **282**, L13.
- Grindlay, J.E., Bailyn, C.D., Cohn, H., Lugger, P.M., Thorstensen, J.R. and Wegner, G., 1988, *Ap. J. (Letters)*, **334**, L25.
- Grindlay, J.E., 1988, in *The Harlow-Shapley Symposium on Globular Cluster Systems in Galaxies*, eds. J.E. Grindlay and A.G. Davis Philip (Dordrecht, Reidel).

- Grindlay, J.E. and Bailyn, C.D., 1988, *Nature*, **336**, 48.
- Gunn, J.E. and Griffin, R.F., 1979, *A.J.*, **84**, 752.
- Gunn, J.E., 1980, in *Globular Clusters*, eds. D. Hanes and B. Madore (Cambridge University Press, Cambridge).
- Hamilton, T.T., Helfand, D.J. and Becker, R.H., 1985, *A.J.*, **90**, 606.
- Harrington, R.S., 1975, *A.J.*, **80**, 1081.
- Harris, W.E. and Racine, R. 1979, *Ann. Rev. Astr. Ap.*, **17**, 241.
- Hartwick, F.D.A., Cowley, A.P. and Grindlay, J.E., 1982, *Ap. J. (Letters)*, **254**, L11.
- Heggie, D.C., 1975, *M.N.R.A.S.*, **173**, 729.
- Herschel, W., 1803, *Phil. Trans. R. Soc.*, **93**, 339.
- Herschel, W., 1804, *Phil. Trans. R. Soc.*, **94**, 353.
- Hertz, P. and Grindlay, J.E., 1983, *Ap. J.*, **275**, 105.
- Hertz, P. and Wood, K.S., 1985, *Ap. J.*, **290**, 171.
- van den Heuvel, E.P.J., van Paradijs, J. and Taam, R.E., 1986, *Nature*, **322**, 153.
- van den Heuvel, E.P.J., 1991, in *Neutron Stars: Theory and Observation*, eds. J. Ventura and D. Pines (Kluwer Academic Publishers, Dordrecht).
- Hewish, A., Bell, S.J., Pilkington, J.D., Scott, P.F. and Collins, R.A., 1968, *Nature*, **217**, 709.
- Higdon, J.C. and Lingenfelter, R.E., 1990, *Astr. Ap.*, **28**, 401.
- Hills, J.G., 1975a, *A.J.*, **80**, 809.
- Hills, J.G., 1975b, *A.J.*, **80**, 1075.
- Hills, J.G. and Fullerton, L.W., 1980, *A.J.*, **85**, 1281.
- Hulse, R.A. and Taylor, J.H., 1974, *Ap. J. (Letters)*, **195**, L51.

- Hut, P. and Bahcall, J.N., 1983, *Ap. J.*, **268**, 319.
- Hut, P., 1983a, *Ap. J.*, **268**, 342.
- Hut, P., 1983b, *A.J.*, **88**, 1549.
- Hut, P., 1983c, *Ap. J. (Letters)*, **272**, L29.
- Hut, P. and Verbunt, F., 1983, *Nature*, **301**, 587.
- Hut, P. and Paczyński, B., 1984, *Ap. J.*, **284**, 675.
- Hut, P. and Inagaki, S., 1985, *Ap. J.*, **298**, 502.
- Hut, P., Makino, J. and McMillan, S., 1988, *Nature*, **336**, 31.
- Hut, P., 1990, in *Proceedings of the Workshop on Self-Gravitating Systems in Astrophysics and Nonequilibrium Processes in Physics* (Kyoto, June 1989).
- Hut, P., Murphy, B.W. and Verbunt, F., *Astr. Ap.*, 1991, in the press.
- Iben, I. and Tutukov, A.V., 1984, *Ap. J. Suppl.*, **54**, 335.
- Illarionov, A.F. and Sunyaev, R.A., 1975, *Astr. Ap.*, **39**, 185.
- Ilovaisky, S.A. in *Topics in X-ray Astronomy, Proc. 23rd ESLAB Symp.*, ESA SP-296, Vol. 1, 145-150 (1989), eds. J. Hunt & B. Battrock, published Paris.
- Johnston, H.M. and Kulkarni, 1991, *Ap. J.*, **368**, 504.
- Johnston, H.M., Kulkarni, S.R. and Goss, W.M., 1991a, in preparation.
- Johnston, H.M., Kulkarni, S.R. and Phinney, E.S., 1991b, in preparation.
- Katz, J.I., 1975, *Nature*, **253**, 698.
- Katz, J.I., 1975, *M.N.R.A.S.*, **183**, 765.
- King, I.R., 1962, *A.J.*, **67**, 471.
- King, I.R., 1966, *A.J.*, **71**, 64.

- Krolik, J.H., Meiksin, A. and Joss, P.C., 1984, *Ap. J.*, **282**, 466.
- Kulkarni, S.R., 1986, *Ap. J. (Letters)*, **306**, 85.
- Kulkarni, S.R. and Narayan, R., 1988, *Ap. J.*, **335**, 755.
- Kulkarni, S.R., Narayan, R. and Romani, R.W., 1990a, *Ap. J.*, **356**, 174.
- Kulkarni, S.R., Goss, W.M., Wolszczan, A. and Middleditch, J., 1990b, *Ap. J. (Letters)*, **363**, L5.
- Kulkarni, S.R., Djorgovski, S. and Klemola, A.R., *Ap. J.*, 1990c, in the press.
- Kulkarni, S.R., Anderson, S.B., Prince, T.A. and Wolszczan, A., 1991, *Nature*, **349**, 47.
- Larson, R.B., 1988, in *The Harlow-Shapley Symposium on Globular Cluster Systems in Galaxies*, eds. J.E. Grindlay and A.G. Davis Philip (Dordrecht, Reidel).
- Latham, D.W., 1989, in *Highlights of Astronomy*, ed. D. McNally (Kluwer Academic Publishers, Dordrecht).
- Lauer, T.R., Holtzman, J.A., Faber, S.M., Baum, W.A., Currie, D.G., Ewald, S.P., Groth, E.J., Hester, J., Kelsall, T., Light, R.M., Lynds, C.R., O'Neil, E.J., Schneider, D.P., Shaya, E.J. and Westphal, J.A., 1991, *Ap. J. (Letters)*, **369**, L45.
- Lee, H.M. and Ostriker, J.P., 1986, *Ap. J.*, **310**, 176.
- Leonard, P.J.T., 1989, *A.J.*, **98**, 217.
- Leonard, P.J.T. and Fahlman, G.G., 1991, *A.J.*, **102**, 994.
- Lewin, W.H.G. and Joss, P.C., *Space Sci. Rev.*, 283 (1981).
- Lugger, P.M., Cohn, H., Grindlay, J.E., Bailyn, C.D. and Hertz, P., 1987, *Ap. J.*, **320**, 482.

- Lynden-Bell, D. and Wood, R., 1968, *M.N.R.A.S.*, **138**, 495.
- Lyne, A.G., Brinklow, A., Middleditch, J., Kulkarni, S.R., Backer, D.C. and Clifton, T.R., 1987, *Nature*, **328**, 399.
- Lyne, A.G., Brinklow, A., Middleditch, J., Kulkarni, S.R., Backer, D.C. and Clifton, T.R., 1987, *Nature*, **328**, 399.
- Lyne, A.G., Biggs, J.D., Brinklow, A. and Ashworth, M., 1988, *Nature*, **332**, 45.
- Lyne, A.G., Manchester, R.N., D'Amico, N., Staveley-Smith, L., Johnston, S., Lim, J., Fruchter, A.S., Goss, W.M. and Frail, D., 1990, *Nature*, **347**, 650.
- Lyne, A.G., 1991, talk presented at the NATO Workshop on "X-ray binaries and the formation of binary and millisecond pulsars," Santa Barbara, 21-25 Jan 1991.
- Makino, J. and Hut, P., *Ap. J.*, 1991, in the press.
- Manchester, R.N. and Taylor, J.H., 1977, *Pulsars* (W.H. Freeman and Company, San Francisco).
- Manchester, R.N., Lyne, A.G., D'Amico, N., Johnston, S., Lim, J. and Kniffen, D.A., 1990, *Nature*, **345**, 598.
- Manchester, R.N., Lyne, A.G., D'Amico, N., Bailes, M. and Lim, J., 1991, *Nature*, **352**, 219.
- Mateo, M., Harris, H.C., Nemec, J. and Olszewski, E.W., 1990, *A.J.*, **100**, 469.
- Mathieu, R.D. and Latham, D.W., 1988, in *The Harlow-Shapley Symposium on Globular Cluster Systems in Galaxies*, eds. J.E. Grindlay and A.G. Davis Philip (Dordrecht, Reidel).
- McCrea, W.H., 1982, in *Progress in Cosmology*, ed. A.W. Wolfendale (Dordrecht, Reidel).

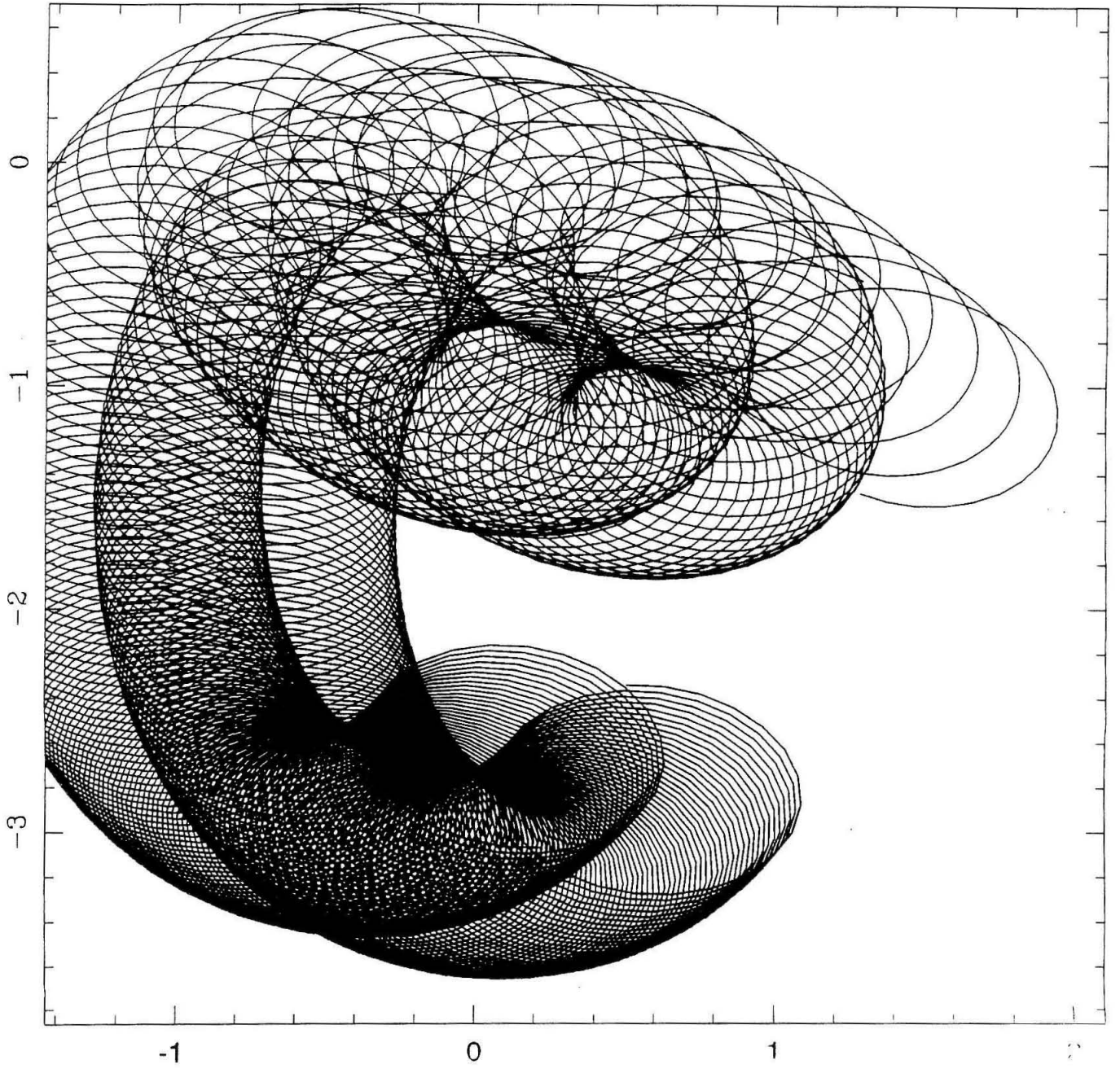
- McMillan, S.L.W., 1986, *Ap. J.*, **306**, 552.
- McMillan, S.L.W., McDermott, P.N. and Taam, R.E., 1987, *Ap. J.*, **318**, 261.
- McMillan, S.L.W., Taam, R.E. and McDermott, P.N., 1990a, *Ap. J.*, **354**, 190.
- McMillan, S.L.W., Hut, P. and Makino, J., 1990b, *Ap. J.*, **362**, 522.
- Meylan, G., 1988, *Astr. Ap.*, **191**, 215.
- Meylan, G., 1989, *Astr. Ap.*, **214**, 106.
- Michel, F.C., 1987, *Nature*, **329**, 310.
- Michell, J., 1767, *Phil. Trans. R. Soc.*, **57**, 234.
- Michell, J., 1784, *Phil. Trans. R. Soc.*, **74**, 56.
- Michie, R.W., 1963, *M.N.R.A.S.*, **125**, 127.
- Michie, R.W. and Bodenheimer, P.H., 1963, *M.N.R.A.S.*, **126**, 269.
- Mikkola, S., 1983, *M.N.R.A.S.*, **203**, 1107.
- Mikkola, S., 1984a, *M.N.R.A.S.*, **207**, 115.
- Mikkola, S., 1984b, *M.N.R.A.S.*, **208**, 75.
- Morbey, C.L. and Griffin, R.F., 1987, *Ap. J.*, **317**, 343.
- Murphy, B.W. and Cohn, H.N., 1988, *M.N.R.A.S.*, **232**, 835.
- Murphy, B.W., Cohn, H.N. and Hut, P., 1990, *M.N.R.A.S.*, **245**, 335.
- Murphy, B.W., Rutten, R.G.M., Callanan, P.J., Seitzer, P., Charles, P.A., Cohn, H.N. and Lugger, P.M., 1991, *Nature*, **351**, 130.
- Murphy, B.W. and Phinney, E.S., 1991, in preparation
- Narayan, R., Fruchter, A.S., Kulkarni, S.R. & Romani, R. 1990, in *Proc. 11th North American Workshop on CVs and LMXRBs* (ed. C.W. Mauche), (in the press).

- Narayan, R. and Ostriker, J.P., 1990, *Ap. J.*, **352**, 222.
- Naylor, T. and Charles, P.A., 1989, *M.N.R.A.S.*, **236**, 1P.
- Nomoto, K. and Kondo, Y., 1991, *Ap. J.*, **367**, L19.
- Ostriker, J.P., 1988, in *The Harlow-Shapley Symposium on Globular Cluster Systems in Galaxies*, eds. J.E. Grindlay and A.G. Davis Philip (Dordrecht, Reidel).
- Pacini, F., 1967, *Nature*, **216**, 567.
- Patterson, J. and Raymond, J.C., 1985, *Ap. J.*, **292**, 535.
- Patterson, J. and Raymond, J.C., 1985, *Ap. J.*, **292**, 550.
- Peebles, P.J.E. and Dicke, R.H., 1968, *Ap. J.*, **154**, 891.
- Peters, P.C. 1964, *Phys. Rev.*, **136**, 1224.
- Peterson, R.C., Seitzer, P. and Cudworth, K., 1989, *Ap. J.*, **347**, 251.
- Phinney, E.S., *M.N.R.A.S.*, 1991, in the press.
- Phinney, E.S. and Verbunt, F., 1990, *M.N.R.A.S.*, **248**, 24P.
- Phinney, E.S. and Kulkarni, S.R., *Nature*, 1991, in the press.
- Phinney, E.S. and Sigurdsson, S., 1991a, *Nature*, **349**, 220.
- Phinney, E.S. and Sigurdsson, S., 1991b, in preparation.
- Piotto, G., King, I.R. and Djorgovski, S., 1988, *A.J.*, **96**, 1918.
- Predehl, P., Hasinger, G. and Verbunt, F., *Astr. Ap.*, 1991, in the press.
- Press, W.H. and Teukolsky, S.A., 1977, *Ap. J.*, **213**, 183.
- Priedhorsky, W.C. and Holt, S.S., 1987, *Space Science Reviews*, **45**, 291.
- Priedhorsky, W.C. and Verbunt, F., 1988, *Ap. J.*, **333**, 895.

- Prince, T.A., Anderson, S.B., Kulkarni, S.R. and Wolszczan, A., 1991, *Ap. J. (Letters)*, **374**, 41.
- Pringle, J.E., 1989, *M.N.R.A.S.*, **239**, 361.
- Pryor, C., Latham, D.W. and Hazen-Liller, M.L., 1985, in *Dynamics of Star Clusters*, IAU Symposium No. 113, ed. J. Goodman and P. Hut (Dordrecht, Reidel), p. 99.
- Pryor, C., McClure, R.D., Hesser, J.E. and Fletcher, J.M., 1989, in *Dynamics of Dense Stellar Systems*, ed. D. Merritt (Cambridge University Press) p. 175.
- Pryor, C., Schommer, R.A. and Olszewski, E.W., 1990, *Steward Observatory, University of Arizona preprint*.
- Rappaport, S., Putney, A. and Verbunt, F., 1990, *Ap. J.*, **345**, 210.
- Rasio, F.A. and Shapiro, S.L., 1991, *Ap. J.*, **377**, 559.
- Roberts, M.S., 1988, in *The Harlow-Shapley Symposium on Globular Cluster Systems in Galaxies*, eds. J.E. Grindlay and A.G. Davis Philip (Dordrecht, Reidel).
- Romani, R.W., Kulkarni, S.R. and Blandford, R.D., 1987, *Nature*, **329**, 309.
- Romani, R.W., 1990a, *Ap. J.*, **357**, 493.
- Romani, R.W., 1990b, *Nature*, **347**, 741.
- Romani, R.W. and Weinberg, M.D., 1991, *Ap. J.*, **372**, 487.
- Ruffert, M. and Müller, E., 1990, *Astr. Ap.*, **238**, 116.
- Shapiro, S.L. and Teukolsky, S.A., 1983, *Black Holes, White Dwarfs and Neutron Stars: The Physics of Compact Objects* (John Wiley & Sons).
- Shara, M.M., Moffatt, A.F.J. and Potter, M., 1990, *A.J.*, **99**, 1858.

- Shaw, S.J. and White, R.E., 1986, *A.J.*, **91**, 312.
- Seitzer, P., Peterson, R. and Cudworth, K.M., 1989, in *Dynamics of Dense Stellar Systems*, ed. D. Merritt (Cambridge University Press) p. 175.
- Siegel, C.L. and Moser, J.K., 1971, *Lectures on Celestial Mechanics* (Springer, Berlin, Heidelberg, New York).
- Sigurdsson, S. and Phinney, E.S., 1991, in *PhD Thesis*.
- Smith, G.H., Wood, P.R., Faulkner, D.J. and Wright, A.E., 1990, *Ap. J.*, **353**, 168.
- Spitzer, L., 1969, *Ap. J.*, **158**, L139.
- Spitzer, L. and Hart, M.H., 1971a, *Ap. J.*, **164**, 399.
- Spitzer, L. and Hart, M.H., 1971b, *Ap. J.*, **166**, 483.
- Spitzer, L. and Shull, J.M., 1975, *Ap. J.*, **201**, 773.
- Spitzer, L. and Thuan, T.X., 1972, *Ap. J.*, **175**, 31.
- Spitzer, L., 1987, *Dynamical Evolution of Globular Clusters* (Princeton University Press).
- Talbot, F., 1871, *Proc. Roy. Soc.*, **20**, 386.
- Tayler, R.J. and Wood, P.R., 1975, *M.N.R.A.S.*, **171**, 467.
- Taylor, J.H. and Weisberg, J.M., 1989, *Ap. J.*, **345**, 434.
- Thorne, K.S. and Żytkow, A.N., 1977, *Ap. J.*, **212**, 832.
- Tout, C.A., 1991, *M.N.R.A.S.*, **250**, 701.
- Trimble, V., 1976, in *Structure and Evolution of Close Binary Systems*, IAU Symposium No. 73, ed. P. Eggleton, S. Mitton and J. Whelan (Dordrecht, Reidel), p. 369.
- VandenBerg, D.A. and Faulker, D.J., 1977, *Ap. J.*, **218**, 415.

- VandenBerg, D.A., 1978, *Ap. J.*, **224**, 394.
- VandenBerg, D.A., 1983, *Ap. J. Suppl.*, **51**, 29.
- Verbunt, F. and Hut, P., 1987, in *The Origin and Evolution of Neutron Stars*, eds. D.J. Helfand and J.H. Huang (Dordrecht, Reidel).
- Verbunt, F., van den Heuvel, E.P.J., van Paradijs, J. and Rappaport, S., 1987, *Nature*, **329**, 312.
- Verbunt, F., Lewin, W.H.G. and van Paradijs, J., 1989, *M.N.R.A.S.*, **241**, 51.
- Verbunt, F., 1990, in *Neutron Stars and Their Birth Events*, ed. W. Kundt (Dordrecht, Reidel).
- Webbink, R.F., 1984, *Ap. J.*, **277**, 355.
- Wheeler, J.A., 1966, *Ann. Rev. Astr. Ap.*, **4**, 393.
- Wijers, R.A.M.J. and van Paradijs, J., 1991, *Astr. Ap.*, **241**, L37.
- Wolszczan, A., 1991, *Nature*, **350**, 688.
- Zahn, J.P., 1989, *Astr. Ap.*, **220**, 112.
- Zahn, J.P. and Bouchet, L., 1989, *Astr. Ap.*, **223**, 112.



Chapter 2

Binary–single star interactions in Globular Clusters

in collaboration with

E.S. Phinney,

California Institute of Technology

To be submitted to the *Astrophysical Journal*

Abstract

An extensive series of three-body interactions involving hard binaries and single stars was calculated for different mass-ratios, by direct integration. Cross-sections for different interactions are presented and discussed. We find that mass-ratios of order two lead to significant and interesting differences in interaction compared with the equal mass case. Previous calculations concentrated on the equal mass case or extreme mass-ratios. Resonances are followed and are found to contribute strongly to the *a posteriori* calculated collision cross-section. We find that for moderately soft binaries exchange of heavy field stars is the dominant process and after such an exchange the physical cross-section for a subsequent interaction increases, even though the binary is hardened by the interaction. For very hard binaries, dissipative interactions dominate the cross-section.

“Two stars keep not their motion in one sphere”

W. Shakespeare, *Henry IV*

1. Introduction

Following the discovery of the first millisecond pulsar in the Galaxy (Backer *et al.*, 1982), globular clusters were identified as possible millisecond pulsar nurseries (Alpar *et al.*, 1982). The first cluster millisecond pulsar was found in short order (Hamilton *et al.*, 1985, Lyne *et al.*, 1987), and over thirty cluster millisecond pulsars are now known (Phinney and Kulkarni, 1990, and references therein, Bailyn, 1990, Lyne, 1991). The question of how old evolved systems, like the globular clusters, can contain apparently young, active objects like pulsars presents an interesting challenge. Although timing measurements can only give an estimate of the age of these pulsars, lifetime constraints, from orbital decay by gravitational radiation (Anderson *et al.* 1990a), among others, strongly suggest that some of these systems at least are being formed currently.

We consider the possibility that pulsar recycling is enhanced in globular clusters by binary–single star interactions. Binary interactions can increase the cross-section for recycling processes and weaken the density dependence of the probability of a non-pulsing neutron star undergoing an interaction leading to its rebirth as a pulsar. In addition, binary interactions lead to predictable distributions of binary pulsars, ejection of pulsars from the core of clusters, and, in some cases, to the ejection of the pulsar from the cluster. We also note recent evidence for a population of abnormal stars in cluster cores, particularly in post-core collapse clusters (Djorgovski *et al.*, 1988, Piotto *et al.*, 1988, Meylan, 1989, Aurière *et al.*, 1990, Djorgovski *et al.*, 1990, Mateo, 1990).

In order to estimate the relevant cross-sections, we have carried out an extensive Monte-Carlo simulation of three-body interactions by direct integration. Many previous three-body calculations have been carried out (Hills, 1975a,b, Hut and Bahcall, 1983, Hut, 1983b, Hut and Inagaki, 1985, Hills and Fullerton, 1980, Fullerton and Hills, 1982, McMillan, 1986, Rappaport, Putney and Verbunt, 1990), but most have been optimised for other systems of interest; Hut and Bahcall restricted themselves to the equal mass case and concentrated on soft binaries, with a small sample of hard equal mass binaries considered by Hut and Inagaki. Hills only considered encounters with zero impact parameter; Hills and Fullerton and Fullerton and Hills concentrated on the effects of extreme mass-ratios. McMillan considered the equal mass case, modeling dissipative encounters for very hard binaries, assuming main-sequence stars with polytropic equations of state. Rappaport *et al.* considered binaries with mass-dependent orbital period and specifically excluded resonances.

We have concentrated on obtaining a complete set of data, at a statistically significant level, for encounters between point-mass stars with unequal masses and hard binaries. Resonant encounters were followed as long as feasible, the vast majority being resolved. The resulting cross-sections are used to provide an estimate for the interaction rate in dense globular clusters, and in the future will provide a basis for further modeling of cluster evolution and dissipative encounters in cluster cores.

We consider a system of three point masses m_1, m_2, m_3 , moving under Newtonian gravity, with two of the masses, m_1, m_2 , initially bound. The third (field) star, $m_3 (= m_f)$, is initially at spatial infinity, moving with velocity v_∞ relative to the binary. We define $m_i = \frac{m_i}{m_S}$, in terms of an arbitrary scale mass, m_S , and,

without loss of generality, choose $m_1 \geq m_2$. For other physical systems we may consider a scaling mass $m'_S \neq m_S$, and scale appropriately.

In the center-of-mass frame of the trinary system, there is a well defined relative velocity at infinity, v_c , for a binary with semi-major axis a_{in} ,

$$\begin{aligned} v_c &= \sqrt{Gm_S \frac{m_1 m_2 (m_1 + m_2 + m_3)}{m_3 (m_1 + m_2)} \frac{1}{a}} \\ &= \frac{Gm_T \mu_{12}}{a m_3}, \end{aligned} \tag{1.1}$$

$\mu_{12} = m_1 m_2 / (m_1 + m_2)$, $m_T = m_1 + m_2 + m_3$, at which the field star possesses exactly sufficient energy to ionize the binary. We will be concerned almost solely with hard binaries, that is, those systems in which the field stars have velocity at infinity less than v_c . *A priori*, we have not set the physical semi-major axis of the binary, and can only consider the relative energy of the field star at infinity and the binary, since the unit of mass is arbitrary in the three-body calculation. Dimensions are introduced only in discussion of collisions and physical cross-sections. Thus the same set of runs describes interactions between white dwarfs and between main-sequence stars. Keeping in mind the physical situation we are interested in, the unit of mass was implicitly taken to be that of the canonical neutron star, $m_S = M_{NS} = 1.4 M_\odot$. This provides relative scaling for the choices of other masses of interest. With this choice, stars of mass $m_i = 1$ should, in the present context, be thought of as neutron stars (or heavy white dwarfs). Then the turn-off mass of a typical globular cluster ($\approx 0.7 M_\odot$) is $m_i = 0.5$. The initial mass-function in globular clusters is very uncertain, it may be steeper than the Salpeter mass-function (Chernoff and Weinberg, 1990), but recent results suggest that it may be no steeper than the Salpeter mass-function, and may even be flatter (Phinney, 1990). It is certain that light stars are more numerous than heavy stars, so the typical companion in a binary would be expected to be

somewhat less massive than the turnoff mass, so, somewhat arbitrarily, we chose $m_i = 0.35$ and $m_i = 0.4$ as reasonable representative masses. We do not expect any physics to depend critically on the exact mass-ratio, but the fact that there is a difference of order two in the masses is significant. As clusters are mass-segregated, we do not expect to find many light stars in the core, where neutron stars are expected to congregate. Very light stars, $m \sim 0.1 M_\odot$, are thought to evaporate from the cluster on a relatively short time scale (Spitzer, 1987), while the core population is expected to consist mainly of degenerate stars, binaries and the heaviest main-sequence stars. Heavy white dwarfs (masses $1.0-1.2 M_\odot$) should be more numerous than neutron stars, and undergo similar interactions.

In a three-body encounter, interactions may be classified into two groups: prompt interactions and resonances. We adopt the same criterion for defining resonances as used by Hut and Bahcall, that the root-mean-square separation of the three stars has more than one minimum. The result of an interaction is classified into one of four groups: flybys, consisting of the same outgoing state as the ingoing state (symbolically denoted $(1, 2) + (3) \rightarrow (1, 2) + (3)$); exchanges, where the field star becomes a part of the final state binary ($(1, 2) + (3) \rightarrow (1) + (2, 3)$ and $(1, 2) + (3) \rightarrow (1, 3) + (2)$); ionisation, where all three stars are unbound ($(1, 2) + (3) \rightarrow (1) + (2) + (3)$), and unresolved encounters. Flybys and exchanges may be either prompt or resonant, while ionisations are always prompt. In addition we consider collision cross-sections, where two of the stars are considered to have merged, while the third star may either remain bound to the merged object, or may escape to infinity (symbolically $(1, 2) + (3) \rightarrow ((a + b), c)$ and $(1, 2) + (3) \rightarrow (a + b) + (c)$, respectively).

As only a finite number of combinations of masses can be considered, a physically reasonable subset was picked. A complete set of runs was calculated for

masses $\{1.0, 1.0, 1.0\}$, with $v_\infty/v_c \in [0.0625, 1.0]$, binned in velocity in four logarithmic intervals, with a large proportion of the runs in the low velocity bins. These runs provided a basis for comparison with the unequal mass cross-sections, and, by comparing with the results obtained by Hut and Bahcall, the correctness and accuracy of our calculations could be checked. A complete set of runs was obtained for mass-ratios $\{0.5, 0.35, 1.0\}$, $\{1.0, 0.35, 0.5\}$ and $\{1.0, 0.4, 1.0\}$, for $v_\infty/v_c \in [0.05, 1.05]$.

The focus of the study was on the low velocity ($v_\infty/v_c \in [0.05, 0.15]$) encounters, so the majority of computing time was devoted to these encounters so as to have a statistically useful sample. Where appropriate the runs were then rebinned logarithmically. As the computer time needed to resolve resonances decreased sharply with v_∞/v_c , the runs at higher v_∞/v_c did not consume much additional computer time.

An additional series of runs were calculated for $v_\infty/v_c \in [0.05, 0.15]$, in order to check inferred scaling laws and possible contributions from encounters between very hard binaries and light stars. These calculations were performed for mass-ratios $\{1.0, \frac{0.8}{2^n}, 1.0\}$, for $n = 1-7$. One set of runs was calculated for the mass-ratio $\{1.0, 1.0, 0.4\}$ with $v_\infty/v_c \in [0.05, 0.15]$ and one set was calculated for mass-ratio $\{1.0, 0.001, 1.0\}$ for $v_\infty/v_c \in [1.0, 1.5]$.

The sampling was uniform in v_∞/v_c , though clearly physical systems have some distribution, $\zeta(\mathbf{v}_i)$, (typically Maxwellian or a truncated Maxwellian) of velocities. We did not wish to restrict ourselves to any specific choice of $\zeta(\mathbf{v})$, but given $\sigma(X, v_\infty)$, we can integrate over $\zeta(\mathbf{v}_{i,j}) dv_\infty$ to obtain a velocity averaged cross-section. The integration over $\zeta(\mathbf{v})$ is nontrivial, as the cross-section is a function of $|\mathbf{v}_b - \mathbf{v}_f|$ (Sigurdsson and Phinney, 1991), but as first approximation, we can consider $\sigma(X, \bar{v}_\infty)$.

The mass-ratios were chosen to investigate the physical scenarios likely to be of interest. The mass-ratios chosen model encounters between neutron stars or heavy white dwarfs and main-sequence stars: with $\{0.5, 0.35, 1.0\}$ appropriate for encounters between degenerates and main-sequence binaries or main-sequence-giant binaries; $\{1.0, 0.35, 0.5\}$ describing turnoff mass stars or giants encountering binaries composed of a neutron star/heavy white dwarf and a main-sequence star, and $\{1.0, 0.4, 1.0\}$ modeling encounters between a neutron star/heavy white dwarf-main-sequence binary encountering another neutron star/heavy white dwarf. The set with mass-ratio $\{1.0, 1.0, 0.4\}$ provides an estimate of the perturbation a neutron star-neutron star binary suffers from background main-sequence stars and white dwarfs. See Table 1 for summary of possible run interpretations: “NS” denotes a neutron star; “MS” denotes a main-sequence star; “G” denotes a giant or a sub-giant; and “T” denotes a main-sequence star at the turnoff point in the Hertzsprung-Russell diagram.

The series with mass-ratios $\{1.0, m_2, 1.0\}$ was calculated to examine systematic variations with mass-ratio of exchanged stars for hard binaries, and the “gravitational Fermi acceleration” exchange mechanism. Clearly for $m_2 \ll 1$, the system becomes physically unrealistic. For example, in a cluster core with dispersion 10 km s^{-1} , the mean relative velocity at infinity is $\approx 14 \text{ km s}^{-1}$. In order for a $0.001 M_{NS}$ star in orbit about a neutron star to encounter another neutron star at $v_\infty/v_c = 0.10$, we would require $v_c = 140 \text{ km s}^{-1}$, which implies a semi-major axis of only $2 \times 10^{-4} AU$, which is likely to be less than the stellar radius. Such systems are still physically interesting for m_2 as low as 0.01, with PSR1957+20 being an example. The run with mass-ratios $\{1.0, 0.001, 1.0\}$ extended the investigation of light star exchanges, and provided some data at higher, more realistic v_∞/v_c .

2. Methods

We assume that there is a population of binaries in globular clusters, having some distribution of semi-major axis. The majority of our calculations were with zero initial eccentricity. A set of runs was calculated for binaries with eccentricity 0.5 and 0.7, to check the variation in cross-sections with eccentricity. Calculations by Hut and Bahcall indicate that the cross-section scales in proportion to $1 + e$, and that there should be no other large systematic effects in cross-section due to non-zero initial eccentricity. In globular clusters, interactions perturb an initial eccentricity distribution on a time scale short compared to the time scale for changing the semi-major axis distribution. There is no data on the eccentricity distribution of globular cluster binaries; the Galactic distribution of binary eccentricity is thought to be $P(e) = 2e$. We note that there is reasonably good evidence for the existence of at least one spectroscopic binary in a globular cluster (Pryor *et al.*, 1985), and that recent observations are consistent with a significant primordial binary population (Pryor *et al.*, 1989, 1990) In general, a binary will move through a background of field stars of number density $n(t, \mathbf{r})$, with mean relative velocity v_∞ . The probability, $P(X)$, of a process X taking place, in time $T = t_f - t_i$, can be written

$$P(X) = 1 - e^{-\int_{t_i}^{t_f} R(X, t') dt'} \quad (2.1)$$

The rate for a process X to take place, $R(X)$, can be written

$$R(X) = \langle n(t, \mathbf{r}) v_\infty \sigma(X) \rangle, \quad (2.2)$$

where $\sigma(X)$ is the cross-section for process X to take place. To define σ , consider the binary in its center-of-mass rest frame. Without loss of generality, we consider a symmetric flux of field stars, uniform in area at infinity. Each star has some

projected impact parameter b , from the center-of-mass of the binary. Clearly a star passing some arbitrarily large projected distance b from the binary center-of-mass will not interact. Allowing for gravitational focusing, but still treating the binary as a point mass, a star with projected impact parameter b at infinity would have a pericenter p .

$$p = \frac{Gm_T}{v_\infty^2} \left(\sqrt{1 + b^2 \left(\frac{v_\infty^2}{Gm_T} \right)^2} - 1 \right). \quad (2.3)$$

For $Gm_T/v_c^2 b \gg 1$ we have

$$\begin{aligned} p &\simeq b^2 \frac{v_\infty^2}{2Gm_T} \\ &= \left(\frac{v_\infty}{v_c} \right)^2 \left(\frac{b}{2a_{in}} \right) \frac{\mu_{12}}{m_3} b. \end{aligned} \quad (2.4)$$

Note that for $\mu_{12} \ll m_3$, p is small. We define

$$\sigma(X) = f(X) \pi b_{max}^2, \quad (2.5)$$

where $f(X)$ is the fraction of field stars with impact parameters $b < b_{max}$ which undergo interaction X . Clearly

$$\lim_{b_{max} \rightarrow \infty} f(X) \rightarrow 0, \quad (2.6)$$

for any non-trivial interaction, in such a way that σ converges. For flybys, the cross-section clearly does not converge, although the cross-section for finite perturbations during flybys does converge (*i.e.* given finite change $\delta > 0$ in some physical quantity during process X , then $\exists \epsilon > 0$ such that, cross-section for change $\delta' \geq \delta$, $\sigma(\delta X)$, converges, $\lim_{b_{max} \rightarrow \infty} \sigma(\delta X) \rightarrow \epsilon$).

In practise σ is computed with a finite b_{max} and a compromise must be maintained between ensuring that b_{max} is large enough that σ has converged, and the total number of encounters that can feasibly be calculated with finite resources.

It is useful to define a dimensionless cross-section, $\tilde{\sigma}$, in terms of the geometric cross-section of the binary πa_{in}^2 ,

$$\tilde{\sigma}(X) = \frac{\sigma(X)}{\pi a_{in}^2} \left(\frac{v_\infty}{v_c} \right)^2, \quad (2.7)$$

where $(\frac{v_\infty}{v_c})^2$ is included to remove this dependence on gravitational focusing at low v_∞/v_c . The time scale for interactions is then

$$\begin{aligned} T_X &= R(X)^{-1} \\ &= \langle n(t, \mathbf{r}) \pi a_{in}^2 \left(\frac{v_c}{v_\infty} \right) \tilde{\sigma}(X) \rangle^{-1}. \end{aligned} \quad (2.8)$$

In physical units, for hard binaries ($v_\infty < v_c$), the interaction time scale, for a particular binary, can be conveniently written

$$T_X = 1.5 \times 10^{10} g(m_i)^{-1} a_{AU}^{-1} n_4^{-1} \left\langle \frac{1}{v_{10}} \right\rangle^{-1} \tilde{\sigma}(X)^{-1} \text{ years}, \quad (2.9)$$

where

$$g(m_i) = \frac{m_1 m_2 (m_1 + m_2 + m_3)}{m_3 (m_1 + m_2)}, \quad (2.10)$$

a_{AU} is the semi-major axis in astronomical units, $n_4 = n(t, \mathbf{r})/10^4 \text{ pc}^{-3}$ is the number density of field stars, and $v_{10} = v_\infty/10 \text{ km s}^{-1}$ is the relative velocity at infinity. For $\mu_{12} \ll m_3$, a renormalised cross-section $\tilde{\sigma}' = g(m_i)\tilde{\sigma}$ is more useful. Table 2 shows $g(m_i)$, v_c and v_c in km s^{-1} as a function of semi-major axis and scale mass m_S .

Given $R(X)$, and some assumptions about $n(t, \mathbf{r})$, $\zeta(v_\infty(t, \mathbf{r}), m_i)$, the fraction of primordial binaries, f_b , and the initial mass-function, we can calculate the expected numbers of various interactions and the properties of the current binary population and products of binary interactions. Detailed discussion of these properties is deferred to a later chapter.

A population of primordial binaries in globular clusters will significantly affect the dynamical evolution of the cluster (Hut, 1983c, Cohn and Hut, 1984, Hut and

Paczynski, 1984, Goodman and Hut, 1989, McMillan *et al.*, 1990b, Murphy *et al.*, 1990). We hope to use the results of this work to extend the ongoing work on cluster collapse and to attempt to produce a self-consistent model of primordial binary evolution during collapse.

We follow Hut and Bahcall in choosing $b \leq b_{max} = (C/v_\infty + 0.6(1 + e_{in}))a_{in}$, distributed uniformly in b_{max}^2 . We chose $C = 4$ for runs $\{1, 1, 1\}$, $\{1, 0.35, 0.5\}$, $\{1, 0.8, 1\}$ and $\{1, 0.4, 1\}$. For mass-ratios $\{1, m_2, 1\}$, $m_2 \leq 0.2$, we chose $C = 3$. For the set of runs with mass-ratio $\{0.5, 0.35, 1\}$, most runs were made with $C = 4$, some had $C = 3$. For a number of sets of initial values, initially done for $C = 4$, an additional set of runs was made with $C = 3$, in order to obtain better statistics for some low cross-section interactions of interest.

With this choice of impact parameter, the unperturbed field star with maximum impact parameter, b_{max} , approaches within a few a_{in} of the binary center-of-mass, so the typical encounter with $b < b_{max}$ will involve a non-perturbative interaction between the field star and the binary.

It can be useful to consider separately the first pass of the field star and the binary, and the subsequent trajectory. For large pericenters, ($p/a_{in} \gg 1$) the majority of first pass encounters produces a negligible energy transfer (compared to $\min\{\frac{1}{2}(m_3(m_1 + m_2)/m_T)v_\infty^2, Gm_1m_2/a_{in}\}$), approximated by (Heggie, 1975),

$$\langle \Delta E \rangle \simeq -A \left(\frac{p}{a_{in}} \right)^{3/2} e^{-B \left(\frac{p}{a_{in}} \right)^3}. \quad (2.11)$$

We define energy change to be negative, if energy is transferred to the field star, that is the binary binding energy becomes more negative. Here,

$$\begin{aligned} A &= \xi \sqrt{2} \left(\frac{Gm_1m_2}{a_{in}} \right)^{7/4} \left(\frac{m_1 + m_2}{m_1m_2} \right)^{1/4} \frac{m_3}{G^{3/2}m_T^2\sqrt{m_1m_2}} a_{in}^{3/2} v_\infty^{3/2} \\ &= \xi \sqrt{2} \left(\frac{G(m_1 + m_2)}{a_{in}} \right)^{1/4} \frac{m_1m_2m_3}{m_T^2} v_\infty^{3/2} \end{aligned}, \quad (2.12)$$

where ξ is a geometric factor of order unity, and

$$B = \frac{1}{3} \frac{1}{(m_1 + m_2)\sqrt{m_T}} \left(\frac{m_1 m_2}{m_3} \right)^{3/2} \left(\frac{v_\infty}{v_c} \right)^3. \quad (2.13)$$

For smaller p , the energy transfer may be significant, in which case one of several paths may be followed: the energy transfer may be to the field star (possibly accompanied by a prompt exchange), leading to the field (exchanged) star receding to infinity, with velocity, $v_{\infty_{new}} > v_\infty$; or, energy may be transferred from the field star to the binary. If the energy transfer is small

$$\Delta E < \frac{1}{2} \left(\frac{m_3(m_1 + m_2)}{m_T} \right) v_\infty^2 = \Delta E_{crit}, \quad (2.14)$$

then the binary will remain intact and the field star (or exchanged star in the case of prompt exchange) will recede to infinity with $v_{\infty_{new}} < v_\infty$ ($v_{\infty_{new}} < \sqrt{m_3/m_{ejected}}v_\infty$ in case of prompt exchange). If $\Delta E \geq \Delta E_{crit}$, and $v_\infty < v_c$, the field star cannot escape to infinity, and a resonance occurs. If $v_\infty > v_c$, the binary may be ionised, or a prompt exchange may occur; no resonance is possible.

It is worth noting that in the point mass approximation it is impossible to form a stable hierarchical triple in a binary–single star encounter (Hut, 1983b and references therein). Although a field star may be captured into a wide, eccentric orbit, the pericenter of the orbit will be at approximately the same distance from the binary center-of-mass as the initial closest approach which led to the energy transfer establishing the orbit. As energy transfer was necessarily to the binary, the binary orbit will now be wider (and typically more eccentric) than it was initially. It is therefore inevitable that the system will undergo a second, strong perturbation, involving energy transfer of the same order as that which led to the formation of the triple. Using the same argument, if the system is still bound at that point, it will, inevitably, experience another perturbation of the same order

as the second perturbation. This process will eventually perturb the pseudo-stable triple until it disrupts, ejecting one star, leaving a new binary and field star. Typically, any triple formed will disrupt in a few dynamical times (the dynamical time being determined by the period of the outer star); only a very small fraction lasts more than 10^3 dynamical times. A resonance may go through several hierarchical pseudo-stable triples before being resolved, but, except for a set of relative measure zero, none will be stable. We note the family of stable non-hierarchical orbits found by Hénon (Hénon, 1976), and conjecture that at most a set of orbits of relative measure zero can be captured into that family of orbits.

3. Calculation

To calculate the cross-sections for various processes of interest, a Monte-Carlo simulation of 7.5×10^4 runs was carried out by direct integration of the three-body equations of motion. The calculations were done following the method described by Hut and Bahcall, with some modifications. The first two masses were initially set to be in a binary with semi-major axis $a_{in} = 1$, while the field star was initially at a distance of $20 a_{in}$ from the center of mass of the binary. Treating the binary as a point mass, the field star trajectory was then integrated forward to periastron, still assuming the binary to be a point mass. The initial phase of the binary was set randomly at that time, and the phase at the time the field star was at the initial distance calculated. The total energy of the system, E_T , was then calculated exactly. The velocity of the field star should not be set to that it would have at $20 a$ if the binary were a point mass, the reason being that the total energy would not be the desired one. For example, at a distance D from the binary center-of-mass, the error in energy which would result from treating the

binary as a point mass is, for a circular orbit, to first non-zero order,

$$\frac{\Delta E_f}{E_f} = \frac{M_1 M_2}{(M_1 + M_2)^2} \left(\frac{a}{D}\right)^2 \frac{1}{2} (3 \cos^2 \psi - 1), \quad (3.1)$$

where $E_f = -GM_f(M_1 + M_2)/D$, $\psi = \frac{\pi}{2} - \theta \sin \phi$, θ is the angle of the field star relative to the binary orbital axis and ϕ is the phase of the binary. In order to keep the initial conditions consistent with the specified conditions at infinity, the magnitude of the velocity of the field star at D is adjusted so that the total energy was exactly equal to that specified when the field star was at infinity. This gives a prescription for uniform, reproducible choice of angular variables, while allowing a well-defined total energy for the system. This is largely for convenience of analysis, as the binning of results is done by velocity at infinity, and the analysis programs checked for error in integration by recalculating the exact extrapolated velocity at infinity. It should be noted that the choice of initial phase is still well defined, as the projected time of periastron is not equal to the actual time at periastron in either choice of initial conditions.

The calculations were carried out on DECstation 3100s by direct integration, using a fourth order Runge-Kutta integration scheme with adaptive stepsize ($dt = \epsilon' r_{ij_{min}}/v_{ij_{max}}$) and quality control. We found that even for very small ϵ' , energy conservation to accuracy 2ϵ , ($\delta E/|E| \leq \epsilon \times |E| + \epsilon \times KE$), was not a useful constraint on stepsize for the high eccentricity orbits which develop during resonant encounters of interest. The problem arises because the binary energy is given by $E_b = -GM_1 M_2/2a_{in}$, independent of eccentricity. At high eccentricity, residual numerical errors in integration give orbits with an approximately constant semi-major axis, a_{in} , but varying eccentricity. With energy conservation and position quality control as the only constraint on the stepsize, the integrator will over or under-step leading to a drift in the calculated eccentricity of subsequent binary orbits. Therefore we imposed an additional requirement that angular momentum

be conserved to one part in 10^5 . To test the stability of the integrator, binaries with eccentricity of 0.999 were run for several hundred orbits, and the trajectory checked for drift. When explicit angular momentum conservation was relaxed, the integrator would drift, leading to a clear shift in the pericenter of the orbit. Imposing angular momentum conservation explicitly eliminated the problem with highly eccentric orbits and gave us energy conserved to better than one part in 10^7 (for most runs energy conservation was several orders of magnitude better still). Other integration schemes were tested and were found to be either no faster than Runge–Kutta or to have convergence problems. Regularisation or analytic approximations were not used in order to have a consistent calculation method for the entire trajectory. It should be noted that when a heavy star is exchanged for a light star in a binary, the final semi-major axis $a_f \sim \frac{m_{heavy}}{m_{light}} a_{in} \gg a_{in}$. Thus it becomes necessary to follow some encounters to very large separation, R , as R/a_f is not necessarily large even though R/a_{in} is large. This procedure, although computationally intensive, assured that most physically relevant interactions were included; in particular most field stars left marginally bound by the first encounter with the binary were followed until the interaction was complete. As we are interested in physical systems, runs in which stellar separation approached zero ($\min\{r_{ij}\} \leq 5 \times 10^{-5} a_{in}$, in practise) were considered to have led to stellar collision and were halted.

The accuracy of the positions and velocities thus calculated was checked by running identical initial conditions with half the maximum stepsize, and the final conditions were compared after 5×10^5 integration steps. Inevitably highly resonant trajectories were found to be chaotic, that is small changes in initial conditions lead to large changes in final condition (Siegel and Moser, 1971, Hut, 1983b). It was impossible to repeat all resonant runs, resonances consumed most

of the computer time spent on these calculations, but a small sample was re-run, both at double integration precision and at normal integration precision with initial condition differing by approximately $10^{-6} a_{in}$ in initial position, and similar fractional error in initial velocity. All runs integrated with identical initial conditions (to double precision) were exactly reproduced when integrated with half initial and maximum integration step-size, for 10^5 timesteps. Several highly resonant runs (more than 5×10^5 integration steps) were integrated with slightly perturbed initial conditions, and all deviated radically from the original trajectory within a few hundred thousand integration steps. There is no point in attempting to maintain arbitrary precision in these simulations, as not only are the chaotic trajectories scattered into one another, causing effectively a minor randomisation of already random initial conditions, but physical effects ignored in these calculations, such as finite stellar size and dissipation make such precision in initial conditions meaningless.

Each run was in the first instance permitted to run for 10^6 time steps, in order to give as much time as practicable to resolving resonances. Runs were halted when the separation between the final binary and the final field star exceeded $30 a_{in}$, when the maximum number of permitted time steps was exceeded, or when the separation between any pair of stars was less than $5 \times 10^{-5} a_{in}$. After each set of runs was halted, the final conditions were analysed and resonances and unresolved interactions were picked out by extrapolating the final positions and velocities analytically to infinity. To do this, we considered the potential energy of each star with respect to the other stars in turn, and choose the pair with the lowest binding energy as a candidate bound pair. The relative velocity between the third star and the new binary's center-of-mass is calculated and extrapolated to infinity. If the extrapolated velocity at infinity was finite and positive, the orbital parameters of the new binary were calculated, and if the eccentricity was

less than one, the system was considered to be resolved. If the eccentricity was greater than or equal to one, and the kinetic energy of each star was larger than the binding energy of that star, then the system was assumed to have ionised. Any system not ionised or resolved into a binary and a free field star was assumed to be resonant or an eccentric, wide-orbit trinary and was flagged for further integration. Colliding systems, ($r_{min} < 5 \times 10^{-5} a_{in}$), were noted separately after each run was halted. This approach is very conservative, in any case of doubt the integration is continued, a resolved system will then be resolved unambiguously.

The closest approach between each pair of stars was stored, as were the positions and velocities of each star at the moment of closest approach between any pair of stars. Due to limited available memory storage, the positions and velocity could not be stored for each close encounter. This leads to some loss of information. In particular, if in the analysis one or more of the stars is assumed degenerate, the closest encounter may have involved a degenerate and not be close enough for collision, while an encounter between a different pair of non-degenerate stars, though not as close, may have been dissipative. As we did not want to restrict the calculations to consideration of a particular stellar type, this was unavoidable, given finite data storage available. A major limiting factor in these calculations was available data storage space. To decide, *a posteriori*, whether a particular closest encounter was dissipative or collisional, a stellar radius, R_* , and tidal radius, R_t , had to be assumed. The interaction radius could be set to some fraction of the initial binary semi-major axis, or a stellar model was assumed, with

$$R_* = \beta \left(\frac{M_*}{M_\odot} \right)^\alpha R_{in}. \quad (3.2)$$

The tidal radius, $R_t = f_t R_*$, where $f_t \sim 3$, for main-sequence stars, and somewhat less for giants (Fabian *et al.*, 1975, Press and Teukolsky, 1977, Lee and Ostriker,

1986, McMillan *et al.*, 1987, 1990a, Bailyn, 1988). For most purposes, the interaction radius of a degenerate was assumed to be zero. A significant fraction of runs with low relative velocity at infinity, led to a trinary consisting of a wide binary with the third star in a very wide orbit about the other two. These, and any close resonance still in progress after 10^6 integration steps, were separately integrated for up to 8×10^6 timesteps (16×10^6 total, for $\{1, 0.0125, 1\}$) in an attempt to resolve as many runs as possible. The unresolved runs were halted when the separation between the final binary and the final field star was $2^n \times 30 a_{in}$ for ($n = 1, \dots, 5$), when collision was certain ($r_{min} < 5 \times 10^{-5}$), or when the maximum number of permitted time steps was exceeded. After each set of reruns was completed the final conditions were re-analysed and n incremented, until the final field star was $960 a$ from the final binary, at which point, in the clusters of interest, perturbations from other field stars would be likely to significantly disturb the orbit and the field star could be considered to be at effective spatial infinity. The fraction of unresolved runs ranged from less than 0.1%, for high velocity runs with approximately equal masses, to almost 10%, for the run $\{1, 0.0125, 1\}$. Typically about 0.1% of the runs were found to be certain collisions ($r_{min} < 5 \times 10^{-5}$). For low velocity runs ($v_\infty/v_c \in [0.05, 0.15]$), of order 1% were still resonant. For the low mass ratio runs, a few percent, the fraction increasing with decreasing m_2 , were metastable trinaries, with the field star on an orbit about the binary with apastron greater than $10^3 a_{in}$.

4. Results

4.1. Recoil and Energy Transfer

There exists a critical value $v_{\infty_c}(m_i) \sim v_c$ for which the average energy transfer $\langle \Delta E \rangle$ in an encounter is zero. For $v_{\infty} < v_{\infty_c}$, $\langle \Delta E \rangle < 0$. Values of v_{∞_c} for mass-ratios $\{0.5, 0.35, 1.0\}$, $\{1.0, 0.35, 0.5\}$ and $\{1.0, 0.4, 1.0\}$ are shown in Figure 1a. The mean energy transferred varies slowly with v_{∞}/v_c near v_{∞_c} , and binaries near the borderline will slowly random walk away from the critical semi-major axis. Those binaries will either be rapidly ionised, or will slowly harden. Considering flybys only, the picture is quite different; the average energy transfer does not become positive until $v_{\infty} > v_c$, and even then, for mass-ratio $\{0.5, 0.35, 1.0\}$, the average energy transfer is still negative (Figure 1b). For exchanges the mean energy transfer is positive for a larger range of v_{∞}/v_c (Figures 1c,d). For the mass-ratio $\{0.5, 0.35, 1.0\}$ the mean energy transfer is negative for all $v_{\infty}/v_c \leq 1$. When the ejected star is lighter than the field star replacing it, the mean energy transfer is somewhat larger than when the lighter star is ejected (see Tables 4b,c). When a light star is ejected, the mean energy transfer is positive only for a small range in v_{∞}/v_c , if at all (Figure 1d).

This can be understood by noting that the cross-section for ionisation increases rapidly with v_{∞} for $v_{\infty}/v_c > 1$, and is large for $m_f > \mu_{12}$. Interactions that soften the binary are now ionising it. We can therefore conclude; that, during close encounters, a hard binary is rarely softened without being ionised or exchanged. For $v_{\infty}/v_c \ll 1$ the probability of softening the binary becomes vanishingly small. At higher v_{∞}/v_c the final binary is more likely to be hardened if the field star exchanged into the binary was more massive than the star

ejected. To consider in detail the energy transfer during an encounter, it is useful to define the fractional energy transfer, Δ . The binary binding energy is $E_{fin} = -GM_S m_a m_b / a_{fin}$, where m_a and m_b are the masses of the stars constituting the final binary, giving

$$\begin{aligned}\Delta &= (E_{in} - E_{fin}) / E_{in} \\ &= 1 - \frac{a_{in} m_a m_b}{a_{fin} m_1 m_2}\end{aligned}\quad (4.1)$$

$E_{in} = -GM_S m_1 m_2 / a_{in}$ is the initial binary binding energy.

The distribution of semi-major axis of the binary after any interaction can be modeled by

$$\sigma(a_{fin}/a_{in}|X) = \frac{N_1 a_{fin} e^{(a_{fin}-a_0)}}{e^{N_2 (\frac{v_\infty}{v_c})(a_{fin}-a_0)} + 1}, \quad (4.2)$$

where N_1 ($\sim \sigma(X)$), N_2 (~ 3), are normalising constants. For exchanges, where field star mass m_f exchanges into the binary and star mass m_e is ejected, $a_0 \approx a_{in} \times (1 + v_\infty/v_c) \frac{m_f}{m_e}$ (see Figures 2a,b, 3). The motivation for the form of the fit can be understood by noting that for $v_\infty \rightarrow 0$ the maximum final semi-major axis is simply $a_{fin} = a_{in} \times \frac{m_f}{m_e}$, and for $v_\infty \ll v_c$ the cutoff for $a_{fin} > a_{in} \times \frac{m_f}{m_e}$ is faster than exponential. For small a_{fin} the best fit is linear in a_{fin} .

After interaction, the new relative velocity at infinity, v'_∞ , is given by

$$v'_\infty = \sqrt{\frac{m_3(m_1 + m_2)}{m_e(m_a + m_b)} v_\infty^2 + \frac{2m_T E_{in}}{m_e(m_a + m_b)} \Delta} \quad (4.3)$$

(see Figure 4). The binary recoil velocity follows trivially from momentum conservation in the center-of-mass frame, $v_{rec} = \frac{m_e}{m_T} v'_\infty$. Typically $m_a + m_b \gg m_e$, so the ejected star has large relative velocity at infinity in the center-of-mass frame. As a test of the correctness of the analysis program, the extrapolated velocities at infinity were compared with the range of possible velocities, given the range of v_∞/v_c and the calculated a_{fin}/a_{in} . All calculated velocities fell within the

allowed range, with a reasonable distribution in velocity, as shown in Figure 13. Integrating $\sigma(a_{fin}/a_{in})$ numerically, we find that for flybys, $\sigma(\Delta < -0.1)$ as a function of v_∞/v_c , is fairly flat up to $v_\infty/v_c \sim 0.5$, and decreases exponentially for $v_\infty/v_c \gtrsim 0.7$.

For exchanges we find that Δ is not sensitive to the mass-ratio of the interacting stars, in contrast to the results obtained by Hills and Fullerton. Hills and Fullerton concentrated their work on large mass-ratio encounters at zero impact parameters. At zero impact parameter the total angular momentum, \mathbf{J} , of the system is determined by the angular momentum of the binary, whereas at large impact parameter the angular momentum is dominated by the field star,

$$\mathbf{J} = (M_1 M_2) \sqrt{\frac{a_{in} G}{(M_1 + M_2)}} \hat{\mathbf{z}} + b v_\infty \left(\frac{M_f (M_1 + M_2)}{M_T} \right) \hat{\mathbf{z}}'. \quad (4.4)$$

Here, $\hat{\mathbf{z}}$ is the unit normal to the plane of the binary, $\hat{\mathbf{z}}'$ is the unit normal to the plane defined by the unperturbed orbit of the field star about the binary center-of-mass at infinity. For $m_2 < m_f$ and $b \gg 0$, the initial binary angular momentum is negligible. In general $\hat{\mathbf{z}}$ is not parallel to $\hat{\mathbf{z}}'$, and for typical b the net angular momentum, $J = |\mathbf{J}|$, is large compared to the binary angular momentum. Only in the small region of phase space $p \ll a$, or $p \lesssim a$ and $\hat{\mathbf{z}}$ anti-parallel to $\hat{\mathbf{z}}'$, is the total angular momentum small. After an exchange the binary is unlikely to have less angular momentum than it had initially. The semi-major axis and eccentricity of the final binary are determined by angular momentum conservation (and energy conservation). To extend the analogy with atomic physics, the ejected star is typically in an s-state, or a low l-state; high l-states have low probability. We believe that the result of Hills and Fullerton was an artifact of the zero-impact parameter initial conditions, and not applicable generally. This is of some importance, as the cross-section for further interaction is dependent on a_{fin} , and

we find that a_{fin} after exchange is typically m_f/m_e larger than would be inferred from Hills and Fullerton’s results.

We find that exchanges are possible for very small m_2 , which might appear to contradict the conclusion reached by Heggie; it should however be noted that Heggie considered systems with fixed v_∞ , and thus increasing v_∞/v_c as m_2 gets smaller. Here we fix v_∞/v_c , which becomes physically unrealistic for very small m_2 , as noted above (excepting exotic objects, such as neutron star–massive black hole binaries encountering a massive black hole, for which we might have $m_2 \ll m_{1,3}$ and $v_\infty/v_c \ll 10^{-2}$, without tidal disruption of the less massive member of the binary).

4.2. Exchanges

The cross-section for exchanges converges as $b \rightarrow \infty$, and for $v_\infty \lesssim v_c$, the dimensionless cross-section, $\tilde{\sigma}$, decreases slowly with increasing velocity (Tables 4a,b,c). The cross-section for ejecting the heavier member of the initial binary is proportionally larger at high v_∞/v_c ; the ratio of probability of exchange is very approximately $\propto (1 + v_\infty/v_c)m_{e2}/m_{e1}$ for $m_f > m_e$. For $m_f < m_e$ the cross-section for exchange decreases very rapidly with m_f/m_e . For the set of mass-ratios $\{1, m_2, 1\}$,

$$g(m_i)\tilde{\sigma}((1, 2) + (3) \rightarrow (1, 3) + (2)) \simeq 5.5, \quad (4.5)$$

approximately constant to within 10%, at $v_\infty/v_c \in [0.05, 0.15]$.

For $m_f \gg m_e$, qualitatively the exchange mechanism can be thought as being one of two types: “hooking” and “gravitational Fermi acceleration.” In hooking, the field star orbit is prograde relative to the binary orbit, and $m_1 (> m_2)$ is captured into orbit about the field star without the field star coming near the

lighter of the binary members, as illustrated in Figure 5a. The light star is ejected with velocity comparable to its orbital velocity, and the two heavier stars are bound in a wide, eccentric orbit. In gravitational Fermi acceleration, the field star orbit is retrograde and makes a close approach to the lighter of the binary members. The light star is scattered through a large angle $\sim 180^\circ$, carrying away sufficient energy to leave the original field star bound. The name follows from the analogous electro-magnetic process (see Figure 5b). In the case $m_1 \simeq m_3 (= m) \gg m_2$, the binary recoils with speed $v_{13} \sim 0.3\sqrt{m_2/m_3}\sqrt{Gm_3/a_f}$.

As previously noted, in general the total angular momentum, \mathbf{J} , is not parallel to the direction of the binary angular momentum $\hat{\mathbf{z}}$. The direction of the angular momentum of the final binary will therefore not, in general, be parallel to $\hat{\mathbf{z}}$. This is of particular interest if mass-transfer has taken place in the initial binary, and the spin, \mathbf{s} , of the neutron star member of the initial binary is aligned with the orbital angular momentum. After exchange, the spin will, in general, no longer be aligned with the orbital angular momentum of the binary. However, analysis of the results shows that the spin direction is not totally randomised; some memory is retained of the original binary orbital angular momentum direction. Roughly two-thirds of the final binaries had $\mathbf{s} \cdot \mathbf{J} > 0$. This is easily understood by noting that the cross-section for exchanges is somewhat larger for field stars coming in on prograde orbits. Unfortunately, in practise determination of the sign of $\mathbf{s} \cdot \mathbf{J}$ does not seem possible, although radio observations of pulsars may indicate the magnitude (Wolszczan, 1991). In parentheses, we note that, in principle, the sign of $\mathbf{s} \cdot \mathbf{J}$ may be determined by measuring the polarization of gravitational waves emitted by the system, a difficult observation in practise. Figure 14 shows the distribution of flybys, shown as points, and exchanges, shown as triangles and crosses for ejections of stars 1 and 2 respectively. The plot shows z-component of

the total angular momentum of the system plotted against the transverse component of the total angular momentum with the same sign as \mathbf{J}_x arbitrarily assigned for ease of presentation. The exchanges are asymmetric about $\mathbf{J}_z = 0$, showing the preference for prograde exchanges, and completely contained within the circle of flybys, showing the beam diameter was sufficient to include all interactions of interest.

The ratio of the time scale for significant hardening to that for exchange is of great importance, as it determines whether main-sequence binaries are removed and replaced by binaries containing the heavier degenerate stellar remnants. Considering the runs with mass-ratios $\{0.5, 0.35, 1.0\}$, $\{1.0, 0.35, 0.5\}$, $\{1.0, 0.4, 1.0\}$ and $\{1.0, 1.0, 1.0\}$, using equation 2.9, we find that

$$\frac{T_h}{T_e} = \frac{\tilde{\sigma}_e}{\tilde{\sigma}_h}, \quad (4.6)$$

where $\tilde{\sigma}_e = \tilde{\sigma}(X : (1, 2) + (3) \rightarrow (1) + (2, 3)) + \tilde{\sigma}(X : (1, 2) + (3) \rightarrow (1, 3) + (2))$, and $\tilde{\sigma}_h = \tilde{\sigma}(\Delta < -0.1)$. Numerically, $\tilde{\sigma}_f \sim 2 \times \tilde{\sigma}_e$, and using the numerical integration of $\sigma(a_{fin}/a_{in})$ we find

$$\frac{T_h}{T_e} > 1 \Rightarrow \frac{v_\infty}{v_c} > 0.5. \quad (4.7)$$

That is, moderately hard main-sequence binaries are *more likely to be exchanged* than significantly hardened by massive (neutron stars or heavy white dwarfs) field stars. In particular, whereas the time scale for hardening main-sequence binaries with semi-major axis of a few AU down to less than $0.5 AU$, in a moderately dense ($n_4 \sim 0.3$) cluster core, is greater than the cluster core collapse time scale, we would expect the majority of these main-sequence binaries to have been exchanged and hardened by heavy, degenerate field stars, assuming such a population is present in the cluster core. After an exchange, the physical cross-section of the resulting binary is larger than it was before the exchange, and we would expect

significant hardening or exchange of a second degenerate into the binary on a time scale short compared to the time scale for the first exchange. For binaries with an initial semi-major axis of the order of an AU , the probability of the exchange leading to a binary recoil velocity large enough to eject the binary from the core is vanishingly small. The ejected light main-sequence star may escape the core, and may even be ejected from the cluster. A degenerate-degenerate binary is not likely to undergo an exchange interaction with a main-sequence star; it may however be hardened by main-sequence field stars, and can undergo collisions with main-sequence field stars. Thus, once the primordial population of main-sequence binaries, with semi-major axis of order an AU , in the core, has been replaced by degenerates, the population of optical binaries is small, and determined by the equilibrium exchange rate for main-sequence field stars, and primordial main-sequence binaries that have recently arrived in the core from the outer parts of the cluster, through dynamical friction. There will still be a population of hard ($a_{in} \ll 1 AU$) main-sequence binaries in the core, and these will continue to interact with the degenerate field stars and binaries. In very dense cluster core ($n_4 \gg 1$), even these will be destroyed, but the process is delayed because a binary with a period of the order of a day will have a large recoil velocity (see Figure 4) after a significant hardening or exchange and will be ejected from the dense core, possibly from the cluster, although in most cases the binary will return to the core through dynamical friction on a time scale comparable to or shorter than the interaction time scale (Phinney and Sigurdsson, 1991).

4.3. Eccentricity

Tables 4a,b,c show mean final eccentricity from each set of encounters. The

mean eccentricity for flybys is renormalised to

$$\langle e_{(n)} \rangle = \left\langle \frac{b}{b_{m_0}} \right\rangle^2 \langle e \rangle, \quad (4.8)$$

where $b_{m_0} = (4/v_\infty + 0.6(1+e))a_{in}$, so that runs with different C can be compared. For flybys $\langle e_{(n)} \rangle$ is approximately constant for a given mass-ratio; the actual value depends on the choice of C , with $\lim_{C \rightarrow \infty} \langle e_{(n)} \rangle = 0$. The distribution in eccentricities is consistent with $\sigma(\delta e \rightarrow 0) \propto 1/\delta e$, and clearly diverges as expected.

For exchanges we do not renormalise the mean eccentricity, as the final eccentricity is only dependent on whether an exchange took place, not on how small the largest periastron was. Comparing runs made with $C = 4$ and $C = 3$ suggests that the sample of exchanges is complete, that we included all of the exchange “peninsulas” (Hut 1983b), see Figure XXX. $\langle e \rangle \simeq 0.67$ for $0.3 < m_i/m_f < 3$, increasing linearly for ejection of smaller masses. For $m_2 \ll m_f$, $\langle e \rangle \approx 1 - 1.3 \frac{m_2}{m_f}$ for exchanges ejecting m_2 . The distribution in e can be fitted in most cases by either

$$P(e) = 2e \quad (4.9)$$

or $P(e) = a_1 e + a_2 e^2$. Imposing

$$\langle e \rangle = \int_0^1 e P(e) de, \quad (4.10)$$

and

$$\left(\frac{dP(e)}{de} \right) \Big|_{e_{max}} = 0, \quad (4.11)$$

we get

$$\begin{aligned} a_1 &= \frac{3\langle e \rangle}{1 - \frac{3}{8e_{max}}} \\ a_2 &= -\frac{1}{e_{max}}. \end{aligned} \quad (4.12)$$

Given the statistical uncertainty in fitting the curves, it is a good approximation to take $e_{max} = \langle e \rangle$ for $\mu_{12} \sim m_f$. For $\mu_{12} \ll m_f$, the minimum eccentricity is non-zero, and

$$a_1 \mapsto \frac{3\langle e \rangle}{1 - \frac{3}{8e_{max}} - e_0^3 \left(1 - \frac{3e_0}{8e_{max}}\right)}, \quad (4.13)$$

where e_0 is the minimum eccentricity. Typically $e_0 \gtrsim 1 - (10 \times \frac{\mu_{12}}{m_f}) > 0$. See Figures 6a,b for examples of eccentricity distribution.

If the initial eccentricity, e_{in} , of the binary was non-zero, the total cross-sections for any non-trivial interaction were larger by a factor of approximately $(1 + e_{in})$. The mean eccentricity after exchange was not sensitive to initial eccentricity, while flybys perturbed the eccentricity away from its initial value, e_{in} , with a similar distribution as for the case $e_{in} = 0$.

4.4. Close Approach

In order to estimate collision rates in the encounters, an analytic approximation to the cross-section for a star, m_i , to approach within some distance r_{ij} , of star m_j , is useful. In the cases of interest, we are often not interested in all close encounters, as a close approach between two degenerates is rarely of interest. A useful approximation was found to be

$$\tilde{\sigma}(\min\{r_{ij}, r_{jk}, \dots\} \geq r_{min}) = \sigma_1 \left(\frac{r_{min}}{a_{in}}\right)^\gamma, \quad (4.14)$$

with γ, σ_1 , fit (piecewise) to the numerical results. Some examples are shown in Figures 7–12. Best linear fit was made to a log–log plot, keeping the coefficients as simple rationals, with the proviso that the error not exceed one (or two at most) standard deviations. Table 3 gives the fits to γ and $\log \sigma_1$. The fits were made for cumulative closest approach between any pair of non-degenerate stars (*i.e.* r_{ij}

was not included if $m_i = 1 = m_j$, except for the set $\{1.0, 1.0, 1.0\}$). Fits to γ are accurate to 0.05 for $r_{min} \gtrsim 10^{-2}$, somewhat less accurate for smaller r_{min} .

We can then write the collision time scale, T_c , as

$$T_c = 1.5 \times 10^{10} g(m_i)^{-1} a_{AU}^{-1+\gamma} n_4^{-1} \left\langle \frac{1}{v_{10}} \right\rangle^{-1} \sigma_1^{-1} r_{min}^{-\gamma} \text{ years.} \quad (4.15)$$

Using equation 3.2, and $R_{cl} = 0.05 \text{ AU}$, we get

$$T_c = \frac{(200)^\gamma 1.5 \times 10^{10}}{\sigma_1 g(m_i) (\beta f_t)^\gamma} \left(\frac{M_*}{M_\odot} \right)^{-\alpha\gamma} n_4^{-1} \left\langle \frac{1}{v_{10}} \right\rangle^{-1} a_{AU}^{-1+\gamma} \text{ years.} \quad (4.16)$$

It is illustrative to consider some simple examples of tidal encounters. We assume $\alpha = 1 = \beta$ in the discussion below. If we have $m_1 = m_2 = m_3$, then if all the stars are $0.7M_\odot$ main-sequence stars,

$$T_c = 1.4 \times 10^{10} \frac{a_{AU}^{-0.6}}{n_4} \left\langle \frac{1}{v_{10}} \right\rangle^{-1} \text{ years.} \quad (4.17)$$

That is, a 0.1 AU binary in a cluster core of density $5 \times 10^4 \text{ pc}^{-3}$, and dispersion 10 km s^{-1} will undergo an interaction leading to a stellar collision in 10^{10} years, on average. If there are 10^3 such binaries in the core, there will be a collision every 10^7 years on average. In the case of a $(0.7, 0.5)M_\odot$ binary interacting with a $1.4M_\odot$ neutron star, the collision time scale is

$$T_c = 3.8 \times 10^{10} \frac{a_{AU}^{-0.33}}{n_4} \left\langle \frac{1}{v_{10}} \right\rangle^{-1} \text{ years.} \quad (4.18)$$

In this case a 0.1 AU binary will have a collision on average every $1.6 \times 10^{10}/f_n$ years, if in a cluster core of density $5 \times 10^4 \text{ pc}^{-3}$, and dispersion 10 km s^{-1} , with neutron stars composing a fraction f_n of the total number of stars. In the case of a neutron star-main sequence binary (with $M_* = 0.55M_\odot$), the time scale is $1.2 \times 10^{10}/f_n$ years, in the same environment. For harder binaries, the unequal mass case collision time scale actually becomes shorter than in the equal mass case,

as the slower dependence on a_{AU} overtakes the larger total cross-section in the equal mass case. For softer binaries, the main-sequence binaries are more likely to collide, but, as we argue above, in cluster cores we expect exchanges to have removed and hardened most moderately soft main-sequence binaries. Very soft binaries will be ionised on a time scale short compared to any collision time scale, except in the outer parts of the cluster, and cores of very low density clusters.

We find that for the mass sequence $\{1, m_2, 1\}$, for $v_\infty \in [0.05, 0.15]$, γ is fit by

$$\gamma = \frac{7}{12} - \frac{1}{6} \log m_2, \quad (4.19)$$

for $m_2 \in [0.0125, 0.4]$, with a somewhat steeper dependence on m_2 for $m_2 > 0.4$.

It is useful to consider the ratio of time scale for exchange, T_e , with the time scale for collision, T_c . Using equations 2.9 and 4.19, we get

$$\frac{T_c}{T_e} = \left(\frac{200}{\beta f_t}\right)^\gamma \left(\frac{M_*}{M_\odot}\right)^{-\alpha\gamma} \frac{\tilde{\sigma}_e}{\sigma_1} a_{AU}^\gamma. \quad (4.20)$$

For $\tilde{\sigma}_e$ defined as above, $\frac{\tilde{\sigma}_e}{\sigma_1} \approx 0.4$, for the mass-ratios considered. With $f_t = 3.1$ and $\alpha = 1 = \beta$, as above, and $M_* = 0.7M_\odot$,

$$\frac{T_c}{T_e} \approx 0.4 \times 10^{2\gamma} a_{AU}^\gamma. \quad (4.21)$$

For, $\gamma \sim 0.5 - 0.7$, we find that $T_c/T_e \geq 1$, for $a_{AU} \sim 0.03 - 0.06$. Thus binary-single star encounters, involving neutron stars or heavy white dwarfs, and medium mass main-sequence stars, for binaries with periods longer than a couple of days, have a larger cross-section for exchange than collision. Typically after an exchange, the final binary is harder than the initial binary, but has a larger physical cross-section than the initial binary, by a factor of approximately m_f/m_e , due both to the larger final semi-major axis and the stronger gravitational focusing. We would therefore expect many collisions to involve hard binaries, with periods

of order a day. For short period binaries, non-perturbative encounters with main sequence stars are more likely to result in a dissipative encounter than a significant hardening or an exchange, even if the other stars involved are degenerate.

5. Conclusion

Neutron stars are expected to be formed in the early stages of globular cluster evolution. No star formation is observed in globular clusters today, and the lifetimes of neutron star progenitors are much shorter than the age of Galactic globular clusters. Assuming that a significant fraction of the primordial neutron stars was retained by the young cluster, the pulsars initially formed would have spun down and become quiescent $\lesssim 10^9$ years after their formation. Further, it is thought that most pulsars are born spinning relatively slowly (Narayan and Ostriker, 1990), and with large ($B \sim 10^{12-13}$ G), magnetic fields. In contrast, the pulsars observed in globular clusters today tend to have short periods and relatively low inferred magnetic fields (Phinney and Kulkarni, 1990). Accretion Induced Collapse (AIC) provides a second possible channel for neutron star formation (Michel, 1987, Bailyn and Grindlay, 1990, Nomoto and Kondo, 1991), which could, in principle, allow rapidly rotating, low field pulsars to be generated in the current epoch. However, most white dwarfs are expected to disrupt rather than collapse when accreting over the Chandrasekhar limit, and there is some question that AIC can produce millisecond pulsars in the numbers required to explain observations (Verbunt *et al.*, 1989).

In order to account for the observed presence of active pulsars in these ancient systems, it is therefore conjectured that quiescent neutron stars can be brought back to life as pulsars through recycling. The neutron star is assumed to accrete matter, gaining angular momentum, and possibly regenerating magnetic field, until the pulsar emission mechanism starts up again and a new pulsar is observed.

Accreting an amount of matter δm , onto a neutron star, mass M_{NS} , can spin it up to a period P , where P is given by

$$P = 0.2 \left(\frac{M_{NS}}{\delta m} \right)^{3/4} I_{45}^{3/4} \text{ ms}, \quad (5.1)$$

where I_{45} is the moment of inertia of the neutron star in 10^{45} g cm^2 . The spin-up is not sensitive to the exact accretion mechanism (Phinney and Kulkarni, 1990), assuming Eddington limited accretion, and the absence of efficient ‘‘propeller mechanisms.’’

$$\delta m = \int_{t_i}^{t_f} \dot{m}(t') dt', \quad (5.2)$$

where $\dot{m}(t)$ is the accretion rate. A characteristic timescale is defined by $T_{acc} = \delta m / \dot{m}$, and the total number of pulsars produced from Low Mass X-ray Binaries (LMXBs) can be estimated to be

$$N_{pulsars} = N_{LMXBs} \frac{\tau_{pulsar}}{T_{acc}}, \quad (5.3)$$

where τ_{pulsar} is the characteristic pulsar lifetime. A neutron star accreting mass at a rate \dot{m} radiates at $L = \epsilon \dot{m} c^2$, where $\epsilon \sim 0.1$. Accreting neutron stars are thought to be efficient X-ray emitters, and, as such, are relatively easily detectable, even at relatively low accretion rates. X-ray sources have been detected in globular clusters (Hertz and Grindlay, 1983, Grindlay *et al.*, 1984, Hertz and Wood, 1985, Friedhorsky and Holt, 1987), and there is a relatively large population of LMXBs in Galactic globular clusters, but if estimates of LMXB lifetimes are accurate, then the number of cluster LMXBs is about two orders of magnitude too small to account for the pulsar population observed (Kulkarni *et al.*, 1990a, Hut *et al.*, 1991, Kulkarni and Narayan, 1988, Wijers and van Paradijs, 1991). LMXBs are thought to form when a neutron star companion star overflows its Roche lobe and accretion commences; alternatively some LMXBs in clusters may be formed by

tidal capture of a main-sequence star or giant by a neutron star. LMXBs have relatively modest accretion rates, $\dot{m} \lesssim 10^{-8} M_{\odot} \text{ y}^{-1}$ and have large estimated accretion times. It is possible that rapid accretion takes place after tidal capture or neutron star main-sequence collisions. Calculations indicate that tidal capture by single neutron stars can account for the existence of only a few pulsars, and that most of those should be in the core of high density clusters (Romani *et al.*, 1987, Verbunt *et al.*, 1987). As more pulsars in globular clusters are discovered, it has become clear that another channel for pulsar recycling must exist (Phinney and Kulkarni, 1990, Fruchter and Goss, 1990, Kulkarni *et al.*, 1990a,b, Johnston *et al.*, 1991a,b).

The possibility of binary interactions in globular clusters has long been appreciated, and suggested as a path for creating both blue stragglers (Leonard, 1989, Leonard and Fahlman, 1991) and pulsars (Phinney and Kulkarni, 1990). Evidently, with a significant number of binaries present, binary-binary interactions must be considered. Unfortunately, the number of free parameters in binary-binary interactions is much larger than in binary-single star interaction, and a complete simulation of binary-binary interactions would require excessive computing time. Simulations carried out so far (Mikkola, 1983, 1984a,b) would indicate that this is not a severe problem; that binary-binary interactions are rapidly resolved into a hierarchical system with one or two stars acting as distant observers, and the interaction proceeding as a perturbed resonant three-body encounter. Binary-binary interactions should contribute a qualitatively similar distribution in final states as resonant three-body interactions, with a cross-section approximately a factor of ten larger, due to the larger geometric cross-section and somewhat enhanced gravitational focusing.

A primary requirement of any attempt to account for the recycled pulsars observed is to estimate the total number of recyclars that might be formed in globular clusters; the expected number as a function of cluster density, mass and evolutionary history; the proportion of binary pulsars and the spatial distribution of the cluster pulsars.

Most stellar encounters cause only a minor perturbation in the eccentricity and semi-major axis of a binary. As the impact parameter is reduced the effect of the encounter becomes larger, until qualitative changes can take place in the orbital parameters of the binary. If $v_\infty > v_c$ the binary may be ionised, leading to three free stars receding separately to infinity. We will mostly be concerned with encounters for which $v_\infty \ll v_c$. A large fraction of such encounters is resonant, but, ultimately, all resonances are resolved. In the point mass approximation, the result may either be a system in which the original field star recedes to infinity with the original binary still intact, but with orbital parameters that may be very different from their original values (resonant flybys); or an exchange may have taken place, in which case one of the original binary members was ejected and the field star substituted (resonant exchanges). Non-resonant encounters may also lead to exchanges (prompt exchanges); if not, they are referred to as flybys and typically lead to minor perturbation of the binary orbital parameters. Encounters involving a close approach between non-point stars can be dissipative or collisional. We consider some possible consequences of such tidal encounters later.

If the encounter is dissipative, the field star orbit will have a still smaller semi-major axis, and a subsequent close encounter is again inevitable, unless the dissipation was large enough that the field star is captured into an orbit with semi-major axis much less than that of the initial binary, in which case a

stable hierarchical triple may be formed. In a large percentage of such strongly dissipative encounters, the stars are likely to physically collide, and merge or disrupt. The mass-loss may then leave a disk or reduced remnant in a short period orbit, with the third star now in a somewhat wider orbit about the collided stars. Just such a mechanism may be responsible for some of the recycled cluster pulsars (Finzi, 1978, Krolik *et al.*, 1984, Phinney and Kulkarni, 1990), as a neutron star that has collided with and disrupted a main-sequence star may accrete substantial mass before the rest of the debris is unbound by the energy released by the mass accreted. It is possible that that such a rapidly accreting system will emit mainly very soft X-rays (Patterson and Raymond, 1985a,b), in contrast with normal LMXBs.

Cleary and Monaghan (1989) have simulated a small number of close tidal encounters using SPH. They conclude that point-mass exchange encounters can become resonant when tidal effects are allowed for, and that most, or all, resonances lead to collision. If there is substantial mass-loss, the properties of the orbit of the final system may be affected by any asymmetry in the mass-loss. In particular, a forward jet of matter, carrying angular momentum out of the system, can leave the merged remnant and third star in a tighter orbit than would otherwise be expected. The problem of a (magnetised) degenerate colliding with main-sequence stars is beyond current hydrodynamical codes, and models of unequal mass stellar collisions calculated so far have not shown any evidence for large asymmetric mass-loss (Benz *et al.*, 1987, 1989, 1990, Ruffert and Müller, 1990). In contrast, a binary-binary encounter can lead to the formation of stable hierarchical triples, and simulations indicate a relatively large cross-section for this process (Mikkola, 1983, 1984a,b).

It has been suggested that a large fraction of binaries in globular clusters may have become pseudo-stable hierarchical triples as a consequence of tidal dissipation (Bailyn, 1989, Bailyn and Grindlay, 1987, Bailyn, 1987). The mechanism proposed by Bailyn involves the field star approaching a hard binary on a retrograde orbit. With the total angular momentum small, it is possible for the field star to be captured with simultaneous hardening of the binary, the energy released being dissipated in the stellar tides. If the binary is sufficiently hardened, the resulting triple may be stable. Bailyn does not follow the evolution of the tidal capture triples, and it is not clear what fraction is stable and what fraction is pseudo-stable and will spontaneously decay. The subset of phase space that would leave a dynamically stable triple, without a stellar collision taking place, is small, and we believe that this process will not contribute significantly to the hierarchical triple population; rather any stable triples formed are likely to be the result of a binary-binary interaction.

The simulations carried out have shown the importance of resonant hard binary interactions in high density stellar environments, such as may be found in the cores of globular clusters. The simulations carried out so far have given a fair statistical sampling of possible processes. It is desirable to carry out simulations for a larger range of eccentricities, and somewhat harder binaries (down to say, $v_\infty/v_c \sim 10^{-3}$). It would be worthwhile to increase the sample size by an order of magnitude, to get better statistics on low probability interactions, but a much larger sample is physically unrealistic; the dynamical systems being modeled have themselves not interacted that often, and will show "statistical fluctuations" in their properties comparable to those already obtained in numerical modeling. As a matter of some urgency, it would be useful to get a comparably complete sample of hard binary-binary interactions. This is certainly possible with existing computer technology, although it may not be economical for another few years (Hut,

1990). A major limitation is the amount of data storage necessary to store binary orbital parameters and computational variables. As stable hierarchical trinarities may be produced through binary–binary interactions, the interaction between such trinarities and single stars should also be simulated. Of particular interest is the possibility that the larger semi–major axis may determine a cross–section for resonances with energy transfers characteristic of the scale of the inner binary. If a significant fraction of cluster stars is in such hierarchical trinarities, the collision cross–section may be dominated by these systems.

We find that runs with non–equal masses, with mass–ratios of order two, show significant and interesting differences in behaviour from the equal mass case previously extensively considered. In particular, exchanges of heavy field stars into moderately hard binaries are likely to be a dominant process in cluster cores. The interactions may account for many of the properties and distribution of observed cluster pulsars, and we will consider the various scenarios in a later chapter.

The physical expansion of binary orbits when a heavy star is exchanged in place of a lighter one allows the physical cross–section for subsequent interaction to *increase* even as the binary is hardened. As core–collapse is approached, this process becomes more efficient and collapse may be prevented until physical collisions come to dominate, at which point rapid core–collapse may occur. Clusters in this “binary burning” stage would be expected to have density profiles and core dispersions deviating from a simple multi–mass King profile. The binary burning stage can be prolonged with the recoil ejection of binaries after exchange or hardening, temporarily removing the binary from the core before it is brought back into the core by dynamical friction. A binary that is softened will on average recoil with less energy and angular momentum in the cluster frame, and will subsequently be on an orbit that takes it deeper into the cluster core; as it will

also have a larger semi-major axis, and hence cross-section, it will likely be either ionised very rapidly or exchanged and hardened on a time scale comparable to or shorter than the original interaction time scale. Both processes conspire to remove moderately hard main-sequence and giant binaries from the cores of clusters.

On the whole, where there is overlap, our conclusions are generally consistent with previous work done in the field, except we find that the fractional energy transfer during exchanges is roughly independent of the mass-ratio of exchanged stars, in contradiction of the results obtained by Hills and Hills and Fullerton. We believe this discrepancy is due to the special initial conditions used by Hills and Fullerton. Exchanging a heavy star for a light star in a hard binary hardens the binary while increasing the cross-section for further interactions. For the equal mass case our results are consistent with those obtained by Hut and Bahcall and Hut and Inagaki, to within statistical error.

A realistic hydrodynamic model of stellar tidal encounters and collisions, which could be turned on at close approach would be of great interest, and would remove considerable uncertainty in the outcome of such interactions, currently modeled impulsively. Of particular interest would be an accurate model of a (magnetised) degenerate colliding with a main-sequence star. Currently a number of efforts are under way to simulate realistic stellar collisions (Goodman and Hernquist, 1991, Rasio and Shapiro, 1991, Ruffert and Müller, 1990, Davies *et al.*, 1991), but a systematic search of phase space is beyond current capabilities. Dissipative encounters will reduce the cross-section for moderate recoils which may provide the heating necessary to reverse core collapse (Goodman and Hut, 1989). The substitution of degenerates into primordial main-sequence binaries increases the heating rate. We also note that subtracting colliding systems from unequal-

mass exchanges does not, in general, disproportionately reduce the cross-section for significant recoil (Phinney and Sigurdsson, 1991).

There seems little doubt that binaries play a critical role in the dynamical evolution of globular clusters, and may be able to account for the current plethora of millisecond pulsars observed in the Galactic globular clusters.

References

- Alpar, M.A., Cheng, A.F., Ruderman, M.A. and Shaham, J., 1982, *Nature*, **300**, 728.
- Aurière, M., Ortolani, S. and Lauzeral, C., 1990, *Nature*, **344**, 638.
- Backer, D.C., Kulkarni, S.R., Heiles, C., Davis, M.M. and Goss, W.M., 1982, *Nature*, **300**, 615.
- Bailyn, C.D. and Grindlay, J.E., 1987, *Ap. J.*, **312**, 748.
- Bailyn, C.D. and Grindlay, J.E., 1990, *Ap. J.*, **353**, 159.
- Bailyn, C.D., 1987, *Ap. J.*, **317**, 737.
- Bailyn, C.D., 1988, *Nature*, **332**, 330.
- Bailyn, C.D., 1989, *Ap. J.*, **341**, 175.
- Bailyn, C.D., 1990, in *Proc. of A.S.P. Conference on Formation and Evolution of Star Clusters*, ed. K. Janes (P.A.S.P. Conference Series).
- Benz, W. and Hills, J.G., 1987, *Ap. J.*, **323**, 614.
- Benz, W., Hills, J.G. and Thielemann, F.-K., 1989, *Ap. J.*, **342**, 986.
- Benz, W., Bowers, R.L., Cameron, A.G.W. and Press, W.H., 1990, *Ap. J.*, **348**, 647.
- Chernoff, D.F. and Weinberg, M.D., 1990, *Ap. J.*, **351**, 121.
- Cleary, P.W. and Monaghan, J.J., 1990, *Ap. J.*, **349**, 150.
- Cohn, H. and Hut, P., 1984, *Ap. J. (Letters)*, **277**, L45.
- Davies, M.B., Benz, W. and Hills, J.G., *Ap. J.*, 1991, submitted.
- Djorgovski, S., Piotto, G. and King, I.R., 1988, in *Dynamics of Dense Stellar Systems*, ed. D. Merritt (Cambridge University Press) p. 147.

- Djorgovski, S., Piotto, G., Phinney, E.S. and Chernoff, D., *Ap. J. (Letters)*, 1991, submitted.
- Fabian, A.C., Pringle, J.E. and Rees, M.J., 1975, *M.N.R.A.S.*, **172**, 15P.
- Finzi, A., 1978, *Astr. Ap.*, **62**, 149.
- Fruchter, A.S. and Goss, W.M. 1990, *Ap. J. (Letters)*, **365**, L63.
- Fullerton, L.W. and Hills, J.G., 1982, *A.J.*, **87**, 175.
- Goodman, J. and Hut, P., 1989, *Nature*, **339**, 40.
- Goodman, J. and Hernquist, L., *Ap. J.*, 1991, in the press.
- Grindlay, J.E., Hertz, P, Steiner, J.E., Murray, S.S. and Lightman, A.P., 1984, *Ap. J. (Letters)*, **282**, L13.
- Gunn, J.E. and Griffin, R.F., 1979, *A.J.*, **84**, 752.
- Hamilton, T.T., Helfand, D.J. and Becker, R.H., 1985, *A.J.*, **90**, 606.
- Heggie, D.C., 1975, *M.N.R.A.S.*, **173**, 729.
- Hertz, P. and Grindlay, J.E., 1983, *Ap. J.*, **275**, 105.
- Hertz, P. and Wood, K.S., 1985, *Ap. J.*, **290**, 171.
- Hills, J.G., 1975a, *A.J.*, **80**, 809.
- Hills, J.G., 1975b, *A.J.*, **80**, 1075.
- Hills, J.G. and Fullerton, L.W., 1980, *A.J.*, **85**, 1281.
- Hut, P. and Bahcall, J.N., 1983, *Ap. J.*, **268**, 319.
- Hut, P., 1983a, *Ap. J.*, **268**, 342.
- Hut, P., 1983b, *A.J.*, **88**, 1549.
- Hut, P., 1983c, *Ap. J. (Letters)*, **272**, L29.
- Hut, P. and Paczyński, B., 1984, *Ap. J.*, **284**, 675.

- Hut, P. and Inagaki, S., 1985, *Ap. J.*, **298**, 502.
- Hut, P., 1990, in *Proceedings of the workshop on Self-Gravitating Systems in Astrophysics and Nonequilibrium Processes in Physics*, (Kyoto, June 1989).
- Hut, P., Murphy, B.W. and Verbunt, F., *Astr. Ap.*, 1991, in the press.
- Johnston, H.M., Kulkarni, S.R. and Goss, W.M., 1991a, in preparation.
- Johnston, H.M., Kulkarni, S.R. and Phinney, E.S., 1991b, in preparation.
- Krolik, J.H., Meiksin, A. and Joss, P.C., 1984, *Ap. J.*, **282**, 466.
- Kulkarni, S.R. and Narayan, R., 1988, *Ap. J.*, **335**, 755.
- Kulkarni, S.R., Narayan, R. and Romani, R.W., 1990a, *Ap. J.*, **356**, 174.
- Kulkarni, S.R., Goss, W.M., Wolszczan, A. and Middleditch, J., 1990b, *Ap. J. (Letters)*, **363**, L5.
- Kulkarni, S.R., Anderson, S.B., Prince, T.A. and Wolszczan, A., 1991, *Nature*, **349**, 47.
- Lee, H.M. and Ostriker, J.P., 1986, *Ap. J.*, **310**, 176.
- Leonard, P.J.T., 1989, *A.J.*, **98**, 217.
- Leonard, P.J.T. and Fahlman, G.G., 1991, *A.J.*, **102**, 994.
- Lyne, A.G., Brinklow, A., Middleditch, J., Kulkarni, S.R., Backer, D.C. and Clifton, T.R., 1987, *Nature*, **328**, 399.
- Lyne, A.G., Manchester, R.N., D'Amico, N., Staveley-Smith, L., Johnston, S., Lim, J., Fruchter, A.S., Goss, W.M. and Frail, D., 1990, *Nature*, **347**, 650.
- Lyne, A.G., 1991, talk presented at the NATO Workshop on "X-ray binaries and the formation of binary and millisecond pulsars", Santa Barbara, 21-25 Jan 1991.

- Mateo, M., Harris, H.C., Nemec, J. and Olszewski, E.W, 1990, *A.J.*, **100**, 469.
- McMillan, S.L.W., 1986, *Ap. J.*, **306**, 552.
- McMillan, S.L.W., McDermott, P.N. and Taam, R.E., 1987, *Ap. J.*, **318**, 261.
- McMillan, S.L.W., Taam, R.E. and McDermott, P.N., 1990a, *Ap. J.*, **354**, 190.
- McMillan, S.L.W., Hut, P. and Makino, J., 1990b, *Ap. J.*, **362**, 522.
- Meylan, G., 1989, *Astr. Ap.*, **214**, 106.
- Michel, F.C., 1987, *Nature*, **329**, 310.
- Mikkola, S., 1983, *M.N.R.A.S.*, **203**, 1107.
- Mikkola, S., 1984a, *M.N.R.A.S.*, **207**, 115.
- Mikkola, S., 1984b, *M.N.R.A.S.*, **208**, 75.
- Murphy, B.W., Cohn, H.N. and Hut, P., 1990, *M.N.R.A.S.*, **245**, 335.
- Narayan, R. and Ostriker, J.P., 1990, *Ap. J.*, **352**, 222.
- Nomoto, K. and Kondo, Y., 1991, *Ap. J.*, **367**, L19.
- Patterson, J. and Raymond, J.C., 1985, *Ap. J.*, **292**, 535.
- Patterson, J. and Raymond, J.C., 1985, *Ap. J.*, **292**, 550.
- Phinney, E.S., *M.N.R.A.S.*, 1990, in the press.
- Phinney, E.S. and Kulkarni, S.R., *Nature*, 1991, in the press.
- Phinney, E.S. and Sigurdsson, S., 1991, *Nature*, **349**, 220.
- Piotto, G., King, I.R. and Djorgovski, S., 1988, *A.J.*, **96**, 1918.
- Press, W.H. and Teukolsky, S.A., 1977, *Ap. J.*, **213**, 183.
- Priedhorsky, W.C. and Holt, S.S., 1987, *Space Science Reviews*, **45**, 291.

- Pryor, C., Latham, D.W. and Hazen-Liller, M.L., 1985, *Dynamics of Star Clusters*, IAU Symposium No. 113, ed. J. Goodman and P. Hut (Reidel, Dordrecht), p. 99.
- Pryor, C., McClure, R.D., Hesser, J.E. and Fletcher, J.M., 1989, in *Dynamics of Dense Stellar Systems*, ed. D. Merritt (Cambridge University Press) p. 175.
- Pryor, C., Schommer, R.A. and Olszewski, E.W., 1990, *Steward Observatory, University of Arizona preprint*.
- Rappaport, S., Putney, A. and Verbunt, F., 1990, *Ap. J.*, **345**, 210.
- Rasio, F.A. and Shapiro, S.L., 1991377559
- Romani, R.W., Kulkarni, S.R. and Blandford, R.D., 1987, *Nature*, **329**, 309.
- Romani, R.W. and Weinberg, M.D., 1991, 372, 487 *preprint*.
- Ruffert, M. and Müller, E., 1990, *Astr. Ap.*, **238**, 116.
- Shawl, S.J. and White, R.E., 1986, *A.J.*, **91**, 312.
- Siegel, C.L. and Moser, J.K., 1971, *Lectures on Celestial Mechanics*, (Springer, Berlin, Heiedlberg, New York).
- Sigurdsson, S. and Phinney, E.S., 1991, in preparation.
- Spitzer, L., 1987, *Dynamical Evolution of Globular Clusters*, (Princeton University Press).
- Verbunt, F., van den Heuvel, E.P.J., van Paradijs, J. and Rappaport, S., 1987, *Nature*, **329**, 312.
- Verbunt, F., Lewin, W.H.G. and van Paradijs, J., 1989, *M.N.R.A.S.*, **241**, 51.
- Wijers, R.A.M.J. and van Paradijs, J., 1991, *Astr. Ap.*, **241**, L37.
- Wolszczan, A., 1991, *Nature*, **350**, 688.

Captions

Figure 1a

Mean fractional energy transfer, Δ , weighted by the dimensionless cross-section $\bar{\sigma} = (v_\infty/v_c)^2 \sigma / \pi a_{in}^2$, as function of v_∞/v_c , for three different mass-ratios. We define $v_{\infty crit}$ to be v_∞ where the mean energy transfer is zero. The lines are included to help guide the eye.

Figure 1b

Same as Figure 1a, for flybys only. Note that mean energy transfer becomes negative again for $v_\infty > v_c$ for one of the mass-ratios. This is because ionising interactions are excluded and dominate the positive energy interactions at higher velocities.

Figure 1c

Same as Figure a, but for exchange $X : (1, 2) + (3) \rightarrow (1) + (2, 3)$ only.

Figure 1d

Same as Figure a, but for exchange $X : (1, 2) + (3) \rightarrow (1, 3) + (2)$ only. The cross-section for ejecting star 2 is larger than for ejecting star 1, as $m_2 < m_1$.

Figure 2a

Distribution of final semi-major axis, a_{fin} , for all interactions at $v_\infty/v_c \in [0.05, 0.15]$ for set of runs with mass-ratio $\{1.0, 0.4, 1.0\}$. Note that for ejection of the heavier member of the binary, the distribution in semi-major axis peaks at $a_{fin} < a_{in}$, whereas for the ejection of the lighter member of the binary, the distribution peaks for $a_{fin} \lesssim 2.5 \times a_{in}$.

Figure 2b

Distribution in binary recoil velocity, v_{rec} , after interaction, for all interactions at $v_\infty/v_c \in [0.05, 0.15]$ for set of runs with mass-ratio $\{1.0, 0.4, 1.0\}$. Note that a uniform distribution in initial velocities is being mapped into the final distribution, so the distribution is a non-trivial map from the distribution in a_{fin} .

Figure 3

Same as Figure 2a, but for $v_\infty/v_c \in [0.45, 0.55]$, and mass-ratio $\{0.5, 0.35, 1.0\}$. Note that at higher velocity, the distribution of a_{fin} is broader than for lower v_∞ .

Figure 4

The recoil velocity of a binary after exchange leading to the ejection of the lighter member of the initial binary. The initial relative velocity at infinity was taken to be $0.1 v_c$, which was, for initial period $P_{in} = 24$ hours, equal to 26 km s^{-1} for mass-ratio $\{1.0, 1.0, 1.0\}$, 15 km s^{-1} for mass-ratio $\{0.5, 0.35, 1.0\}$, 22 km s^{-1} for mass-ratio $\{1.0, 0.35, 0.5\}$ and 19 km s^{-1} for the mass-ratio $\{1.0, 0.4, 1.0\}$. The recoil velocity tends to a finite value as $P_{in} \rightarrow \infty$, and for $P_{in} \gtrsim P_{fin}$ is not sensitive to the exact initial period. The cross-section for exchange peaks rather sharply for $P_{in} \gtrsim P_{fin}$, and is exponentially small for $P_{in} \gg P_{fin}$.

Figure 5a

An example of a “hooking” exchange. Here, a massive field star, $m_f = 1$ encounters a binary with stars of mass $\{1.0, 0.1\}$, with $v_\infty/v_c = 0.08$. The light star is ejected, and the two heavy stars form an eccentric binary with $a_{fin} \approx 9a_{in}$. The closest approach between the light star and the field star was approximately $1.5a_{in}$.

Figure 5b

An example of “gravitational Fermi acceleration.” Here, a massive field star, $m_f = 1$ encounters a binary with stars of mass $\{1.0, 0.1\}$, with $v_\infty/v_c = 0.07$.

The light star is ejected, and the two heavy stars form an eccentric binary with $a_{fin} \approx 9a_{in}$. The closest approach between the light star and the field star was approximately $0.12a_{in}$.

Figure 6a

Distribution of final eccentricity, e_{fin} , for all interactions, in set of runs with mass-ratio $\{1.0, 0.4, 1.0\}$, and $v_{\infty}/v_c \in [0.05, 0.15]$.

Figure 6b

Same as Figure 6a, but for $v_{\infty}/v_c \in [0.45, 0.55]$, and mass-ratio $\{0.5, 0.35, 1.0\}$. The run shown was for $C = 3$, the fraction of runs inducing $e_{fin} < 0.05$ during flyby is small, and the cross-section for that bin has not converged. For $C = 4$, the cross-section for final eccentricity induced by flybys maintained the $1/e_{fin}$ profile into the $e_{fin} < 0.05$ bin.

Figure 7

Cumulative cross-section for close approach for mass-ratio $\{1.0, 1.0, 1.0\}$ for $v_{\infty}/v_c \in [0.05, 0.15]$. Compare with Figure 1a in Hut and Inagaki. The two graphs agree everywhere to within a standard deviation. A fit to the curve, made independently of the results of Hut and Inagaki, agrees exactly with their fit.

Figure 8

Cumulative cross-section for close approach for mass-ratio $\{1.0, 0.4, 1.0\}$ for $v_{\infty}/v_c \in [0.05, 0.15]$. The upper curve shows the cumulative cross-section for close approach between any pair of stars, the lower curve restricts the cross-section to close approach between a pair where one of the stars has $m_i \neq 1.0$, and is therefore by assumption not degenerate. In Table 3, fits are given to the lower curve only. The upper curve is included here for comparison.

Figure 9

Cumulative cross-section for close approach for mass-ratio $\{1.0, 0.4, 1.0\}$ for $v_\infty/v_c \in [0.35, 0.65]$.

Figure 10

Cumulative cross-section for close approach for mass-ratio $\{0.5, 0.35, 1.0\}$ for $v_\infty/v_c \in [0.05, 0.15]$.

Figure 11

Cumulative cross-section for close approach for mass-ratio $\{1.0, 0.35, 0.5\}$ for $v_\infty/v_c \in [0.05, 0.15]$.

Figure 12

Cumulative cross-section for close approach for mass-ratio $\{1.0, 0.1, 1.0\}$ for $v_\infty/v_c \in [0.05, 0.15]$.

Figure 13

Final semi-major axis as a function of recoil velocity for low velocity flybys. The solid curve shows the theoretical range in allowed a_{fin}/a_{in} for the range of v_∞/v_c used. All the points fall between the curves, and the distribution in recoil velocities is reasonable.

Figure 14

Scatter plot of flybys and exchanges as a function of J_z and J_\perp .

Tables

Table 1.

Possible interpretations of runs for different mass scales

Run		Interpretation								
Dimensionless masses		Mass unit								
binary	field star	1.4M _⊙			1.1M _⊙			0.7M _⊙		
(0.5,0.35,1.0)		0.7M _⊙	0.49M _⊙	1.4M _⊙	0.55M _⊙	0.39M _⊙	1.1M _⊙	0.35M _⊙	0.25M _⊙	0.7M _⊙
		G/T	MS/WD	NS	MS/WD	MS	HWD	MS	MS	G/T
(1.0,0.35,0.5)		1.4M _⊙	0.49M _⊙	0.7M _⊙	1.1M _⊙	0.39M _⊙	0.55M _⊙	0.7M _⊙	0.25M _⊙	0.35M _⊙
		NS	MS/WD	G/T	HWD	MS	MS/WD	G/T	MS	MS
(1.0,0.4,1.0)		1.4M _⊙	0.56M _⊙	1.4M _⊙	1.1M _⊙	0.44M _⊙	1.1M _⊙	0.7M _⊙	0.28M _⊙	0.7M _⊙
		NS	MS/WD	NS	HWD	MS	HWD	G/T	MS	G/T
(1.0,1.0,0.4)		1.4M _⊙	1.4M _⊙	0.56M _⊙	1.1M _⊙	1.1M _⊙	0.44M _⊙	0.7M _⊙	0.7M _⊙	0.28M _⊙
		NS	NS	MS/WD	HWD	HWD	MS	G/T	G/T	MS
(1.0,1.0,1.0)		1.4M _⊙	1.4M _⊙	1.4M _⊙	N/A			0.7M _⊙	0.7M _⊙	0.7M _⊙
		NS	NS	NS	N/A			G/T/MS		

Table 2.

 $g(m_i)$ and $v_c(m_i)$

Dimensionless masses		$g(m_i)$	v_c	$v_c \sqrt{\frac{1}{a_{AU}}} \sqrt{\frac{M_*}{M_{NS}}} \text{ km s}^{-1}$
binary	field star			
(1.0,1.0,1.0)		1.50	1.22	44
(0.5,0.35,1.0)		0.38	0.62	22
(1.0,0.35,0.5)		0.96	0.98	35
(1.0,0.8,1.0)		1.24	1.16	42
(1.0,0.4,1.0)		0.69	0.83	30
(1.0,0.2,1.0)		0.37	0.61	22
(1.0,0.1,1.0)		0.19	0.44	16
(1.0,0.05,1.0)		0.10	0.31	11
(1.0,0.025,1.0)		0.05	0.22	7.9
(1.0,0.0125,1.0)		0.025	0.16	5.7
(1.0,0.001,1.0)		0.002	0.04	1.4
(1.0,1.0,0.4)		3.00	1.73	62

Table 3.

Fits to $\bar{\sigma}$

Dimensionless masses		r_{ij}	$\frac{v_{\infty}}{v_c}$	$\log \sigma_1$	γ	r_{min}
binary	field star					
(1.0,1.0,1.0)	12,23,31	[0.0625, 0.125]	0.95	0.4	$r_{min} > 10^{-2} a_{in}$	
			1.67	0.75	$r_{min} < 10^{-2} a_{in}$	
			[0.125, 0.25]	0.9	0.4	$r_{min} > 10^{-2} a_{in}$
				1.33	0.67	$r_{min} < 10^{-2} a_{in}$
			[0.25, 0.5]	0.9	0.4	$r_{min} > 10^{-2} a_{in}$
				1.33	0.67	$r_{min} < 10^{-2} a_{in}$
			[0.5, 1.0]	0.85	0.6	$r_{min} > 3 \times 10^{-3} a_{in}$
				1.67	0.95	$r_{min} < 3 \times 10^{-3} a_{in}$
(0.5,0.35,1.0)	23,31	[0.05, 0.15]	1.33	0.67	all r_{min}	
			[0.15, 0.35]	1.33	0.67	all r_{min}
			[0.35, 0.75]	1.33	0.75	$0.3 a_{in} > r_{min} > 3 \times 10^{-3} a_{in}$
			[0.75, 1.15]	1.33	1.0	all r_{min}
(1.0,0.35,0.5)	12,31	[0.05, 0.15]	0.9	0.5	$r_{min} > 10^{-2} a_{in}$	
			1.33	0.75	$r_{min} < 10^{-2} a_{in}$	
			[0.15, 0.35]	0.85	0.5	$r_{min} > 10^{-2} a_{in}$
				1.33	0.75	$r_{min} < 10^{-2} a_{in}$
			[0.35, 0.65]	0.85	0.67	all r_{min}
			[0.65, 1.05]	0.85	0.85	all r_{min}
(1.0,0.8,1.0)	12,23	[0.05, 0.15]	1.0	0.5	$r_{min} > 10^{-2} a_{in}$	
			1.5	0.8	$r_{min} < 10^{-2} a_{in}$	
(1.0,0.4,1.0)	12,23	[0.05, 0.15]	1.25	0.65	$r_{min} > 10^{-2} a_{in}$	
			1.75	0.95	$r_{min} < 10^{-2} a_{in}$	
			[0.15, 0.35]	1.25	0.75	$r_{min} > 10^{-2} a_{in}$
				1.67	1.0	$r_{min} < 10^{-2} a_{in}$
			[0.35, 0.65]	1.2	0.8	all r_{min}
			[0.65, 1.05]	1.2	1.0	all r_{min}
(1.0,0.2,1.0)	12,23	[0.05, 0.15]	1.45	0.7	$r_{min} > 5 \times 10^{-2} a_{in}$	
			1.65	0.9	$r_{min} < 5 \times 10^{-2} a_{in}$	
(1.0,0.1,1.0)	12,23	[0.05, 0.15]	1.67	0.75	all r_{min}	
(1.0,0.05,1.0)	12,23	[0.05, 0.15]	2.0	0.80	all r_{min}	
(1.0,0.025,1.0)	12,23	[0.05, 0.15]	2.3	0.85	all r_{min}	
(1.0,0.0125,1.0)	12,23	[0.05, 0.15]	2.6	0.90	$r_{min} > 10^{-2} a_{in}$	
(1.0,0.001,1.0)	12,23	[1.0, 1.5]	3.75	1.0	all r_{min}	
(1.0,1.0,0.4)	23,31	[0.05, 0.15]	0.3	0.4	$r_{min} > 10^{-2} a_{in}$	
			0.75	0.67	$r_{min} < 10^{-2} a_{in}$	

Table 4a.

Exchange cross-sections and means †

masses	$\frac{v_{max}}{v_c}$	X	$\bar{\sigma}'_X$	$\langle \frac{v_{max}}{v_c} \rangle$	$\langle e_{(n)} \rangle$	$\langle \frac{\Delta E}{E} \rangle$
(1.0,0.8,1.0)	[0.05, 0.15]	(1, 2) + (3) → (1, 2) + (3)	10.5	0.10	0.31	-0.13
		(1, 2) + (3) → (1) + (2, 3)	1.9	0.18	0.65	-0.31
		(1, 2) + (3) → (1, 3) + (2)	3.5	0.15	0.66	-0.35
(1.0,0.4,1.0)	[0.05, 0.15]	(1, 2) + (3) → (1, 2) + (3)	10.5	0.27	0.11	-0.12
		(1, 2) + (3) → (1) + (2, 3)	0.8	0.22	0.62	-0.35
		(1, 2) + (3) → (1, 3) + (2)	4.8	0.13	0.66	-0.45
(1.0,0.2,1.0)	[0.05, 0.15]	(1, 2) + (3) → (1, 2) + (3)	5.2	0.20	0.26	-0.27
		(1, 2) + (3) → (1) + (2, 3)	0.6	0.24	0.68	-0.35
		(1, 2) + (3) → (1, 3) + (2)	5.5	0.11	0.76	-0.68
(1.0,0.1,1.0)	[0.05, 0.15]	(1, 2) + (3) → (1, 2) + (3)	5.4	0.20	0.25	-0.24
		(1, 2) + (3) → (1) + (2, 3)	0.5	0.28	0.73	-0.41
		(1, 2) + (3) → (1, 3) + (2)	5.3	0.08	0.87	-0.70
(1.0,0.05,1.0)	[0.05, 0.15]	(1, 2) + (3) → (1, 2) + (3)	5.5	0.21	0.26	-0.25
		(1, 2) + (3) → (1) + (2, 3)	0.5	0.29	0.72	-0.42
		(1, 2) + (3) → (1, 3) + (2)	5.0	0.05	0.93	-0.75
(1.0,0.025,1.0)	[0.05, 0.15]	(1, 2) + (3) → (1, 2) + (3)	4.4	0.23	0.26	-0.29
		(1, 2) + (3) → (1) + (2, 3)	0.5	0.30	0.70	-0.42
		(1, 2) + (3) → (1, 3) + (2)	5.0	0.04	0.97	-0.77
(1.0,0.0125,1.0)	[0.05, 0.15]	(1, 2) + (3) → (1, 2) + (3)	4.4	0.22	0.26	-0.26
		(1, 2) + (3) → (1) + (2, 3)	0.5	0.28	0.63	-0.40
		(1, 2) + (3) → (1, 3) + (2)	4.2	0.03	0.98	-0.69
(1.0,0.001,1.0)	[1.0, 1.5]	(1, 2) + (3) → (1, 2) + (3)	6.0	0.58	0.29	0.11
		(1, 2) + (3) → (1) + (2, 3)	0.4	0.51	0.77	0.36
		(1, 2) + (3) → (1, 3) + (2)	1.5	0.01	0.99	-0.09
(1.0,1.0,0.4)	[0.05, 0.15]	(1, 2) + (3) → (1, 2) + (3)	16.2	0.04	0.25	-0.09
		(1, 2) + (3) → (1) + (2, 3)	0.18	0.13	0.73	-0.20
		(1, 2) + (3) → (1, 3) + (2)	0.18	0.13	0.73	-0.22

† NOTE: The cross-section for flybys ((1, 2) + (3) → (1, 2) + (3)) is provided for reference only. The total cross-section for flybys depends on the b_{max} used, and is included here to provide the total cross-section and an estimate of the relative cross-sections discussed in section 4.

Table 4b.

Exchange cross-sections and means

masses	$\frac{v_{\text{osc}}}{v_c}$	X	$\bar{\sigma}_X$	$\langle \frac{v_{\text{osc}}}{v_c} \rangle$	$\langle e_{(n)} \rangle$	$\langle \frac{\Delta E}{E} \rangle$
(1.0,1.0,1.0)	[0.0625, 0.125]	$(1, 2) + (3) \rightarrow (1, 2) + (3)$	7.3	0.11	0.36	-0.16
		$(1, 2) + (3) \rightarrow (1) + (2, 3)$	1.7	0.16	0.67	-0.30
		$(1, 2) + (3) \rightarrow (1, 3) + (2)$	1.7	0.16	0.66	-0.29
	[0.125, 0.25]	$(1, 2) + (3) \rightarrow (1, 2) + (3)$	8.1	0.11	0.32	-0.12
		$(1, 2) + (3) \rightarrow (1) + (2, 3)$	1.6	0.16	0.65	-0.28
		$(1, 2) + (3) \rightarrow (1, 3) + (2)$	1.6	0.16	0.65	-0.26
	[0.25, 0.5]	$(1, 2) + (3) \rightarrow (1, 2) + (3)$	8.9	0.15	0.31	-0.10
		$(1, 2) + (3) \rightarrow (1) + (2, 3)$	1.6	0.16	0.66	-0.15
		$(1, 2) + (3) \rightarrow (1, 3) + (2)$	1.6	0.17	0.65	-0.20
	[0.5, 1.0]	$(1, 2) + (3) \rightarrow (1, 2) + (3)$	11.1	0.25	0.29	-0.02
		$(1, 2) + (3) \rightarrow (1) + (2, 3)$	1.6	0.18	0.68	0.19
		$(1, 2) + (3) \rightarrow (1, 3) + (2)$	1.1	0.18	0.66	0.21
(1.0,0.4,1.0)	[0.05, 0.15]	$(1, 2) + (3) \rightarrow (1, 2) + (3)$	14.7	0.11	0.27	-0.12
		$(1, 2) + (3) \rightarrow (1) + (2, 3)$	1.2	0.22	0.62	-0.35
		$(1, 2) + (3) \rightarrow (1, 3) + (2)$	7.0	0.13	0.66	-0.45
	[0.15, 0.35]	$(1, 2) + (3) \rightarrow (1, 2) + (3)$	16.4	0.14	0.25	-0.09
		$(1, 2) + (3) \rightarrow (1) + (2, 3)$	1.4	0.22	0.63	-0.31
		$(1, 2) + (3) \rightarrow (1, 3) + (2)$	6.8	0.13	0.68	-0.40
	[0.35, 0.65]	$(1, 2) + (3) \rightarrow (1, 2) + (3)$	18.6	0.22	0.24	-0.05
		$(1, 2) + (3) \rightarrow (1) + (2, 3)$	1.8	0.23	0.60	-0.11
		$(1, 2) + (3) \rightarrow (1, 3) + (2)$	5.8	0.13	0.70	-0.29
	[0.65, 1.05]	$(1, 2) + (3) \rightarrow (1, 2) + (3)$	22.2	0.35	0.26	-0.01
		$(1, 2) + (3) \rightarrow (1) + (2, 3)$	2.2	0.30	0.58	0.15
		$(1, 2) + (3) \rightarrow (1, 3) + (2)$	3.6	0.16	0.76	0.04

Table 4c.

Exchange cross-sections and means

masses	$\frac{\nu_{ee}}{\nu_e}$	X	$\bar{\sigma}_X$	$\langle \frac{\nu_{res}}{\nu_e} \rangle$	$\langle e_{(n)} \rangle$	$\langle \frac{\Delta E}{E} \rangle$
(0.5,0.35,1.0)	[0.05, 0.15]	(1, 2) + (3) \rightarrow (1, 2) + (3)	26.0	0.12	0.21	-0.07
		(1, 2) + (3) \rightarrow (1) + (2, 3)	5.5	0.21	0.59	-0.64
		(1, 2) + (3) \rightarrow (1, 3) + (2)	9.8	0.15	0.61	-0.50
	[0.15, 0.35]	(1, 2) + (3) \rightarrow (1, 2) + (3)	30.3	0.18	0.22	-0.07
		(1, 2) + (3) \rightarrow (1) + (2, 3)	4.9	0.20	0.57	-0.55
		(1, 2) + (3) \rightarrow (1, 3) + (2)	8.2	0.16	0.64	-0.58
	[0.35, 0.75]	(1, 2) + (3) \rightarrow (1, 2) + (3)	25.2	0.32	0.21	-0.10
		(1, 2) + (3) \rightarrow (1) + (2, 3)	4.8	0.24	0.58	-0.51
		(1, 2) + (3) \rightarrow (1, 3) + (2)	7.8	0.18	0.66	-0.49
	[0.75, 1.15]	(1, 2) + (3) \rightarrow (1, 2) + (3)	36.4	0.51	0.24	-0.02
		(1, 2) + (3) \rightarrow (1) + (2, 3)	4.8	0.30	0.65	-0.27
		(1, 2) + (3) \rightarrow (1, 3) + (2)	4.9	0.24	0.73	-0.40
(1.0,0.35,0.5)	[0.05, 0.15]	(1, 2) + (3) \rightarrow (1, 2) + (3)	13.8	0.06	0.17	-0.07
		(1, 2) + (3) \rightarrow (1) + (2, 3)	0.1	0.22	0.76	-0.26
		(1, 2) + (3) \rightarrow (1, 3) + (2)	2.8	0.10	0.66	-0.27
	[0.15, 0.35]	(1, 2) + (3) \rightarrow (1, 2) + (3)	14.9	0.09	0.17	-0.07
		(1, 2) + (3) \rightarrow (1) + (2, 3)	0.1	0.22	0.76	-0.23
		(1, 2) + (3) \rightarrow (1, 3) + (2)	2.8	0.10	0.67	-0.24
	[0.35, 0.65]	(1, 2) + (3) \rightarrow (1, 2) + (3)	16.9	0.14	0.16	-0.03
		(1, 2) + (3) \rightarrow (1) + (2, 3)	0.2	0.17	0.75	0.08
		(1, 2) + (3) \rightarrow (1, 3) + (2)	2.0	0.11	0.65	-0.08
	[0.65, 1.05]	(1, 2) + (3) \rightarrow (1, 2) + (3)	19.0	0.23	0.00	0.10
		(1, 2) + (3) \rightarrow (1) + (2, 3)	0.5	0.22	0.66	0.51
		(1, 2) + (3) \rightarrow (1, 3) + (2)	1.4	0.12	0.71	0.24

All interactions

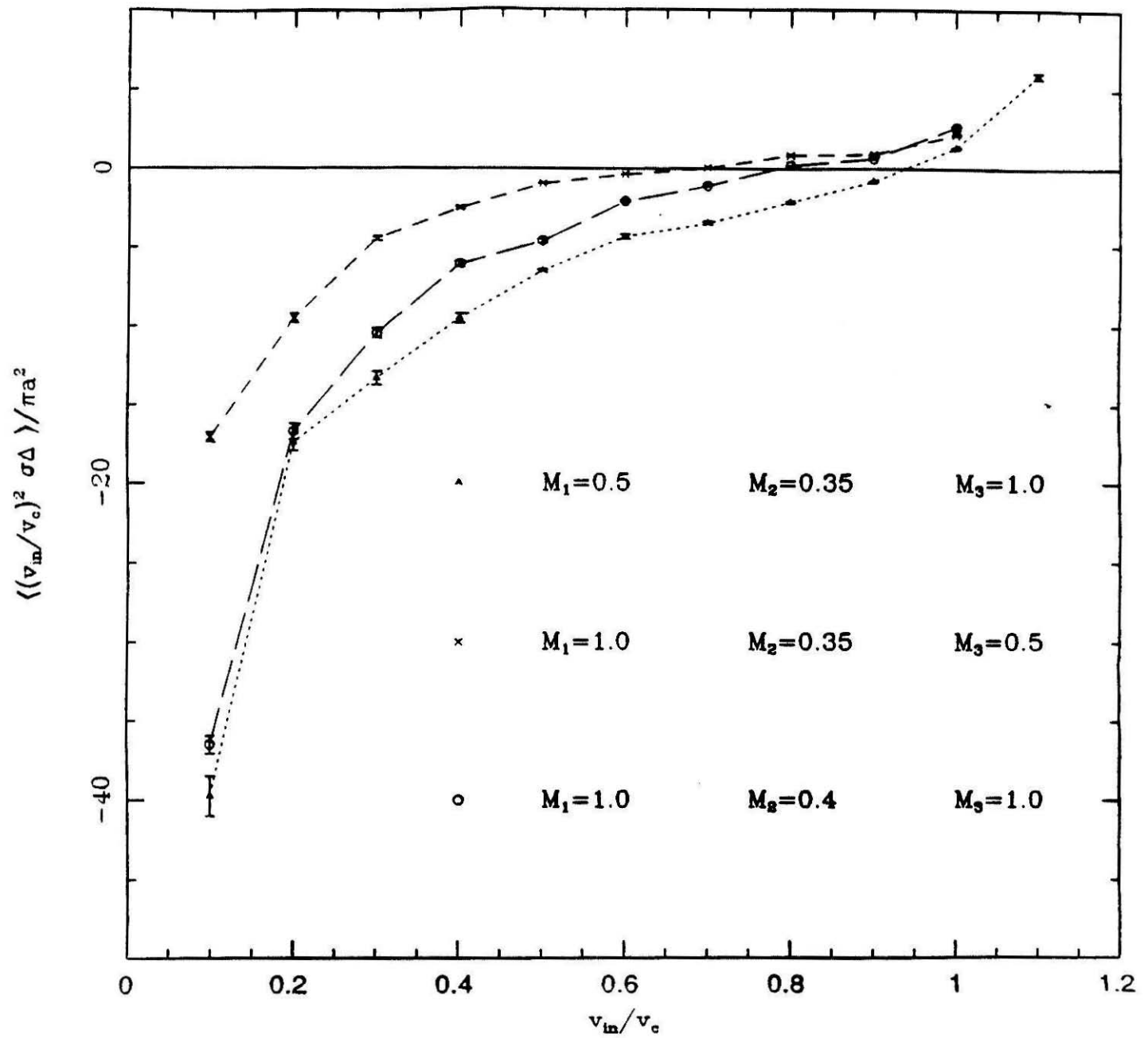


Figure 1a

X:(1,2)+(3)→(1,2)+(3)

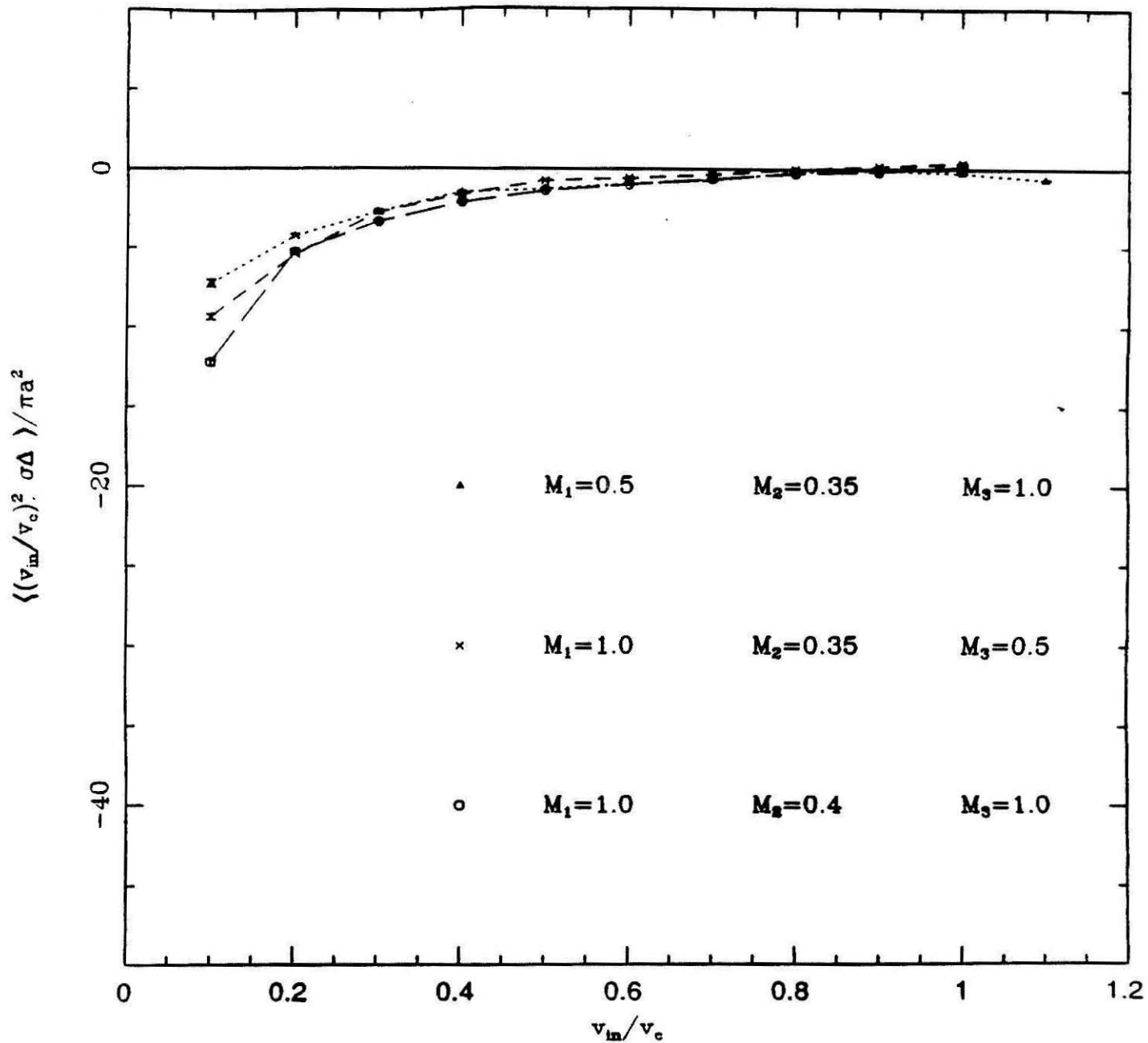


Figure 1b

X:(1,2)+(3)→(1)+(2,3)

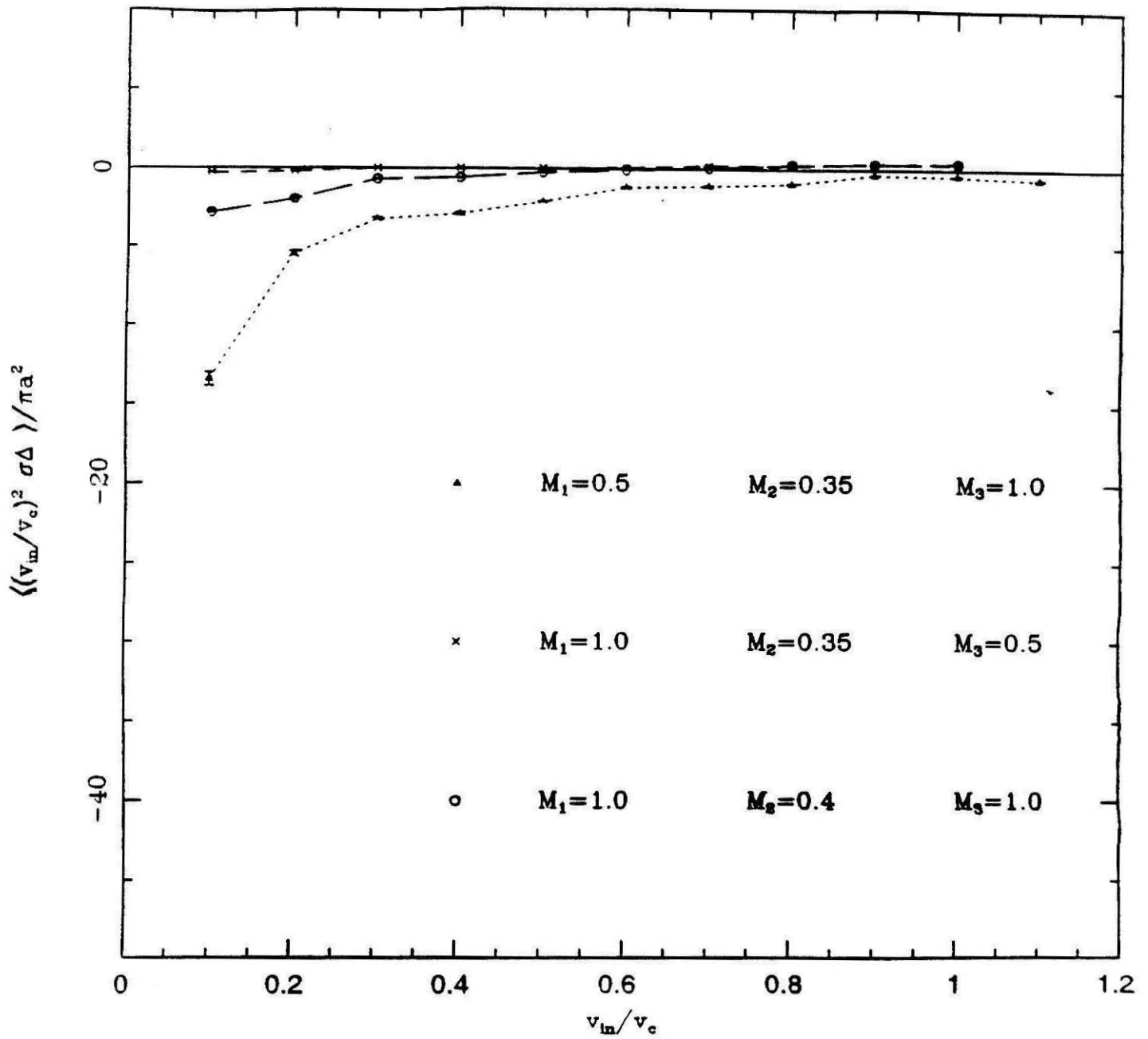


Figure 1c

X:(1,2)+(3)→(1,3)+(2)

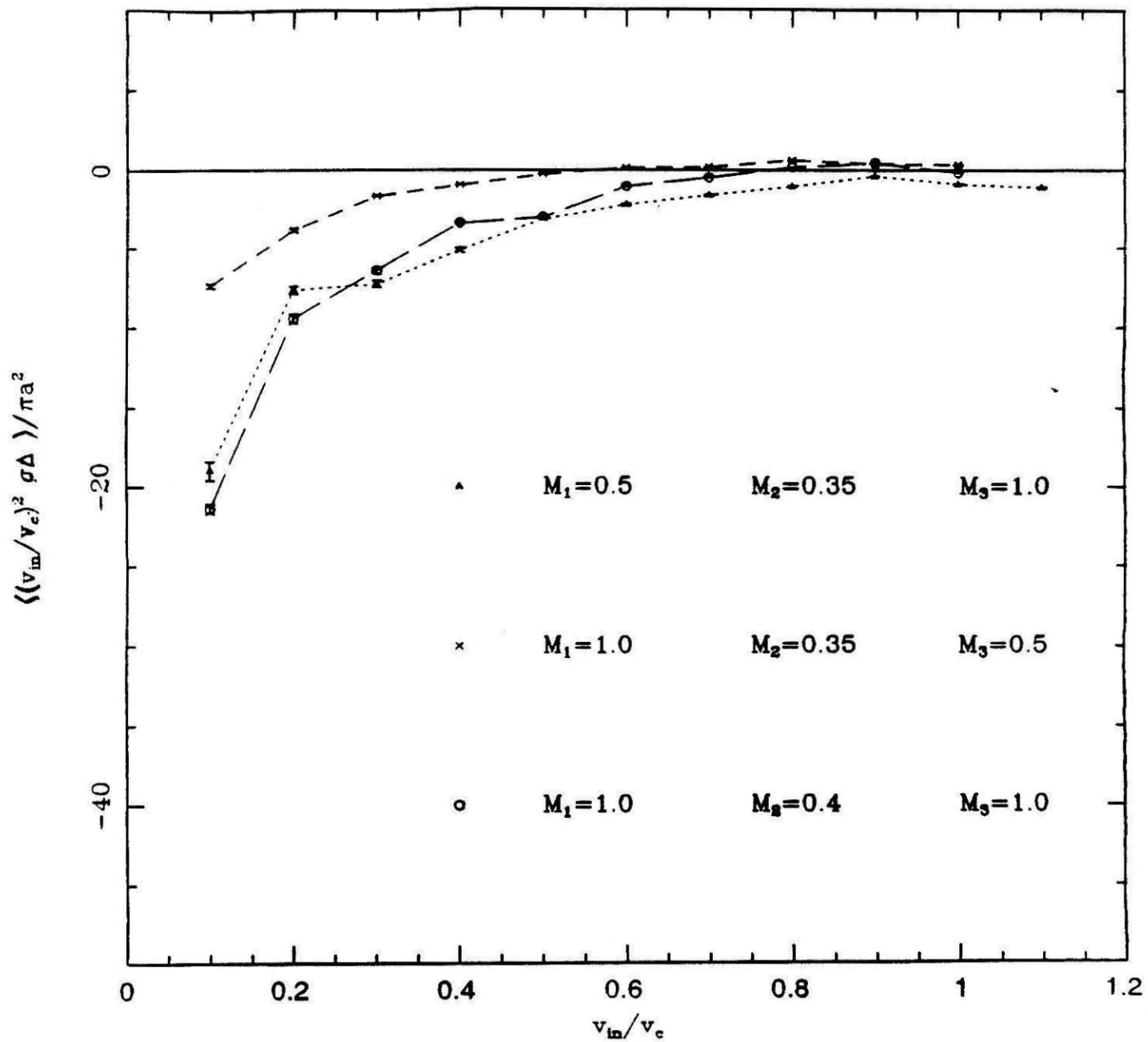


Figure 1d

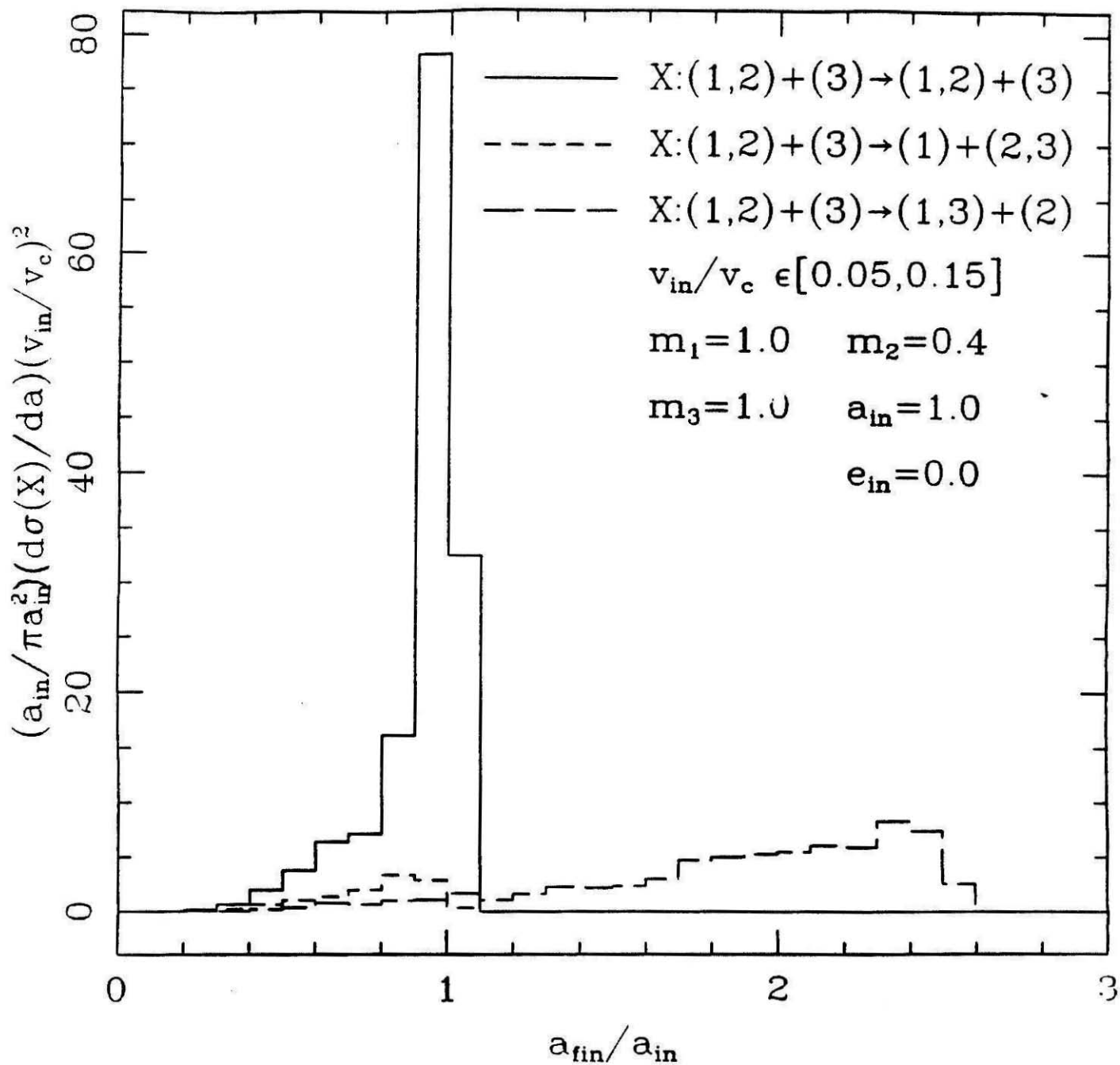


Figure 2a

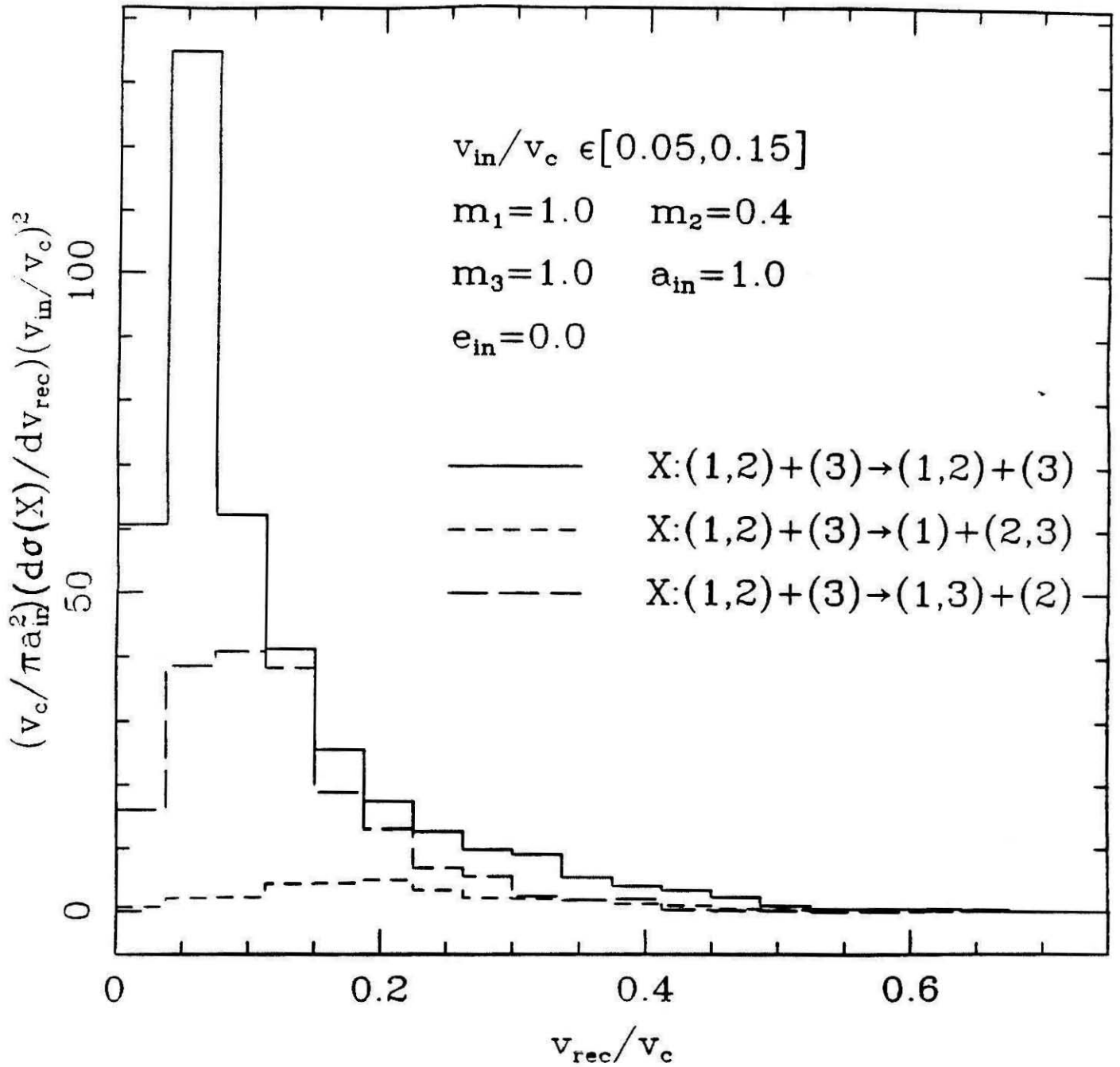


Figure 2b

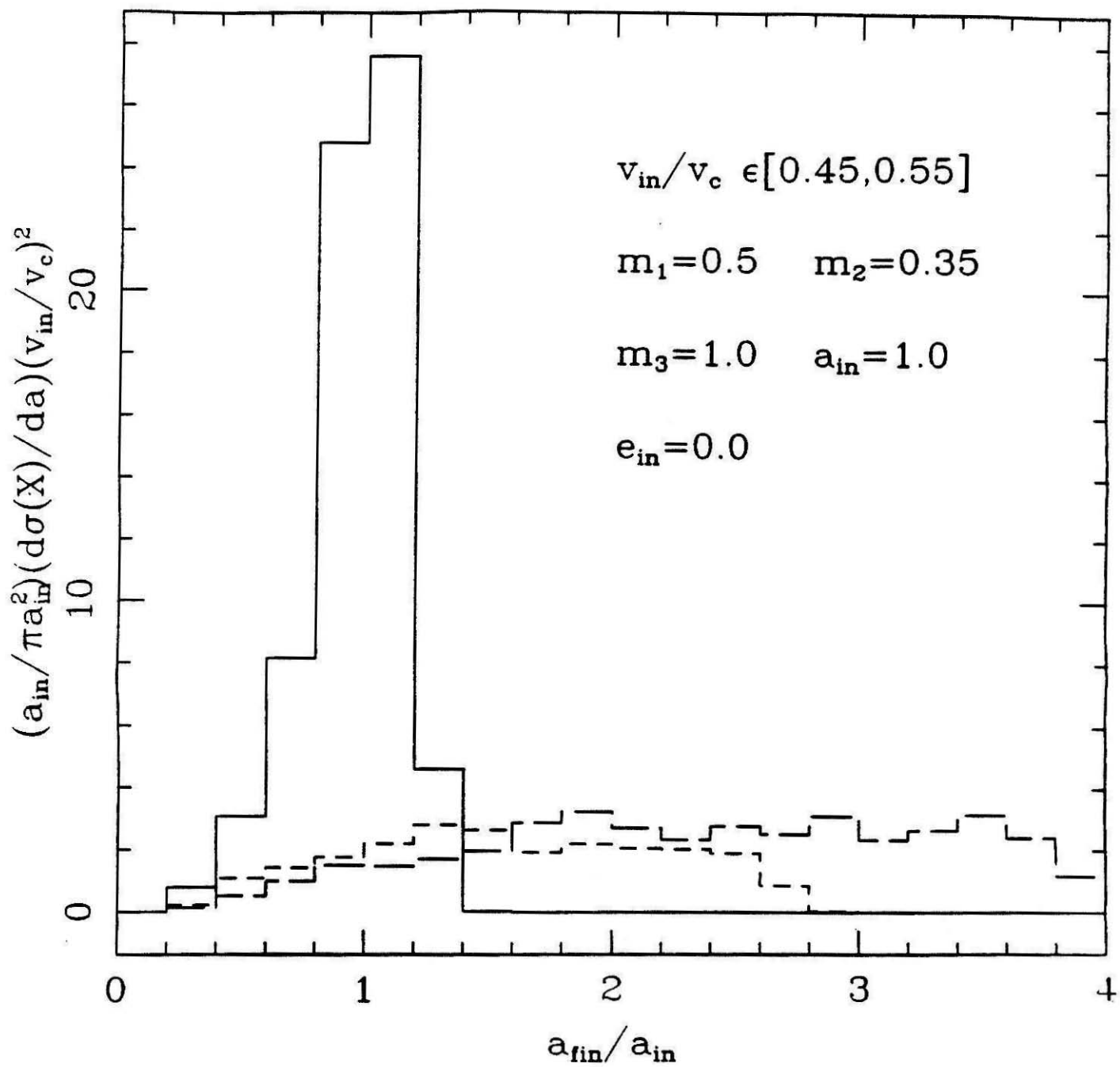


Figure 3

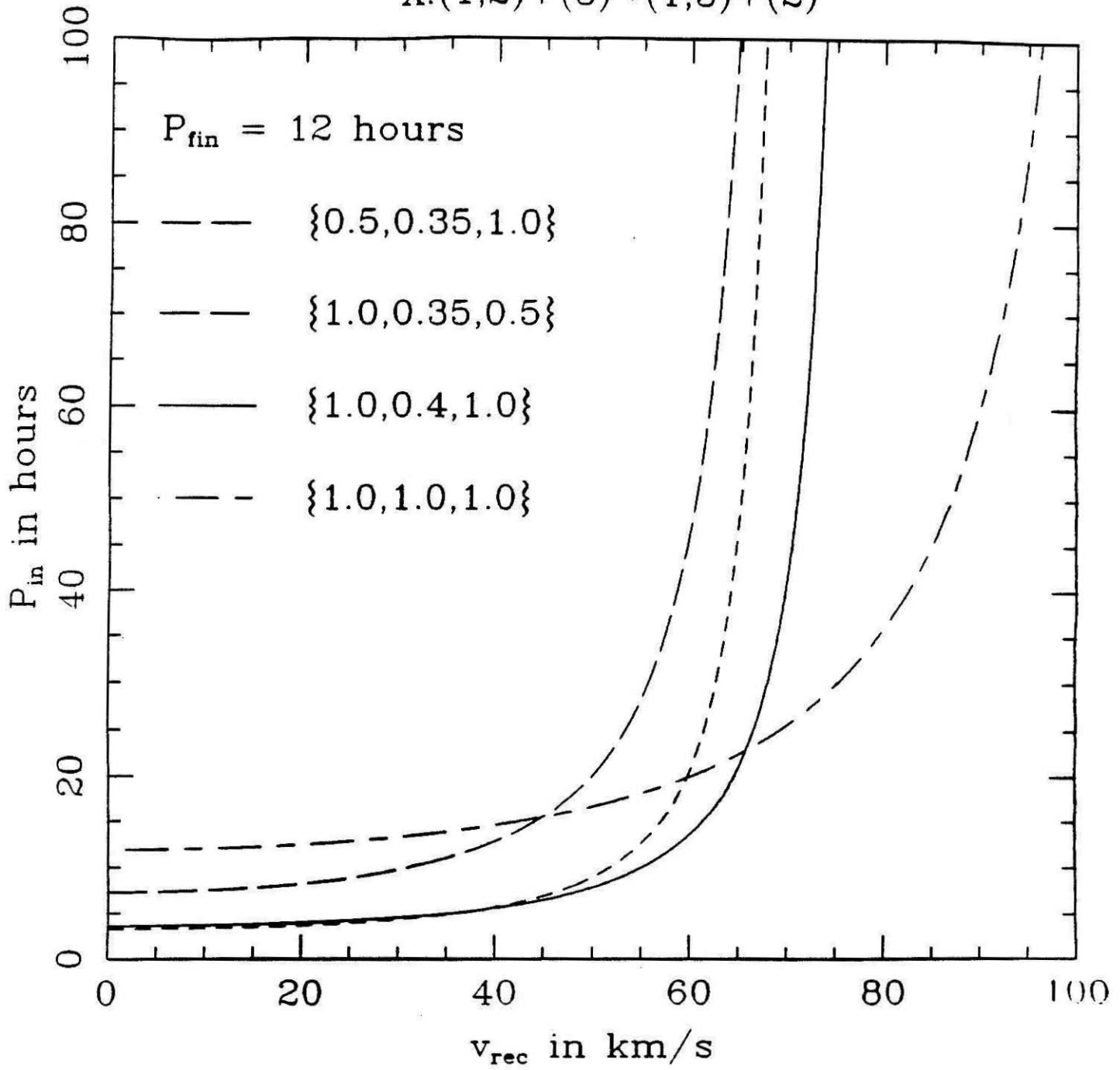
$X:(1,2)+(3) \rightarrow (1,3)+(2)$ 

Figure 4

$$X:(1,2)+(3) \rightarrow (1,3)+(2)$$

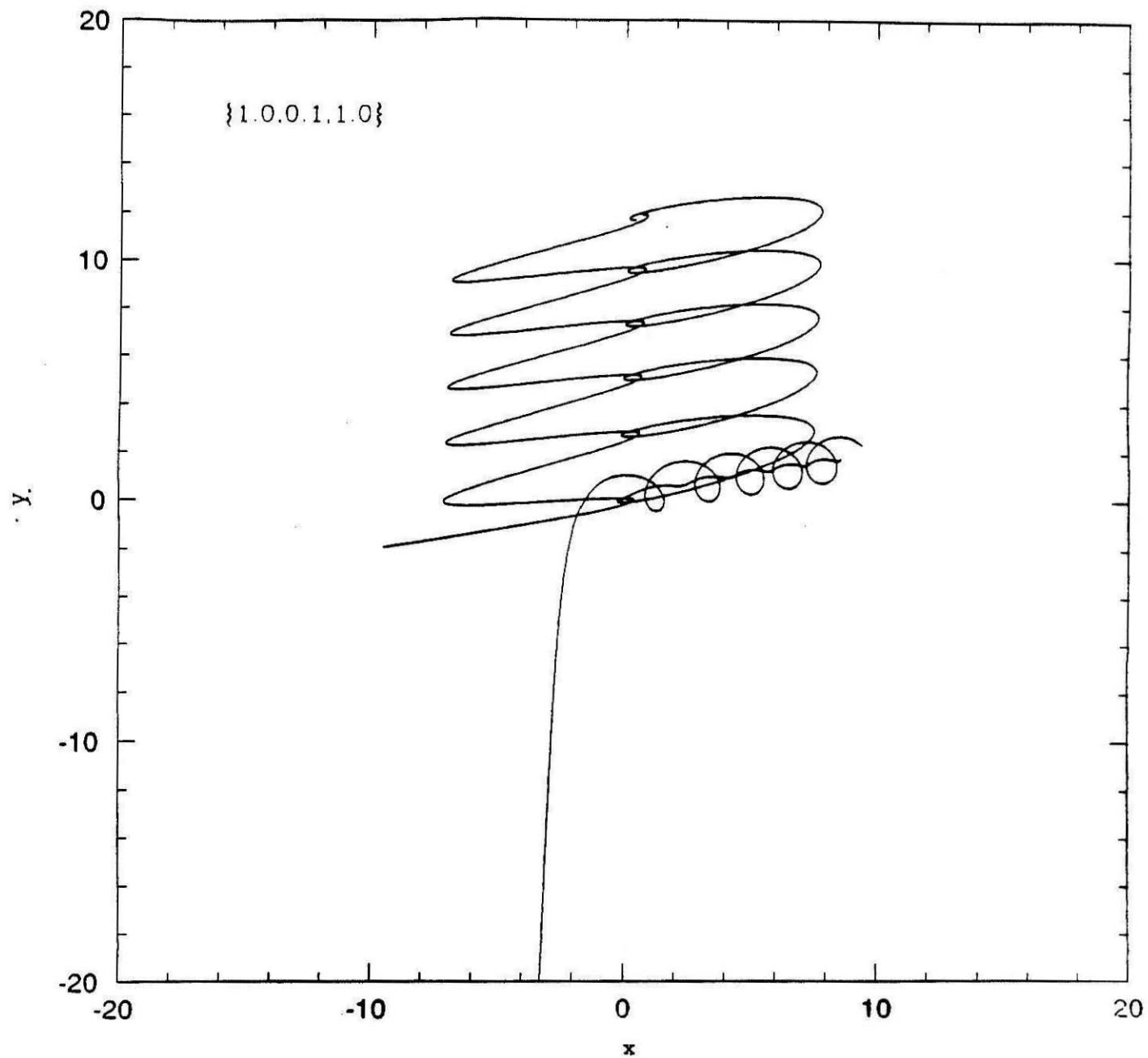


Figure 5a

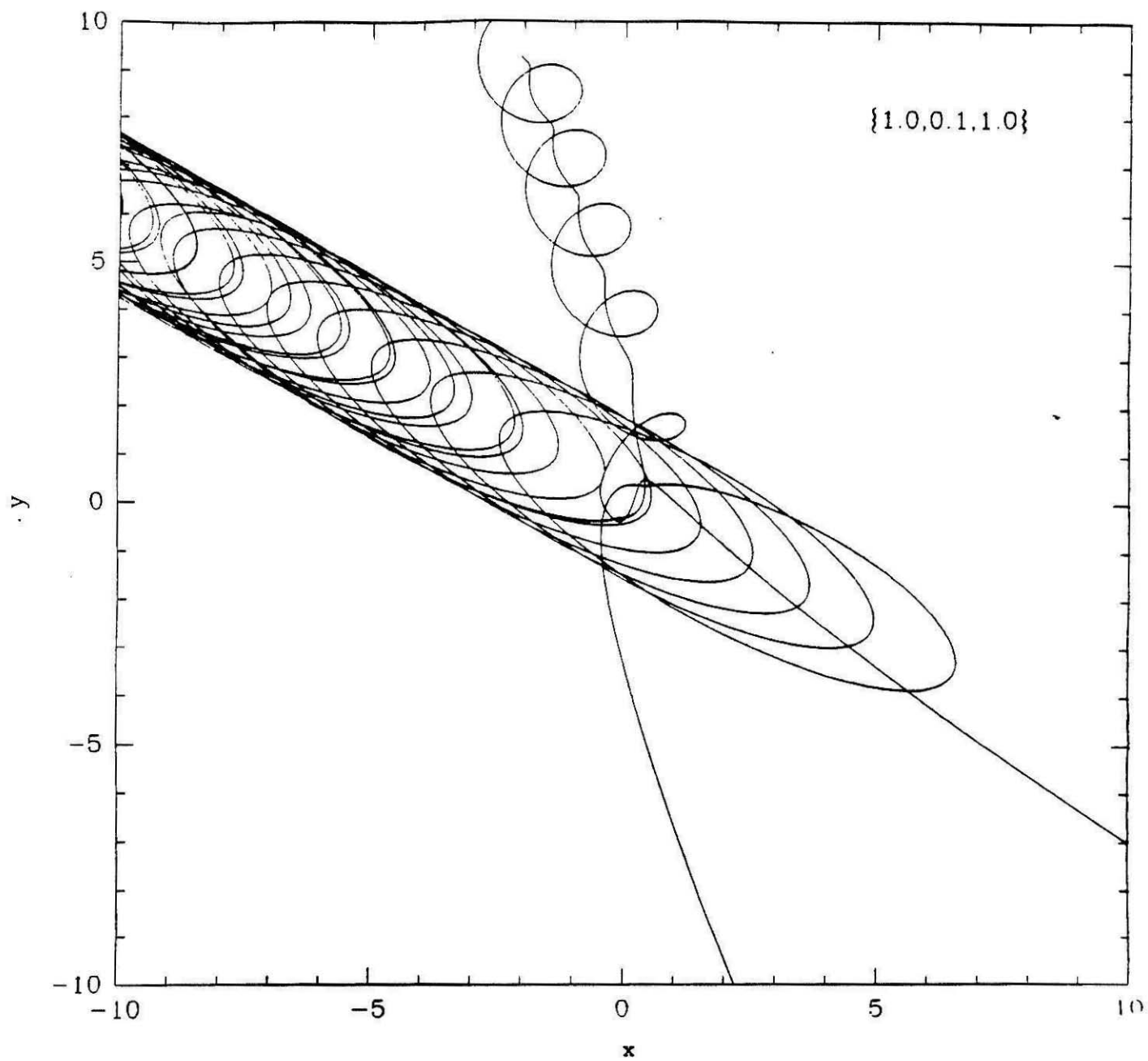
$X:(1,2)+(3) \rightarrow (1,3)+(2)$ 

Figure 5b

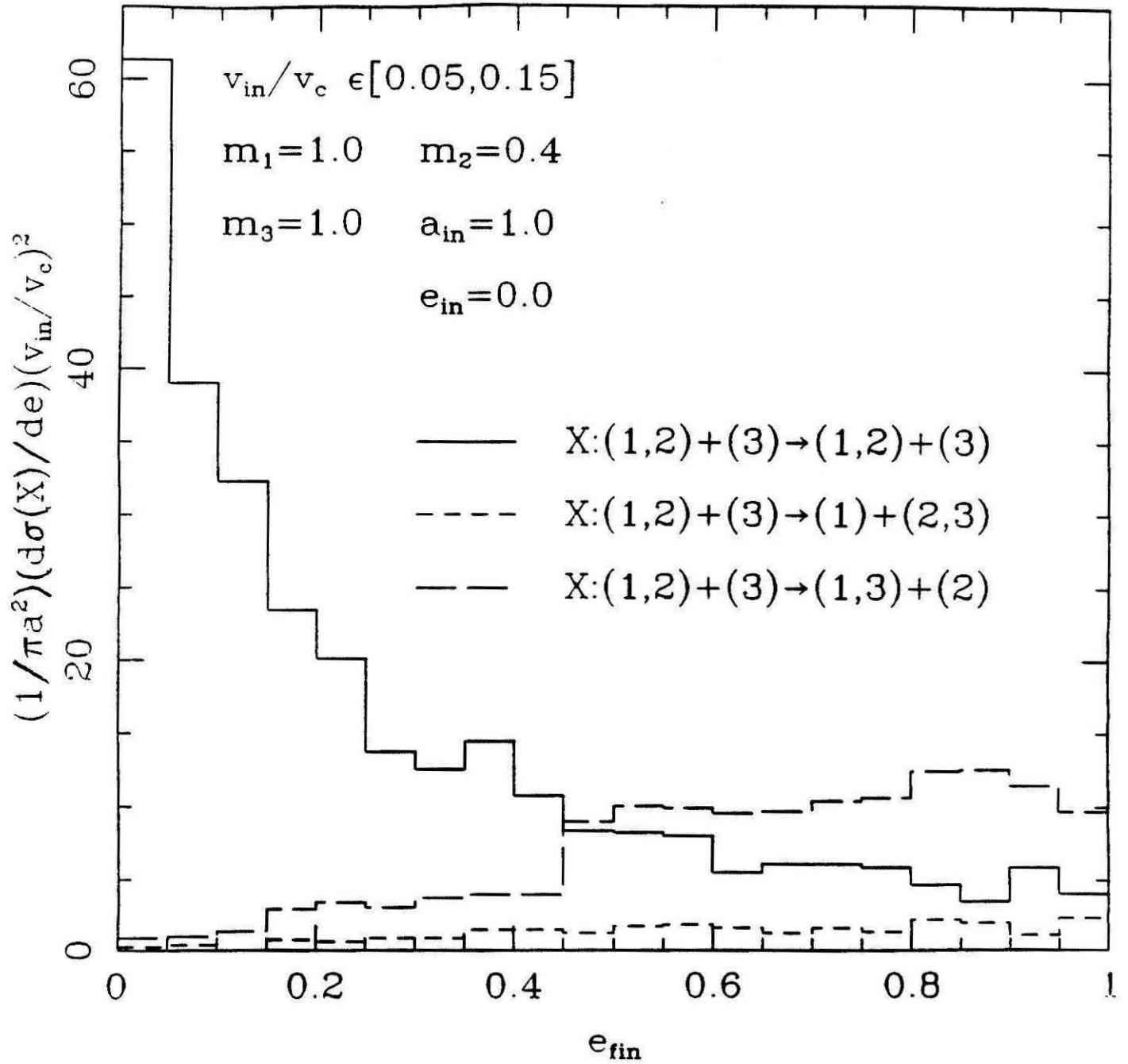


Figure 6a

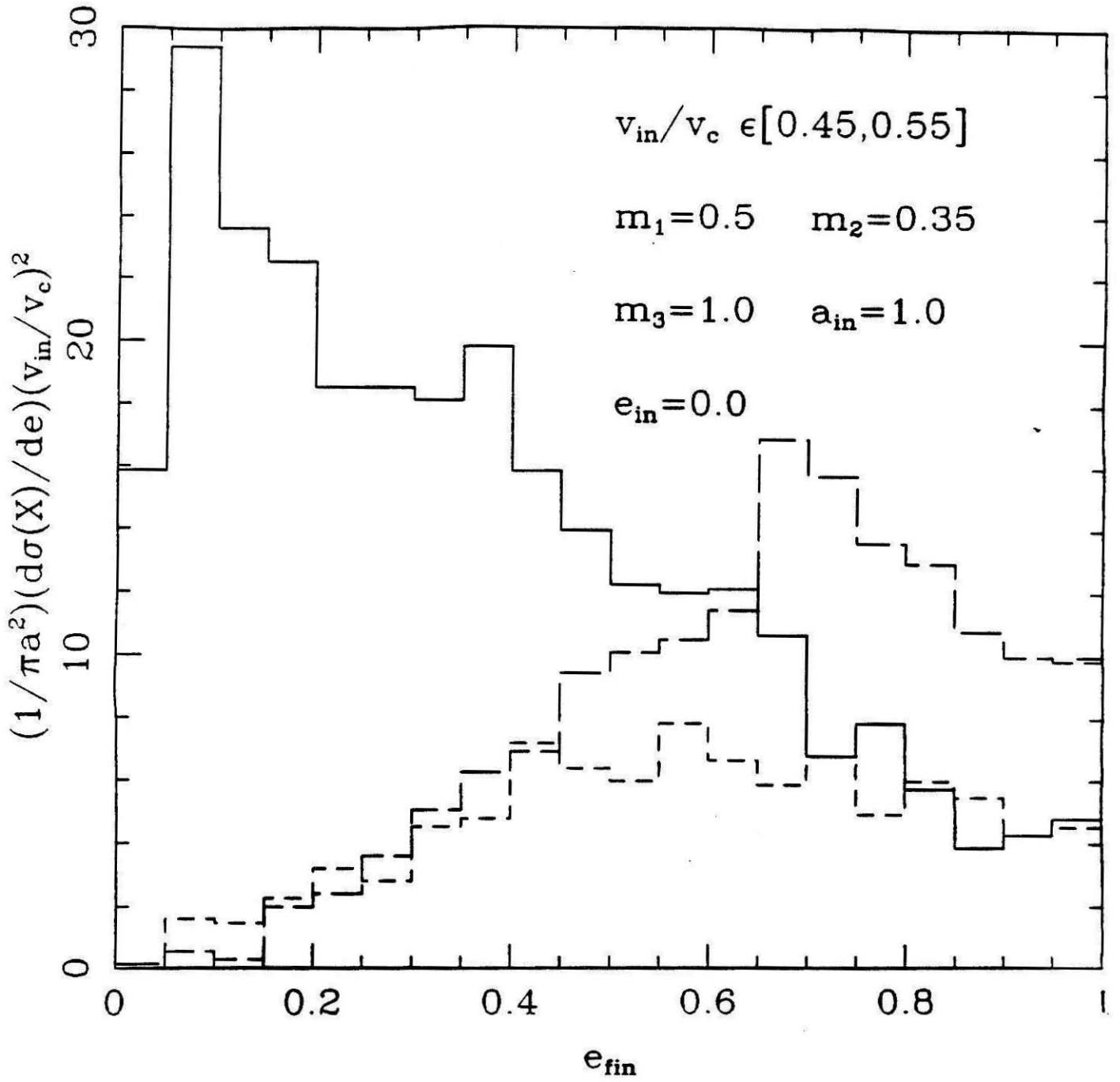


Figure 6b

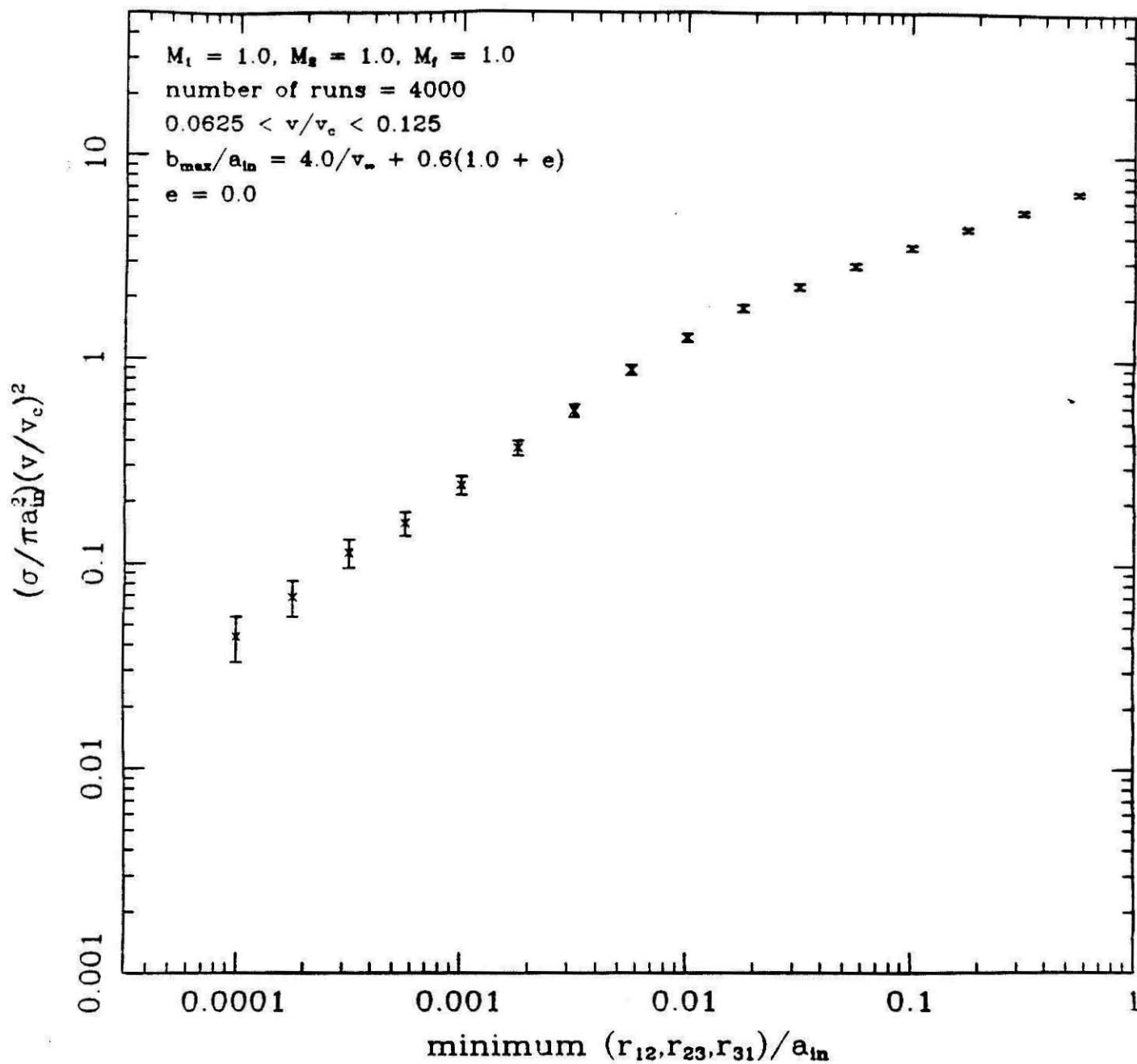


Figure 7

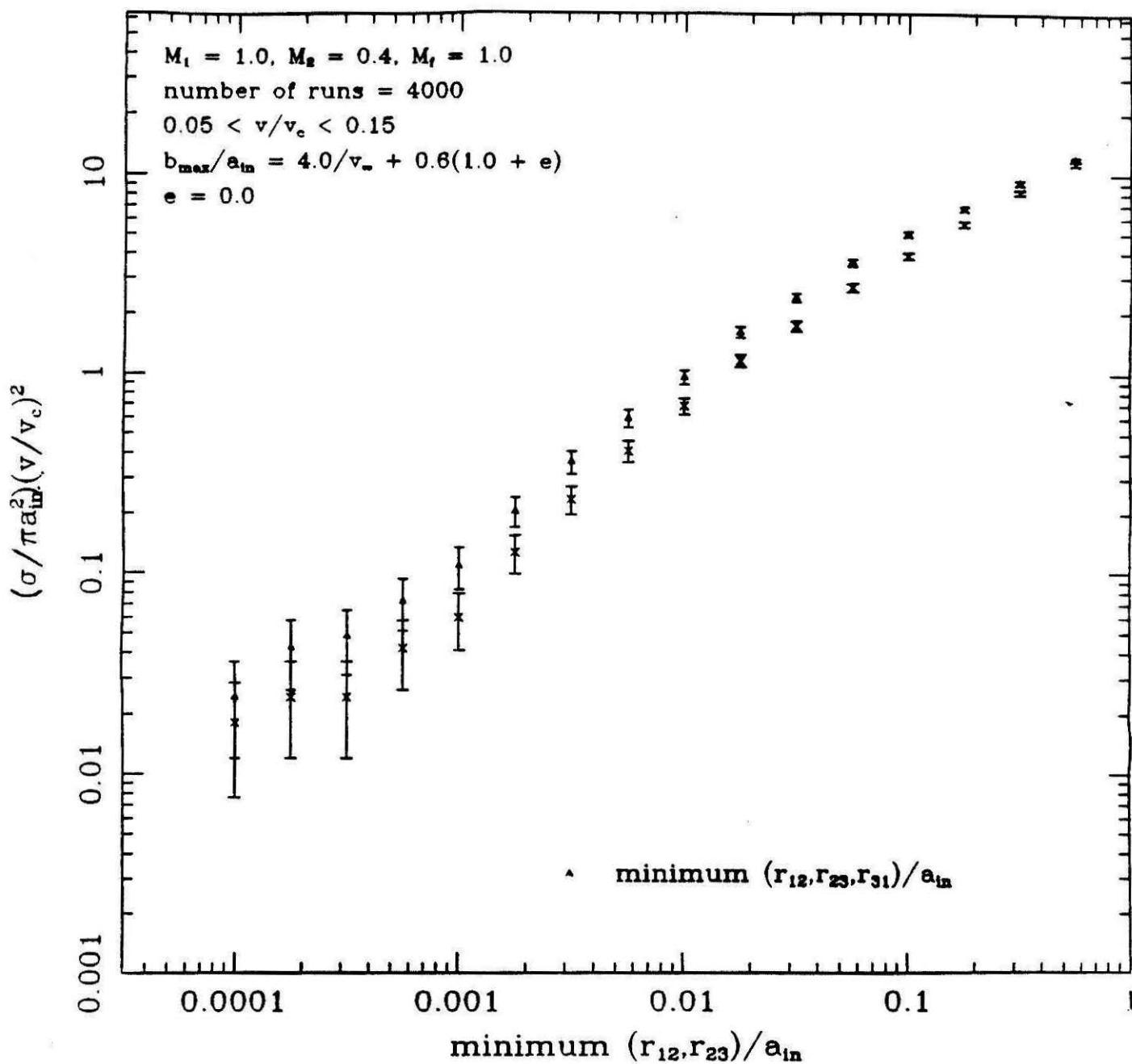


Figure 8

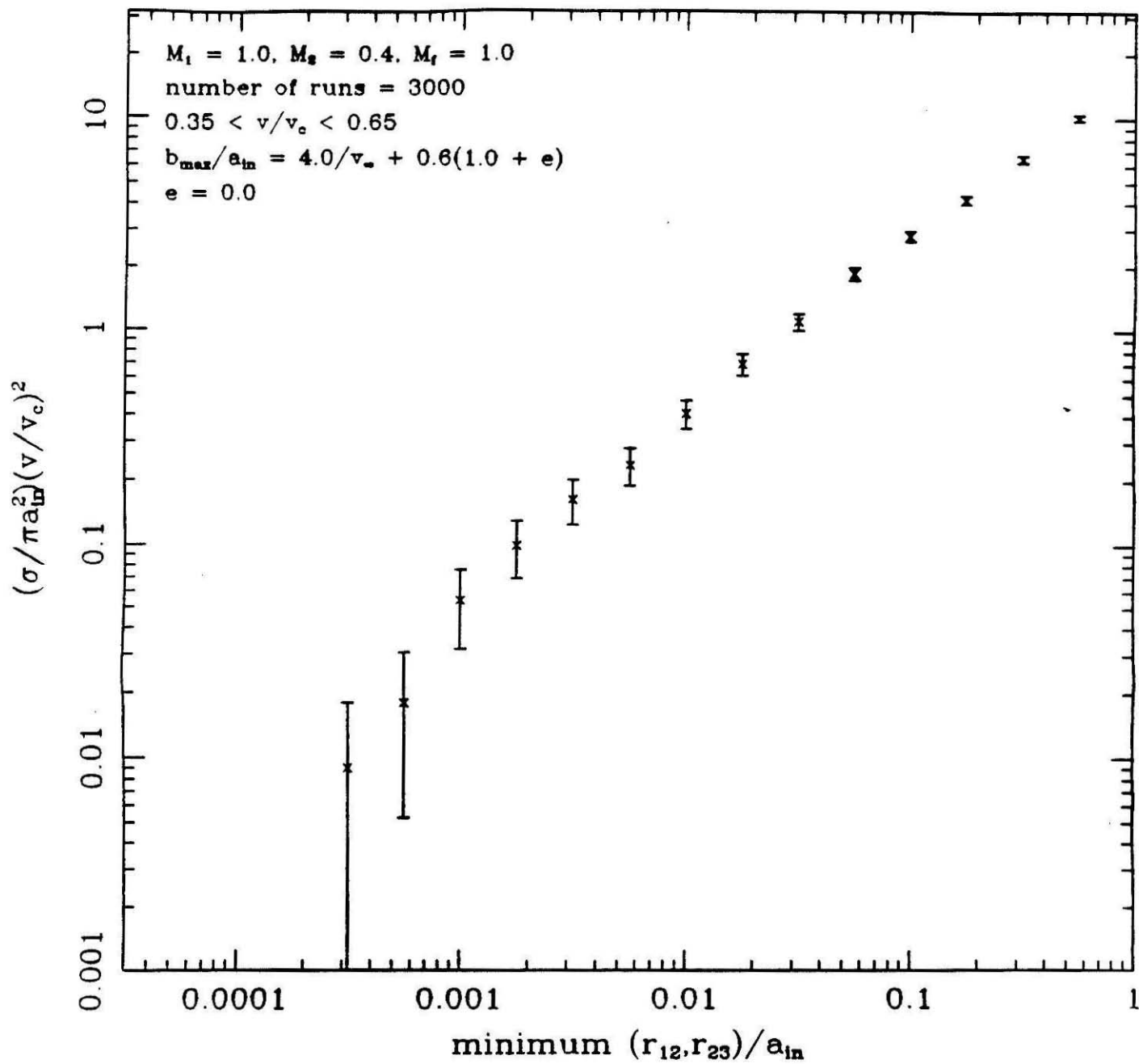


Figure 9

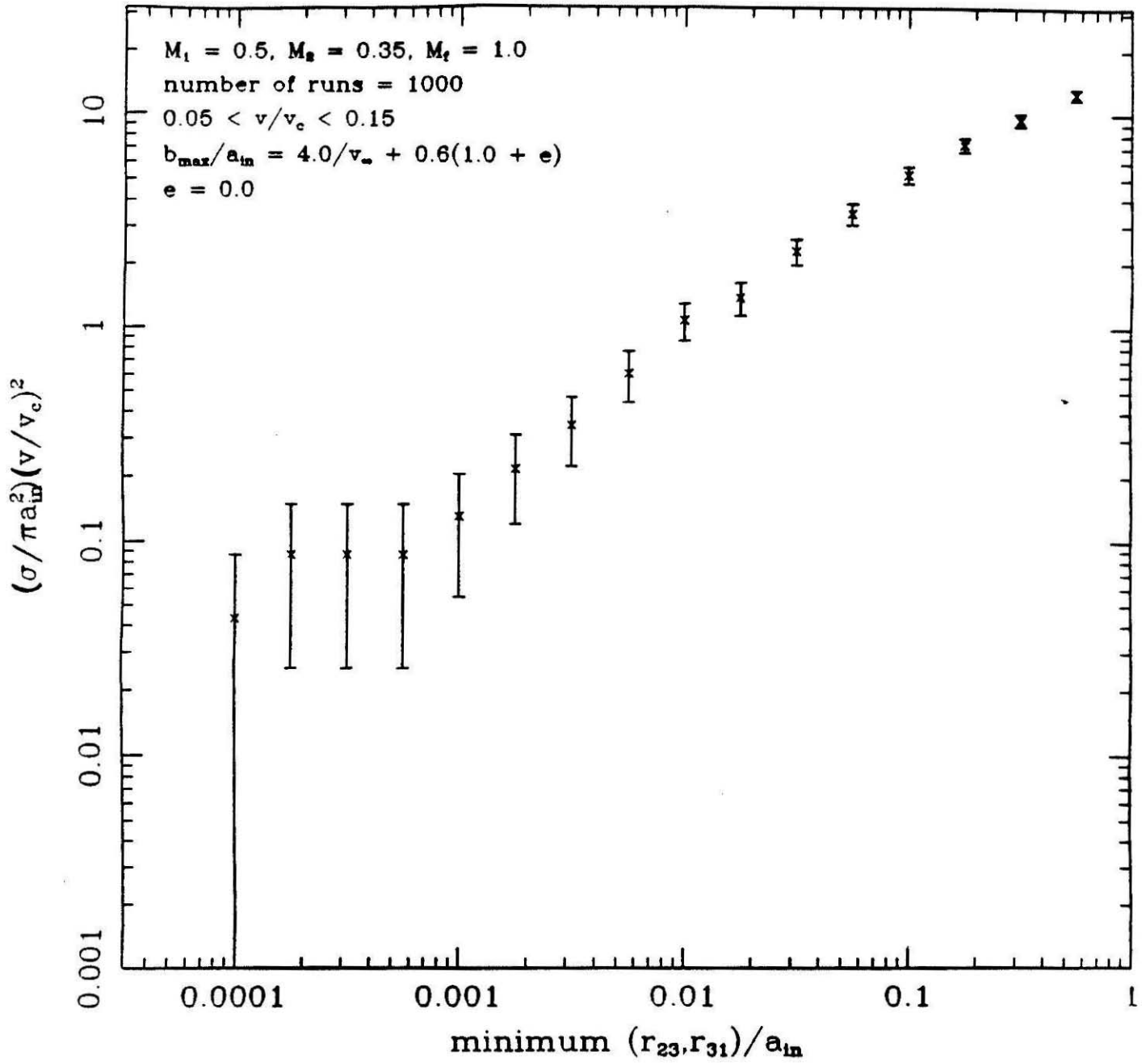


Figure 10

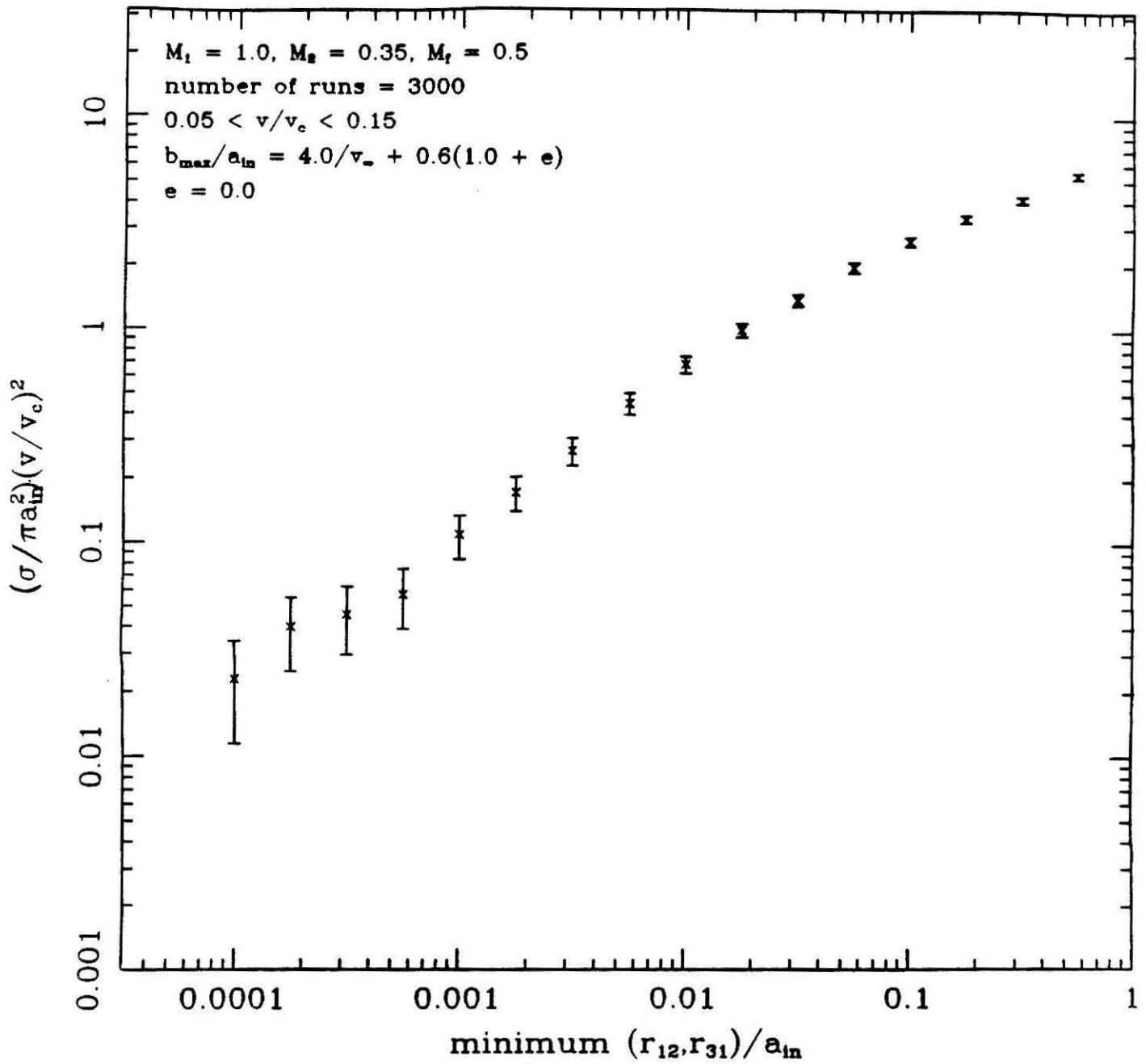


Figure 11

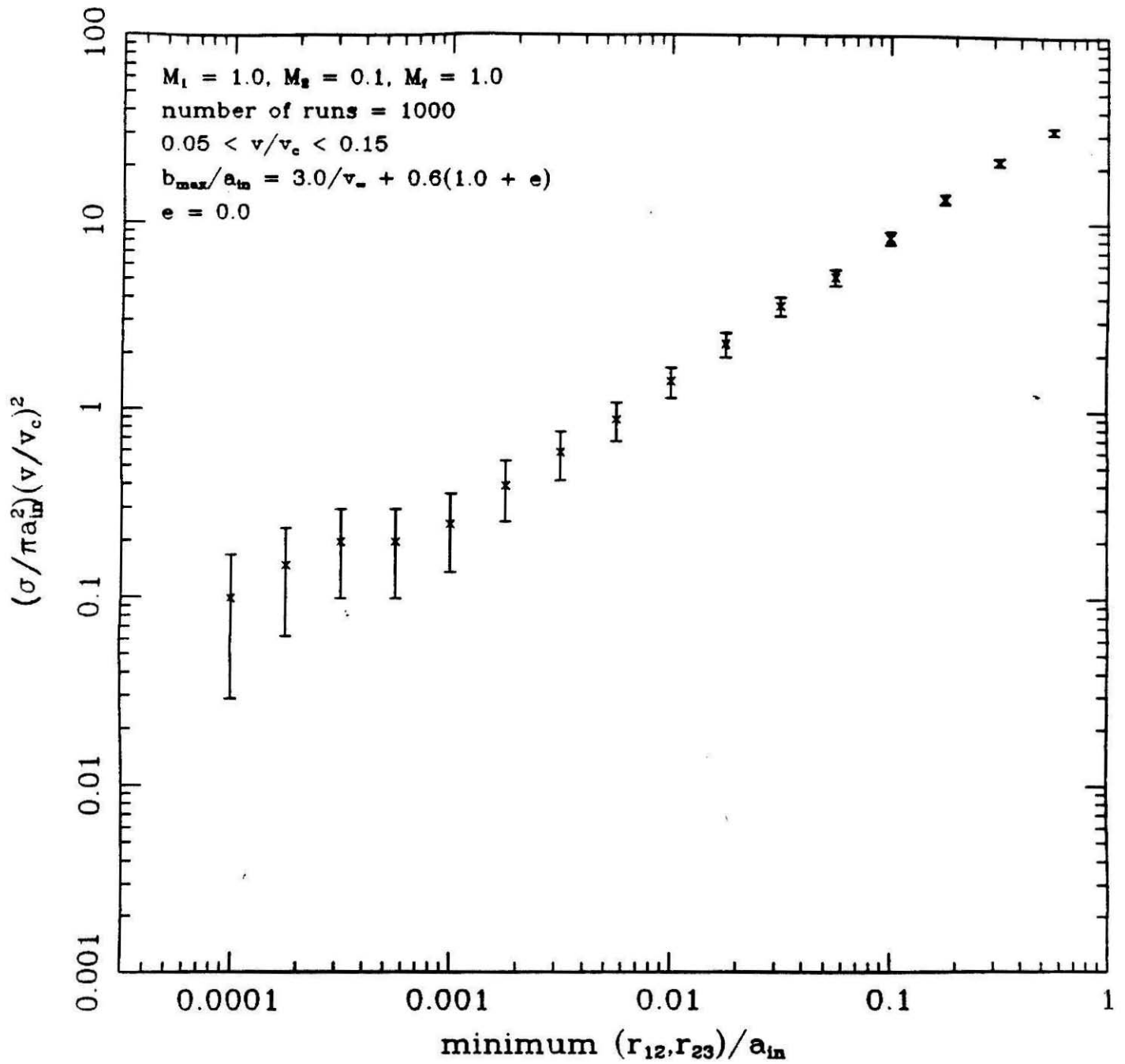


Figure 12

S:(1,2)+(3)→(1,2)+(3)

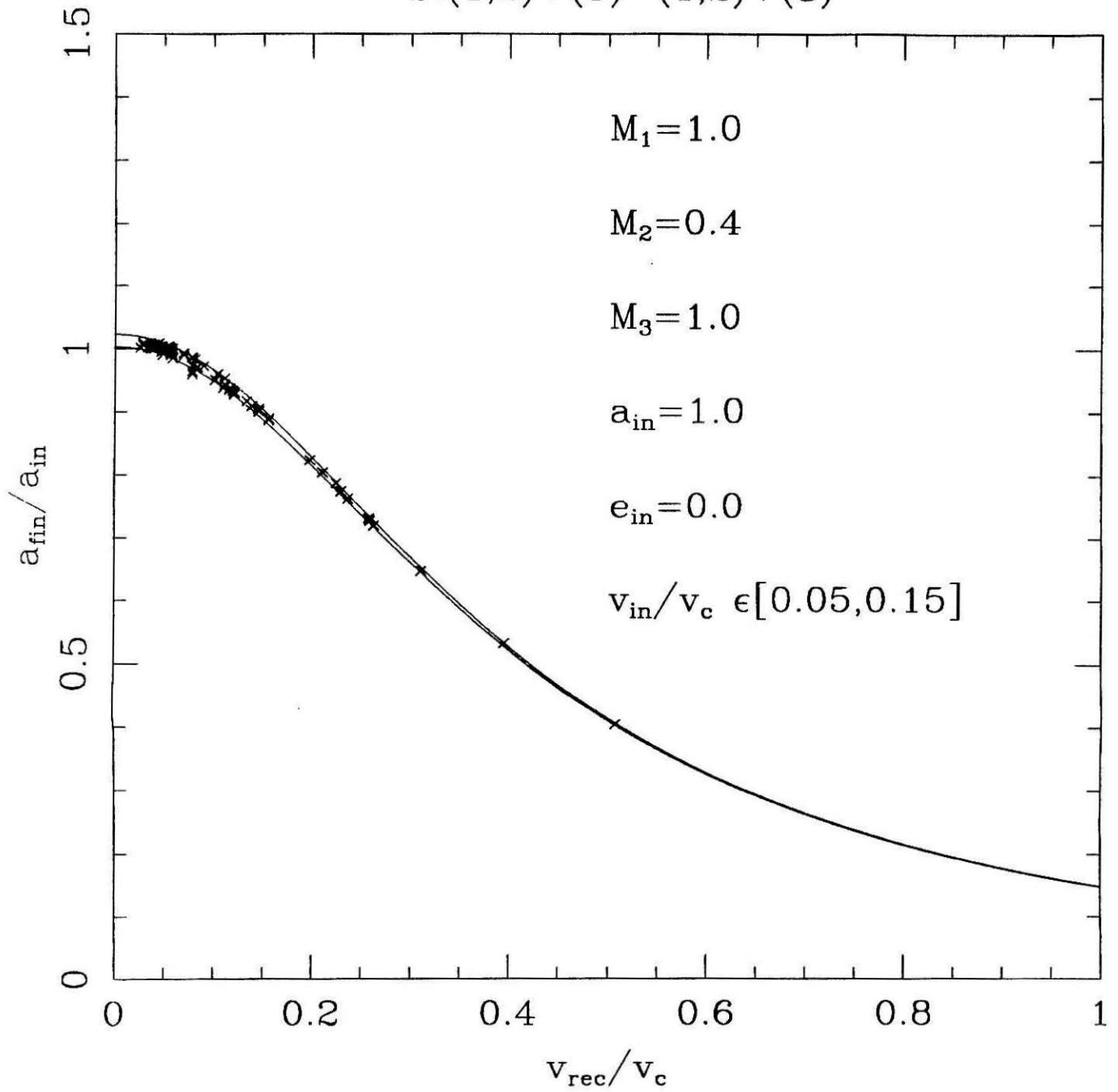


Figure 13

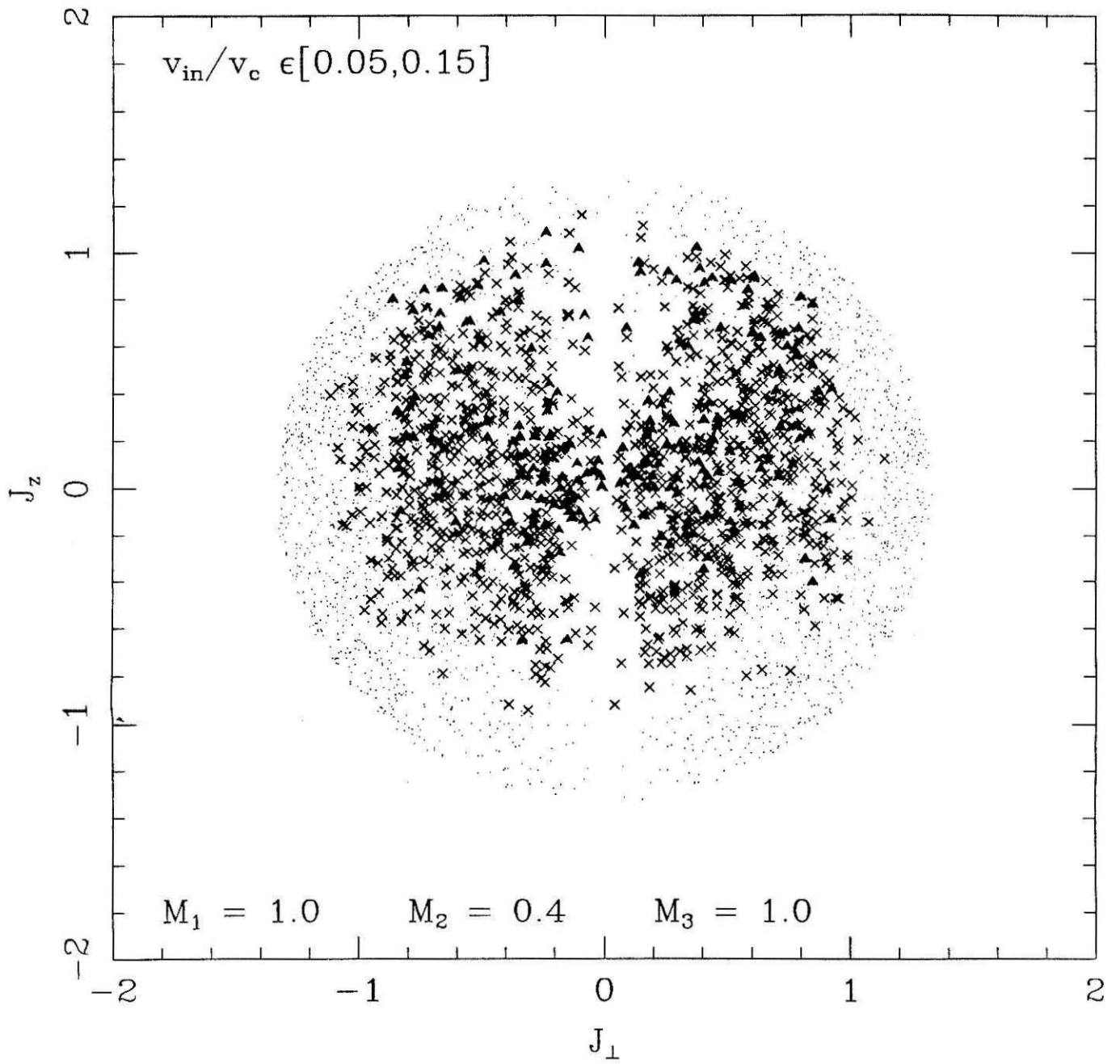


Figure 14



“Since once I sat upon a promontory,
And heard a mermaid on a dolphin’s back
Uttering such dulcimer and harmonious breath,
That the rude sea grew civil at her song,
And certain stars shot madly from their spheres,
To hear the sea-maid’s music.”

W. Shakespeare, *A Midsummer Night’s Dream*

Chapter 3

Ejection of Pulsars and Binaries
to the Outskirts of Globular Clusters

E. S. Phinney & Steinn Sigurdsson

Appeared originally in *Nature* 349 220, 17th January, 1991

Abstract

Three-body interactions can eject stars, singly or in binaries, from the core of a globular cluster to its outskirts, whither dynamical friction may take more than 10^8 years to return them. We show here that such processes can explain why the binary pulsar 2127+11C in M15 (and perhaps 1744-24A in Terzan 5) is now far from the cluster core. A suitable encounter could have given the pulsar enough velocity to eject it to its present position, and also replace its original companion with a neutron star. For ejection of systems like PSR 2127+11C to be probable, the core of M15 must be composed of heavy degenerate stars at a density $\gtrsim 10^7 \text{ pc}^{-3}$, maintained for $\gtrsim 10^8 \text{ y}$, and contain at least 10^3 degenerate stars of $\gtrsim 10^3 M_{\odot}$, of which $\gtrsim 10^2$ are neutron stars; this is consistent with previous dynamical estimates. We show that a natural combination of factors conspires to enable us to see PSR 2127+11C. A binary of longer period could not have received an impulse large enough to escape the core, whereas a binary of shorter period would have been ejected from the cluster or would have collapsed through decay of its orbit by gravitational radiation. Pulsars and pulsar binaries ejected from clusters contribute to the birthrate of recycled pulsars in the inner Galaxy. Similar recoil can occur in hard binaries containing white dwarfs (cataclysmic variables), complicating the task of determining cluster membership of candidates far from cluster centers.

Stars can be ejected to the outskirts of a globular cluster, where the time required for dynamical friction to return them to the core is a significant fraction of the age of the universe. Both binary and single stars can attain high velocities in three-body (or binary-binary) interactions, and perhaps by asymmetric mass-loss during a tidal encounter. Here we show how the binary pulsar 2127+11C in M15 and perhaps 1744-24A in Terzan 5 must have formed in this way. For ejection of systems like PSR 2127+11C to be probable, the core of M15 must be composed of heavy degenerate stars at a density $\gtrsim 10^7 \text{ pc}^{-3}$, maintained for $\gtrsim 10^8 \text{ y}$, and contain at least 10^3 degenerate stars of $\gtrsim 10^3 M_{\odot}$, of which $\gtrsim 10^2$ are neutron stars; this is consistent with previous dynamical estimates. We show that a natural combination of factors conspires to enable us to see PSR 2127+11C. A binary of longer period could not have received an impulse large enough to escape the core. A binary of shorter period would have been ejected from the cluster and/or collapsed through decay of its orbit by gravitational radiation. Pulsars and pulsar binaries ejected from clusters contribute to the birthrate of recycled pulsars in the inner Galaxy. Similar recoil can occur in hard binaries containing white dwarfs (cataclysmic variables), complicating the task of determining cluster membership of candidates far from cluster centers^{1,2}. Neutron stars and binaries, being heavier than the unevolved majority of stars in M15, would in thermal equilibrium be found at the bottom of M15's potential well. Indeed the low mass X-ray binary (LMXB) AC 211^{1,3} and the four single radio pulsars 2127+11A,B,D,E⁴ are all within 0.4 pc of the optical center of M15 (whose U-band core radius* is⁵ $r_0 < 0.1 \text{ pc}$). To reach its current position⁶ projected 2.7 pc from the core of M15, the binary containing PSR 2127+11C must have been ejected, with a speed $\gtrsim 50 \text{ km s}^{-1}$ from the high density central region where it formed (Figure 1).

* Throughout, we define *core radius* as the radius at which the surface density of a specified population of stars falls to half its central value.

PSR 2127+11C has a spin-down age $\tau_c = P/2\dot{P} = 1 \times 10^8$ y (Ref. 6). This suggests that the pulsar was spun up by accretion not much more than τ_c ago. Assuming, as suggested by the mass function, that the binary consists of two 1.4M $_{\odot}$ neutron stars, gravitational radiation will cause the two neutron stars to merge 2×10^8 y from now. Integrating the orbit backwards from the present orbital period and eccentricity ($P_b = 8.05$ h, $e = 0.68$) under the influence of gravitational radiation alone, 10^8 y ago the binary would have had $P_b = 12$ h and $e = 0.75$, and 2×10^8 y ago $P_b = 16$ h and $e = 0.79$. A binary consisting of two compact objects offers no opportunity for accretion or tidal capture. Therefore either the current companion must have been exchanged for the non-degenerate star from which the pulsar was accreting or the pulsar must have been spun up elsewhere, and exchanged into a binary already containing the current companion. We begin with the first possibility.

Since M/L rises steeply^{7,8,9} for $r < 0.1$ pc in M15, most of the stars encountered by a binary there will be heavy degenerate stars. If star 3 encounters a binary of semimajor axis a_i (consisting of stars 1,2) and exchanges with star 2, the recoil velocity v_{13} of the final binary consisting of stars 1,3 with semi-major axis a_f is

$$\left(\frac{v_{13}}{v_c}\right)^2 = \frac{M_2 M_3 (M_1 + M_2)}{(M_1 + M_3)(M_1 + M_2 + M_3)^2} \left[\frac{a_i}{a_f} \frac{M_3}{M_2} - 1 + \left(\frac{v_{in}}{v_c}\right)^2 \right], \quad (1)$$

where v_c , given by

$$v_c^2 = \frac{GM_1 M_2 (M_1 + M_2 + M_3)}{a_i M_3 (M_1 + M_2)} \quad (2)$$

is the relative incoming velocity $v_{in} = (v_3 - v_{12})$ for which the system would have zero total energy. The $(v_{in}/v_c)^2$ in (1) may be neglected for hard binaries, so a_i and the period P_i of the initial binary are uniquely determined by the recoil velocity and the period P_f after exchange. If the pulsar was accreting from its erstwhile

companion, then $M_2 < 0.7M_{\odot}$, the mass of stars just leaving the main sequence. The companion cannot have been very light (such as the $0.02M_{\odot}$ companion of PSR 1957+20), because if $M_2 \ll M_1 = M_3$, most of the exchange cross-section produces only wide $a_f \sim (M_3/M_2)a_i$, extremely eccentric $1-e_f \sim M_2/M_3$ binaries with negligible recoil, $v_{13} \sim 0.3(M_2/M_3)^{1/2}(GM_3/a_f)^{1/2}$. We therefore consider an intermediate mass $M_2 = 0.56M_{\odot} = 0.4M_1$. For $P_f = 12$ h (encounter τ_c ago), a recoil exceeding 50 km s^{-1} requires $P_i > 8$ h, while $P_f = 8$ h (encounter very recently) requires $P_i > 4$ h. In the latter case, a normal main sequence star could have filled its Roche lobe. The pre-encounter orbit will have been circularized by tidal dissipation. As part of a larger investigation of the interaction of cluster binaries with compact objects, we have calculated cross-sections for subsequent exchanges. Our simulations show that the median post-encounter orbit has eccentricity $e_f = 0.7$ (and approximately $d\sigma/de_f \propto e_f$), like that of PSR 2127+11C. The cross-section for exchange with recoil velocity in range dv_{rec} for such a binary (with $P_i = 8P_8$ h) gives a rate of reaction with heavy degenerate stars of $v_{in} = 10 v_{10} \text{ km s}^{-1}$ and density $n_d = 10^6 n_{d6} \text{ pc}^{-3}$ of

$$n_d(d\sigma/dv_{rec})v_{in} = 0.8(d\tilde{\sigma}/dv_{rec})P_8^{2/3}v_{10}^{-1}n_{d6} \text{ per } 10^{10} \text{ y}, \quad (3)$$

where $d\tilde{\sigma}/dv_{rec}$ is shown in Figure 3. Treating the bodies as point masses, the total cross-section for exchange is $\tilde{\sigma} = 7$. For $P_f = 8$ (12) h, recoil velocities exceeding 40, 50, and 65 km s^{-1} have $P_8^{2/3}\tilde{\sigma}(> v_{rec}) = 2.4$ (2.6), 1.4 (1.6), and 0.7 (0.5) respectively. Recoil velocities exceeding 70 km s^{-1} have negligible cross-section. Some 55% of the exchanges are affected by collisions between the main sequence star and one of the neutron stars (see Figure 3); all encounters leading to tidal interactions with the main-sequence star have cross-section $\tilde{\sigma} \sim 10$ (naïve extrapolation of results from encounters of bodies of equal mass^{10,11} would overestimate recoil velocities and the importance of tidal interactions, since exchange

of unequal masses results in significant expansion of the orbit). We note that recycled pulsars in exchange binaries will not have spins \mathbf{S} aligned with the binary orbital angular momentum \mathbf{L} (as expected in binaries where mass transferred from the companion spun up the pulsar). They are thus good candidates for observing geodetic precession of the pulsar spin. But exchanges do not destroy all memory of the initial binary. If $\mathbf{S} \parallel \mathbf{L}$ in the initial binary, some 65% of exchange binaries with high recoil speeds have $\mathbf{S} \cdot \mathbf{L} > 0$, since prograde encounters are more efficient than retrograde ones in hardening binaries.

The radial distribution of pulsars in M15 suggests that the half-mass radius of neutron stars (and other dark remnants of similar mass) is $r_{dh} = 0.2$ pc. The negative \dot{P} s of PSRs 2127+A,D require⁹ that the density of dark remnants rises more steeply than $n_d \propto r^{-2}$ from 0.2 pc to 0.1 pc, where $n_d(0.1 \text{ pc}) \simeq 10^6 \text{ pc}^{-3}$. That the density continues to rise to at least 10^7 pc^{-3} is suggested both by the apparently high velocity dispersion^{7,8} at < 0.05 pc, and by models of the post-core collapse evolution of clusters. These predict¹² that even during maximum expansion during core oscillations, the central density of heavy remnants $n_d(0) > 10^7 \text{ pc}^{-3}$. Binaries, being heavier, will sink to the core between encounters which eject them. Equation (3) shows that the time between encounters which eject the binaries at least as far as PSR 2127+11C is $\lesssim 10^9$ y. Since the mean number of such ejected binaries observed at any one time is

$$\langle N_{ej} \rangle \sim N_{\text{prog}} \langle n_d \rangle \sigma v_{in} T_{ej}, \quad (4)$$

where N_{prog} is the mean number of progenitor binaries in the core at any time, T_{ej} is the lifetime of the ejected binary, and $\langle n_d \rangle$ is the time-average density through which the progenitor binaries move. M15 contains $N_{\text{prog}} = 1$ LMXB, and $T_{ej} \gtrsim 10^8$ y (see Fig. 2), this scenario gives $\langle N_{ej} \rangle \gtrsim 0.1$. Given the uncertainties in the central density, it thus appears possible that PSR 2127+11C was ejected

in this way by an encounter between a heavy remnant and a LMXB. If so, not many more such systems will be found in M15 or the other ~ 20 post core collapse clusters¹³, which contain between them only 10 LMXBs.

The long periods of the pulsars found in M15 suggest that they may have been spun up not by gradual Roche-lobe overflow in a binary, but by accretion of the remains of a tidally disrupted star. If a fraction ϵ_{ak} of the accretion energy were absorbed in the disrupted remains and converted to kinetic energy, accretion of only $10^{-4}M_{\odot}/\epsilon_{ak}$ would unbind the rest of the material, yet provide enough to spin the neutron star (moment of inertia $10^{45}I_{45} \text{ g cm}^2$) up to equilibrium spin for periods

$$P > 50(\epsilon_{ak}/0.1)^{3/4}I_{45}^{3/4} \text{ ms.} \quad (5)$$

The lifetimes of such systems could be very short, $< 10^6$ y, permitting a rate of pulsar formation as high as 100 per 10^8 y while having an expectation value of < 1 system caught in the act (AC 211 may be a longer-lived system contributing negligibly to the pulsar birth-rate). This would resolve the discrepancy between the pulsar birthrate and that of LMXBs.¹⁴

We therefore consider the second possibility: that the pulsar was spun up by the remains of a disrupted star, and subsequently exchanged into a binary containing its present companion. Exchanges into binaries containing a heavy degenerate require, for $P_f = 11$ h, $P_i = 15$ h for $v_{rec} = 50 \text{ km s}^{-1}$ ($\bar{\sigma}(> v_{rec}) = 0.8$) and $P_i = 30$ h for $v_{rec} = 80 \text{ km s}^{-1}$ ($\bar{\sigma}(> v_{rec}) = 0.2$). The exchange rate is given by (3), but with the coefficient (which depends on the mass ratios) increased by a factor of 2.4. The initial eccentricity of the orbit affects $\bar{\sigma}$ only weakly. If not too eccentric, such initial binaries have lifetimes against gravitational radiation approaching the age of the universe. Binary-binary interactions have similar cross-sections and recoil velocities. The expected number of ejected systems is then

$\langle N_{ej} \rangle = N_{PSR} \langle n_{db} \rangle \sigma v_{in} T_{ej}$, where $\langle n_{db} \rangle$ is the time-average density of degenerate binaries through which the pulsars passed. Since $N_{PSR} \sim 3$ (we count only single pulsars in the dense core and as bright as PSR 2127+11C, because only they could give rise to that system), this scenario thus gives $\langle N_{ej} \rangle \simeq \langle n_{db} \rangle / 10^7 \text{ pc}^{-3}$. Relaxation will in their 10^8 y lifetime spread single pulsars over ~ 0.1 pc, where $\langle n_{db} \rangle \lesssim 10^6 \text{ pc}^{-3}$. Thus this scenario is much less probable than the LMXB scenario unless the inner 0.1 pc of M15 is composed largely of hard degenerate binaries.

The eclipsing binary pulsar PSR 1744–24A is located at a projected distance¹⁵ 1.0 pc from the center of Terzan 5. This cluster has $r_0 \sim 0.4$ pc, and a central density $\sim 10^{5.8} M_{\odot} \text{ pc}^{-3}$ (Djorgovski, personal communication). The probability that the binary has formed by recoil-less two-body capture at $> 2.5r_0$ is less than a few percent¹⁶. The recoil velocity required to eject PSR 1744–24A to its projected radius is $\sim 20 - 30 \text{ km s}^{-1}$. The timescale for dynamical friction to carry it back to the core is $\gtrsim 10^{7.5}$ y (Figure 2), and the time for gravitational radiation to bring its two components together is $\lesssim 2 \times 10^8$ y. It thus resembles in some ways PSR 2127+11C. However, its companion is of lower mass, and non-degenerate. Exchange reactions leaving a light star are improbable, especially if the lower central density of Terzan 5 is correct. For tidal capture to give sufficient recoil would require at least 20% of the main-sequence star's mass to be lost in a collimated jet. Existing hydrodynamic simulations^{17,18} seem to show much less mass loss, even for grazing collisions. Furthermore, cluster LMXB's with measured positions are all much closer to their clusters' cores¹⁹ (Liller 1 being a possible exception), suggesting that such asymmetric jets are not common.

It seems more likely either that PSR 1744–24A is a primordial binary hardened by an encounter with another star, or that it is the result of tidal capture during

an encounter between a main sequence star and a binary containing a neutron star. We find that in about 30% of such encounters the third star is unbound, and the tidal binary recoils with $\bar{\sigma}(v_{rec} > 30 \text{ km s}^{-1}) \sim 0.5$ for $P_i < 10 \text{ d}$. This latter process, having by far the largest cross-section, seems most likely if Terzan 5 is being supported against core collapse by a large population of primordial binaries²⁰.

Could PSR 1913+16, the Galactic twin of PSR 2127+11C, have been created in a globular cluster, with a recoil slightly larger, rather than slightly lower than the escape velocity? The seemingly large proper motion²¹ of PSR 1913+16, 140 km s^{-1} relative to its local standard of rest, is consistent with this hypothesis. Difficulties with scenarios for creating PSR 1913+16 in supernova explosions,²² make a cluster origin attractive. But the birth-rates pose a difficulty, however. PSR 1913+16, with lifetime $\sim 10^{8.5} \text{ y}$, was discovered in a survey covering 168 deg^2 along $1/20$ of the Galactic plane; the birthrate is thus $\sim 10^{-7} \text{ y}^{-1}$ if objects like it are found only within 300 pc of the Galactic plane. It lies at a (DM) distance of 6.5 kpc from the Galactic center. The vast majority of the clusters with high central density lie within a projected distance of 2.5 kpc of the Galactic center.¹³ A recoil velocity $v_{ej} > \sqrt{v_{ri}^2 + v_{esc}^2}$ would be required to escape (v_{esc}) one of these clusters, and then rise ($v_{ri} > 100 \text{ km s}^{-1}$) the required distance in the Galactic potential. Such recoil velocities cannot be obtained in physically reasonable three-body encounters, so it is unlikely that PSR 1913+16 could have been ejected from one of those clusters. Possible sources are thus the rare halo PCC clusters (like M15) or clusters of modest central density. Then objects like PSR 1913+16 could be found anywhere within $\sim 10 \text{ kpc}$ of the Galactic center, suggesting a birthrate $\sim 10^{-6.4} \text{ y}^{-1}$, which seems hard to maintain from the rare dense clusters at large Galactocentric radius. A birthrate an order of magnitude lower might be maintained, however, so we are reluctant to reject this idea using rates derived from

statistics of single objects. In any case, there are likely to be several systems like PSR 1913+16 in the inner 2.5 kpc of the Galaxy, ejected from the dense clusters there.

Recent U-band imaging from the Hubble Space Telescope²³ shows that M15 has $r_0 \approx 0.1$ pc, and Meylan, Dubath and Mayor (abstract, American Astronomical Society, 1991) find the central velocity dispersion to be nearly constant at 14 km s^{-1} , in contrast to ref. 8. The parameters chosen for Fig. 1 thus seem almost perfectly appropriate to M15.

Figure Captions

Fig. 1 The turning points of the orbit of a body ejected at speed v_{rec} from radius r_i in the core of a single-mass $W_0 = 12$ ($c = 2.74$) King²⁴ model cluster of core radius r_0 and line-of-sight central velocity dispersion σ . The form of the curve is independent of r_0 and W_0 for $r/r_0 \ll 100$. For PSR 2127+11C to reach its projected distance of 2.7 pc from the core of M15, it must have been ejected at $\gtrsim 50 \text{ km s}^{-1}$, a result confirmed by more sophisticated cluster models⁹.

Fig. 2 The timescale for dynamical friction to carry back to the core a star or binary system of mass M_b ejected with speed v_{rec} from radius r_i . The form of the curve is independent of r_0 for $r_i \gtrsim r_0$. The friction time on the ordinate is labeled for a heavy body of 10^{-5} the cluster mass, but scales inversely as the mass of the heavy body. The friction time is determined largely by the density at pericenter. Perpendicular velocity kicks from cluster stars passing on the outer reaches of the orbit can shift the pericenter of the nearly radial orbit of the ejected body, creating a *distribution* of sinking times with a tail extending to times much larger than indicated by the curve, which neglects such kicks. The width of this distribution of sinking times becomes significant for orbits with initial apocentric distances r_a more than $4(M_b + \langle m \rangle)/\langle m \rangle$ times the initial pericentric distance, where $\langle m \rangle$ is the mean mass of cluster stars encountered near r_a . The timescale for the binary pulsar 2127+11C to sink within M15 is $\sim 5 \times 10^7 (r_p/0.05 \text{ pc}) \text{ y}$. The timescale for the binary pulsar 1744-24A to sink within Terzan 5 is $\gtrsim 1 \times 10^8 \text{ y}$. Uncertainties in the cluster structure, the radii from which the binaries were ejected, and the true r_a make the estimates of sinking time uncertain to at least a factor of 5. Neither system's pericentric distance is likely to have been shifted substantially. Ejected pulsars are most likely to be found near the half-mass radius (3.5 pc for M15): convolution of Fig. 1 and 3 shows that few pulsars will be found beyond

the half-mass radius ($85r_0$), since only a narrow range of ejection velocities have apocentres there. Few will be found inside the half-mass radius, since friction will there rapidly drag them back to the core⁹.

Fig. 3 Differential cross section of binary recoil velocity for exchanges in which a passing heavy star is exchanged for the lightest star in a binary. The final binary consists of two stars of mass $1.0M_h$; the expelled star has mass $0.4M_h$. In the application envisaged here, $M_h = 1.4M_{\odot}$, appropriate for neutron stars or heavy white dwarfs. The initial binary is circular, with semi-major axis a ; v_c is defined in the text, and equals 273 km s^{-1} if the initial period $P_i = 8 \text{ h}$. The light star was treated as a point mass for the solid curve; the dashed and dotted curves show only exchanges in which collisions between a light star of finite radius and either of the heavy stars were avoided. If $P_i = 8 \text{ h}$, the two collision criteria respectively correspond to passage of a main sequence star of radius $R_* = 0.56R_{\odot}$, within $1.07R_*$ and $3.2R_*$ (within which tidal dissipation would modify the orbit) of one of the neutron stars. The total cross-section for heavy star exchanges which leave the light star in the binary is smaller by a factor of 6. The cross sections shown are based on Monte Carlo simulation of 1000 three-body interactions, all integrated to completion. 302 of the interactions contributed to the exchange channel shown here.

References

1. Charles, P.A. in *Topics in X-ray Astronomy, Proc. 23rd ESLAB Symp.*, ESA SP-296, Vol. 1, 129-137 (European Space Agency, Paris, 1989).
2. Shara, M.M., Moffat, A.F.J. & Potter, M. *Astron. J.*, **99**, 1858-1862 (1990).
3. Ilovaisky, S.A. in *Topics in X-ray Astronomy, Proc. 23rd ESLAB Symp.*, ESA SP-296, Vol. 1, 145-150 (1989).
4. Anderson, S.B., Gorham, P.W., Kulkarni, S.R., Prince, T.A. & Wolszczan, A. *Nature* **346**, 42-44.
5. Lugger, P.M., Cohn, H., Grindlay, J.E., Bailyn, C.D., & Hertz, P. *Astrophys. J.* **320**, 482-492 (1987).
6. Anderson, S.B., Kulkarni, S.R., Prince, T.A. & Wolszczan, A. *Nature* (submitted, 1990).
7. Seitzer, P., Peterson, R. & Cudworth, K. in *Dynamics of Dense Stellar Systems* (ed. D. Merritt) 153-156 (Cambridge Univ. Press, 1989).
8. Peterson, R.C, Seitzer, P. & Cudworth, K.M. *Astrophys. J.* **347**, 251-265 (1989).
9. Phinney, E.S. *Mon. Not. R. Astr. Soc.* (submitted, 1990).
10. McMillan, S.L.W. *Astrophys. J.* **306**, 552-564 (1986).
11. Hut, P. & Inagaki, S. *Astrophys. J.* **298**, 502-520 (1985).
12. Murphy, B.W., Cohn, H.N. & Hut, P. *Mon. Not. R. Astr. Soc.*, **245**, 335-349 (1990).
13. Chernoff, D.F. & Djorgovski, S. *Astrophys. J.* **339**, 904-918 (1989).

14. Kulkarni, S.R., Narayan, R. & Romani, R.W. *Astrophys. J.* **356**, 174-183 (1990).
15. Lyne, A.G., Manchester, N., D'Amico, N., Stavely-Smith, L., Johnston, S., Lim, J., Fruchter, A.S., Goss, W.M. & Frail, D. *Nature* **328**, 399 (1990).
16. Verbunt, F. & Meylan, G. *Astron. Astrophys.* **203**, 297-305 (1988).
17. Benz, W. & Hills, J.G. *Astrophys. J.* **323**, 614-628 (1987).
18. Ruffert, M. & Müller, E. *Astron. Astrophys.* **238**, 116 (1990).
19. Grindlay, J.E., Hertz, P., Steiner, J.E., Murray, S.S., & Lightman, A.P. *Astrophys. J.* **282**, L13-L16 (1984).
20. Goodman, J. & Hut, P. *Nature* **339**, 40-43 (1989).
21. Taylor, J.H. & Weisberg, J.M. *Astrophys. J.* **345**, 434-450 (1989).
22. Burrows, A. & Woosley, S. *Astrophys. J.* **308**, 680-684 (1986).
23. Lauer, T.R. *et al.* *Astrophys. J.* **369**, L45 (1991).
24. King, I.R. *Astron. J.*, **71**, 64-75 (1966).

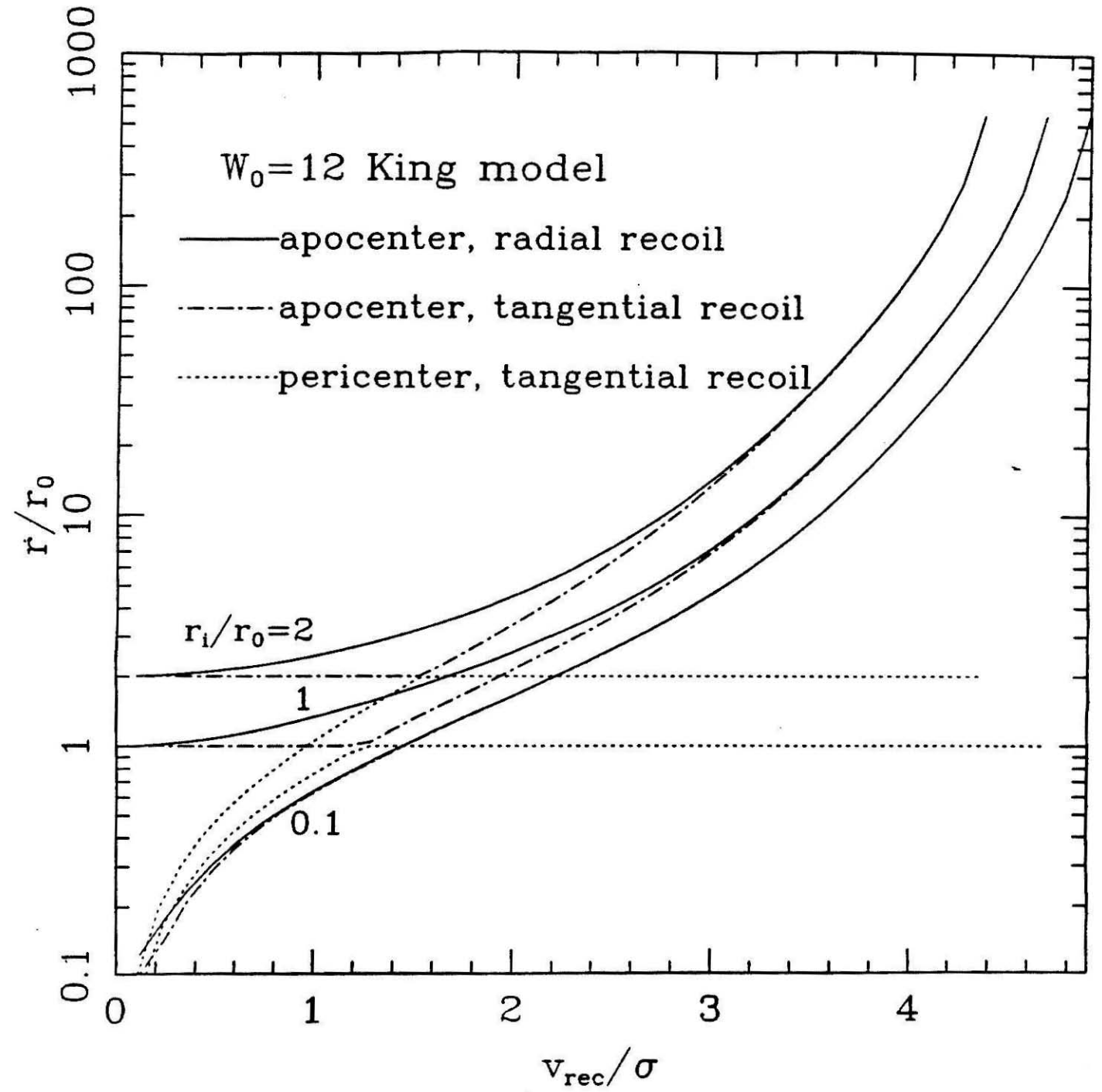


Figure 1

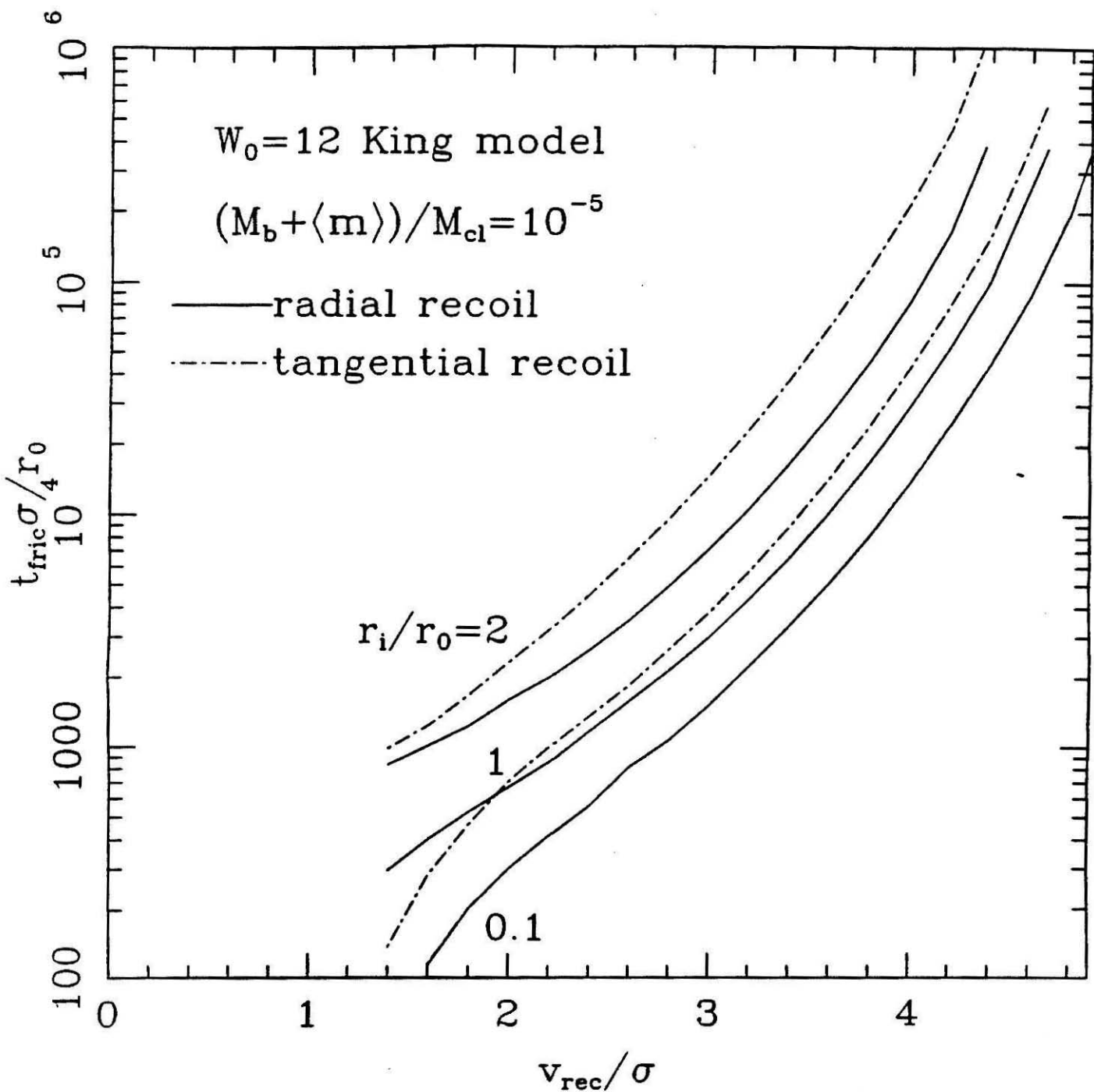


Figure 2

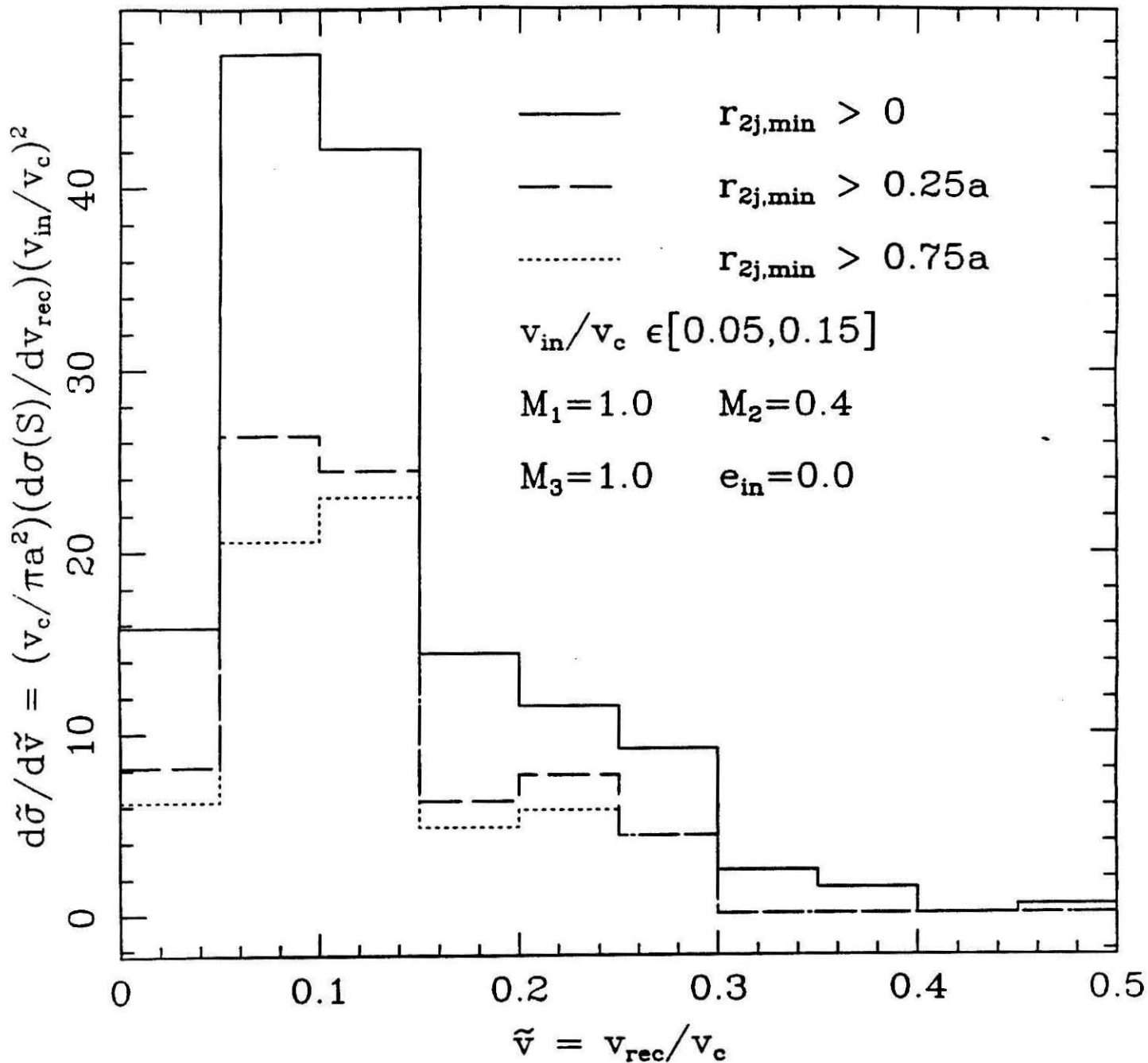
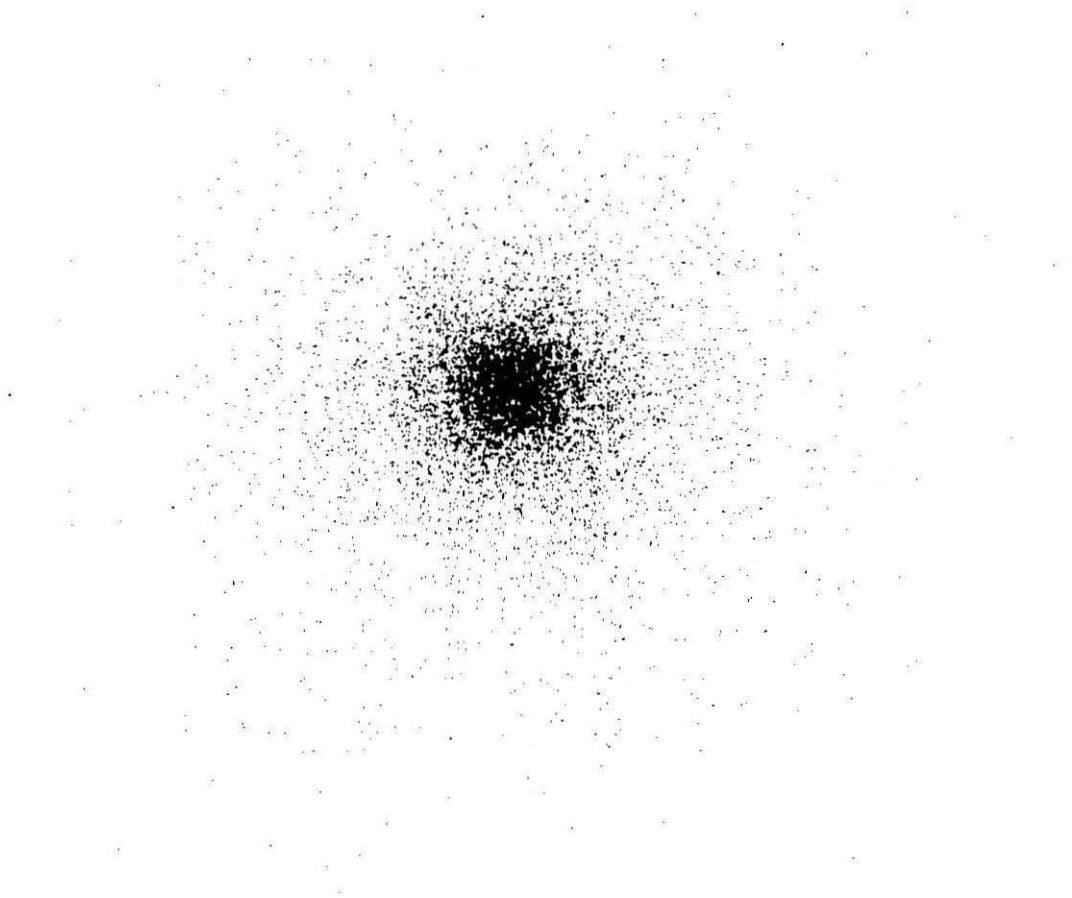
$$S:(1,2)+(3) \rightarrow (1,3)+(2)$$


Figure 3



Chapter 4

Dynamics of Binaries in Globular Clusters

in collaboration with

E.S. Phinney,

California Institute of Technology

To be submitted to the *Astrophysical Journal*

Abstract

The dynamical evolution of a test population of binaries, in a range of globular cluster models, is simulated. Three-body encounter probabilities are calculated, and actual encounters calculated explicitly by Monte Carlo simulations of the encounter parameters. Stars were assumed to have finite radii, permitting calculation of stellar collisions. Stellar mergers were assumed to be completely inelastic and an evaluation of the merged products was made. Heating rates for the cluster were calculated, as were collision rates and the final distribution of binary parameters. It is proposed that many of the pulsars observed in the globular cluster system were produced by three-body encounters involving neutron star collisions.

“When shall the stars be blown about the sky,
 Like the sparks blown out of a smithy and die?
 Surely thine hour has come, thy great wind blows,
 Far-off, most secret, and inviolate Rose?”

W.B. Yeats, *The Secret Rose*

1. Introduction

Globular clusters make possible observational tests of some of the basic ideas in many-body dynamics, and in recent decades substantial theoretical efforts have been made to understand collective phenomena in such systems. Recently, following the discovery of a preponderance of X-ray sources (Katz, 1975, Hertz and Grindlay, 1983, Hertz and Wood, 1985, Lewin and Joss, 1981), and, later, millisecond pulsars (Hamilton *et al.*, 1985, Lyne *et al.*, 1987) in Galactic globular clusters, it has become apparent that there is more to globular cluster dynamics than earlier models have allowed for. The dynamical evolution of globular clusters has attracted more interest, as a possible factor in explaining these discoveries.

It has long been appreciated that the static models of globular clusters developed (King, 1962, 1966, Michie, 1963, Michie and Bodenheimer, 1963) were an approximation, and that the gravothermal instability (Lynden-Bell and Wood, 1968, Katz, 1978) would inevitably lead to cluster mass segregation and core-collapse (Spitzer, 1987, Binney and Tremaine, 1987, and references therein). Extensive simulations of cluster evolution, initially with single mass models, later with more sophisticated multi-mass models, showed that core-collapse was apparently inevitable, and would occur typically in a few half-mass relaxation times (Spitzer and Hart, 1971b, Spitzer and Thuan, 1972, Cohn, 1979, Cohn, 1980, Murphy and Cohn, 1988). Observed cluster profiles suggested that a remarkable number

of clusters were very near core-collapse. Unless we live at a special time in the evolution of the Galaxy, this would appear, *a priori*, to be unlikely. The problem is obviated if core-collapse can be postponed or reversed; to do so requires an energy source to keep the core heated. Amongst the many possible energy sources for slowing core-collapse, binary interactions appear to be the most robust (Elson *et al.*, 1987, Goodman, 1989).

Approximating cluster stars as point masses must fail in the core-collapse limit. As the core density approaches infinity, the finite size of stars becomes important, and dissipative effects start to dominate stellar encounters. It was shown that the formation of hard binaries through three-body interactions and tidal capture, and the subsequent interactions of the binaries might halt and then reverse the collapse of the cluster core (Goodman, 1987, Statler *et al.*, 1987), albeit at very high central densities. If the core is dominated by degenerates, binary formation through three-body interactions dominates. However, binaries formed during core collapse cannot be part of the mechanism postponing core-collapse during the earlier evolutionary phases of the cluster. A possible energy source for postponing core-collapse would be the presence of primordial binaries (Hut, 1983c, Goodman and Hut, 1989).

The binary abundance in the Galaxy and halo has been estimated to be no less than 20%, and possibly as high as 50% (Abt, 1983, 1987, Latham, 1989). Our understanding of stellar formation is not sufficiently developed to state that the initial cluster binary abundance must be similar, but we cannot say with any confidence that there **cannot** have been a primordial binary population in the Galactic globular clusters. An early search for spectroscopic giant binaries found no evidence for the existence of a binary population in the globular clusters (Gunn and Griffin, 1979), but subsequent observations have found a number of binaries (Pryor *et al.*, 1985, 1989, 1990, Mateo *et al.*, 1990, Murphy *et al.*, 1991), and

current observations are consistent with a primordial binary abundance of 10% or more (Pryor, 1989). We will argue below that selection effects and binary dynamics conspire to decrease the number of observable binaries, and that the primordial binary abundance in globular clusters may have been as high as the observed Galactic abundance.

In addition to the intrinsic interest in the effect of cluster binaries on the structure and evolution of the cluster, the presence of a substantial primordial binary population may in large part account for the detection of a large number of X-ray sources and pulsars in Galactic globular clusters.

There are ten classic Low Mass X-ray Binaries (LMXBs) in the Galactic globular clusters (Lewin and Joss, 1981). Compared with a hundred odd in the Galaxy, the number of LMXBs per unit mass in the globular cluster system ($10/10^7 M_{\odot}$, compared to $100/10^{11} M_{\odot}$ in the Galaxy), the number of cluster LMXBs per unit mass appears quite excessive. The launch of *Rosat* has led to the discovery of more cluster X-ray sources, and there are indications that a number of faint, soft X-ray sources are also present in the clusters (Charles, 1989, Predehl *et al.*, 1991). LMXBs are thought to be progenitors of millisecond pulsars (MSPs), and it was soon realised that the abundance of LMXBs might indicate a similar excess of pulsars in clusters (Alpar *et al.*, 1982). The first cluster MSP was soon found (Hamilton *et al.*, 1985, Lyne *et al.*, 1987), and intense searches have now revealed a large number of MSPs and binary MSPs in clusters (Phinney and Kulkarni, 1991, van den Heuvel, 1991). In the Galaxy, a comparison of the inferred birthrates of LMXBs and MSPs suggested that there was an excess of MSPs relative to the LMXBs (Narayan *et al.*, 1990). In the globular clusters, this excess is also present, and possibly worse (Bailyn and Grindlay, 1990, Kulkarni *et al.*, 1990). It seems clear that another class of MSP progenitors may exist; in the Galaxy this second channel for MSP formation may be through massive Be stars (Verbunt,

1990), a channel that is not available in the globular cluster population; a different mechanism for MSP formation must be invoked for the cluster pulsars.

Millisecond pulsars are thought to be old neutron stars that have been recycled, spun up again to short periods, most likely by accreting of order $0.1M_{\odot}$ of matter (van den Heuvel *et al.*, 1986, Verbunt *et al.*, 1987, Phinney and Kulkarni, 1991). That there are neutron stars in globular clusters is evident from the observation of MSPs. As there is no star formation taking place currently in Galactic globular clusters, the neutron stars must be primordial, or, possibly, recently formed by accretion induced collapse (AIC) of heavy white dwarfs (Michel, 1987, Grindlay and Bailyn, 1988). In either instance mass transfer must have taken place recently: if the MSP ancestors are dead, primordial neutron stars, they must accrete to spin up; if the MSP ancestors are heavy white dwarfs, they must accrete to pass over the Chandrasekhar limit (Nomoto and Kondo, 1991). LMXBs are believed to be accreting neutron stars, and hence are good candidates for being the progenitors of at least some millisecond pulsars. The hard tidal capture binaries thought to form during core-collapse are an obvious source of LMXBs; if the star captured is a neutron star, it will be captured in an orbit likely to lead to mass transfer; if the captor is a main-sequence star near turnoff, or a (sub)giant, as is relatively probable in a globular cluster, stellar evolution will also drive mass transfer onto the neutron stars, again leading to a LMXB (Verbunt, 1990). Indeed, five of ten classic cluster LMXBs are in clusters thought to have undergone core-collapse (Djorgovski, private communication); four of the the remaining LMXBs are in very dense clusters, which may have gone through core-collapse. Of the two recently reported sources discovered by *Rosat* (Predehl *et al.*, 1991), one is in a core collapsed cluster, the other is in a dense, possibly core collapsed cluster. The LMXBs have long inferred lifetimes; and consequently low inferred birthrates, they are also readily detectable in even the most distant

cluster. Although many LMXBs are transient, and may not have been observed in their on-state, this does not affect the birthrate argument, as they presumably also do not accrete in the off-state. There are now twenty-nine reported MSPs in the Galactic globular clusters (van den Heuvel, 1991, Manchester *et al.*, 1991). MSPs are hard to detect (Johnston and Kulkarni, 1991, Johnston *et al.*, 1991b). Allowing for selection effects, an enormous population of cluster pulsars is inferred. A number of MSPs have been found in relatively low density clusters (Kulkarni *et al.*, 1990b), in proportions far in excess of those expected from the two body tidal capture scenario (Fruchter and Goss, 1990, Johnston *et al.*, 1991b, Phinney and Kulkarni, 1991).

A possible solution of the MSP birthrate problem is presented by a population of primordial binaries. A binary in a background of stars will undergo occasional close encounters with the field stars. The outcome of such encounters depends, among other things, on the total center-of-mass energy of the three-body system (Heggie, 1975, Hills, 1975a,b, Hut and Bahcall, 1983), parametrised by the ratio of the relative velocity at infinity and a critical velocity, v_∞/v_c . Crudely, for $v_\infty/v_c > 1$, energy is transferred to the binary, for $v_\infty/v_c < 1$ energy is transferred to the field star. In globular clusters, $v_\infty \sim 10 \text{ km s}^{-1}$. An encounter may lead to a change of state in the binary: the original binary may emerge intact with different eccentricity and semi-major axis; one of the members of the binary may be exchanged, leaving the field star as a member of the new binary; there may be tidal encounter or collision between a pair of stars, or it may be ionized if $v_\infty/v_c \geq 1$. For encounters with $v_\infty/v_c < 1$, the encounter may be resonant (Hut and Bahcall, 1983). Collisions are relatively probable during resonant encounters. Cross-sections for various encounter scenarios have been calculated and tabulated extensively (Heggie, 1975, Hills, 1975a,b, Hills and Fullerton, 1980, Fullerton and Hills, 1982, Hut and Bahcall, 1983, Hut, 1983a, Hut and Inagaki, 1985, Mikkola,

1983, 1984a,b, McMillan, 1986, Rappaport *et al.*, 1990, Leonard, 1989, Leonard and Fahlman, 1991, Hut, 1990, Sigurdsson and Phinney, 1991). Of particular interest in globular clusters are encounters leading to stellar collisions. A neutron star (or white dwarf) colliding with a main-sequence star or a (sub)giant is likely to disrupt the star leaving a thick disk around the degenerate (Finzi, 1978, Krolik *et al.*, 1984, Benz *et al.*, 1987, 1989, 1990, Ruffert and Müller, 1990, Davies *et al.*, 1991, Rasio and Shapiro, 1991, Goodman and Hernquist, 1991). Before the disk is disrupted, a substantial amount of matter may accrete onto the degenerate at a very high rate. It is possible that enough matter may be accreted to spin the neutron star up to a MSP (Type I encounters, as classified by Kochanek (1991)). If the accretion is rapid enough, the LMXB lifetime problem is circumvented. In the case of a white dwarf, it is not clear if accretion past the Chandrasekhar limit is possible, and if so, whether a neutron star is formed at that point (Verbunt *et al.*, 1989). Main-sequence star mergers through this channel may, at least in part, account for the “blue stragglers” observed in globular clusters (Leonard, 1989, Leonard and Fahlman, 1991). The cross-section for three-body encounters is more weakly dependent on the core density than the two-body tidal capture scenario, and is consistent with observation (Fruchter and Goss, 1990, Johnston *et al.*, 1991b, Phinney and Kulkarni, 1991). In addition, the time evolving distribution of binary parameters affects the encounter rate, as we attempt to elucidate in part in this paper.

As a cluster collapses, the core density increases, and the binary encounter rate increases. For the stellar mass-ratios expected in cluster binaries, encounters tend to provide positive feedback in the initial stages, leading to an increasing encounter rate, as some binaries are softened, absorbing energy from the cluster. Later in the evolution of the cluster, binaries undergo exchanges which both widen the binary and increase gravitational focusing (Chapter 2), increasing the encounter

(and exchange) rate. As the density increases, this feedback is negated, as binaries start to be disrupted by collisions, or become hard enough that encounters lead to the binaries being ejected on wide, eccentric orbits about the cluster core (Phinney and Sigurdsson, 1991). At all stages up to the disruption of the cluster, a residue of binaries will still be making excursions to the cluster core for the first time, having resided in the cluster halo, with relaxation times of the order of the Hubble time. The energy input from the binaries will slow down the cluster collapse, postponing core-collapse. As the remaining binaries harden, the encounter rate decreases, and each encounter becomes more likely to eject the binary from the core, reducing the energy input from the binaries. Adjusting to the reduced energy input, the core contracts and core-collapse continues.

In this paper, we consider the explicit time evolution of a population of test binaries in a fixed cluster background. A comparison between the collision rate in different cluster models is obtained, as is the expected energy input to the cluster due to binary encounters. Previous estimates of the energy input from binaries have been made from analytic approximations and averaged cross-section (Murphy *et al.*, 1990, Gao *et al.*, 1991) and did not allow for the feedback as binaries undergo rate enhancing encounters, nor the actual probability distribution of encounter parameters, as detailed below. Though our treatment of binary-single star encounters is exact, it should be pointed out that we do not allow for binary-binary encounters. To include a binary population would increase the number of mass groups (N_m) to $O(N_m^2)$, and the computation effort by a corresponding factor. Further, the equilibrium distribution of the binaries is not known, and for dense clusters is most likely dependent on the binary semi-major axis. We hope that our calculations will provide information enabling binary-binary interactions to be included in a consistent manner in future simulations. We note that stable hierarchical tr binaries formed in binary-binary encounters

may be an important collision channel in moderate density clusters, and should be accounted for in a complete cluster simulation.

2. Cluster models

The binaries were evolved in a fixed background cluster model, defined by the density profile $n(\mathbf{r})$ of its stars of mass m_α . The model can be adapted for any density profiles and associated gravitational potential and velocity distribution functions. In this paper we consider simple equilibrium multi-mass Michie–King models only. Future calculations will consider evolution in a more general model, including time varying density distributions.

We follow Binney & Tremaine (1987), and consider a cluster specified by a distribution function, $f^{(N)}(\mathbf{w}_i, t)$, consisting of N particles indexed by i , with phase space coordinates $\mathbf{w}_i = (\mathbf{x}_i, \mathbf{v}_i)$ at time t . The distribution function is normalised,

$$\int f^{(N)}(\mathbf{w}_i, t) d\mathbf{w}_i = 1, \quad (2.1)$$

and obeys a continuity equation,

$$\frac{\partial f^{(N)}}{\partial t} + \sum_{i=1}^N \left[\frac{\partial}{\partial \mathbf{x}_i} \left(f^{(N)} \frac{d\mathbf{x}_i}{dt} \right) + \frac{\partial}{\partial \mathbf{v}_i} \left(f^{(N)} \frac{d\mathbf{v}_i}{dt} \right) \right] = \Gamma(f), \quad (2.2)$$

where $\Gamma(f)$ allows for the time variation in f due to encounters. For conservative forces, with potential Φ ,

$$\frac{d\mathbf{v}_i}{dt} = -\frac{\partial \Phi}{\partial \mathbf{x}_i}, \quad (2.3)$$

and,

$$\frac{d\mathbf{x}_i}{dt} = \mathbf{v}_i, \quad (2.4)$$

this reduces to,

$$\frac{df^{(N)}}{dt} = \frac{\partial f^{(N)}}{\partial t} + \sum_{i=1}^N \left[\mathbf{v}_i \cdot \frac{\partial f^{(N)}}{\partial \mathbf{x}_i} - \frac{\partial \Phi}{\partial \mathbf{x}_i} \cdot \frac{\partial f^{(N)}}{\partial \mathbf{v}_i} \right] = 0. \quad (2.5)$$

The one particle distribution function, $f = f^{(1)}$ is defined by

$$f = \int f^{(N)}(\mathbf{w}_1, \mathbf{w}_2, \dots, \mathbf{w}_N) d\mathbf{w}_2 \dots \mathbf{w}_N, \quad (2.6)$$

and the local spatial density of stars, n , is given by

$$n(\mathbf{x}) = \int f(\mathbf{x}, \mathbf{v}) d^3\mathbf{v}. \quad (2.7)$$

Poisson's equation,

$$\nabla^2\Phi(\mathbf{x}) = 4\pi G\rho(\mathbf{x}), \quad (2.8)$$

relates the local mass density of stars, ρ and the potential Φ .

In general, we considered cluster models defined by one particle distribution functions $f_\alpha(\mathbf{x}, \mathbf{v}, m_\alpha)$, for a discrete set of mass groups, m_α , $\alpha = 1, \dots, N_m$, with corresponding local number densities, n_α , and mass densities, ρ_α . Initially we considered analytic, static models for the distribution function; later we hope to develop more consistent models with a time varying distribution function. In particular, in this paper, we only consider multi-mass Michie-King models,

$$f_\alpha(\varepsilon, \mathbf{J}) = \frac{n_{1_\alpha}}{(2\pi\sigma_\alpha^2)^{3/2}} e^{-\mathbf{J}^2/2r_a^2\sigma_\alpha^2} \left[e^{\varepsilon/\sigma_\alpha^2} - 1 \right], \quad (2.9)$$

where σ_α^2 is the core dispersion of mass group α . r_a , the anisotropy radius, defines at what radius the anisotropy in the distribution becomes significant. \mathbf{J} is the angular momentum of the particle relative to the cluster center-of-mass, and $\varepsilon = -\Phi - \frac{1}{2}m_\alpha v^2$ is the energy of the particle in the cluster center-of-mass frame. n_{1_α} are normalising constants to be determined later. Since $\rho_\alpha = m_\alpha n_\alpha$, we define number and mass total densities, $n(\mathbf{x}) = \sum n_\alpha(\mathbf{x})$, $\rho(\mathbf{x}) = \sum \rho_\alpha(\mathbf{x})$, and mean core mass \bar{m}_c and mean core dispersion, $\bar{\sigma}^2$,

$$\begin{aligned} \bar{m}_c &= \rho_0^{-1} \sum_{\alpha=1}^{N_m} m_\alpha \rho_\alpha(0) \\ \bar{m}_c \bar{\sigma}^2 &= m_\alpha \sigma_\alpha^2, \end{aligned} \quad (2.10)$$

where $\rho_0 = \rho(0)$. Hence we define a scale radius r_0 , analogous to the King radius in single mass King models,

$$r_0 = \sqrt{\frac{9\bar{\sigma}^2}{4\pi G\rho_0}}. \quad (2.11)$$

Each mass group is then scaled independently with scale radius

$$r_{0\alpha} = \sqrt{\frac{\tilde{m}_c}{m_\alpha}} r_0. \quad (2.12)$$

The models reduce to single mass King models for $r_a = \infty$, $N_m = 1$. As a check of the consistency of our code we verified that the models created did indeed reduce exactly to the corresponding King models in that limit. For the current set of numerical calculations, we take $r_a = \infty$, in part to reduce the computing effort needed, mainly because the physical processes of interest are not expected to be sensitive to anisotropy in the halo, such as are observed in real clusters.

This class of models assumes a relaxed distribution of particles in near thermal equilibrium in the core, with a spherically symmetric spatial distribution truncated at some radius, r_t . We define a new potential, $\Psi(r) = \Phi(r_t) - \Phi(r)$. Note reversal of sign, $\nabla\Psi = -4\pi G\rho$. Following the King model analogy, we define a dimensionless parameter, $W_0 = \Psi(0)/\bar{\sigma}^2$, and concentration $c = \log_{10}(r_t/r_0)$. The total mass of the cluster, M , is then given by

$$-\nabla\Psi(r_t) = \frac{GM}{r_t^2}. \quad (2.13)$$

To obtain realistic cluster models, we need to solve for $n_{1\alpha}$ and r_t , given r_0 , W_0 , $n(0) = n_0$, m_α , M and $\bar{\sigma}^2$. In practise, not all the quantities are independent, and some are scale invariant. We pick scale $n_0 = 1$, $r_0 = 1$, and $\bar{\sigma}^2 = 1$, and choose W_0 as an independent parameter determining r_t/r_0 , for the given initial mass function. Our choice of n_0 and $\bar{\sigma}^2$ then uniquely determines M and r_0 in physical units.

To solve for $n_{1\alpha}$ and r_t , we must decide a cluster mass function and the relative abundance of each mass group. The current set of calculations assumes a Salpeter IMF,

$$\frac{dN_*}{dm_*} \propto m_*^{-1-x_*}, \quad (2.14)$$

with canonical value $x_* = 1.35$, though we also considered values of x_* over the range $1.0 \leq x_* \leq 3.5$. In the current calculation, the zero age main-sequence number fraction of each mass group was calculated for a mass range, typically $0.1M_\odot \leq m_* \leq 15M_\odot$. A turnoff mass was selected, $0.8M_\odot$; stars below the turnoff mass were assumed not to evolve significantly on the time scale of the simulation, stars above the turnoff were assumed to have evolved completely before the start of the simulation. Later simulations will allow for explicit stellar evolution during the dynamical evolution. Other initial mass functions, such as Meylan's flat IMF (Meylan, 1988), were also considered.

Stars with mass above the turnoff mass, but below some critical mass, $m_{wd} (= 4.7M_\odot)$, were assumed to have evolved to white dwarfs of mass $0.58 + 0.22 \times (m_* - 1.0)M_\odot$, while stars above mass m_{wd} but below some critical mass, $m_I (= 8.0M_\odot)$, were assumed to disrupt completely; stars with mass greater than m_I , but less than m_{bh} , were assumed to become neutron stars of mass approximately $1.4M_\odot$. For the current set of simulations, $m_{bh} = m_{max} = 15M_\odot$, and our cluster models do not contain black holes; future calculations will include black holes for comparison of the dynamics. Stars with mass greater than m_{bh} would be assumed to become few solar mass black holes (Chernoff and Weinberg, 1990). For the purposes of the current set of simulations, all evolved stars were assumed to have been retained in the cluster; in practise some fraction is expected to be ejected, in particular a substantial fraction of the neutron stars may be ejected. Bins for mass groups were set by hand; the current simulations use the same binning used in Phinney (1991) and Murphy and Phinney (1991). The mass fraction and number fraction, η_α , in each bin were calculated by integrating the evolved initial mass function.

To solve for $n_{1\alpha}$, we followed the method of Da Costa and Freeman (1976, see also Gunn and Griffin, 1979). A trial solution $n_{1\alpha} = \eta_\alpha$ was used, the cluster

model integrated, the actual number fraction of each mass group in the cluster,

$$N_\alpha = 4\pi \int_0^{r_t} n(r) r^2 dr, \quad (2.15)$$

was calculated and compared with η_α ; a new solution

$$n_{1_\alpha} = n_{1_\alpha} \times \left(\frac{\eta_\alpha}{N_\alpha} \right)^j, \quad (2.16)$$

$j = 1$, was then substituted, and the integration iterated. For a few cluster models, with extreme values of the cluster parameters, linear iteration failed to converge, the iteration getting caught in a bistable (or multistable) solution, so after a certain number of iterations, typically 50 or 100, we set $j = j/2$, and continued the iteration. This guarantees convergence to the local fixed point of the iteration.

To integrate the cluster model, we integrated for Ψ in radial coordinates $\xi = \log_{10} (1 + r^2/r_0^2)$, with implicit scaling $n(0) = 1$, $\bar{\sigma}^2 = 1$. Substituting equation 2.9 into equation 2.7, and using equation 2.11, we obtain

$$\begin{aligned} \frac{d}{d\xi} \left[\left(\frac{2(e^\xi - 1)^{3/2}}{e^\xi} \right) \frac{d}{d\xi} \right] \Psi(\xi) = - \sum_\alpha \frac{e^\xi (e^\xi - 1)^{1/2}}{2} 9n_{1_\alpha} \frac{1}{\bar{\rho}_\alpha} \\ \times \left[e^{\frac{\Psi(\xi)}{\sigma_\alpha^2}} \operatorname{erf} \left(\sqrt{\frac{\Psi(\xi)}{\sigma_\alpha^2}} \right) - \sqrt{\frac{4\Psi(\xi)}{\pi\sigma_\alpha^2}} \left(1 + \frac{2\Psi(\xi)}{3\sigma_\alpha^2} \right) \right], \end{aligned} \quad (2.17)$$

where $\bar{\rho}_\alpha$ are normalising constants,

$$\bar{\rho}_\alpha = \frac{\bar{m}_c}{m_\alpha} \left[\operatorname{erf} \left(\sqrt{\frac{\Psi(0)}{\sigma_\alpha^2}} \right) e^{\frac{\Psi(0)}{\sigma_\alpha^2}} - \sqrt{\frac{4\Psi(0)}{\pi\sigma_\alpha^2}} \left(1 + \frac{2\Psi(0)}{3\sigma_\alpha^2} \right) \right]. \quad (2.18)$$

For isotropic Michie–King models, an analytic expression can be obtained for the integral in equation 2.7, as above. Equation 2.17 was integrated using a simple leapfrog integrator with boundary conditions $\Psi(0) = W_0$, and $\nabla\Psi(0) = 0$ (in practise the integration was started at finite r with $\nabla\Psi(\delta r) \propto \delta r$). ξ was incremented

in variable steps up to $r = r_t$, defined by $\Psi(r = r_t) = 0$. Stepsize was proportional to r for $r < 1$, and constant in ξ for $r > 1$, providing the highest density of steps near $r = 0$ and near the core boundary. Typically the converged model required $O(10^2)$ integration steps, although the intermediate integrations often required more integration steps. The model was considered to have converged when $\max |1 - \eta_\alpha/N_\alpha| < \delta (= 10^{-3})$. Cluster parameters were not found to be sensitive to δ for small δ , nor was there significant variation in the cluster parameters when the integration step was reduced by an order of magnitude, indicating that a robust solution had been found. After convergence, $n(r)$, $\Psi(r)$ and $\nabla\Psi(r)$ were saved, as were each of $n_\alpha(r)$. A cubic spline fit was also made to each of the quantities above (using standard IMSL spline fitting routines), and the breakpoints and coefficients for each fit were saved for future use. In addition the mass density, $\rho_\alpha(r)$ and the projected surface density $\Sigma_\alpha(r)$ were calculated and saved. Density profiles obtained were compared with previous published calculations (Gunn and Griffin, 1979, Da Costa and Freeman, 1976, Meylan, 1988) and were found to be in good agreement, providing an additional test of the models. The half mass radius r_h was also calculated, as was the dispersion profile, $\sigma_\alpha^2(r)$. Given a luminosity function, a surface brightness profile can be constructed. Model luminosity functions assuming the light profile is dominated by giants indicated that the core radius, r_c , ($\Sigma_L(r_c) = \Sigma_L(0)/2$), was typically somewhat less than the scale radius r_0 , approaching equality for more concentrated models and flatter IMFs.

A set of models was constructed by choosing W_0 and an initial mass function. The density profiles and concentrations were calculated, and comparison with real cluster profiles was made, selecting appropriate n_0 and $\bar{\sigma}^2$, in an attempt to reproduce observed core radii, core dispersion and cluster concentrations. A number of cluster models were used, chosen to be somewhat representative of the clusters M3, M13, M15 and 47Tuc. In the case of M15, the cluster was fit to the

core profile (Lauer *et al.*, 1991), requiring a very high concentration model that probably fits the outer parts of the cluster poorly. Reasonable models were fit to M3 and M13 data, while several models were run for 47Tuc to get comparative interaction rates, and estimates of the number of pulsars that might be produced. We assumed the luminosity profile was dominated by (sub)giants. The choice of IMF was dictated by recent results from pulsar acceleration limits (Phinney, 1991), in particular for 47Tuc we chose not to use the models fit by Meylan (1989), in anticipation that they underestimate the number of neutron stars in the core. Measurements of pulsar period derivatives in the near future should severely constrain the cluster mass function. The high mean core mass flattens the giant core profile, forcing a choice of larger W_0 to reproduce the observed concentration.

3. Dynamics

3.1. Initial Conditions

An ensemble of binaries was evolved in model clusters, for a fixed length of time, using a cluster of DECstation 3100s. We evolved binaries of mass $m_b (= m_1 + m_2)$, eccentricity e , semi-major axis, a , in a fixed background potential, $\Psi(r)$, as calculated in the previous section. The binary masses were drawn independently and at random from the initial mass function, with a proviso that we may require $m_i > m_{i_{min}}$, and specify the stellar type. The initial eccentricity was selected from a distribution, $P(e) = 2e$, except that we required any binary containing a (sub)giant to have initial $e = 0$, irrespective of binary period or evolutionary stage of the giant. Observations suggest that Population II binaries with orbital periods less than 10 days also have $e = 0$ (Abt, 1983), but as any encounter will perturb the eccentricity away from zero, we decided not to impose that condition. The semi-major axis was selected from a uniform $\log(a)$ distribution, $a_{min} \leq a \leq a_{max}$. After selecting $m_{1,2}$, the stellar type was determined (main-sequence, giant/subgiant, white dwarf or neutron star) by comparing a random number with the fractional abundance of each stellar type in that mass-group. The stellar type was coded with an integer flag, and the stellar radius, R_* , was calculated. We assumed

$$R_* = \beta \left(\frac{m_\alpha}{M_\odot} \right)^\alpha R_{\odot}, \quad (3.1)$$

with $\alpha = 1.0 = \beta$ for main-sequence stars, $\alpha = -1/3$, $\beta = 0.0162$ for white dwarfs (Shapiro and Teukolsky, 1983), and $\alpha = 0.0 = \beta$ for neutron stars.

As we did not allow for explicit stellar evolution, (sub)giants were assumed to occur with constant probability for any star in the turnoff mass group ($0.63M_\odot \geq m \geq 0.8M_\odot$). The total probability of a star in that mass group being a (sub)giant

was assumed to be 0.095 (fraction of cluster age (sub)giant of that mass lasts), with a distribution of stellar radius such that $t(R_* > R) \propto R^{-3/2}$. Assuming a giant lifetime of 4.7×10^7 years for $R = 10R_\odot$, (Fahlman *et al.*, 1985), for a power-law IMF we get a probability distribution for the fraction of stars in the turnoff mass group with radius $> R$, f_g ,

$$f_g(R_* > R) = \frac{4.7 \times 10^7}{7 \times 10^{10}} \frac{0.8^{-1-x_*}}{\frac{1}{x_*}((0.63^{-x_*}) - (0.8^{-x_*}))} \left(\frac{R_*}{10R_\odot}\right)^{-3/2} \quad (3.2)$$

After calculating the stellar radius, if $2(R_{*1} + R_{*2}) \leq a(1 - e)$, we required $a = a + f_c(R_{*1} + R_{*2})/(1 - e)$, in order to avoid immediate merger of the stars. For most runs, $f_c = 2 < f_t$; this was deliberate in anticipation that an encounter with a contact binary ($a \leq f_t(R_{*1} + R_{*2})$) would perturb the binary sufficiently for the system to undergo an energetic event. In the absence of a better understanding of binary formation we assumed the binary members may be picked independently from the evolved IMF (Tout, 1991), but we note that in practise binary masses may be correlated; in particular, mass transfer in the protostar phase, and during giant evolution for binaries containing evolved stars, may bias the mass function.

The binary was placed in the cluster at radius, r , selected from the density distribution, $\rho_\alpha(r)$, of one of the mass groups, with velocity, v , picked from the local dispersion for that mass group. Both the initial positions and velocities were assumed to be isotropic in the cluster center-of-mass frame. The initial distribution was deliberately chosen not to be the relaxed equilibrium distribution of stars mass m_b , in order to permit the binaries to relax naturally. To pick the velocity, the peak of the velocity distribution was estimated,

$$\max_v f_\alpha(v) = f_\alpha(v_m),$$

for the mass group chosen, with

$$\begin{aligned} v'^2 &= 2 \left(1 - e^{-\frac{\Psi(r)}{2\sigma_\alpha^2}} \right) \\ v_m^2 &= 2 \left(1 - e^{\frac{v'^2}{2} - \frac{\Psi(r)}{2\sigma_\alpha^2}} \right), \end{aligned} \tag{3.3}$$

and a velocity was chosen from the distribution by Monte–Carlo selection, scaled down by the relative mass of the binary.

The binaries were evolved in the cluster center–of–mass frame according to

$$\ddot{\mathbf{r}} = \nabla\Psi(r) + \mathbf{a}_{\text{dyf}} + \mathbf{a}_{\text{kick}}, \tag{3.4}$$

where $\nabla\Psi(r)$ is the potential gradient due to the mass interior to r , \mathbf{a}_{dyf} is the dynamical friction experienced by the binary, and \mathbf{a}_{kick} is the effective acceleration due to scattering by individual stars in the cluster. The dynamical friction experienced by the binary is due to the drag on the binary from the perturbed distribution of stars in the cluster; it acts to circularize cluster orbits, and tends to cause binaries with masses larger than \bar{m}_c to sink towards the cluster core (Binney and Tremaine, 1987, Chandrasekhar, 1943). The kicks are due to the fluctuating force felt by the binary due to inhomogeneities in the actual stellar distribution. The kicks are time averaged, and a large kick may be due to a single close encounter or the cumulative effect of many smaller perturbations from distant stars. The kicks tend to increase the eccentricity of the orbit in the cluster, and to eject stars from the core. For binaries, close encounters will strongly perturb the binary orbit, and significant energy transfer may take place, sufficient to eject one or both of the binary and encountered star from the cluster. We calculate the effects of such close encounters separately and explicitly.

To calculate \mathbf{a}_{dyf} and \mathbf{a}_{kick} , we first calculated the diffusion coefficients, $D(\Delta(v_i))$, $D(\Delta v_i \Delta v_j)$ (Binney and Tremaine, 1987). We consider a local orthonormal basis, $\{\hat{\xi}, \hat{\zeta}, \hat{\eta}\}$, relative to the binary, defined by the binary’s position,

\mathbf{r} , and velocity, \mathbf{v} , in the cluster center-of-mass frame, with unit vectors

$$\begin{aligned}\hat{\xi} &= \frac{\mathbf{v}}{v} \\ \hat{\zeta} &= \frac{\mathbf{r} \times \mathbf{v}}{|\mathbf{r} \times \mathbf{v}|} \\ \hat{\eta} &= \frac{(\mathbf{r} \cdot \mathbf{v})\mathbf{v} - v^2\mathbf{r}}{v\sqrt{r^2v^2 - (\mathbf{r} \cdot \mathbf{v})^2}},\end{aligned}\tag{3.5}$$

$\mathbf{r} = \{x, y, z\}$, $\mathbf{v} = \{v_x, v_y, v_z\}$, then force components along the $\hat{\xi}$ direction are parallel to the binary's direction of motion, and $\hat{\zeta}$, $\hat{\eta}$ define two equivalent (by symmetry) components perpendicular to the direction of motion. Hence we have three independent diffusion coefficients, $D(\Delta v_{\parallel})$, $D(\Delta v_{\parallel}^2)$ and $D(\Delta v_{\perp}^2)$.

Defining

$$\mu = \frac{4\pi GM}{9 r_0 \bar{\sigma}^2},\tag{3.6}$$

we find

$$\begin{aligned}\mathbf{a}_{\text{dyf}} &= D(\Delta v_{\parallel}) \\ &= \sum_{\alpha} \frac{81}{4\pi} \frac{(m_b + m_{\alpha})}{M} \mu \ln(\Lambda) \frac{1}{v^2} \frac{1}{\bar{\rho}_{\alpha}} \\ &\quad \times \left(\operatorname{erf}\left(\frac{v}{\sqrt{2}\sigma_{\alpha}}\right) e^{\frac{\Psi}{\sigma_{\alpha}^2}} - \frac{v}{\sigma_{\alpha}} e^{\frac{\Psi}{\sigma_{\alpha}^2} - \frac{v^2}{2\sigma_{\alpha}^2}} - \frac{1}{3} \left(\frac{v}{\sigma_{\alpha}}\right)^3 \right),\end{aligned}\tag{3.7}$$

where $\ln \Lambda \sim 10$ is the Coulomb logarithm. Some care must be maintained in evaluating \mathbf{a}_{dyf} near turning points in the orbit, as finite precision in evaluating the integral to double precision can produce sign errors in the dynamical friction, especially at evaluations of intermediate steps in the integration step, leading to spurious systematic expansion of the orbit in the cluster. This can be a serious problem for nearly radial trajectories, integrated with maximal timesteps, as is necessary to complete the calculation in finite time. To deal with the underflow, the dynamical friction can either be set to zero, or the sign reversed. As the magnitude of the dynamical friction is always small when a sign error may occur,

either method is adequate. The other two components are given by

$$\begin{aligned}
D(\Delta v_{\parallel}^2) &= \sum_{\alpha} \frac{27}{\sqrt{2\pi}} \frac{m_{\alpha}}{M} \mu \ln(\Lambda) \frac{1}{v} \frac{1}{\tilde{\rho}_{\alpha}} \\
&\quad \times \left(\frac{3}{2} \sqrt{2\pi} \frac{\sigma_{\alpha}^2}{v^2} \operatorname{erf}\left(\frac{v}{\sqrt{2\sigma_{\alpha}^2}}\right) e^{\frac{\Psi}{\sigma_{\alpha}^2}} - 3 \frac{\sigma_{\alpha}}{v} e^{\frac{\Psi}{\sigma_{\alpha}^2} - \frac{v^2}{2\sigma_{\alpha}^2}} \right. \\
&\quad \left. - \frac{v}{\sigma_{\alpha}} \left(\frac{\Psi}{\sigma_{\alpha}^2} - \frac{3}{10} \frac{v^2}{\sigma_{\alpha}^2} + 1 \right) \right), \\
D(\Delta v_{\perp}^2) &= \sum_{\alpha} \frac{81}{\sqrt{2\pi}} \frac{m_{\alpha}}{M} \mu \ln(\Lambda) \frac{1}{v} \frac{1}{\tilde{\rho}_{\alpha}} \\
&\quad \times \left(\sqrt{\frac{\pi}{2}} \left(1 - \frac{\sigma_{\alpha}^2}{v^2} \right) \operatorname{erf}\left(\frac{v}{\sqrt{2\sigma_{\alpha}^2}}\right) e^{\frac{\Psi}{\sigma_{\alpha}^2}} + \frac{\sigma_{\alpha}}{v} e^{\frac{\Psi}{\sigma_{\alpha}^2} - \frac{v^2}{2\sigma_{\alpha}^2}} \right. \\
&\quad \left. - \frac{2}{3} \frac{v}{\sigma_{\alpha}} \left(\frac{\Psi}{\sigma_{\alpha}^2} - \frac{1}{10} \frac{v^2}{\sigma_{\alpha}^2} + 1 \right) \right).
\end{aligned} \tag{3.8}$$

We model \mathbf{a}_{kick} by random fluctuations in velocity, $\Delta \mathbf{v}$,

$$\mathbf{a}_{\text{kick}} = \frac{\Delta \mathbf{v}}{\Delta t}, \tag{3.9}$$

with

$$\begin{aligned}
\Delta v_{\parallel}^2 &= \varsigma_i^2 (D(\Delta v_{\parallel}^2) \Delta t) \\
\Delta v_{\perp}^2 &= \varsigma_i^2 (D(\Delta v_{\perp}^2) \Delta t),
\end{aligned} \tag{3.10}$$

where ς_i is a random number of mean 0, standard deviation 1, chosen here from a normal distribution. Assuming isotropy, in our coordinate system, this becomes

$$\begin{aligned}
\Delta v_{\xi} &= \varsigma_i \sqrt{D(\Delta v_{\parallel}^2) \Delta t} \\
\Delta v_{\zeta} &= \varsigma_i \sqrt{\frac{1}{2} D(\Delta v_{\perp}^2) \Delta t} \\
\Delta v_{\eta} &= \varsigma_i \sqrt{\frac{1}{2} D(\Delta v_{\perp}^2) \Delta t},
\end{aligned} \tag{3.11}$$

transforming to the cluster center-of-mass coordinates, we find directly the ran-

dom fluctuations in velocity,

$$\begin{aligned}
\Delta v_x &= \Delta v_\xi \frac{v_x}{v} + \Delta v_\eta \frac{(\mathbf{r} \cdot \mathbf{v})v_x - v^2 x}{v\sqrt{r^2 v^2 - (\mathbf{r} \cdot \mathbf{v})^2}} + \Delta v_\zeta \frac{y v_z - z v_y}{\sqrt{r^2 v^2 - (\mathbf{r} \cdot \mathbf{v})^2}} \\
\Delta v_y &= \Delta v_\xi \frac{v_y}{v} + \Delta v_\eta \frac{(\mathbf{r} \cdot \mathbf{v})v_y - v^2 y}{v\sqrt{r^2 v^2 - (\mathbf{r} \cdot \mathbf{v})^2}} + \Delta v_\zeta \frac{z v_x - x v_z}{\sqrt{r^2 v^2 - (\mathbf{r} \cdot \mathbf{v})^2}} \\
\Delta v_z &= \Delta v_\xi \frac{v_z}{v} + \Delta v_\eta \frac{(\mathbf{r} \cdot \mathbf{v})v_z - v^2 z}{v\sqrt{r^2 v^2 - (\mathbf{r} \cdot \mathbf{v})^2}} + \Delta v_\zeta \frac{x v_y - y v_x}{\sqrt{r^2 v^2 - (\mathbf{r} \cdot \mathbf{v})^2}}.
\end{aligned} \tag{3.12}$$

The trajectory of the binary was integrated in the cluster center-of-mass frame, using a 4th order Runge-Kutta integrator with quality control. The integrator only integrated the smooth force components, $\nabla\Psi$ and \mathbf{a}_{dyf} ; the contributions from the random kicks were added after each integration step. With the random kicks added, the quality control on the integrator need not be very stringent, which shortens integration time significantly. To check the accuracy of the integrator, it was run with both dynamical friction and kicks set to zero, and the stability of orbits in the cluster was confirmed; quality control was set to be sufficient to prevent any drift in the orbits. The integration time scale follows naturally from the units selected, $t_{\text{scale}} = r_0/\bar{\sigma}$; typical integration times were 10^{10} years, requiring $10^6/t_n$ integration steps or more. The time step used was variable,

$$\Delta t = \epsilon t_n \left(\frac{1.0 + r}{1.0 + v} \right), \tag{3.13}$$

where $\epsilon \approx 0.1$, and $t_n \geq 1$ is a time scaling factor, used to allow faster integration by integrating “super-orbits” rather than real orbits. If $t_n \neq 1$ the $\nabla\Psi$ contribution to the force was integrated as if $t_n = 1$, with the contribution due to dynamical friction and kicks scaled as t_n and $\sqrt{t_n}$ respectively. The assumption is that each orbit is representing an average over t_n , orbits with secular perturbations scaled appropriately. In order to integrate a sufficiently large sample of binaries for a sufficiently long time, we chose $t_n \sim 20 - 30$. Care must be taken

with t_n large, or the kicks become large compared to the smooth force components. In practise, with a normal distribution of kicks, a few binaries were kicked into escape trajectories during runs with $t_n \gg 10$, so an additional requirement that $\Delta v_{x,y,z} < \max\{v/5, \delta\}$ was added, effectively truncating the normal distribution of ς . The truncation could not be proportional to v for very small v , lest heavy binaries freeze in the core, after settling by dynamical friction, which is unphysical, and causes numerical pathologies. Binaries could still escape through a succession of kicks, or, by recoil from encounters leading to the binary hardening substantially. We also noted a small fraction of the binaries on radial orbits were kicked onto trajectories beyond the half-mass radius, and the pericenter of the orbit then kicked out to several core radii before dynamical friction could reduce the apocenter significantly, at which point the relaxation time for the trajectory was typically longer than the integration time.

3.2. Encounters

At each step of the binary's trajectory, the probability of an encounter with a field star, mass m_α , $P_\alpha(r, t)$, was evaluated. To calculate P_α , we integrated over the local field star velocity distribution, $f_\alpha(r, v)$, calculating the probability that a field star is on a trajectory with pericenter p relative to the binary's center of mass. We say an encounter has occurred if $p \leq sa$ for some value $s (= C + D(1 + e))$, $D = 4$, $C = 0.6$) (Hut and Bahcall, 1983). An encounter is specified by the pericenter, the relative velocity at infinity between the binary and the field star, and the phase angles of the binary and the field star relative to the binary axis. An encounter was selected by picking a random number, uniformly distributed on $[0, 1]$, and comparing it with $P = \sum_\alpha P_\alpha$. If P was greater than or equal to the random number, an encounter was deemed to have occurred. Calculating P_α is the most computing intensive task in the simulation. $v(r)$ is not uniquely defined, due to the

varying angular momentum of the trajectory from dynamical friction and kicks, and hence $P(r, v)$ must be calculated at each point in the trajectory. Tabulation of $P(r, v)$ was considered, but as the integral could be evaluated in closed form for the distribution chosen, it was more economical to evaluate it explicitly. For more general distribution functions it would probably be better to tabulate $P(r, v)$, and only calculate the partial integrals as needed. To calculate P , we calculated the rate of encounters, R ,

$$\begin{aligned} R(r, v) &= \sum_{\alpha} \int n_{\alpha}(r) \sigma(\mathbf{v}, \mathbf{v}_*) |\mathbf{v} - \mathbf{v}_*| f_{\alpha}(\mathbf{v}_*) d^3 \mathbf{v}_* \\ &= \sum_{\alpha} n_{\alpha}(r) I_{\alpha}, \end{aligned} \quad (3.14)$$

with encounter cross-section, $\sigma(\mathbf{v}, \mathbf{v}_*)$, given by

$$\sigma(\mathbf{v}, \mathbf{v}_*) = \pi(sa)^2 + \frac{2\pi G(m_b + m_{\alpha})(sa)}{|\mathbf{v} - \mathbf{v}_*|^2}, \quad (3.15)$$

and

$$P(r, v) = \Delta t R(r, v) \quad \text{for } \Delta t R(r, v) \ll 1. \quad (3.16)$$

Assuming isotropic velocity distribution, we find

$$\begin{aligned} I_{\alpha} &= \int_0^{v_{\alpha}} \sigma(\mathbf{v}, \mathbf{v}_*) |\mathbf{v} - \mathbf{v}_*| f_{\alpha}(v_*) v_*^2 dv_* \\ &= \frac{8\pi^2}{3} (sa)^2 v^2 [I_1 + I_2] + 8\pi^2 G(m_b + m_{\alpha})(sa) [I_3 + I_4] \end{aligned} \quad (3.17)$$

where I_i are given by

$$\begin{aligned} I_1 &= \int_0^{\min\{v, v_{\alpha}\}} \frac{v_*^2}{v} \left(3 + \left(\frac{v_*}{v} \right)^2 \right) f_{\alpha}(v_*) dv_* \\ I_2 &= \Theta(v_{\alpha} - v) \int_v^{v_{\alpha}} v_* \left(1 + 3 \left(\frac{v_*}{v} \right)^2 \right) f_{\alpha}(v_*) dv_* \\ I_3 &= \int_0^{\min\{v, v_{\alpha}\}} \frac{v_*^2}{v} f_{\alpha}(v_*) dv_* \\ I_4 &= \Theta(v_{\alpha} - v) \int_v^{v_{\alpha}} v_* f_{\alpha}(v_*) dv_*, \end{aligned} \quad (3.18)$$

where $\Theta(x)$ is the Heaviside function,

$$\Theta(x) = \begin{cases} 0, & \text{if } x < 0; \\ 1, & \text{if } x \geq 0. \end{cases} \quad (3.19)$$

For the isotropic Michie model we can calculate I_i analytically. The integration was carried out using Mathematica, with the results checked using Macsyma and by hand. Defining

$$\begin{aligned} \mu_\alpha &= \frac{m_\alpha}{i\tilde{m}_c} \\ C_\alpha &= \frac{n_{1\alpha}\mu_\alpha^{3/2}}{(2\pi)^{3/2}} \\ W(r) &= \frac{\Psi(r)}{\bar{\sigma}^2} \end{aligned} \quad (3.20)$$

note that $\mu_\alpha W(r) = \Psi(r)/\sigma_\alpha^2$ with $v_0 = \min\{v, v_\alpha\}$, we obtain

$$\begin{aligned} I_1 &= \frac{C_\alpha}{v^3} \left[3\sqrt{\frac{\pi}{2}} \frac{1}{\mu_\alpha^{5/2}} \operatorname{erf}\left(\sqrt{\frac{\pi}{2}}v_0\right) e^{\mu_\alpha W(r)} \right. \\ &\quad \left. - \frac{v_0}{\mu_\alpha} \left(v_0^2 + \frac{3}{\mu_\alpha}\right) e^{\mu_\alpha W(r) - \frac{1}{2}\mu_\alpha v_0^2} - \frac{v_0^5}{5} \right] + 3I_3 \\ I_2 &= \Theta(v_\alpha - v) C_\alpha \left[\frac{v^2}{4} - \frac{v_\alpha^4}{4v^2} + \frac{1}{\mu_\alpha v} \left(\frac{2}{\mu_\alpha v} + v\right) e^{\mu_\alpha W(r) - \frac{1}{2}\mu_\alpha v^2} \right. \\ &\quad \left. - \frac{1}{\mu_\alpha v} \left(\frac{2}{\mu_\alpha v} + \frac{v_\alpha^2}{v}\right) e^{\mu_\alpha W(r) - \frac{1}{2}\mu_\alpha v_\alpha^2} \right] + I_4 \\ I_3 &= \frac{C_\alpha}{v} \left[\sqrt{\frac{\pi}{2}} \frac{1}{\mu_\alpha^{3/2}} \operatorname{erf}\left(\sqrt{\frac{\pi}{2}}v_0\right) e^{\mu_\alpha W(r)} - \frac{v_0}{\mu_\alpha} e^{\mu_\alpha W(r) - \frac{1}{2}\mu_\alpha v_0^2} - \frac{v_0^3}{3} \right] \\ I_4 &= \Theta(v_\alpha - v) C_\alpha \left[\frac{v^2}{2} - \frac{v_\alpha^2}{2} + \frac{1}{\mu_\alpha} \left(e^{\mu_\alpha W(r) - \frac{1}{2}\mu_\alpha v^2} - e^{\mu_\alpha W(r) - \frac{1}{2}\mu_\alpha v_\alpha^2} \right) \right]. \end{aligned} \quad (3.21)$$

At each integration step, $P(v_\alpha = \sqrt{2\Psi(r)})$ was calculated. If an encounter was deemed to have occurred, then $P_\alpha(v_\alpha)$ was evaluated as a function of v_α . Which mass group the encounter involves was determined by comparing the fractional probability of $P_\alpha(v_\alpha = \sqrt{2\Psi(r)})$ with the total probability of the encounter taking place, and then v_α was determined by comparing the fractional probability of encounter taking place at different v_α , for that mass group.

Given v_α , we chose the relative velocity, $v_\infty = |\mathbf{v} - \mathbf{v}_*|$, and hence the impact parameter such that $p \leq sa$. We define χ to be the angle between \mathbf{v}_α and \mathbf{v} ,

$$\cos \chi = \frac{\mathbf{v} \cdot \mathbf{v}_\alpha}{vv_\alpha}. \quad (3.22)$$

For the isotropic Michie distribution function, an analytic expression for $\chi \in [0, \pi]$ can be found. We picked a random number ς_i , uniform on $[0, 1]$, and chose χ from

$$\varsigma_i = \frac{R(\chi|m_\alpha, v_\alpha)}{R(\pi|m_\alpha, v_\alpha)}. \quad (3.23)$$

Integrating, and defining some auxiliary variables,

$$\begin{aligned} c_0 &= |v - v_\alpha| \\ c_1 &= |v + v_\alpha| \\ \beta &= \frac{2G(m_b + m_\alpha)}{sa} \\ \gamma &= -c_0(1 - \varsigma_i)(c_0^2 + \beta) - c_1\varsigma_i(c_1^2 + \beta), \end{aligned} \quad (3.24)$$

we find after some algebra, that χ satisfies

$$t^3 + \beta t + \gamma = 0, \quad (3.25)$$

where $t = \sqrt{v^2 + v_\alpha^2 - 2vv_\alpha \cos \chi}$, and hence

$$\cos \chi = \left[\frac{(A + B)^2 - (v^2 + v_\alpha^2)}{-2vv_\alpha} \right], \quad (3.26)$$

where $A + B$ is the solution of the cubic,

$$\begin{aligned} t &= A + B \\ A &= \sqrt[3]{-\frac{\gamma}{2} + \sqrt{\frac{\gamma^2}{4} + \frac{\beta^3}{27}}} \\ B &= -\sqrt[3]{\frac{\gamma}{2} + \sqrt{\frac{\gamma^2}{4} + \frac{\beta^3}{27}}}. \end{aligned} \quad (3.27)$$

Knowing v_∞ , and the maximum pericenter, we calculated the maximum impact parameter, adjusted for gravitational focusing. Given the maximum impact parameter, we picked the actual impact parameter, distributed uniformly in the area of the beam provided by the maximum permitted impact parameter. The beam is symmetric about the axis between the binary and the field star, and a phase angle for the approaching field star was picked at random, as was the angle of the binary axis relative to the axis joining the stars. Given the field star mass group, the field star stellar type and radius R_{*3} were set, using the same algorithm used to select the radii and stellar type of the binary members. It should be noted that the collision probability per integration step was typically less than the range of built-in random number generators in most computers ($1/(2^{31} - 1)$ for DEC3100s), and to get a reliable encounter rate the random number range must be extended. We used a uniform conditional probability distribution providing a smooth distribution to less than 10^{-14} , which was sufficient for our purposes. If the random number chosen was less than 10^{-7} , the probability was scaled up by 10^7 , and a new random number was drawn uniformly on the interval $(0, 1)$, and compared with the scaled encounter probability. This provides independent uniform sampling to less than 10^{-14} , provided the random number generator has no sampling correlations.

Having chosen an impact parameter, relative velocity and phase angle, the encounter was integrated explicitly, using the three-body integration scheme described in Sigurdsson & Phinney (1991). The binary parameters and the relative velocity were scaled to units where $a = 1$, and the three-body trajectory was calculated explicitly until resolved, or the number of integration steps exceeded a fixed maximum ($= 2 \times 10^6$ steps; previous calculations indicated that a very small proportion of encounters required more than 10^6 steps). Every 20,000 integration steps the state of the system was checked to see if the encounter was

resolved. Explicit provision was made for tidal encounters leading to a merger, merger being assumed if the separation between any pair of stars was less than $f_t \times (R_{*i} + R_{*j})$, $f_t \approx 3.1$ (Lee and Ostriker, 1986). If a merger occurred, the orbital parameters of the resulting system were calculated, assuming an impulsive merger of the two stars, and no mass loss. The stellar type and radius of the merged star were also determined. If the resulting system was bound, the new binary was returned to the cluster for further integration. After each encounter was complete, the final state binary was returned to the main integrator for further integration. If no binary existed after the encounter (system was ionized, or merged leaving the third star unbound) the run was halted and a new binary was picked. If a binary was available for integration, its position in the cluster was updated assuming linear extrapolation of the binary's pre-encounter velocity in the cluster center-of-mass frame, and the velocity in the cluster was adjusted to allow for the outcome of the interaction. For very soft binaries on orbits well outside the core, the encounter rate was dominated by softening encounters with the lowest mass stars. To avoid spending excessive computing time on these gradual ionizations, a binary was arbitrarily considered to be effectively ionized if its semi-major axis exceeded $1.2 \times \max\{a_i, a_{max}(= 10 AU)\}$, as ionization for binaries that wide is virtually inevitable, and collisions during encounters are very unlikely for a binary like that. It is possible that a small number of exchanges were missed because of this scheme. The integration of the binary trajectory in the cluster center-of-mass was then continued for the time specified, at which point the final state of the binary was saved and a new binary was picked. A typical run consisted of 100–350 binaries, with evolution times from 5×10^8 years to 10^{10} years, less concentrated clusters being evolved for longer times.

4. Results

Simulations were run using six cluster models, the parameters of which are listed in Tables 1 and 2. Sample cluster profiles are illustrated in Figures 1a and b. The model parameters were chosen with consideration of the Galactic globular clusters M13 (Model 1), M3 (Model 2) 47Tuc (Models 3–5) and M15 (Model 6). Cluster models were fit to the core radii, the concentration, the central luminosity and the core dispersion. With a given IMF, it is not possible in general to fit all observables exactly with a multi-mass King model. The core radius, r_c , is a fixed function of the scale radius, r_0 , for a given luminosity function, and $r_0 \propto \bar{\sigma}^{3/2}/\rho_0$, and increasing the core density to match the observed luminosity requires either increasing the dispersion, or accepting a smaller calculated core radius. Flattening the IMF initially increases r_0 , as \bar{m}_c increases and the (sub)giant core profile flattens. Flattening the IMF too much, however, increases the proportion of dark remnants in the core and reduces the number fraction in the core of (sub)giants, requiring a further increase in the core density to maintain the core luminosity, reducing the core radius. The problem can be circumvented by either changing the luminosity function, using a different shape IMF, or appealing to the as yet undetermined dynamical effects of a substantial binary core population. We chose the latter. Using multi-mass models results in a choice of W_0 larger than the comparable single-mass models. For the clusters M3 and M13, an error during the fit led to the clusters' luminosity profiles being fit to mass-group 6 rather than mass-group 8, the (sub)giant group. As a consequence, the clusters are somewhat underluminous and have smaller core radii and concentrations than observations would indicate, but the models calculated are still representative of an interesting set of cluster parameters, perhaps more representative of M5 or NGC6569. For

the M15 model we chose a very concentrated model, hoping to match the core profile, being primarily interested in the binary core population dynamics.

47Tuc could not be adequately fit with a Salpeter IMF, multi-mass King model. Meylan (1989) chose a broken IMF to obtain a reasonable fit to 47Tuc, the model essentially makes the current epoch (sub)giant population a preferred mass range, the IMF being flat for $M_* < 0.63 M_\odot$, and steep for all evolved stars. We chose not to use this IMF, in part because it is implausible, *a priori*, that the current turnoff mass should be special in primordial star formation, and in part because Meylan's model only has from 0.01% to 0.5% of the cluster mass in neutron stars, which would appear unlikely in view of the pulsar population (Manchester *et al.*, 1991). In particular, a 0.01% neutron star population implies a total of less than 100 neutron stars in the cluster, compared to the eleven pulsars observed. To model 47Tuc we considered three models bracketing the parameters of the observed cluster. Model 3 is definitely underdense and somewhat underluminous; Model 5 is overdense, and has a higher dispersion and smaller core than observed; Model 4 is probably the closest approximation to the real cluster, but is underluminous, has a slightly smaller core and slightly higher dispersion than the one observed.

The relative encounter probabilities for a sample of trajectories in some of the models are shown in Figures 2–14. The mean cluster encounter rate is dominated by the stars in the core, and, in general, the most probable encounter is with a neutron star or a white dwarf. For trajectories lying entirely outside the core, the total encounter probability is small, and invariably dominated by the lowest mass stars. Thus, even very wide binaries are liable to be hardened if outside the core. The critical velocity, v_c , is given by

$$v_c = \sqrt{GM_S \frac{m_1 m_2 (m_1 + m_2 + m_3)}{m_3 (m_1 + m_2)} \frac{1}{a}}, \quad (4.1)$$

and if $m_3 < m_{1,2}$ v_c increases rapidly. Binaries that would ionize in the core are hardened in the halo. This is in contrast with the single-mass models in which ionization of wide binaries is considerably more efficient, whereas in the multi-mass models the wide binaries may harden sufficiently through encounters with low mass stars in the outskirts of the cluster, and become “hard” by the time they reach the core through dynamical friction, where they have an appreciable chance of encountering the more massive stars.

We define a notation for the encounters, similar to that in Sigurdsson and Phinney (1991). For flybys and exchanges, we define X_i , by $X_1 : (1, 2) + (3) \rightarrow (1, 2) + (3)$, $X_2 : (1, 2) + (3) \rightarrow (1) + (2, 3)$ and $X_3 : (1, 2) + (3) \rightarrow (1, 3) + (2)$. For collisions, we define C_i , by $C_1 : (1, 2) + (3) \rightarrow (1 + 2) + (3)$, $C_2 : (1, 2) + (3) \rightarrow (3 + 2) + (1)$, $C_3 : (1, 2) + (3) \rightarrow (3 + 1) + (2)$, $C_4 : (1, 2) + (3) \rightarrow ((1 + 2), (3))$, $C_5 : (1, 2) + (3) \rightarrow ((3 + 2), (1))$, $C_6 : (1, 2) + (3) \rightarrow ((3 + 1), (2))$, respectively. Unresolved resonances are denoted by a R . Tables 5a–g give the various encounter parameters and outcomes.

The rate of various processes, X , $\Gamma(X)$, is estimated by,

$$\Gamma = f_b(f_r)f_w \frac{n_R}{N_b} N_* \frac{\tau}{T}, \quad (4.2)$$

where f_b is the binary fraction of the cluster (adjusted from the primordial fraction for the range of semi-major axis under consideration, allowing for ionization and hardening), $f_b \sim 0.1 - 0.5$, f_r is the retention rate for the stellar types considered, assumed unity for all except neutron stars, f_w is the binary weight, as shown in Table 3, n_R is the rate observed out of N_b simulations computed, $N_* \sim 10^6$ is the total number of stars in the cluster, and τ is the mean lifetime of the observable result of the process (*e.g.*, pulsar or blue straggler), compared to the duration of the simulation, T . For example, for run 5.1.1, considering pulsar formation, $f_w = 0.046$, $n_R/N_b = 3/100$, assume $f_b = 0.2$ and $f_r = 0.33$, and $N_* = 3 \times 10^6$,

then if a bright recycled pulsar is visible for $\tau = 5 \times 10^8$ years, and $T = 5 \times 10^9$ years, we find $\Gamma(\#PSR) = 27$, sufficient to account for the number observed, for a reasonable set of cluster parameters. As noted previously, Model 5 is probably denser than 47Tuc, in comparison, for runs 4.3.1 and 2 the same calculation gives $\Gamma = 1$, strongly suggesting the real cluster is intermediate between the two models. The rate calculated must be used with some care, as the binary parameters input are not necessarily representative of a real cluster. In particular, the numbers of short period, high eccentricity binaries is likely high, as is the number of contact binaries. However, in a concentrated cluster a number of such binaries will form during the evolution of the cluster, by binary encounters and orbital evolution, so it is not valid to eliminate such binaries from the model either. The actual collision rate is higher than calculated, as a consequence of the calculation of many of the most interesting encounters being terminated during an extended resonance. This is unavoidable, as following the resonances further is prohibitively demanding of computer time. This is partly compensated for by the fact that all tidal encounters are assumed to lead to merger, whereas in practise maybe only half merge. Calculation of the exact rate must await a complete sampling of the collision parameters by hydrodynamical calculations. Parenthetically, note the eccentricity algorithm setting the eccentricity of binaries containing giants to zero, was inadvertently triggered by some heavy white dwarf and neutron star containing binaries for which the minimum primary mass was greater than the giant mass, resulting in a number of hard zero-eccentricity binaries, as seen in Table 5.

The outcome of the various runs is shown in Table 4 and Figures 16–17. The mean energy transfer per binary was evaluated, and is tabulated in Table 4. The energy transfer is positive if energy is transferred from the binary to the cluster,

i.e., the binary binding energy becomes more negative. Ionized binaries were considered to have zero final binding energy. If a binary collided at any stage during its evolution it was excluded from the energy transfer calculation. This biases the result to underestimate the heating, as many of these binaries underwent substantial hardening before colliding. However, some of those were in turn softened or ionized subsequently, thus contributing to the cooling, and some were ejected from the cluster producing radiative cooling of the core, partly compensating for the underestimate. Another bias is produced by the unresolved encounters, of which there were a several, particularly in runs 4.2.2, 5.2.1 and 6.1.1. The resonant encounters were of two types, true resonances, involving neutron stars and white dwarfs in hard binaries, and unstable hierarchial triples in wide eccentric orbits, which may involve non-degenerate stars. Such resonant encounters are likely to be with hard binaries that might have provided substantial heating had the encounter been resolved. Thus, the mean heating rate is underestimated, particularly for Models 5 and 6.

For Models 1, 2, 3 the mean energy transfer per binary is small and is unlikely to have a significant effect upon the evolution of the cluster. For the other runs a significant mean heating rate was found, large enough that the binary heating may hold off core collapse in Models 4 and 5, and reverse core collapse in Model 6. As expected, run 6.2.1 had a negligible heating rate, but in run 6.2.2 the heating rate was surprisingly high, due to a couple of binaries that reached the core and started hardening. The low heating rate in runs 4.2.2, 4.3.1 and 4.3.2 is due to the large number of ionizations in those runs; in a real cluster the binaries ionized would probably have been ionized earlier in the evolution of the cluster. The low heating rate in runs 3.3.1 and 3.4.1 may be due to the choice of too small a a_{max} . The heating rate is sensitive to the initial binary population assumed and the implicit assumptions made about the past dynamical evolution of those binaries.

For calculation of general cross-sections for energy transfer the reader is referred to Sigurdsson and Phinney (1991).

The binaries chosen in this set of runs were all heavier than the turnoff mass-group (excepting run 2.3.1, which was run to obtain a comparison of light binary relaxation), and are thus expected to mass segregate, concentrating to a greater extent than the visible component of the cluster, except to the extent that some of the turnoff stars may themselves be in binaries. Even for binaries initially beyond the half-mass radius, the mass segregation was noticeable, in part because a proportion of those binaries were on elliptical orbits with pericentre inside the half-mass radius where the relaxation time becomes shorter, in part because the relaxation time for binaries with mass $> \bar{m}_c$ is shorter than Hubble time, even beyond the half-mass radius (see Gunn and Griffin, 1979, for discussion of the dependence of the relaxation time on mass). The binaries that drifted beyond the tidal radius are of some concern, although we note that physically they may still be bound to the cluster and would re-enter. With the form of the kicks chosen a binary will have $\Delta v/v \sim 1$, due to kicks, in the course of about 100 orbits, and a binary at the tidal radius will orbit the cluster order 100 times in a Hubble time, so the proportion that exit the cluster would appear not to be unreasonable. It would appear that even in moderate density clusters like M3, the binaries containing (sub)giants and a companion star massive enough to produce an observable velocity variation in the (sub)giant, will have segregated efficiently to the core. We note that most binary searches are performed beyond the half-mass radius, due to problems with crowding in the core, in particular Gunn and Griffin's search contained mostly (sub)giants in the halo of M3. In the more concentrated clusters, no (sub)giant binaries should survive in the core (noting that giant binaries must have semi-major axis of order 0.1 AU or more in order for the companion star to survive the evolution of the giant). Test runs

showed that light binaries were uninteresting for our immediate purpose, as they do not segregate efficiently, and thus spend little time in the core; they provide less gravitational focusing and thus have smaller encounter rates; they are easily ionized at fixed semi-major axis, and thus the probability of a resonant encounter is less, and they are not observable in real clusters. We do note that light binaries play a role in post-core collapsed clusters, such as our Model 6, by providing fresh moderately wide binaries to the core as the light binaries in the halo diffuse in and exchange heavy field stars into the binary, leading to a more rapid drift to the core through stronger dynamical friction, and thus a higher exchange rate, until the new binary is ejected or undergoes a collision. This is illustrated in run 6.2.2, where a 42 day light main-sequence star binary reached the core, a neutron star was exchanged into the binary, producing a high eccentricity 18 day binary, releasing $14 kT$ in the process, mostly in the recoil of the main-sequence star ejected. The ejected star recoiled at $5\bar{\sigma}$, insufficient to escape from the cluster, placing it on a very radial orbit.

In the high interaction rate clusters there were a significant number of ejections past the half-mass radius, that then started relaxing again to the core, and out of the cluster. This is illustrated in Figures 16a-h and 17a-p. Binaries ejected with an apocentre less than the half-mass radius will segregate back to the core in a few core relaxation times (see Phinney and Sigurdsson, 1991, Phinney, 1991), in particular a neutron star binary ejected short of the half-mass radius during an exchange or a collision, will relax back to the core in a time scale comparable to the lifetime of the pulsar. Binaries that contain neutron stars that were ionized during or after a collision remain in the core. Thus we expect most single pulsars to remain in the core of the binary, as will any wide binary pulsars. The exceptions being pulsars that were ejected in a binary hard enough to merge through orbital decay (from gravitational radiation or the evolution of the companion),

and those are liable to be ejected from the cluster. Although the majority of neutron star collisions resulted in a binary, most were wide enough to be subsequently ionized, and we find the ratio of single pulsars to binary pulsars expected to be approximately 2:1. It is interesting to note that if the merged neutron star forms a Thorne-Żytkow object (Thorne and Żytkow, 1977), and the resulting binary is hard enough to escape ionization, the orbit of the binary may circularise through envelope drag in the Thorne-Żytkow object before the envelope is blown away, and a pulsar in a moderately wide, **circular** binary may result. The pulsars in M4 and M53 may be examples of such systems, although other genesis may be more likely, as discussed above. The velocities calculated for the product of collisions are not reliable, and are probably somewhat overestimated by our calculations. Thus we may overestimate by a factor of order two the number of ejected pulsars. Accurate estimates of the recoil following collision will require extensive hydrodynamical simulations of collisions during three-body encounters.

A number of main-sequence star mergers were observed, even in the low density models. It is possible that the rate of main-sequence mergers is sufficient to account for the “blue stragglers” observed in the globular clusters. Leonard has considered this scenario in considerable detail (Leonard, 1989, Leonard and Fahlman, 1991). For Model 1 we find $\Gamma(\#BS) = 11$, assuming $f_r = 1$ and $\tau = 6 \times 10^9$ years. As the simulations concentrate on binaries containing degenerates, they are liable to underestimate the blue straggler creation rate. By comparison, run 3.3.1 implies 200 blue stragglers created in 47Tuc, although the uncertainty is high. A higher rate would be obtained in the low density clusters if a substantial fraction of the binaries has mass-segregated in those clusters, as the low density models were run with a broad initial distribution of binaries.

5. Conclusion

The encounter rate observed, and the parameters of the colliding systems involving neutron stars are consistent with the ratio and distribution of single and binary pulsars observed in the Galactic globular system. In particular, the ratio of single to binary pulsars is accounted for, and the presence of binary pulsars M15C and Trz5A outside their cluster cores is explained. As found previously (Phinney and Sigurdsson, 1991) a number of binary neutron stars were found to be ejected from the cluster after colliding, and of order 10 short period binary pulsars with a neutron star or white dwarf companion might be expected in the Galaxy, having been ejected from core collapsed globular clusters.

It is clear that a critical component of three-body interactions is the time evolution of the binary population parameters. In order to account for the pulsars in 47Tuc, the cluster must have mass-segregated, with the current binary population very concentrated, and starting to eject binaries out to the half-mass radius. The interaction rate in the core is then dominated by 10–100 day binaries, the wider binaries having either ionized or hardened. In M15 the 100 day binaries are mostly hardened or disrupted, the encounter rate being dominated by binaries of periods with less than or order of 10 days. Further, while evolving to core-collapse, through the 47Tuc phase, most of the binaries will have had heavy white dwarfs or neutron stars exchanged in place of the main-sequence stars (see table 5). Consequently we expect a number of stars near the turnoff mass on high speed radial orbits with pericenters in the core and apocenters beyond the half-mass radius. By the time core collapse is reached, a significant fraction of the neutron stars may be in neutron star–neutron star binaries. The simulations try to anticipate this process to some extent by the choice of range of semi-major axis and initial concentration of the binaries evolved. A more realistic time evolution

profile of the binary population would be obtained by evolving a broad initial population in a time varying cluster model.

The white dwarf interaction rate was found to be somewhat greater than the neutron star interaction rate, as expected, and it is possible that white dwarf collisions with stars, or even other white dwarfs may provide the high accretion rate apparently necessary for accretion induced collapse. The merger of white dwarfs has been considered in detail (Webbink, 1984), but not with consideration of accretion induced collapse. It is possible that this may provide a significant channel for pulsar creation.

In order for this model to account for the 47Tuc pulsar population, the globular cluster parameters are strongly constrained. It is necessary that the IMF of the rich clusters have $x_* \sim 1$, at least for masses at and above the turnoff mass, in contradiction to the models favoured by observations, although those models do assume $f_b = 0$. Alternatively, the minimum zero age main-sequence mass sufficient to produce a neutron star must be considerably less than the $8 M_{\odot}$ assumed here. There are some suggestions that stars of mass as low as $5 M_{\odot}$ may produce neutron stars. The IMF will probably be determined in the next few years by observations of pulsars \ddot{P} . Observations of pulsar M15A already suggest that a flat IMF is favoured (Phinney, 1991). It is further necessary that f_r be high, with values closer to 0.4 strongly favoured. Alternatively, it may be that f_r is large for binary neutron stars, the opposite conclusion was reached by Hut and Verbunt (1983). For the simulations to account for the pulsars observed, it is desirable that $f_b > 0.2$. A primordial binary fraction of 0.5 is preferred, noting that binaries with $a > 10 AU$ are rapidly ionized in the clusters concerned, and the primordial binary semi-major axis distribution may extend to $10^5 AU$, implying less than half the primordial binaries survive one relaxation time. Alternatively, if the binary semi-major axis distribution is peaked around $0.2 AU$, as suggested by Trimble (1976),

neutron star collision rates in 47Tuc class models are enhanced in proportion to the excess at that radius. A substantial neutron star and binary population is still required to account for the pulsars in the low density globular clusters. High pulsar formation rate is also favoured by the more concentrated models, suggesting that 47Tuc has a core density greater than $1 \times 10^5 M_{\odot} \text{pc}^{-3}$, although it is probably not necessary to require densities as high as $3 \times 10^5 M_{\odot} \text{pc}^{-3}$.

The evolution of a complete range of binaries in a time evolving cluster model, from zero age through collapse, is necessary to ultimately determine the correct parameter. Such a calculation needs to allow for stellar evolution and binary orbital evolution through gravitational radiation. The heating rates calculated here and in Sigurdsson and Phinney (1991) should contribute to the development of a self-consistent cluster evolution model. The inclusion of binary-binary encounters is necessary if $f_b \sim 0.5$, and it would be desirable to include encounters with hierarchical tr binaries. Some progress is being made towards systematically calculating such encounters (Hut, 1990). At a later stage we expect to make calculations in a time varying background. By using the estimated energy release during the evolution, and iterating the calculation of the evolution of the cluster collapse, we hope to eventually produce partially self-consistent models of cluster evolution.

It is possible to account for the pulsars observed in the Galactic globular clusters through the interactions of binaries and neutron stars, assuming some reasonable values of the globular cluster parameters.

References

- Abt, H.A., 1983, *Ann. Rev. Astr. Ap.*, **21**, 343.
- Abt, H.A., 1987, *Ap. J.*, **317**, 353.
- Alpar, M.A., Cheng, A.F., Ruderman, M.A. and Shaham, J., 1982, *Nature*, **300**, 728.
- Bailyn, C.D. and Grindlay, J.E., 1990, *Ap. J.*, **353**, 159.
- Benz, W. and Hills, J.G., 1987, *Ap. J.*, **323**, 614.
- Benz, W., Hills, J.G. and Thielemann, F.-K., 1989, *Ap. J.*, **342**, 986.
- Benz, W., Bowers, R.L., Cameron, A.G.W. and Press, W.H., 1990, *Ap. J.*, **348**, 647.
- Binney, J. and Tremaine, S., 1987, *Galactic Dynamics*, (Princeton University Press).
- Chandrasekhar, S., 1943, *Ap. J.*, **97**, 255.
- Charles, P.A. in *Topics in X-ray Astronomy, Proc. 23rd ESLAB Symp.*, ESA SP-296, Vol. 1, 129-137 (1989), eds. J. Hunt & B. Battrock, published Paris.
- Chernoff, D.F. and Weinberg, M.D., 1990, *Ap. J.*, **351**, 121.
- Cohn, H., 1979, *Ap. J.*, **234**, 1036.
- Cohn, H., 1980, *Ap. J.*, **242**, 765.
- Da Costa, G.S. and Freeman, K.C., 1976, *Ap. J.*, **206**, 128.
- Davies, M.B., Benz, W. and Hills, J.G., *Ap. J.*, 1991, submitted.
- Elson, R. and Hut, P., 1987, *Ann. Rev. Astr. Ap.*, **25**, 565.
- Fahlman, G.G., Richer, H.B. and Vandenberg, D.A., 1985, *Ap. J. Suppl.*, **58**, 225.

- Finzi, A., 1978, *Astr. Ap.*, **62**, 149.
- Fruchter, A.S. and Goss, W.M. 1990, *Ap. J. (Letters)*, **365**, L63.
- Fullerton, L.W. and Hills, J.G., 1982, *A.J.*, **87**, 175.
- Gao, B., Goodman, J., Cohn, H. and Murphy, B.W., 1991, *Ap. J.*, **370**, 567.
- Goodman, J., 1987, *Ap. J.*, **313**, 576.
- Goodman, J., 1989, in *Dynamics of Dense Stellar Systems*, ed. D. Merritt (Cambridge University Press) p. 183.
- Goodman, J. and Hut, P., 1989, *Nature*, **339**, 40.
- Goodman, J. and Hernquist, L., *Ap. J.*, 1991, in the press.
- Grindlay, J.E. and Bailyn, C.D., 1988, *Nature*, **336**, 48.
- Gunn, J.E. and Griffin, R.F., 1979, *A.J.*, **84**, 752.
- Hamilton, T.T., Helfand, D.J. and Becker, R.H., 1985, *A.J.*, **90**, 606.
- Heggie, D.C., 1975, *M.N.R.A.S.*, **173**, 729.
- Hertz, P. and Grindlay, J.E., 1983, *Ap. J.*, **275**, 105.
- Hertz, P. and Wood, K.S., 1985, *Ap. J.*, **290**, 171.
- van den Heuvel, E.P.J., van Paradijs, J. and Taam, R.E., 1986, *Nature*, **322**, 153.
- van den Heuvel, E.P.J., 1991, in *Neutron Stars: Theory and Observation*, eds. J. Ventura and D. Pines (Kluwer Academic Publishers, Dordrecht).
- Hills, J.G., 1975a, *A.J.*, **80**, 809.
- Hills, J.G., 1975b, *A.J.*, **80**, 1075.
- Hills, J.G. and Fullerton, L.W., 1980, *A.J.*, **85**, 1281.
- Hut, P. and Bahcall, J.N., 1983, *Ap. J.*; **268**, 319.
- Hut, P., 1983a, *Ap. J.*, **268**, 342.

- Hut, P., 1983c, *Ap. J. (Letters)*, **272**, L29.
- Hut, P. and Verbunt, F., 1983, *Nature*, **301**, 587.
- Hut, P. and Inagaki, S., 1985, *Ap. J.*, **298**, 502.
- Hut, P., 1990, in *Proceedings of the workshop on Self-Gravitating Systems in Astrophysics and Nonequilibrium Processes in Physics*, (Kyoto, June 1989).
- Johnston, H.M. and Kukarni, S.R., 1991, *Ap. J.*, **368**, 504.
- Johnston, H.M., Kulkarni, S.R. and Phinney, E.S., 1991b, in preparation.
- Katz, J.I., 1975, *Nature*, **253**, 698.
- Katz, J.I., 1975, *M.N.R.A.S.*, **183**, 765.
- King, I.R., 1962, *A.J.*, **67**, 471.
- King, I.R., 1966, *A.J.*, **71**, 64.
- Kochanek, C.S., *Ap. J.*, 1991, submitted.
- Krolik, J.H., Meiksin, A. and Joss, P.C., 1984, *Ap. J.*, **282**, 466.
- Kulkarni, S.R., Narayan, R. and Romani, R.W., 1990a, *Ap. J.*, **356**, 174.
- Kulkarni, S.R., Goss, W.M., Wolszczan, A. and Middleditch, J., 1990b, *Ap. J. (Letters)*, **363**, L5.
- Latham, D.W., 1989, in *Highlights of Astronomy*, ed. D. McNally (Kluwer Academic Publishers, Dordrecht).
- Lauer, T.R., Holtzman, J.A., Faber, S.M., Baum, W.A., Currie, D.G., Ewald, S.P., Groth, E.J., Hester, J., Kelsall, T., Light, R.M., Lynds, C.R., O'Neil, E.J., Schneider, D.P., Shaya, E.J. and Westphal, J.A., 1991, *Ap. J. (Letters)*, **369**, L45.
- Lee, H.M. and Ostriker, J.P., 1986, *Ap. J.*, **310**, 176.
- Leonard, P.J.T., 1989, *A.J.*, **98**, 217.

- Leonard, P.J.T. and Fahlman, G.G., 1991, *A.J.*, **102**, 994.
- Lewin, W.H.G. and Joss, P.C., *Space Sci. Rev.* 283 (1981)
- Lynden-Bell, D. and Wood, R., 1968, *M.N.R.A.S.*, **138**, 495.
- Lyne, A.G., Brinklow, A., Middleditch, J., Kulkarni, S.R., Backer, D.C. and Clifton, T.R., 1987, *Nature*, **328**, 399.
- Manchester, R.N., Lyne, A.G., D'Amico, N., Bailes, M. and Lim, J., 1991, *Nature*, **352**, 219.
- Mateo, M., Harris, H.C., Nemec, J. and Olszewski, E.W, 1990, *A.J.*, **100**, 469.
- McMillan, S.L.W., 1986, *Ap. J.*, **306**, 552.
- Meylan, G., 1988, *Astr. Ap.*, **191**, 215.
- Michel, F.C., 1987, *Nature*, **329**, 310.
- Michie, R.W., 1963, *M.N.R.A.S.*, **125**, 127.
- Michie, R.W. and Bodenheimer, P.H., 1963, *M.N.R.A.S.*, **126**, 269.
- Murphy, B.W. and Cohn, H.N., 1988, *M.N.R.A.S.*, **232**, 835.
- Murphy, B.W., Cohn, H.N. and Hut, P., 1990, *M.N.R.A.S.*, **245**, 335.
- Murphy, B.W., Rutten, R.G.M., Callanan, P.J., Seitzer, P., Charles, P.A., Cohn, H.N. and Lugger, P.M., 1991, *Nature*, **351**, 130.
- Murphy, B.W. and Phinney, E.S., 1991, in preparation.
- Narayan, R., Fruchter, A.S., Kulkarni, S.R. & Romani, R. 1990, in *Proc. 11th North American Workshop on CVs and LMXRBs*, (ed. C.W. Mauche) (in the press).
- Nomoto, K. and Kondo, Y., 1991, *Ap. J.*, **367**, L19.
- Phinney, E.S., *M.N.R.A.S.*, 1990, submitted.
- Phinney, E.S. and Kulkarni, S.R., *Nature*, 1991, in the press.

- Phinney, E.S. and Sigurdsson, S., 1991, *Nature*, **349**, 220.
- Predehl, P., Hasinger, G. and Verbunt, F., *Astr. Ap.*, 1991, in the press.
- Pryor, C., Latham, D.W. and Hazen-Liller, M.L., 1985, in *Dynamics of Star Clusters*, IAU Symposium No. 113, ed. J. Goodman and P. Hut (Dordrecht, Reidel), p. 99.
- Pryor, C., McClure, R.D., Hesser, J.E. and Fletcher, J.M., 1989, in *Dynamics of Dense Stellar Systems*, ed. D. Merritt (Cambridge University Press) p. 175.
- Pryor, C., Schommer, R.A. and Olszewski, E.W., 1990, *Steward Observatory, University of Arizona preprint*.
- Rappaport, S., Putney, A. and Verbunt, F., 1990, *Ap. J.*, **345**, 210.
- Rasio, F.A. and Shapiro, S.L., 1991377559
- Ruffert, M. and Müller, E., 1990, *Astr. Ap.*, **238**, 116.
- Shapiro, S.L. and Teukolsky, S.A., 1983, *Black Holes, White Dwarfs and Neutron Stars: The Physics of Compact Objects*, (John Wiley & Sons).
- Sigurdsson, S. and Phinney, E.S., 1991, in *PhD Thesis*.
- Spitzer, L. and Hart, M.H., 1971a, *Ap. J.*, **164**, 399.
- Spitzer, L. and Hart, M.H., 1971b, *Ap. J.*, **166**, 483.
- Spitzer, L. and Thuan, T.X., 1972, *Ap. J.*, **175**, 31.
- Spitzer, L., 1987, *Dynamical Evolution of Globular Clusters*, (Princeton University Press).
- Statler, T.S., Ostriker, J.P. and Cohn, H.N., 1987, *Ap. J.*, **316**, 626.
- Thorne, K.S. and Żytkow, A.N., 1977, *Ap. J.*, **212**, 832.

- Trimble, V., 1976, in *Structure and Evolution of Close Binary Systems*, IAU Symposium No. 73, ed. P. Eggleton, S. Mitton and J. Whelan (Dordrecht, Reidel), p. 369.
- Tout, C.A., 1991, *M.N.R.A.S.*, **250**, 701.
- Verbunt, F., van den Heuvel, E.P.J., van Paradijs, J. and Rappaport, S., 1987, *Nature*, **329**, 312.
- Verbunt, F., Lewin, W.H.G. and van Paradijs, J., 1989, *M.N.R.A.S.*, **241**, 51.
- Verbunt, F., 1990, in *Neutron Stars and Their Birth Events*, ed. W. Kundt (Dordrecht, Reidel).
- Webbink, R.F., 1984, *Ap. J.*, **277**, 355.

Captions

Table 1

Table of mass-groups for the models run. x_* is the exponent of the initial mass function, the second column shows the index of mass groups. m_{hi} and m_{lo} are the upper and lower boundaries on each mass group, respectively, while \bar{m} is the mean mass of that mass group. f_m is the fraction of the total mass of the cluster in that mass group, f_n is the number fraction of that mass group in the cluster and f_L is the fraction of that mass group that is luminous. Model 6 was run with $x_* = 1.00$ but only had eight mass groups; the lowest mass group covered the range covered by mass groups 1-3 in this table, the other mass groups were the same.

Table 2

The parameters of the six models used in the calculations. x_* is the exponent of the initial mass function, as before, W_0 is the ratio of the depth of the potential to the mean core dispersion, as described in the text, r_t is the tidal radius of the cluster, r_0 is the mean "King radius" as defined in the text, n_0 is the core density, \bar{m}_c is the mean stellar mass in the core, $\bar{\sigma}(0)$ is the mean core dispersion and M_T is the total mass of the cluster.

Table 3

The parameters of the individual runs. The runs are arbitrarily labeled, and the number of binaries in each run is given. Runs with for which the number of binaries is not a multiple of 50 were prematurely terminated by computer crashes. The fourth column gives the mass group index according to whose radial distribution the binaries were initially placed. We expect the relaxed distribution of the binaries to be concentrated (neglecting encounter recoil), with the heavier

binaries more concentrated than the most concentrated single star mass group. For Models 1 and 2 we started with a broad distribution and allowed the binaries to relax during the calculation. For Models 3, 4 and 5 the initial concentration was higher, as we expect the binaries in such clusters to be relaxed and the integration time was not sufficient to relax a very broad distribution. For Model 6 the initial concentration followed the most massive group for half the runs, as integration time was short and we were interested in the interactions of the core binaries; the other half of the runs had a broader initial concentration to provide a comparison of relaxation and reaction rates. Columns five and six show the integration time and the “super-orbit” scale factor respectively. The scale factor was chosen conservatively to be 20–30 for these runs, except for an extended run of Model 4 where it was chosen to be 60, partly in order to check the scaling, and run 2.3.1 which was done to check the relaxation time scale of light binaries. Columns seven and eight show the range in initial binary semi-major axis in AU. The range was generally chosen so that the maximum size binary was marginally soft. Exceptions are a couple of runs with very wide binaries to check ionisation rates, and the high initial concentration runs for Model 6 where wide binaries are not expected to be found at all. The minimum semi-major axis was generally chosen such that a binary in the core had an encounter probability $\ll 1/N_b$ over the integration time. For the high initial concentration runs for Model 6, the minimum semi-major axis was limited by finite stellar size and time scales for orbital decay through gravitational radiation. Columns eight and nine show the minimum mass imposed on the stars in the binary in M_\odot . The last column shows the binary weight, f_w , the fraction of the total number of binaries that have the members with masses in the range imposed, assuming the binaries drawn independently from the IMF. The weight does not include the restriction in semi-major axis which should be factored separately into f_b .

Table 4.

A summary of the outcome of each run, showing the mean (log) initial energy of the binaries in units of $kT(= \bar{m}_c \bar{\sigma}^2)$, the mean energy transfer per binary in the same units, the total number of collisions during the runs, the total number of exchanges of the primary star ($\#X_2$) and the companion star ($\#X_3$), respectively, and the total number of ionisations, X_I . The total number of ionisations if one includes binaries where a collision left the third star in an orbit about the merged remnant wide enough to be subsequently ionised is shown bracketed, where appropriate.

Tables 5a–g.

The parameters of individual runs resulting in collisions, exchanges, or “interesting” resonances, the process being shown in the third column, following the notation described in the text. The stars involved are designated by n, w, m and g, for neutron stars, white dwarfs, main–sequence stars and (sub)giants respectively. The mass in solar masses is shown to one (or two, where required) significant figures as a subscript. For (sub)giants, the stellar radius is also indicated by a superscript, in units of $\log_{10}(R_*/R_\odot)$. The initial and final period of the binary is shown in hours, and the eccentricity before and after the encounter is also shown. The specific energy and angular momentum of the binary after the encounter is also shown, with $E_c = \frac{1}{2}v^2/\sigma^2 - W(r/r_0)$ and $J_c = |(\mathbf{r}/r_0) \times (\mathbf{v}/\sigma^2)|$. Where appropriate, the time for the system to decay through gravitational radiation is shown for parameters before the encounter, τ_i , and after the encounter, τ_f .

Figures 1a–b

Volume density profiles for Models 1 and 4 respectively. Shown to illustrate the model profiles calculated.

Figures 2a–b

Relative encounter probability for different radial trajectories for binaries in Model 1 and Model 4 respectively. The trajectories show the relative integrated probability of an encounter at different radii for trajectories of binaries moving radially out from the core at different speeds, the lower speed trajectories clearly having the lower apocentres. The trajectories were integrated in the absence of dynamical friction and kicks. v_i is the initial (tangential) velocity of the binary. $v_i = \{1.0, 2.0, 2.5, 3.0, 3.3\}$, in Figure 2a, and $v_i = \{1.5, 2.0, 3.0, 4.0\}$ in Figure 2b.

Figure 3

Integrated relative encounter probability as a function of radius for the trajectory shown in Model 1. Integrated encounter probability along the trajectory was 2.8×10^{-5} .

Figure 4

Relative integrated encounter probabilities for different mass groups (shown by index) for a 1 AU binary in Model 1, on the same trajectory as shown in Figure 3. Note that the remnant groups dominate the encounter rate in the core, while the lightest mass group dominates outside the core.

Figure 5

Integrated relative encounter probability as a function of radius for the trajectory shown in Model 2. Integrated encounter probability along the trajectory was 1.1×10^{-5} .

Figure 6

Relative integrated encounter probabilities for different mass groups (shown by index) for a 1 AU binary in Model 2, on the same trajectory as shown in Figure

5. The turnoff mass group dominates the encounter rate for this model, in the core.

Figure 7

Probability per unit time of an encounter for a 1 AU binary on a radial trajectory in Model 3. Shown as representative of the order of magnitude encounter probabilities expected in the model.

Figure 8

Integrated relative encounter probability as a function of radius for the trajectory shown in Model 3. Integrated encounter probability along the trajectory was 6.5×10^{-5} .

Figure 9

Relative integrated encounter probabilities for different mass groups (shown by index) for a 1 AU binary in Model 3, on the same trajectory as shown in Figure 7. Note that the integrated encounter probability is dominated by mass group 10 (neutron stars) even for a trajectory that extends to two core radii.

Figure 10

Probability per unit time of an encounter for a 1 AU binary on a moderately elliptical trajectory near the half-mass radius in Model 4. Shown as representative of the order of magnitude encounter probabilities expected in the model.

Figure 11

Integrated relative encounter probability as a function of radius for the trajectory shown in Figure 10. Integrated encounter probability along the trajectory was 3.3×10^{-6} .

Figure 12

Relative integrated encounter probabilities for different mass groups (shown by index) for a 1 *AU* binary in Model 4, on the same trajectory as shown in Figure 10. Note that the integrated encounter probability is dominated by mass group 1 (the lightest stars), with the second largest contribution coming from the light white dwarf/moderate mass star group. The contribution to the encounter probability from mass group 10 is negligible on this trajectory.

Figure 13

Integrated relative encounter probability as a function of radius for the trajectory shown in Model 6. Integrated encounter probability along the trajectory was 8.2×10^{-4} .

Figure 14

Relative integrated encounter probabilities for different mass groups (shown by index) for a 1 *AU* binary in Model 4, on the same trajectory as shown in Figure 13. Note that the integrated encounter probability is dominated by mass group 10, as will be the case for any trajectory that penetrates the core.

Figures 15a–b

The initial radial distribution of binaries plotted against the log of the binary binding energy. Figure 15a shows the distributions for runs 1.1.1, 2.1.1, 3.3.1 and 3.4.1, and 4.2.1 and 4.2.2, going from top left to bottom right. Figure 15b shows the distributions for runs 4.3.1 and 4.3.2, 5.1.1 and 5.2.1, 6.1.1 and 6.1.2, and 6.2.1 and 6.2.2, respectively.

Figures 16a–h

The initial and final radial distribution of binaries in the cluster, shown binned in \log_2 spaced bins, for the runs indicated.

Figures 17a-p

Final distribution of the binaries for the various runs indicated. The fate of each binary is indicated by the symbol plotted. A binary which underwent no encounters is plotted as plain point. If the binary had encounter(s) which did not lead to an exchange, ionisation or collision, a "flyby," the binary is plotted as an open polygon, the number of sides being equal to $2 + \text{no. of flybys}$. If the binary underwent an exchange, a horizontal cross is superposed on the polygon, and the number of sides of the polygon is incremented by 2 for a type X_2 exchange or 3 for a type X_3 exchange. If the binary was ionised, the number of sides of the polygon was incremented by 4, and $\log(E_b/kT)$ was set to -1 exactly to fit the outcome on the plot. The radial position of the ionisations plotted was incremented by an arbitrary amount to fit on the plot. Most ionisations took place inside the core. Note that each binary may have undergone a combination of the various encounters.

If the binary underwent a collision, it was plotted with a different symbol. The number of sides of the symbol was determined by the algorithm above, and in addition was incremented by 1-6 according to the various collision scenarios. If the collision led to a merger of two of the stars with the third star ejected, the increment was 1, 2 or 3 according to whether the field star, the primary star or the companion star was ejected. If the collision led to a merger of two of the stars and the third star remained bound to the merged remnant, the increment was 4-6 according to whether the field star, the primary or the companion star was the bound star, respectively. If the collision involved two main-sequence stars only, it was plotted with a skeletal star symbol; if the collision involved a (sub)giant and a main-sequence star or another (sub)giant, the symbol was a re-entrant star symbol; and if the collision involved a white dwarf or a neutron

star the symbol used was a solid polygon. If the collision produced a merged remnant with the third star bound, the integration was continued with the new binary. A number of these binaries were subsequently ionised, and are shown at $\log(E_b/kT) = -1$, above the regular ionisations, where appropriate. The binaries shown at the top of each plot were ejected from the cluster. In each run a small fraction of binaries remained in the halo of the cluster and drifted out past the tidal radius through random kicks, without undergoing any encounters. Physically not all these binaries would be lost from the cluster, depending on the external environment around the cluster at the time, the Galactic tidal field in particular. A significant proportion of the exchanged and/or collided binaries were also ejected, and are shown where appropriate.

For the more concentrated models, we also show the fate of those binaries containing neutron stars on a separate plot (labeled "NS only"). If the binary did **not** contain a neutron star initially, or if the binary was in collision where one of the stars colliding was a neutron star, a small "n" is plotted below the symbol for that binary. If the final binary contained two neutron stars, or was involved in a collision where one of the stars colliding **and** the third star were neutron stars, a small "N" is plotted below the symbol for the binary. Note that no binary contained two neutron stars initially.

Tables

Table 1.

Multi-mass models

x_*	Mass group	m_{hi}	m_{lo}	\bar{m}	f_m	f_n	f_L
1.35	1	0.157	0.100	0.1235	0.2339	0.4571	1.000
	2	0.200	0.157	0.1761	0.1105	0.1514	1.000
	3	0.250	0.200	0.2228	0.0975	0.1514	1.000
	4	0.310	0.250	0.2779	0.0824	0.0716	1.000
	5	0.390	0.310	0.3460	0.0836	0.0583	1.000
	6	0.500	0.390	0.4396	0.0836	0.0459	1.000
	7	0.630	0.500	0.5668	0.1343	0.0572	0.526
	8	0.800	0.630	0.7042	0.1155	0.0396	0.588
	9	1.250	0.800	0.9659	0.0428	0.0107	0.000
	10	1.570	1.250	1.3634	0.0158	0.0028	0.000
1.00	1	0.157	0.100	0.1242	0.1539	0.3681	1.000
	2	0.200	0.157	0.1764	0.0821	0.1382	1.000
	3	0.250	0.200	0.2232	0.0787	0.1047	1.000
	4	0.310	0.250	0.2782	0.0718	0.0767	1.000
	5	0.390	0.310	0.3465	0.0787	0.0674	1.000
	6	0.500	0.390	0.4404	0.0855	0.0577	1.000
	7	0.630	0.500	0.5686	0.1647	0.0861	0.477
	8	0.800	0.630	0.7055	0.1577	0.0664	0.520
	9	1.250	0.800	0.9745	0.0835	0.0255	0.000
	10	1.570	1.250	1.3697	0.0436	0.0094	0.000

Table 2.

Cluster models

Model	x_*	W_0	r_t/r_0	r_0/pc	r_h/r_0	n_0/pc^{-3}	\bar{n}_c/M_\odot	$\sigma(0)/\text{km s}^{-1}$	M_T/M_\odot
1	1.35	6	16.0	1.52	3.24	2×10^4	0.51	12	7.3×10^5
2	1.35	9	36.5	1.41	7.11	1×10^4	0.68	9	1.0×10^6
3	1.35	12	73.5	0.65	14.8	8×10^4	0.83	13	2.3×10^6
4	1.00	12	87.5	0.57	17.6	1×10^5	1.01	14	2.6×10^6
5	1.00	12	83.5	0.35	17.6	3×10^5	1.01	15	1.9×10^6
6	1.35	18	263	0.1	57.2	3×10^6	1.11	15	2.6×10^6

Table 3.

Run parameters

Model	run	N_b	In. conc.	T	t_n	a_{max}	a_{min}	M_{1m}	M_{2m}	f_w
1	1.1.1	350	6	10^{10}	20	20.0	0.1	0.50	0.39	3.2×10^{-2}
2	2.1.1	250	6	10^{10}	20	10.0	0.05	0.50	0.39	3.2×10^{-2}
	2.1.2	59	6	10^{10}	30	100.0	10.0	0.50	0.25	4.1×10^{-2}
	2.2.1	100	10	10^{10}	30	5.0	0.05	0.63	0.39	2.0×10^{-2}
	2.3.1	250	6	10^{10}	100	10.0	0.05	0.20	0.00	4.6×10^{-1}
3	3.3.1	100	8	5×10^9	20	3.0	0.003	0.50	0.39	3.2×10^{-2}
	3.4.1	100	8	5×10^9	20	3.0	0.003	0.80	0.50	2.1×10^{-3}
4	4.1.1	100	8	5×10^9	20	10.0	0.01	0.50	0.39	4.6×10^{-2}
	4.2.1	46	10	5×10^9	20	10.0	0.01	0.80	0.50	6.5×10^{-3}
	4.2.2	100	10	5×10^9	20	10.0	0.01	0.80	0.50	6.5×10^{-3}
	4.3.1	100	10	5×10^9	30	5.0	0.005	0.63	0.39	1.9×10^{-2}
	4.3.2	100	10	5×10^9	60	5.0	0.005	0.63	0.39	1.9×10^{-2}
5	5.1.1	100	8*	5×10^9	20	5.0	0.005	0.50	0.39	4.6×10^{-2}
	5.2.1	87	8*	5×10^9	20	5.0	0.005	0.80	0.50	6.5×10^{-3}
6	6.1.1	100	10	5×10^8	30	0.5	0.0005	0.80	0.63	1.3×10^{-3}
	6.1.2	100	10	5×10^8	30	1.0	0.001	0.50	0.39	3.2×10^{-2}
	6.2.1	35	8	5×10^8	20	10.0	0.01	0.50	0.25	3.3×10^{-1}
	6.2.2	90	8	5×10^8	20	10.0	0.01	0.50	0.25	3.3×10^{-1}

* For Model 5 only 8 mass groups were used

Table 4.

Cluster models

Model	run	$\langle \log(E_{b,in}/kT) \rangle$	$\langle \Delta E_b/kT \rangle$	#coll.	# X_2	# X_3	# X_I
1	1.1.1	1.26	-2.9×10^{-2}	1	4	3	27
2	2.1.1	1.67	8.0×10^{-2}	0	2	1	3
	2.1.2	-0.47	-7.5×10^{-2}	0	2	3	22
	2.2.1	1.73	6.1×10^{-2}	0	0	0	0
	2.3.1	1.15	-9.5×10^{-4}	0	0	0	0
3	3.3.1	2.32	-7.7×10^{-4}	1	1	1	1(2)
	3.4.1	2.52	6.9×10^{-3}	0	0	1	1
4	4.1.1	1.70	7.6×10^{-2}	1	2	5	3(4)
	4.2.1	2.00	2.85	0	7	5	6
	4.2.2	2.00	0.25	3	8	13	12(14)
	4.3.1	1.91	-3.1×10^{-2}	2	3	5	16(18)
	4.3.2	2.08	-6.7×10^{-2}	2	7	8	14(15)
5	5.1.1	1.82	0.57	8	8	12	8(13)
	5.2.1	2.31	6.3	6	13	22	9
6	6.1.1	3.02	8.7	16	16	12	3(10)
	6.1.2	2.22	2.4	14	9	16	9(18)
	6.2.1	1.25	4.1×10^{-4}	0	2	1	0
	6.2.2	1.36	0.15	0	1	1	1

Table 5a.

Outcome of individual runs

run	#	X	Stars	P_{in}	P_{out}	e_i	e_f	E_c	J_c	Comment
1.1.1	7	X_2	$w_{0.9}, g_{0.7}^{0.01}, w_{0.7}$	5850	3850	.11	.90	-4.17	0.23	
	26	X_2	$m_{0.7}, m_{0.4}, w_{0.7}$	4932	6625	.24	.23	-5.39	0.03	
	197	X_3	$w_{0.5}, m_{0.7}, m_{0.7}$	2712	5575	.84	.85	-5.30	0.08	
	211	C_4	$m_{0.7}, w_{0.7}, m_{0.12}$	2379	4444	.93	.22	-3.66	0.93	Softens
	307	X_3	$m_{0.5}, m_{0.7}, w_{0.9}$	7693	24475	.99	.99	-5.01	0.21	Ionizes
2.1.1	249	X_2	$w_{0.9}, m_{0.5}, n_{1.4}$	11.2	13.4	.88	.28	> 0		Ejected
3.3.1	7	X_3	$m_{0.7}, m_{0.4}, w_{0.7}$	577	301	.13	.41	-11.4	0.22	
	89	C_1	$m_{0.7}, m_{0.7}, n_{1.4}$	18.3		.89		-10.4	0.49	
3.4.1	51	X_3	$w_{0.9}, w_{0.9}, n_{1.4}$	630	587	.34	.44	-11.6	0.15	Hardens
4.1.1	9	X_2	$m_{0.7}, n_{1.4}, n_{1.4}$	196	490	.87	.64	-11.2	0.21	Hardens
	19	X_2	$w_{0.5}, n_{1.4}, n_{1.4}$	619	522	.35	.92	-10.6	0.10	
	45	C_1	$m_{0.7}, w_{0.5}, w_{0.9}$	475		.86	.99	-9.40	0.88	
	61	X_3	$m_{0.5}, n_{1.4}, n_{1.4}$	2336	5678	.75	.51	-11.3	0.06	Ionizes
	67	R	$w_{0.5}, m_{0.4}, n_{1.4}$	16.6		.82		-11.2	0.29	May Collide
	79	X_3	$w_{0.5}, w_{0.7}, n_{1.4}$	704	283	.49	.35	-5.28	0.80	
	99	X_3	$n_{1.4}, m_{0.5}, n_{1.4}$	1220	5987	.92	.85	-11.1	0.29	Ionizes

Table 5b.

run	#	X	Stars	P_{in}	P_{out}	e_i	e_f	E_c	J_c	Comment
4.2.1	1	X_2	w _{0.9} , m _{0.7} , n _{1.4}	99	3750	.70	.94	-10.4	0.23	Ionizes
	5	X_2	n _{1.4} , w _{0.9} , n _{1.4}	147	145	.00	.96	-10.3	0.54	
	8	X_3	n _{1.4} , w _{0.7} , n _{1.4}	730	340	.83	.59	-9.11	0.94	Hardens
	8	X_3	n _{1.4} , n _{1.4} , n _{1.4}	97.6	25.1	.95	.64	-10.8	0.08	
	9	R	w _{0.9} , n _{1.4} , n _{1.4}	35.5		.34		-9.78	0.56	May Collide
	13	X_3	w _{0.9} , m _{0.7} , n _{1.4}	242	222	.00	.56	-10.5	0.76	Hardens
	16	X_2	n _{1.4} , w _{0.5} , m _{0.7}	6.96		.76	.76	-11.1	0.07	
	19	X_2	w _{0.9} , w _{0.9} , n _{1.4}	3102	2934	.10	.98	-11.3	0.23	Ionizes
	22	X_2	w _{0.9} , n _{1.4} , n _{1.4}	44.8	72.8	.00	.42	-10.4	0.17	Hardens
	23	X_2	w _{0.9} , n _{1.4} , w _{0.9}	106	11.5	.19	.87	-9.30	1.30	WD Ejected
	40	X_3	w _{0.9} , w _{0.7} , n _{1.4}	53.4	183	.56	.78	-10.8	0.33	
	41	X_2	w _{0.9} , m _{0.7} , n _{1.4}	1230	879	.88	.30	-11.4	0.04	Hardens
	41	X_3	n _{1.4} , m _{0.7} , n _{1.4}	670	1713	.44	.86	-11.7	0.06	Ionizes
4.2.2	2	X_2	n _{1.4} , m _{0.5} , n _{1.4}	3775	4219	.25	.88	-7.46	1.16	Softens
	2	C_1	n _{1.4} , m _{0.5} , w _{0.9}	6786		.99		-10.2	0.02	Single Pulsar
	12	X_3	n _{1.4} , w _{0.5} , n _{1.4}	1344	8732	.57	.61	-11.7	0.09	Ionizes
	16	R	w _{0.9} , w _{0.7} , n _{1.4}	21.2		.85		-11.2	0.15	May Collide
	24	X_3	w _{0.9} , m _{0.5} , n _{1.4}	5540	4197	.49	.45	-11.5	0.23	Ionizes
	32	C_1	w _{0.9} , m _{0.7} , w _{0.9}	119		.98		-10.9	0.29	
	33	X_3	w _{0.9} , m _{0.5} , n _{1.4}	4216	1820	.26	.92	-11.0	0.13	Softens
	33	X_3	n _{1.4} , w _{0.9} , n _{1.4}	2527	3387	.64	.50	-11.3	0.06	Ionizes
	48	X_2	w _{0.9} , w _{0.5} , n _{1.4}	4.62	5.33	.82	.87	> 0		Ejected
	49	X_3	w _{0.9} , n _{1.4} , n _{1.4}	127	118	.34	.45	-8.14	1.05	
	50	X_2	w _{0.9} , n _{1.4} , n _{1.4}	431	509	.00	.76	-10.8	0.22	Hardens
	57	X_3	w _{0.9} , w _{0.7} , n _{1.4}	118	349	.57	.55	-8.84	0.65	
	57	X_2	n _{1.4} , w _{0.9} , n _{1.4}		423	.55	.69	-11.0	0.16	Hardens
	57	C_5	n _{1.4} , w _{0.9} , m _{0.7}	157	217	.69	.84	-4.11	1.61	Hardens
	57	R	n _{1.4} , M _{1.6} , n _{1.4}	157		.57		-10.8	0.52	Second Collision?
	58	R	w _{0.9} , n _{1.4} , n _{1.4}	46.4		.97	.55	-11.2	0.21	
	66	X_2	n _{1.4} , w _{0.5} , n _{1.4}	2632	4059	.47	.73	-10.2	0.73	Ionized
	73	X_3	w _{0.9} , n _{1.4} , n _{1.4}	0.87	0.84	.58	.39	> 0		Ejected
									$\tau_i = 8.10^9$	$\tau_f = 2.10^{10}$
	80	X_3	n _{1.4} , w _{0.9} , n _{1.4}	3640	4741	.12	.53	-11.4	0.19	Hardens
	80	X_2	n _{1.4} , n _{1.4} , n _{1.4}	1039	1266	.63	.80	-10.5	0.30	Hardens
	81	X_3	n _{1.4} , m _{0.7} , n _{1.4}	502	1246	.90	.82	-11.1	0.21	Hardens
	86	X_3	n _{1.4} , w _{0.9} , w _{0.9}	284	267	.59	.31	-11.2	0.37	

Table 5c.

run	#	X	Stars	P_{in}	P_{out}	e_i	e_f	E_c	J_c	Comment
4.3.1	1	C_4	w _{0.9} , m _{0.7} , n _{1.4}	925		.66	.92	-11.2	0.13	Ionizes
	23	C_1	m _{0.7} , n _{1.4} , n _{1.4}	9.2		.93		-7.06	0.55	Single Pulsar
	24	X_2	w _{0.7} , w _{0.9} , n _{1.4}	164		.91	.61	-11.5	0.12	
	24	X_3	n _{1.4} , w _{0.9} , n _{1.4}		374	.61	.51	-10.8	0.04	
	43	X_3	w _{0.9} , w _{0.9} , n _{1.4}	273	675	.49	.99	-10.2	0.23	
	44	X_2	m _{0.7} , w _{0.9} , n _{1.4}	370	562	.85	.43	-10.6	0.66	
	71	X_2	w _{0.9} , w _{0.5} , n _{1.4}	105	160	.30	.17	-8.99	0.51	Hardens
	79	X_3	w _{0.9} , m _{0.7} , n _{1.4}	806	1649	.48	.57	-9.82	0.16	Ionizes
	4.3.2	6	X_3	w _{0.9} , m _{0.5} , n _{1.4}	595	1110	.80	.64	-9.89	0.91
7		X_2	m _{0.7} , n _{1.4} , w _{0.9}	169	77	.70	.49	-10.3	0.36	
14		C_1	m _{0.7} , m _{0.7} , n _{1.4}	12.5		.86	.87	-8.59	1.83	Contact Binary
32		C_4	n _{1.4} , m _{0.5} , w _{0.9}	273	1595	.95	.90	-9.95	0.66	Ionized
43		X_3	w _{0.7} , m _{0.7} , n _{1.4}	1685	2001	.33	.96	-11.8	0.08	Hardens
43		X_2	n _{1.4} , w _{0.7} , n _{1.4}	1390	1059	.96	.83	-11.6	0.07	Ionizes
53		X_2	w _{0.9} , w _{0.5} , w _{0.9}	2477	3130	.96	.51	-11.0	0.35	Ionizes
67		X_3	w _{0.9} , m _{0.5} , n _{1.4}	973	2719	.72	.88	-11.0	0.02	Ionizes
74		X_3	n _{1.4} , w _{0.9} , n _{1.4}	688	1837	.95	.79	-10.9	0.11	Ionizes
76		X_2	w _{0.9} , w _{0.7} , n _{1.4}	1198	1231	.16	.73	-11.1	0.27	Hardens
76		X_2	w _{0.9} , n _{1.4} , n _{1.4}	1191	2519	.79	.93	-11.2	0.12	Ionizes
100	X_2	w _{0.9} , m _{0.7} , n _{1.4}	158	208	.50	.77	-10.1	0.23		

Table 5d.

run	#	X	Stars	P_{in}	P_{out}	e_i	e_f	E_c	J_c	Comment
5.1.1	3	X_3	$n_{1.4}, m_{0.4}, n_{1.4}$	184	1005	.70	.97	-10.5	0.77	Ionizes
	4	X_3	$m_{0.7}, n_{1.4}, n_{1.4}$	206	158	.09	.92	-10.6	0.36	Hardens
	8	C_1	$w_{0.7}, m_{0.4}, w_{0.9}$	14.4		.96	.96	-9.11	0.50	Contact Binary
	10	X_3	$w_{0.5}, m_{0.4}, n_{1.4}$	67.3	110	.23	.52	-8.01	2.21	Hardens
	10	X_3	$n_{1.4}, w_{0.5}, n_{1.4}$	58.7	79.6	.94	.46	-8.39	0.81	Hardens
	10	X_3	$n_{1.4}, n_{1.4}, n_{1.4}$	31.3	22	.97	.28	-9.20	0.31	
	12	X_3	$m_{0.7}, g_{0.7}^{0.12}, w_{0.9}$	645	883	.00	.46	-11.7	0.11	Hardens
	12	X_2	$m_{0.7}, w_{0.9}, w_{0.9}$	645	991	.58	.64	-11.5	0.11	
	12	X_2	$w_{0.9}, w_{0.9}, n_{1.4}$	645	1036	.64	.80	-8.81	0.74	Softens
	12	X_2	$w_{0.9}, n_{1.4}, n_{1.4}$	1074	1323	.78	.75	-11.4	0.04	Ionizes
	13	R	$w_{0.7}, n_{1.4}, n_{1.4}$	1.20		.82		-3.11	0.69	May Collide $\tau_i = 2.10^9$
	16	X_2	$m_{0.7}, m_{0.5}, n_{1.4}$	1114	876	.95	.69	-10.6	0.46	Softens
	16	C_1	$n_{1.4}, m_{0.5}, n_{1.4}$	1596		.87		-11.4	0.06	Single Pulsar
	31	C_1	$m_{0.7}, w_{0.9}, w_{0.9}$	56.8		.88		-9.63	0.07	
	33	X_2	$w_{0.5}, w_{0.9}, n_{1.4}$	612	1367	.35	.99	-11.1	0.17	Softens
	36	C_1	$m_{0.5}, n_{1.4}, n_{1.4}$	10.2		.93	.93	-10.5	0.30	Single Pulsar
	40	X_2	$g_{0.7}^{0.15}, m_{0.7}, n_{1.4}$	2556	3578	.00	.00	-8.00	0.36	Ionizes
	43	X_2	$m_{0.7}, m_{0.4}, n_{1.4}$	237	228	.68	.95	> 0		Ejected
	53	X_3	$n_{1.4}, m_{0.5}, n_{1.4}$	1393	2835	.79	.65	-10.5	0.17	Softens
	54	C_4	$m_{0.5}, n_{1.4}, n_{1.4}$	15.5	45.5	.93	.87	-3.11	1.54	Binary Pulsar, Hardens
	66	C_1	$w_{0.7}, m_{0.7}, w_{0.7}$	315		.99	.99	-9.59	0.47	
	70	X_3	$w_{0.7}, w_{0.5}, w_{0.9}$	32.9	30.1	.99	.91	-10.9	0.29	Hardens
	85	C_1	$m_{0.7}, g_{0.7}^{0.14}, n_{1.4}$	131		.96	.96	-10.2	0.49	
	87	C_1	$w_{0.5}, w_{0.5}, n_{1.4}$	892		.99	.99	-5.40	1.65	Contact Binary
	89	X_3	$n_{1.4}, w_{0.5}, n_{1.4}$	573	954	.92	.75	-10.3	0.29	Hardens
	90	R	$m_{0.7}, n_{1.4}, n_{1.4}$	5.42	15.3	.59		-3.40	0.34	May Collide
	91	X_3	$w_{0.7}, w_{0.9}, n_{1.4}$	1288	1099	.98	.96	-9.49	0.21	Hardens

Table 5e.

run	#	X	Stars	P_{in}	P_{out}	e_i	e_f	E_c	J_c	Comment
5.2.1	2	R	$w_{0.9}, w_{0.7}, n_{1.4}$	48.5		.39		-10.6	0.21	May Collide
	3	X_3	$w_{0.9}, w_{0.7}, n_{1.4}$	245	200	.37	.21	-10.9	0.22	Softens
	3	X_3	$n_{1.4}, w_{0.9}, n_{1.4}$	291	396	.97	.99	-11.5	0.28	Softens
	5	X_3	$n_{1.4}, w_{0.9}, n_{1.4}$	554	399	.78	.95	-9.47	0.23	Softens
	6	C_6	$w_{0.9}, n_{1.4}, n_{1.4}$	14.8	52.7	.02	.48	> 0		Binary Pulsar, Ejected
	7	X_2	$w_{0.9}, n_{1.4}, w_{0.9}$	89.5	92.2	.51	.71	-9.93	0.40	Hardens
	7	X_3	$n_{1.4}, w_{0.9}, w_{0.9}$	31.7	27.6	.96	.59	-11.5	0.59	
	10	R	$n_{1.4}, n_{1.4}, n_{1.4}$	3.06		.00		-9.71	0.07	
	12	R	$w_{0.9}, n_{1.4}, n_{1.4}$	3.06		.88	.86	-11.5	0.05	
									$\tau_i = 5.10^9$	
	14	C_4	$w_{0.9}, n_{1.4}, w_{0.7}$	0.36	2.34	.82	.90	> 0		Binary Pulsar, Ejected
									$\tau_i = 10^8$	
	22	X_3	$n_{1.4}, w_{0.5}, n_{1.4}$	23.2	26.3	.76	.63	-9.11	0.87	Hardens
	29	X_3	$w_{0.9}, w_{0.9}, n_{1.4}$	45.3	87.8	.65	.58	-10.3	0.17	Hardens
	30	X_2	$n_{1.4}, w_{0.9}, n_{1.4}$	889	741	.54	.41	-11.7	0.05	Hardens
	30	X_2	$n_{1.4}, w_{0.9}, n_{1.4}$	691	763	.58	.22	-11.9	0.04	Hardens
	30	X_3	$n_{1.4}, w_{0.9}, n_{1.4}$	561	614	.93	.75	-10.8	0.18	Hardens
	30	X_2	$n_{1.4}, w_{0.9}, n_{1.4}$	614	625	.68	.34	-11.1	0.25	Hardens
	30	X_3	$n_{1.4}, n_{1.4}, n_{1.4}$	544	223	.34	.42	-11.3	0.25	Hardens
	30	X_2	$n_{1.4}, n_{1.4}, n_{1.4}$	213	143	.42	.95	-10.9	3.12	Hardens
	30	X_3	$n_{1.4}, n_{1.4}, m_{0.7}$	122	50.1	.92	.66	-9.96	0.77	Hardens
	30	X_3	$n_{1.4}, m_{0.7}, n_{1.4}$	50.1	31.4	.88	.71	-10.8	0.62	
	33	C_6	$w_{0.9}, g_{0.7}^{0.17}, w_{0.7}$	50.8	554	.00	.17	> 0		Ejected
	40	X_3	$n_{1.4}, w_{0.5}, n_{1.4}$	423	1531	.59	.49	-10.4	0.57	Hardens
	41	X_3	$n_{1.4}, m_{0.7}, n_{1.4}$	10.4	23.5	.91	.99	-11.4	0.17	Hardens
	42	R	$w_{0.9}, n_{1.4}, n_{1.4}$	3.06		.08		-8.25	1.57	May Collide
	46	X_3	$w_{0.9}, n_{1.4}, n_{1.4}$	18.5	18.0	.57	.89	+2.08	0.90	Ejected
	47	C_6	$w_{0.9}, n_{1.4}, w_{0.9}$	3.70	11.8	.00	.83	> 0		Ejected
	51	X_3	$n_{1.4}, w_{0.9}, n_{1.4}$	17.6	24.9	.94	.37	-8.44	0.42	
	51	X_2	$n_{1.4}, n_{1.4}, n_{1.4}$	24.9	17.7	.37	.87	-4.45	0.95	

52	X_2	$w_{0.9}, n_{1.4}, n_{1.4}$	129	237	.00	.69	-7.61	0.60	Hardens
54	X_2	$w_{0.9}, n_{1.4}, n_{1.4}$	0.36	0.35	.86	.31	> 0		Ejected
								$\tau_i = 3.10^7$	$\tau_f = 1.10^9$
58	X_3	$n_{1.4}, g_{0.7}^{0.12}, n_{1.4}$	61.3	45.3	.36	.60	-7.49	0.41	Hardens, Ejected
59	X_3	$w_{0.9}, w_{0.9}, n_{1.4}$	648	567	.90	.21	-11.5	0.20	
59	X_3	$n_{1.4}, w_{0.9}, n_{1.4}$	567	981	.21	.44	-11.6	0.10	Softens
62	X_2	$n_{1.4}, m_{0.7}, n_{1.4}$	354	360	.48	.96	-10.7	0.26	Softens
65	X_3	$n_{1.4}, m_{0.5}, n_{1.4}$	95.0	255	.94	.31	-10.4	0.70	Hardens
66	X_3	$n_{1.4}, w_{0.5}, n_{1.4}$	41.6	58.9	.31	.51	-10.8	0.41	
66	X_2	$n_{1.4}, n_{1.4}, n_{1.4}$	58.9	51.3	.51	.45	-9.81	0.27	
73	C_5	$n_{1.4}, m_{0.7}, w_{0.9}$	111.3	96.9	.75	.61	-11.2	0.05	Hardens, Ejected
75	C_4	$w_{0.9}, m_{0.7}, n_{1.4}$	1.97	5.15	.56	.43	> 0		Ejected
80	X_3	$w_{0.9}, m_{0.5}, n_{1.4}$	211	219	.26	.63	-10.1	0.69	Hardens
85	X_2	$w_{0.9}, w_{0.5}, n_{1.4}$	955	1994	.65	.48	-10.5	0.50	Ionizes

Table 5f.

run	#	X	Stars	P_{in}	P_{out}	e_i	e_f	E_c	J_c	Comment
6.1.1	1	X_2	w _{0.9} , w _{0.7} , n _{1.4}	77.8	110	.77	.94	-16.9	0.15	
	2	C_6	w _{0.9} , n _{1.4} , w _{0.7}	0.25	0.32	.00	.68	-3.79	1.47	
									$\tau_i = 1.10^9$	$\tau_f = 2.10^8$
	3	X_3	w _{0.9} , m _{0.7} , n _{1.4}	55.9	49.3	.72	.68	-16.6	0.37	Hardens
	3	X_2	w _{0.9} , n _{1.4} , n _{1.4}	15.8	14.0	.93	.82	-14.6	0.48	
	3	X_2	n _{1.4} , n _{1.4} , n _{1.4}	14.0	20.5	.86	.90	-16.0	0.74	Hardens
	4	C_4	w _{0.9} , m _{0.7} , w _{0.9}	2.81	6.08	.58	.27	-5.19	0.61	Contact Binary
	5	C_4	w _{0.9} , w _{0.9} , n _{1.4}	0.17	1.30	.86	.80	> 0		Contact Binary, Ejected
	6	X_2	n _{1.4} , w _{0.7} , n _{1.4}	5.98	4.67	.15	.69	-10.1	2.28	
	6	X_2	n _{1.4} , w _{0.7} , n _{1.4}	4.72	3.18	.69	.37	+0.69	0.44	Ejected
	9	X_3	n _{1.4} , w _{0.9} , n _{1.4}	3.81	5.00	.02	.44	-0.39	7.81	
	13	R	n _{1.4} , n _{1.4} , n _{1.4}	0.37		.83				
									$\tau_i = 5.10^7$	
	14	C_1	w _{0.9} , n _{1.4} , n _{1.4}	0.52		.00				Single Pulsar
	17	X_3	w _{0.9} , m _{0.7} , n _{1.4}	40.8	30.6	.00	.75	-16.9	0.17	
	17	X_3	n _{1.4} , w _{0.9} , n _{1.4}	30.6	11.5	.75	.83	-15.2	0.17	Hardens
	22	C_1	w _{0.9} , m _{0.7} , n _{1.4}	29.3		.95		-12.6	1.42	
	28	C_4	w _{0.9} , w _{0.9} , n _{1.4}	0.59	4.86	.93	.91	-3.25	1.63	Contact Binary
									$\tau_i = 2.10^7$	
	29	R	w _{0.9} , n _{1.4} , n _{1.4}	1.63		.85	.80	-17.7	0.04	May Collide
	34	X_2	w _{0.9} , w _{0.9} , n _{1.4}	11.4	4.96	.05	.97	-17.6	0.04	Hardens
	35	C_1	w _{0.9} , w _{0.7} , w _{0.9}	0.93	4.96	.97				Contact Binary
	36	X_2	w _{0.9} , w _{0.7} , w _{0.9}	32.1	31.2	.00	.82	-16.4	0.16	Hardens
	36	X_3	w _{0.7} , w _{0.9} , n _{1.4}	31.2	44.9	.67	.70	-15.4	0.65	
	36	X_2	n _{1.4} , w _{0.7} , n _{1.4}	44.9	31.7	.70	.92	-17.6	0.08	Hardens
	36	X_2	w _{0.7} , n _{1.4} , n _{1.4}	31.7	40.1	.25	.46	-16.8	0.28	Hardens
	41	C_5	w _{0.9} , g _{0.7} ^{0.24} , n _{1.4}	2.38	0.52	.00	.72	> 0		Binary Pulsar, Ejected
	44	X_3	w _{0.9} , m _{0.7} , w _{0.9}	9.81	4.97	.09	.49	-6.77	1.33	
	45	X_3	w _{0.9} , m _{0.7} , n _{1.4}	26.8	39.6	.03	.22	-13.2	1.58	
	45	X_3	n _{1.4} , w _{0.9} , n _{1.4}	39.6	25.3	.22	.46	-13.9	0.26	Hardens
	45	X_3	n _{1.4} , n _{1.4} , n _{1.4}	25.3	17.9	.58	.58	-15.6	1.01	Hardens
	50	X_2	w _{0.9} , m _{0.7} , n _{1.4}	70.9	64.2	.06	.91	-17.2	0.29	
	50	C_4	m _{0.7} , n _{1.4} , n _{1.4}	64.2		.93	.81	-17.2	0.30	Ionizes
	60	R	w _{0.9} , w _{0.7} , n _{1.4}	0.81		.00		-15.8	0.38	May Collide
	61	C_4	n _{1.4} , m _{0.7} , n _{1.4}	4.00	23.9	.70	.91	-11.9	0.87	Binary Pulsar, Hardens
	62	X_2	w _{0.9} , n _{1.4} , n _{1.4}	16.1	22.2	.00	.43	-16.8	0.37	Hardens
	65	X_2	w _{0.9} , g _{0.7} ^{0.76} , n _{1.4}	9.85	8.75	.00	.70	> 0		Ejected

67	X_3	$w_{0.9}, g_{0.7}^{0.11}, n_{1.4}$	65.5	62.4	.00	.07	-15.3	0.27	Hardens
73	X_2	$w_{0.9}, w_{0.9}, w_{0.9}$	58.9	21.5	.78	.54	-16.6	0.46	Hardens
73	C_6	$w_{0.9}, w_{0.9}, w_{0.9}$	21.5	11.0	.64	.67	> 0		Ejected
76	C_6	$w_{0.9}, w_{0.9}, n_{1.4}$	5.51	0.42	.85	.68	> 0		Binary Pulsar, Ejected
$\tau_f = 6 \times 10^8$									
78	C_4	$w_{0.9}, m_{0.7}, w_{0.9}$	27.3		.95	.71	-15.6	0.47	Ionizes
81	C_1	$w_{0.9}, m_{0.7}, w_{0.9}$	3.57		.77	.88	-13.3	1.62	
82	X_2	$w_{0.9}, w_{0.7}, n_{1.4}$	0.46	0.58	.96	.83	-8.34	1.02	
$\tau_i = 2 \cdot 10^7$ $\tau_f = 3 \cdot 10^8$									
85	X_2	$n_{1.4}, w_{0.7}, n_{1.4}$	1.25	1.23	.04	.82	-8.85	2.33	
91	X_3	$w_{0.9}, w_{0.7}, n_{1.4}$	6.03	11.6	.69	.85	> 0		Ejected
94	C_4	$w_{0.9}, m_{0.7}, w_{0.9}$	1.05	0.80	.56	.38	> 0		Ejected

Table 5g.

run	#	X	Stars	P_{in}	P_{out}	e_i	e_f	E_c	J_c	Comment
6.1.2	7	C_5	$w_{0.7}, g_{0.7}^{0.11}, n_{1.4}$	3.90	1.40	.00	.53	-5.04	3.38	Binary Pulsar
	11	X_3	$w_{0.5}, m_{0.4}, n_{1.4}$	91.7	96.9	.96	.39	-14.6	1.65	
	12	C_6	$m_{0.5}, n_{1.4}, n_{1.4}$	0.96	7.87	.64	.88	-11.1	1.32	Hardens
	16	X_3	$m_{0.7}, m_{0.4}, n_{1.4}$	9.49	10.7	.77	.58	-13.5	0.20	
	16	X_3	$n_{1.4}, m_{0.7}, n_{1.4}$	10.7	17.9	.58	.78	-15.3	1.37	Hardens
	18	X_3	$m_{0.7}, m_{0.7}, w_{0.9}$	247	138	.00	.95	-16.2	0.26	Hardens
	23	X_2	$w_{0.7}, n_{1.4}, n_{1.4}$	1.73	2.60	.95	.66	-7.83	0.97	
	23	X_3	$n_{1.4}, n_{1.4}, n_{1.4}$	2.60	1.78	.66	.46	-10.1	1.43	
	28	X_3	$m_{0.5}, w_{0.5}, w_{0.9}$	22.9	29.1	.91	.95	-15.9	0.62	
	28	X_2	$w_{0.9}, w_{0.5}, n_{1.4}$	29.1	24.5	.95	.89	> 0		Ejected
	30	X_3	$n_{1.4}, m_{0.4}, n_{1.4}$	2.11	9.58	.82	.79	-13.7	0.67	Hardens
	32	X_2	$w_{0.7}, m_{0.7}, n_{1.4}$	20.4	50.2	.89	.68	-12.6	0.89	
	32	X_2	$m_{0.7}, n_{1.4}, n_{1.4}$	50.2	104	.83	.84	-16.4	0.19	
	32	X_3	$n_{1.4}, n_{1.4}, n_{1.4}$	104	55.9	.88	.74	-16.3	0.48	Hardens
	45	C_1	$m_{0.5}, g_{0.7}^{0.68}, w_{0.9}$	48.4		.66	.92	-8.10	0.41	
	47	X_2	$m_{0.7}, m_{0.7}, n_{1.4}$	9.29	16.5	.67	.07	-12.8	0.74	
	48	C_1	$m_{0.5}, m_{0.7}, n_{1.4}$	45.0		.93	.99	-12.3	1.31	
	50	C_1	$m_{0.5}, m_{0.7}, w_{0.9}$	2.05		.45	.73	-11.9	0.68	
	54	C_5	$w_{0.7}, m_{0.5}, n_{1.4}$	34.2		.60	.70	-14.8	0.17	Ionizes
	55	X_3	$g_{0.7}^{0.08}, m_{0.5}, n_{1.4}$	2.41	5.86	.00	.59	-8.94	1.04	
	62	C_4	$m_{0.7}, w_{0.5}, n_{1.4}$	4.14	1.87	.59	.87	> 0		Ejected
	67	X_3	$w_{0.9}, m_{0.7}, n_{1.4}$	1.07	2.05	.56	.21	-8.13	2.53	Hardens, Ejected
	68	C_1	$m_{0.7}, m_{0.5}, n_{1.4}$	47.1		.63	.97	-16.1	0.86	
	71	C_5	$m_{0.5}, m_{0.7}, n_{1.4}$	39.5		.90	.51	-16.5	0.54	Single Pulsar
	73	C_4	$m_{0.7}, w_{0.7}, n_{1.4}$	7.54	13.7	.73	.51	-11.1	2.94	Hardens
	76	X_3	$m_{0.5}, m_{0.5}, n_{1.4}$	3.74	3.32	.50	.29	-6.74	1.32	
	79	C_1	$m_{0.5}, w_{0.5}, n_{1.4}$	62.6		.97		-13.3	1.02	Contact Binary
	80	C_1	$m_{0.7}, w_{0.5}, w_{0.9}$	85.0		.98		-11.6	1.46	Contact Binary
	86	C_1	$m_{0.7}, m_{0.4}, n_{1.4}$	10.3		.82	.77	-7.12	0.14	
	94	X_3	$m_{0.5}, m_{0.4}, n_{1.4}$	36.3	116	.08	.66	-17.3	0.22	
	99	C_4	$g_{0.7}^{0.28}, n_{1.4}, n_{1.4}$	5.47	25.7	.00	.87	-11.9	3.18	Binary Pulsar, Hardens
	100	X_2	$w_{0.5}, n_{1.4}, n_{1.4}$	45.7	122	.72	.16	-15.2	0.93	

Model 1

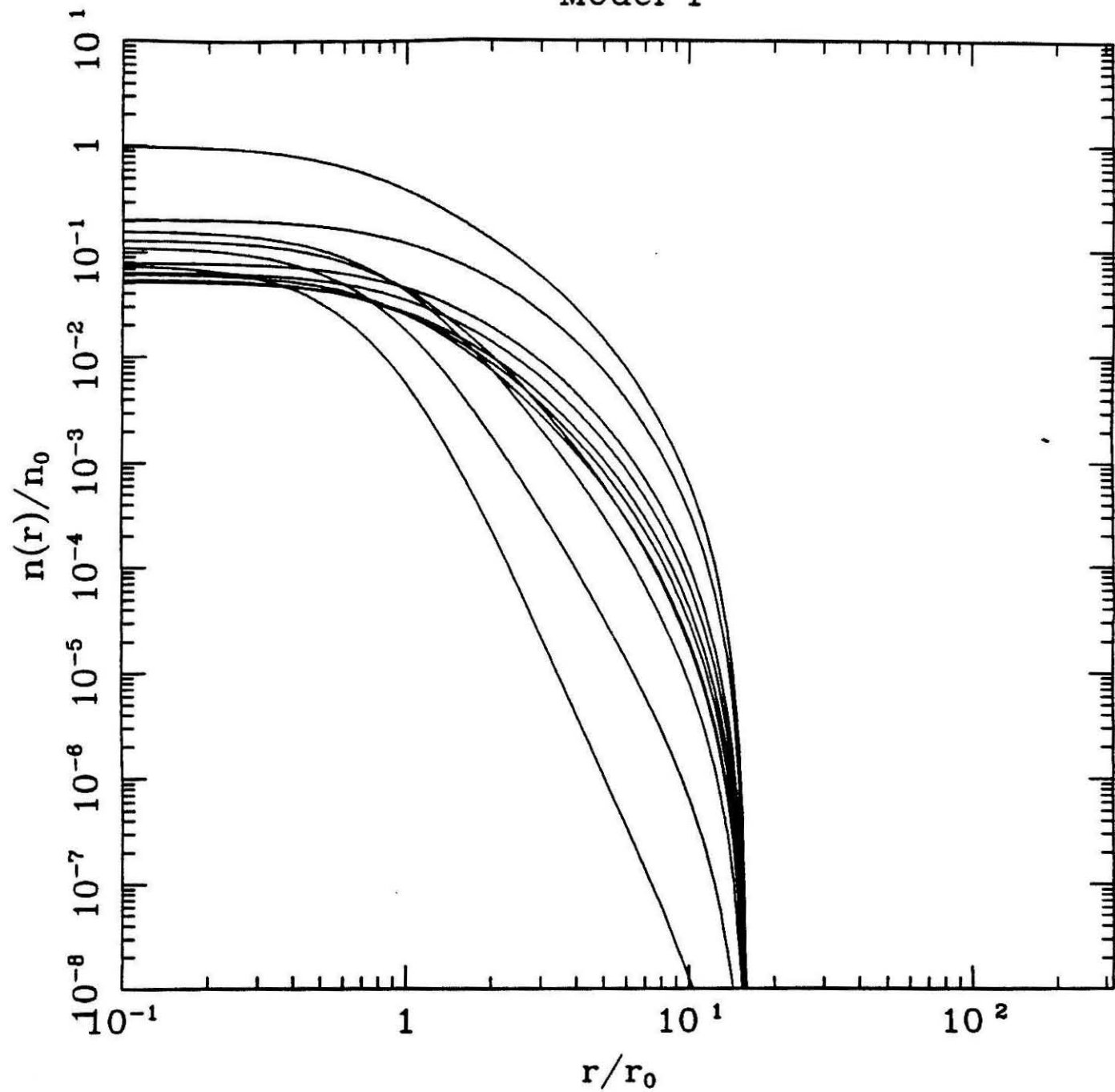


Figure 1a

Model 4

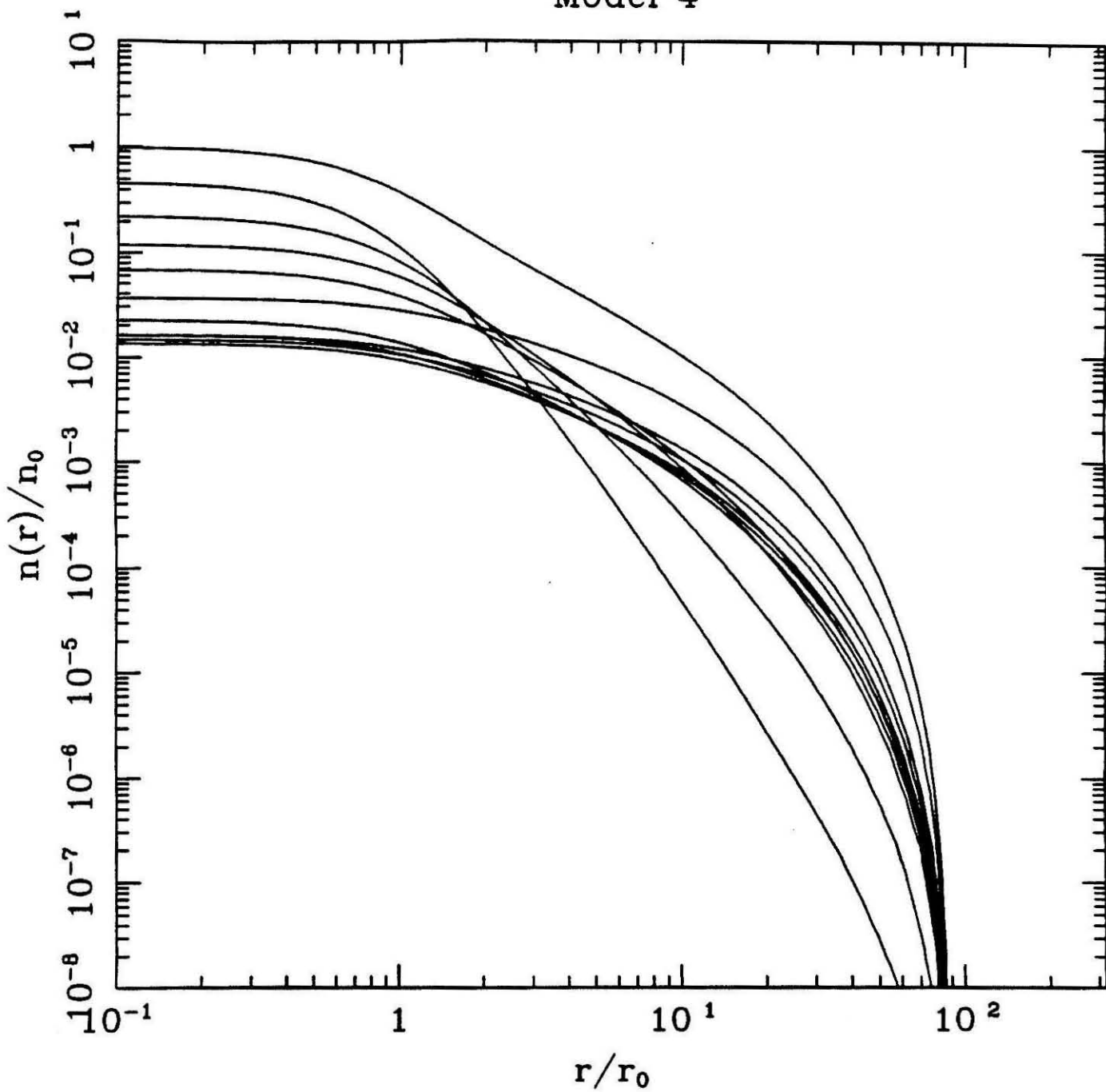


Figure 1b

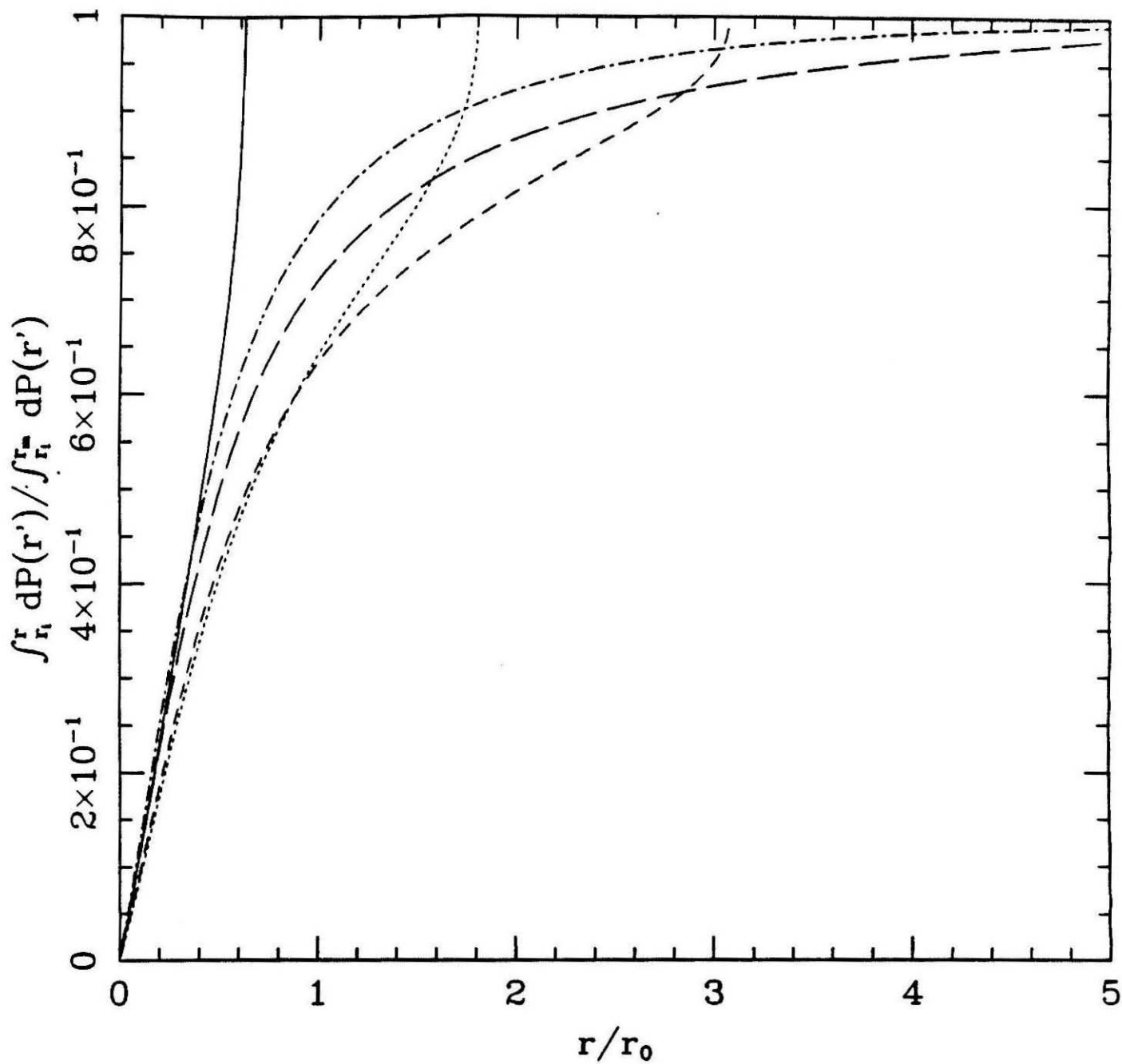
M13 Model 1, $a = 1 \text{ AU}$, $M_b = M_\odot$, $v_i = 1.0-3.3$ 

Figure 2a

47Tuc Model 4, $a = 1$ AU, $M_b = 1.68 M_\odot$, $v_1 = 1.5 - 4.0$

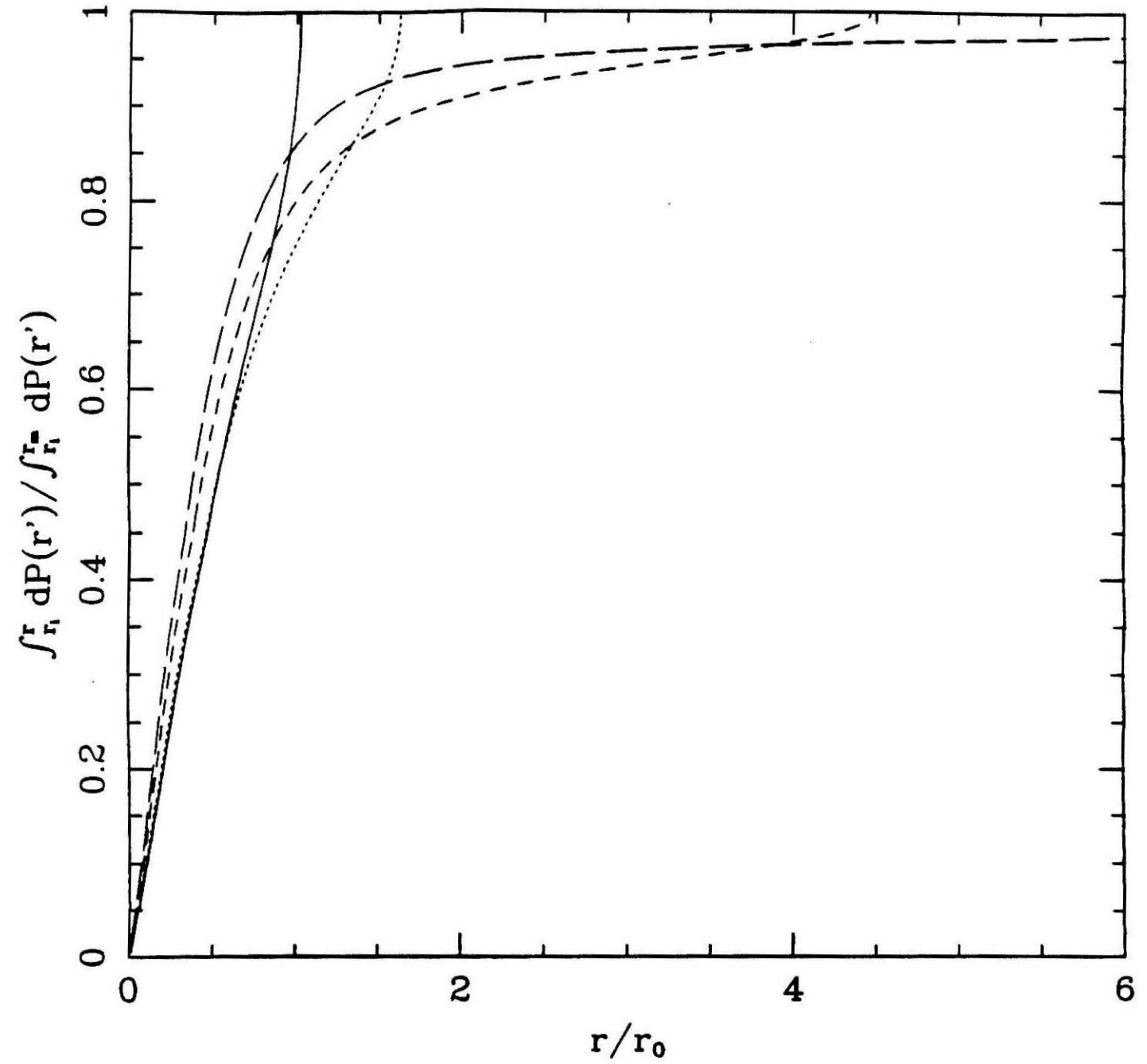


Figure 2b

M13 Model 1, $a = 1$ AU, $M_b = 1.93 M_\odot$, $v_i = 2.5$

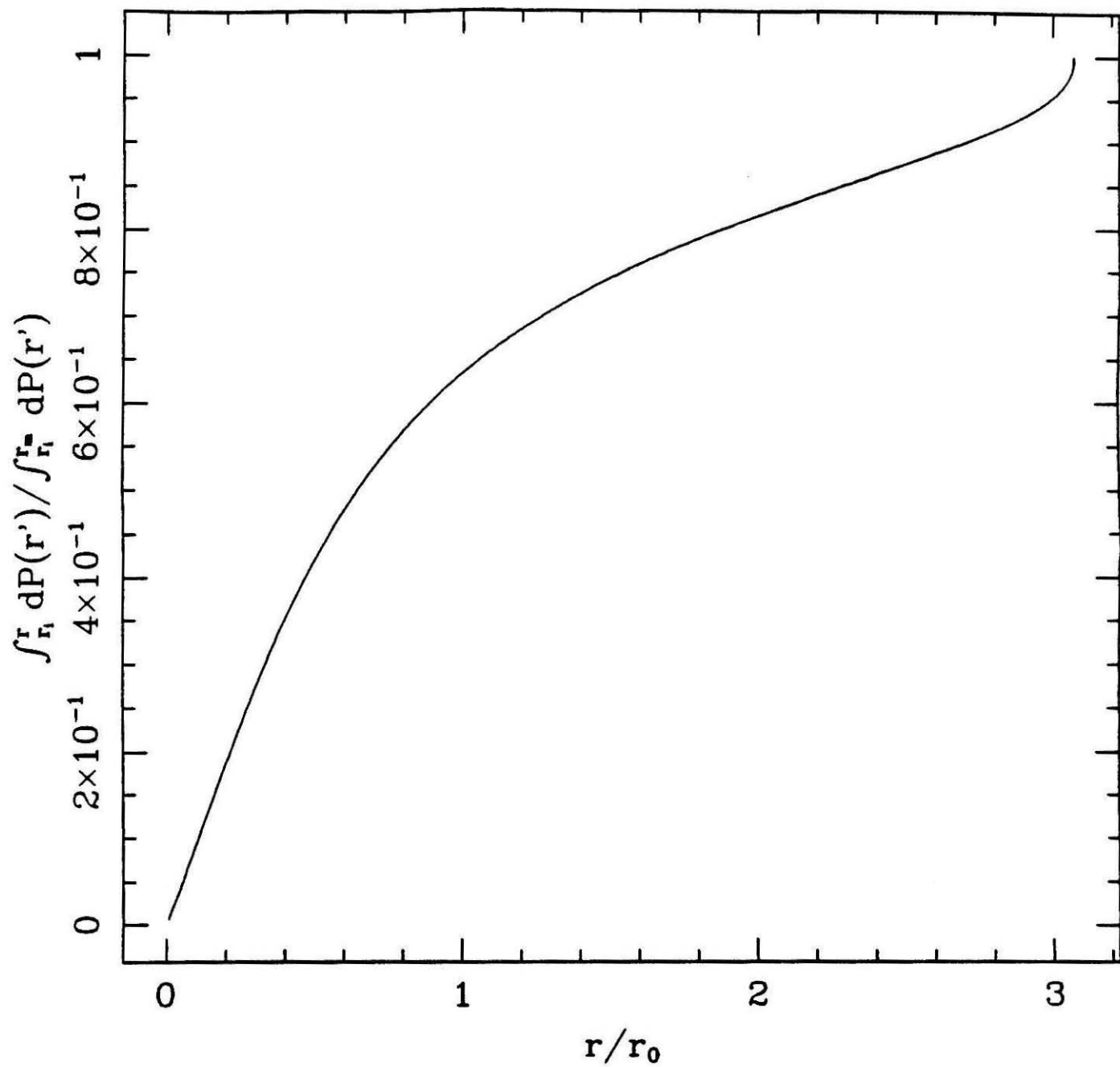


Figure 3

M13 Model 1, $a = 1 \text{ AU}$, $M_b = 1.93 M_\odot$, $v_1 = 2.5$

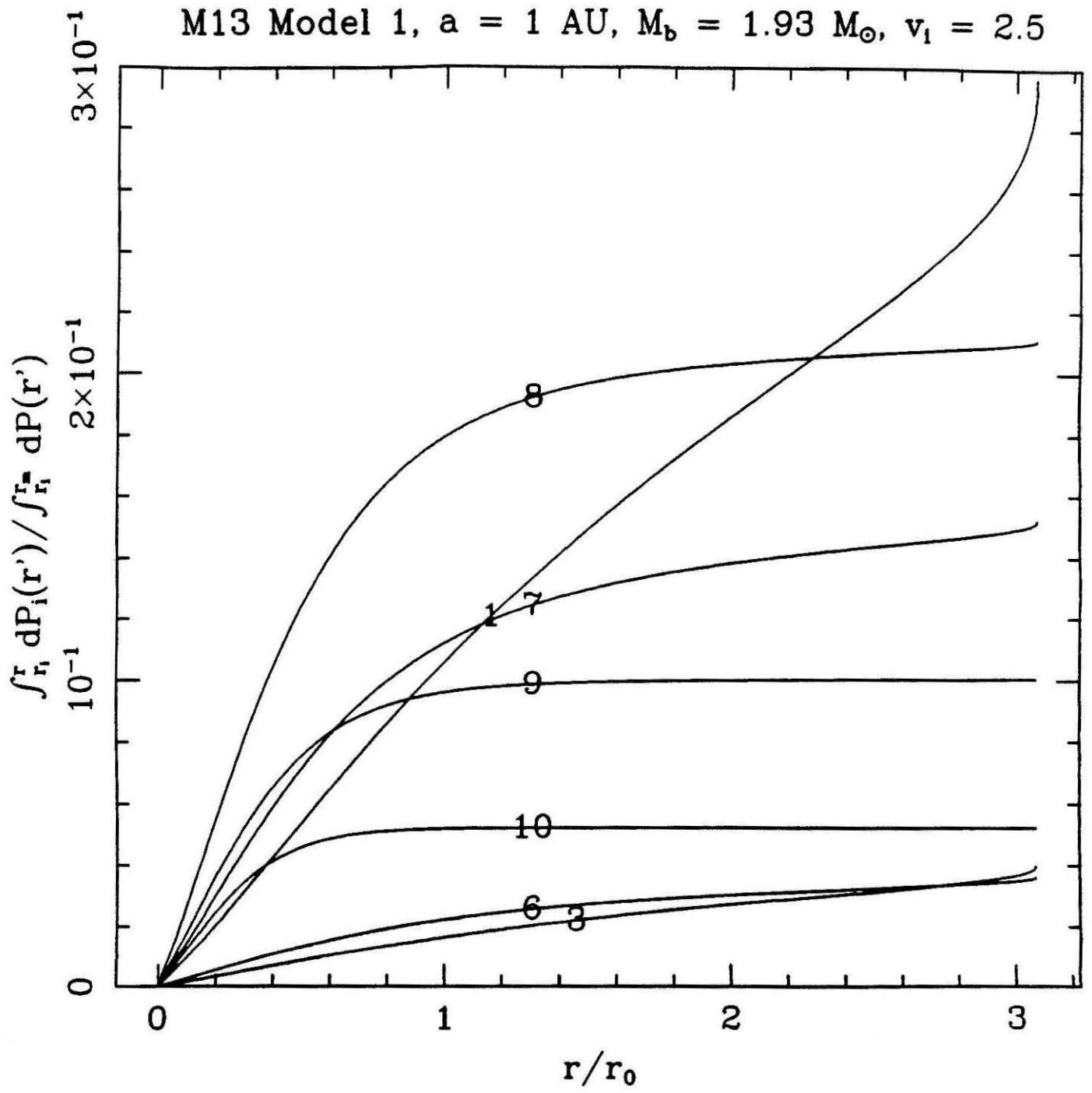


Figure 4

M3 Model 2, $a = 1$ AU, $M_b = 1.27 M_\odot$, $v_1 = 2.5$

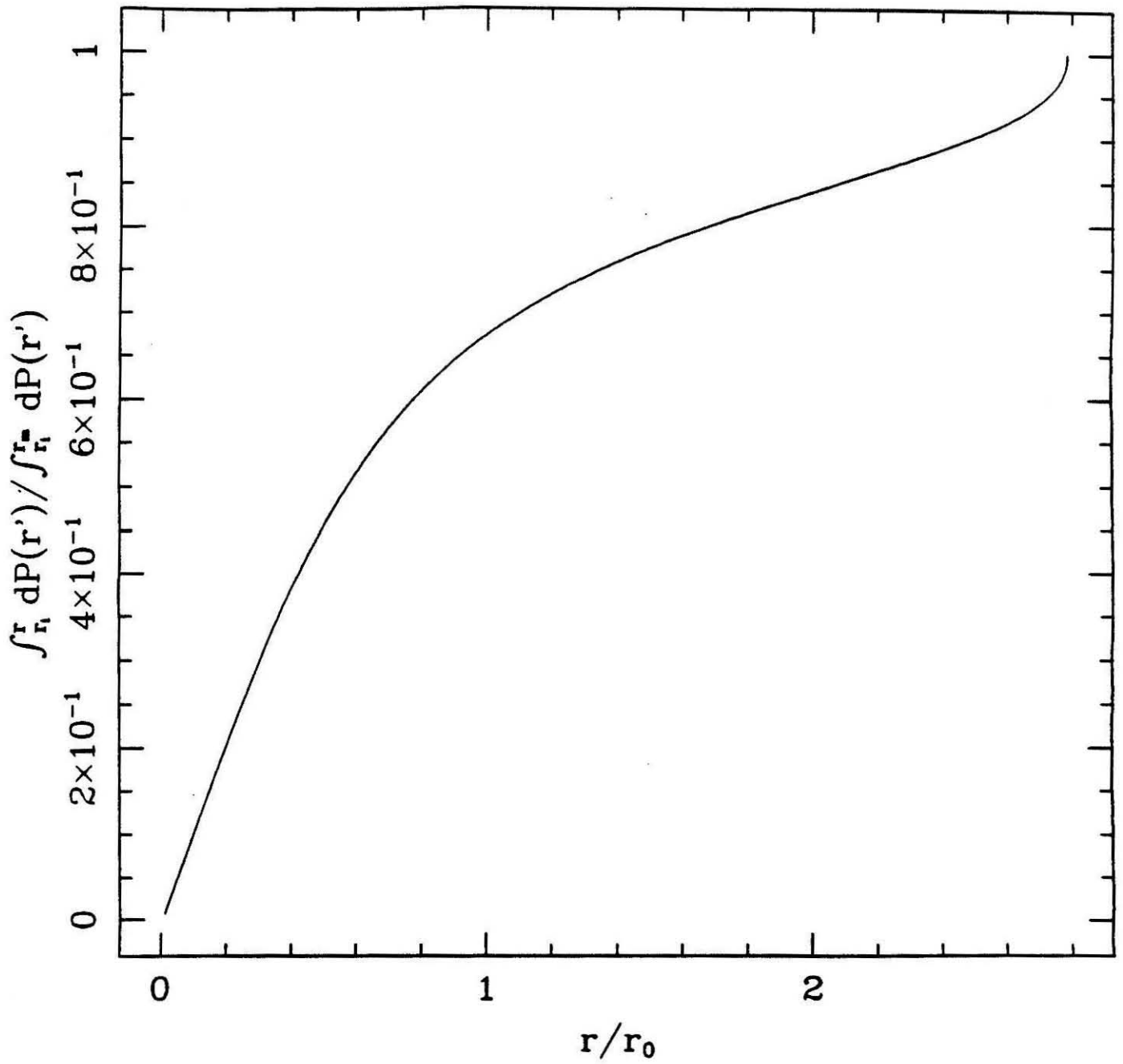


Figure 5

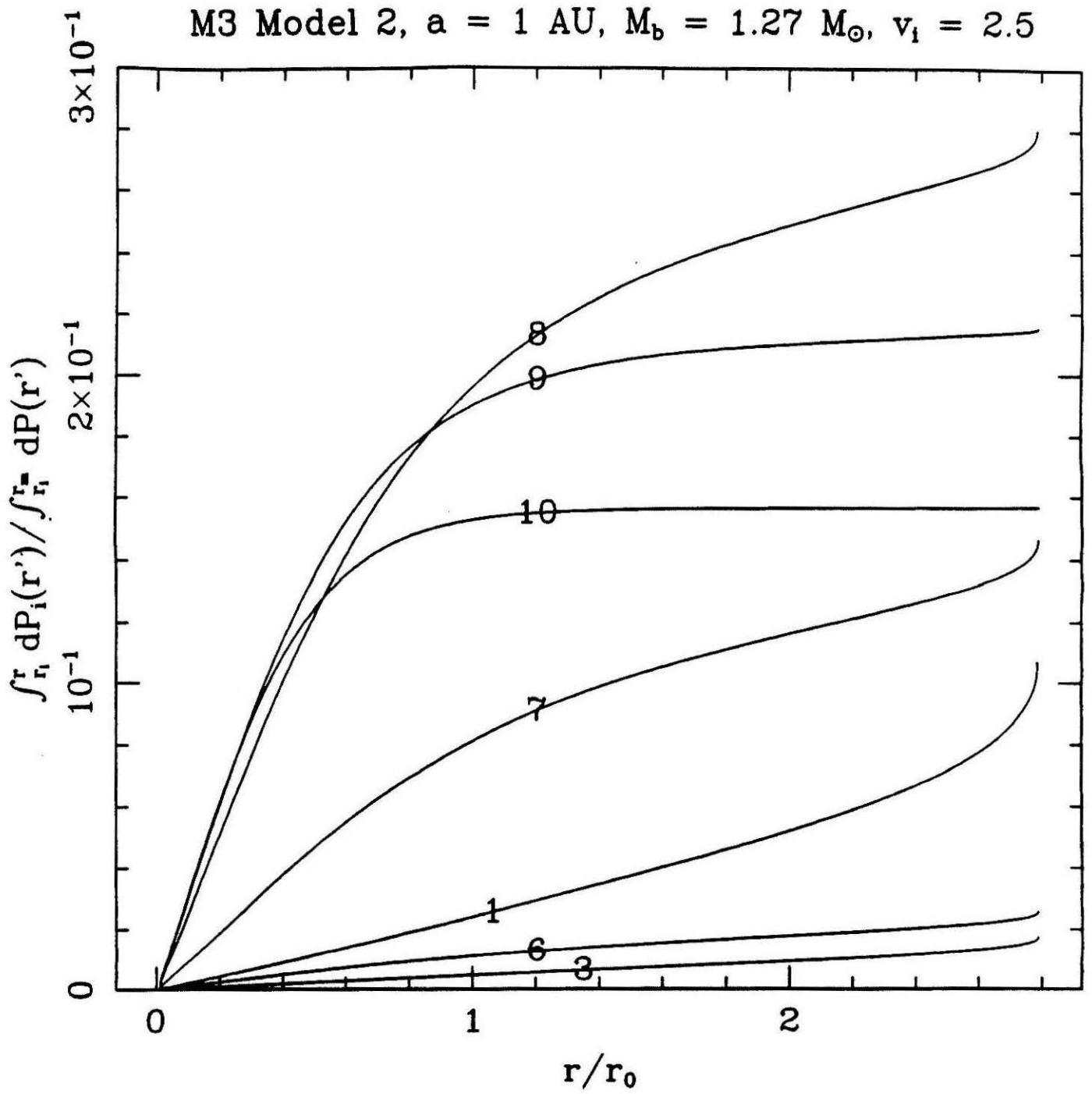


Figure 6

47Tuc Model 3, $a = 1$ AU, $M_b = 1.13 M_\odot$, $v_i = 2.5$

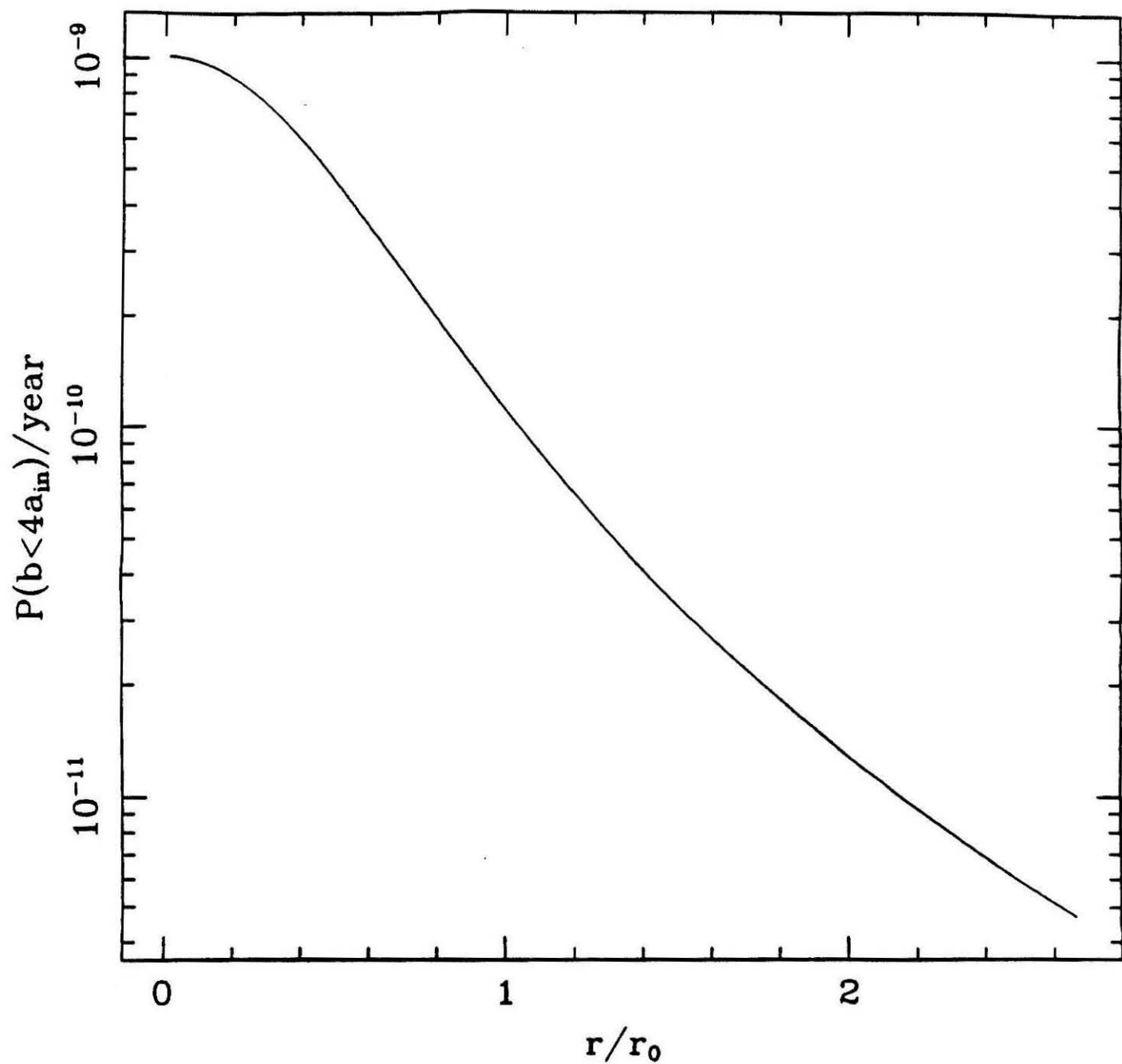


Figure 7

47Tuc Model 3, $a = 1$ AU, $M_b = 1.13 M_\odot$, $v_1 = 2.5$

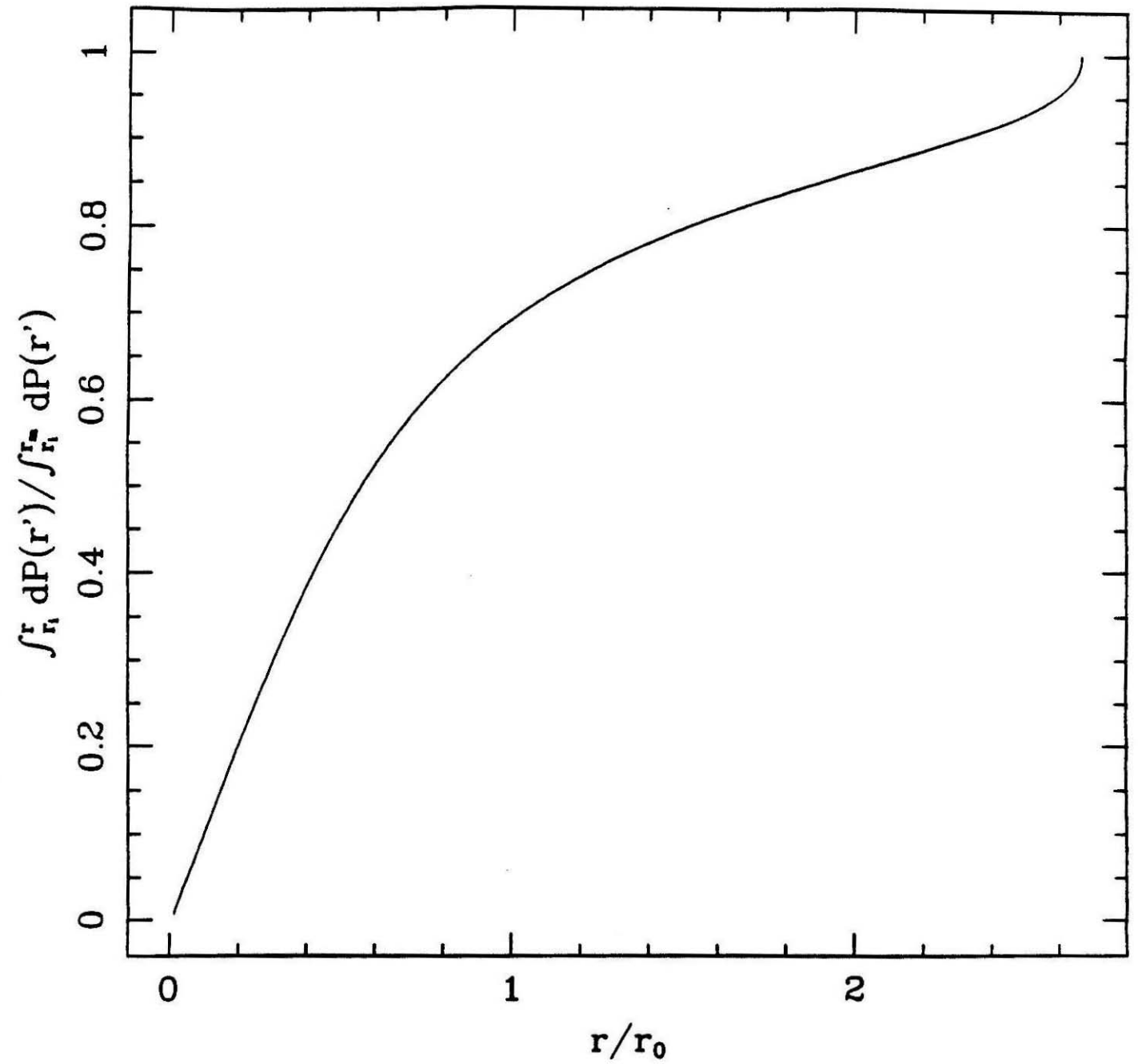


Figure 8

47Tuc Model 3, $a = 1$ AU, $M_b = 1.13 M_\odot$, $v_i = 2.5$

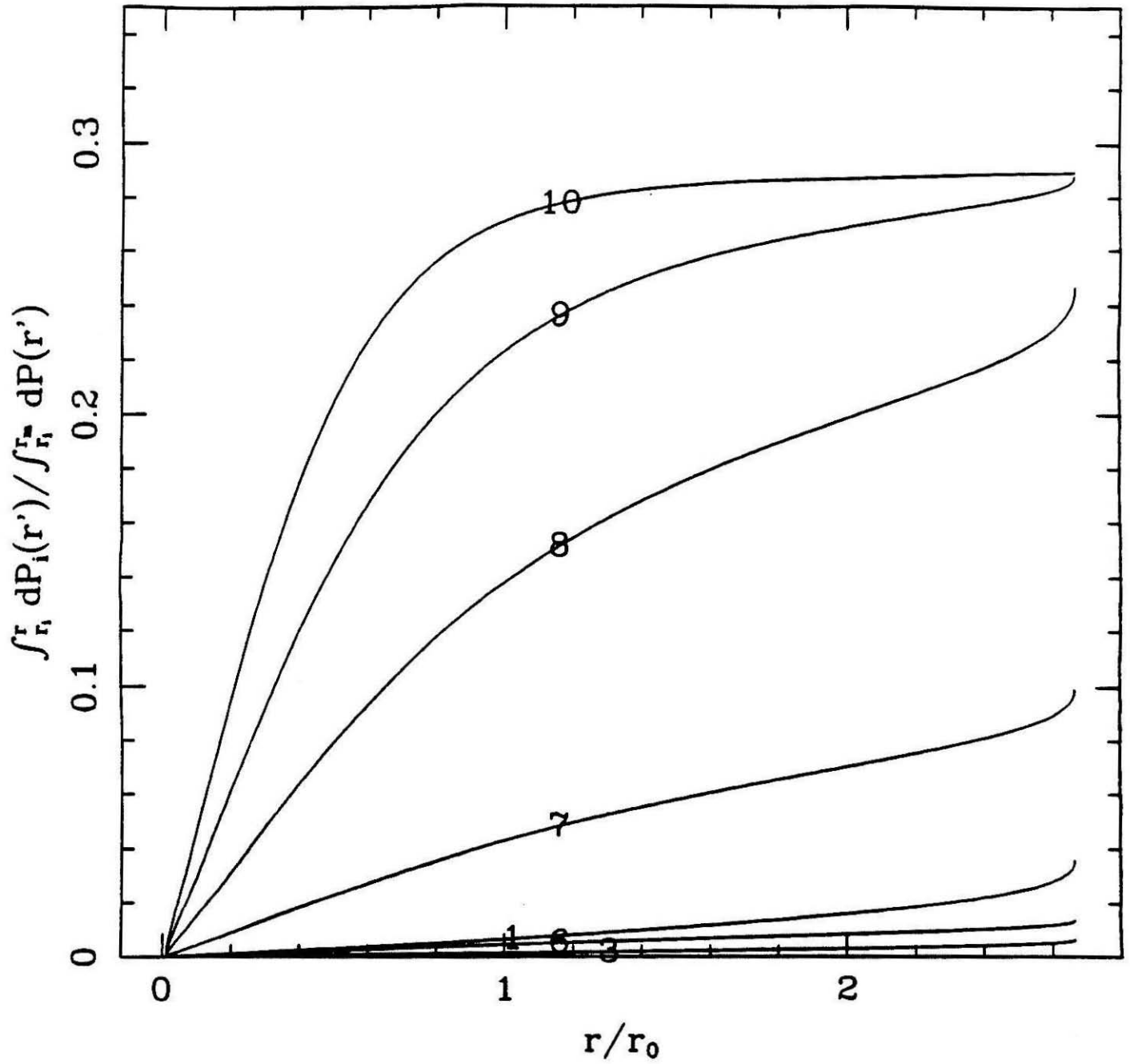


Figure 9

47Tuc Model 4, $a = 1$ AU, $M_b = 1.68 M_\odot$, $v_1 = 2.5$

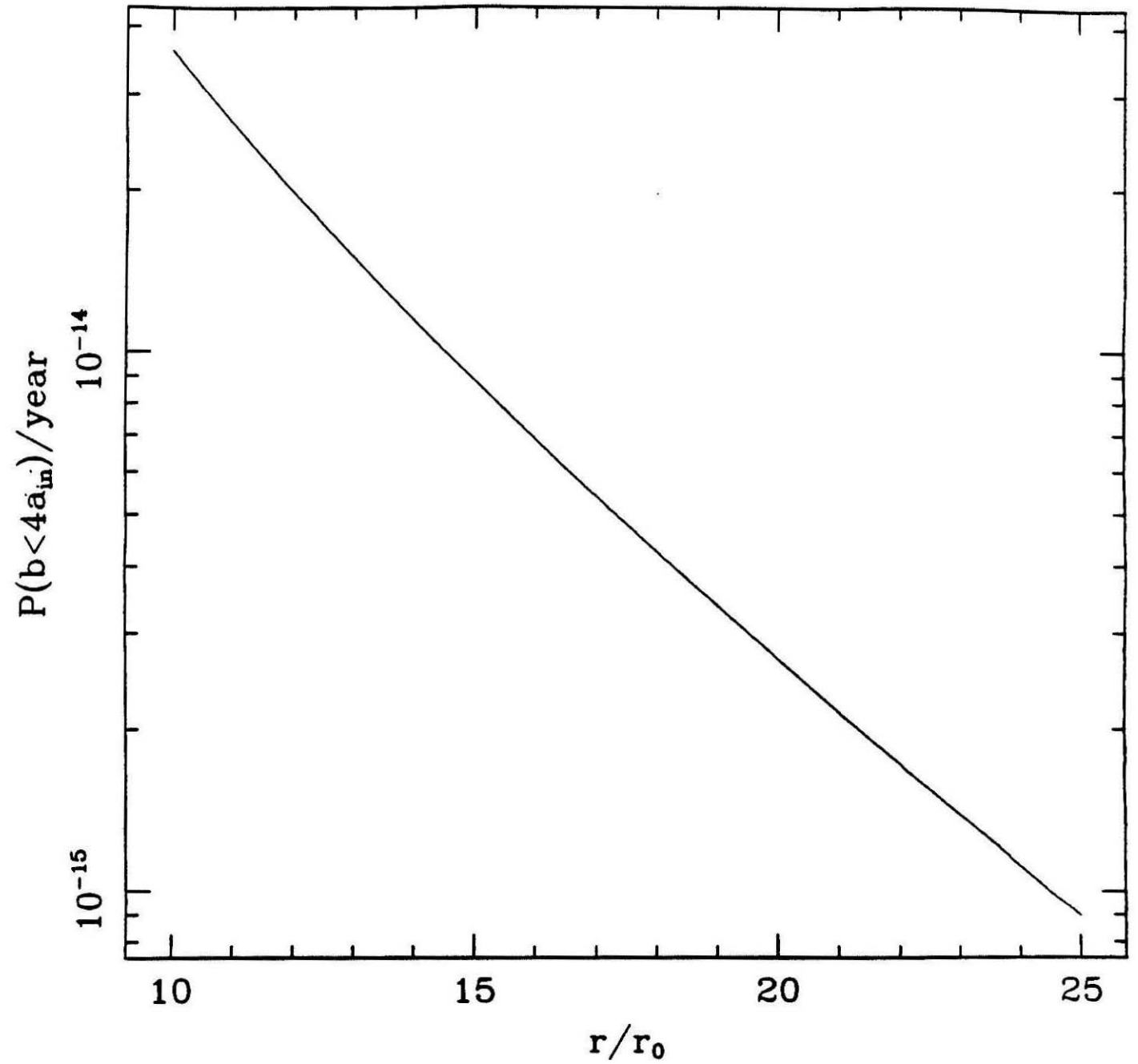


Figure 10

47Tuc Model 4, $a = 1$ AU, $M_b = 1.68 M_\odot$, $v_1 = 2.5$

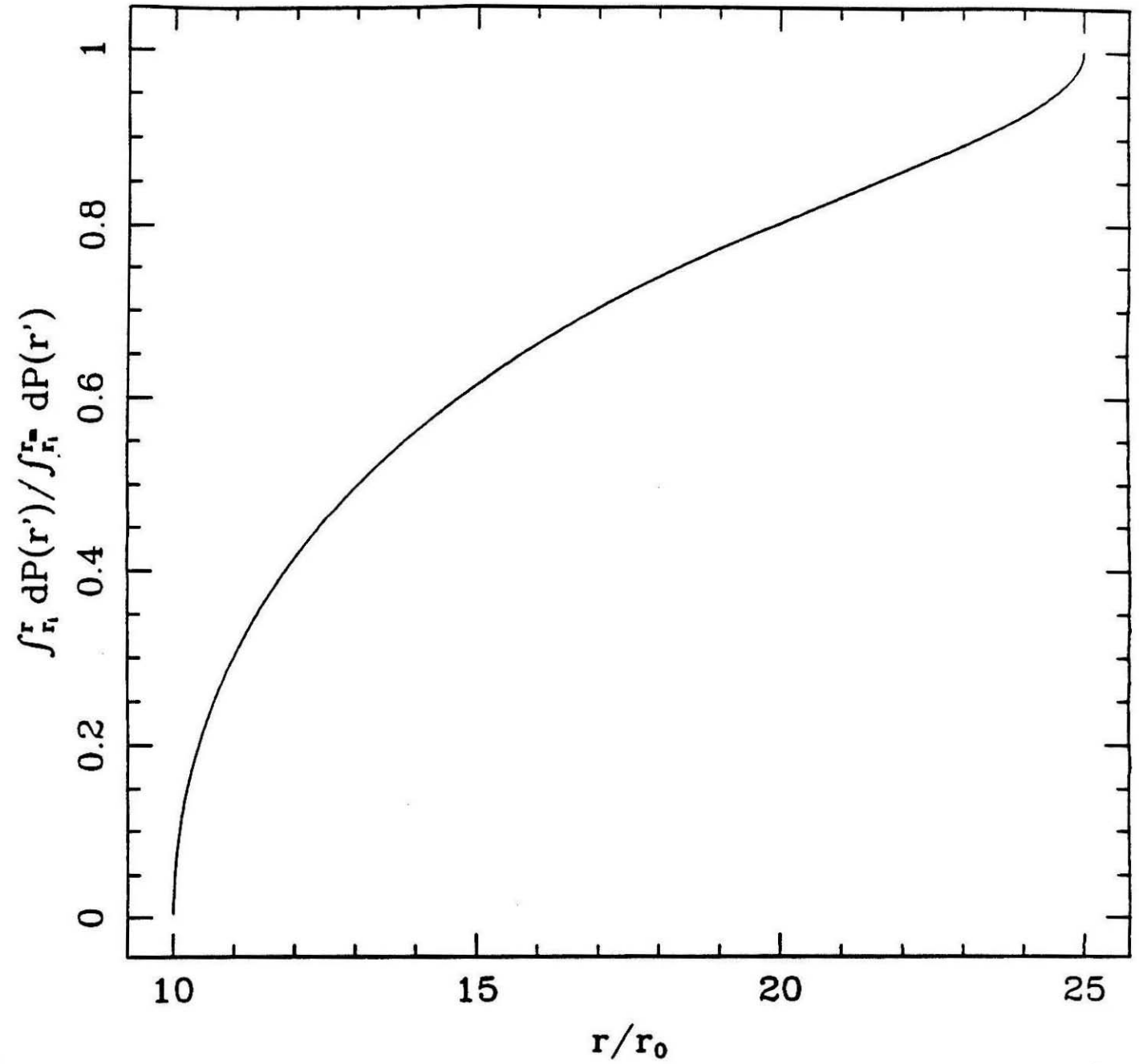


Figure 11

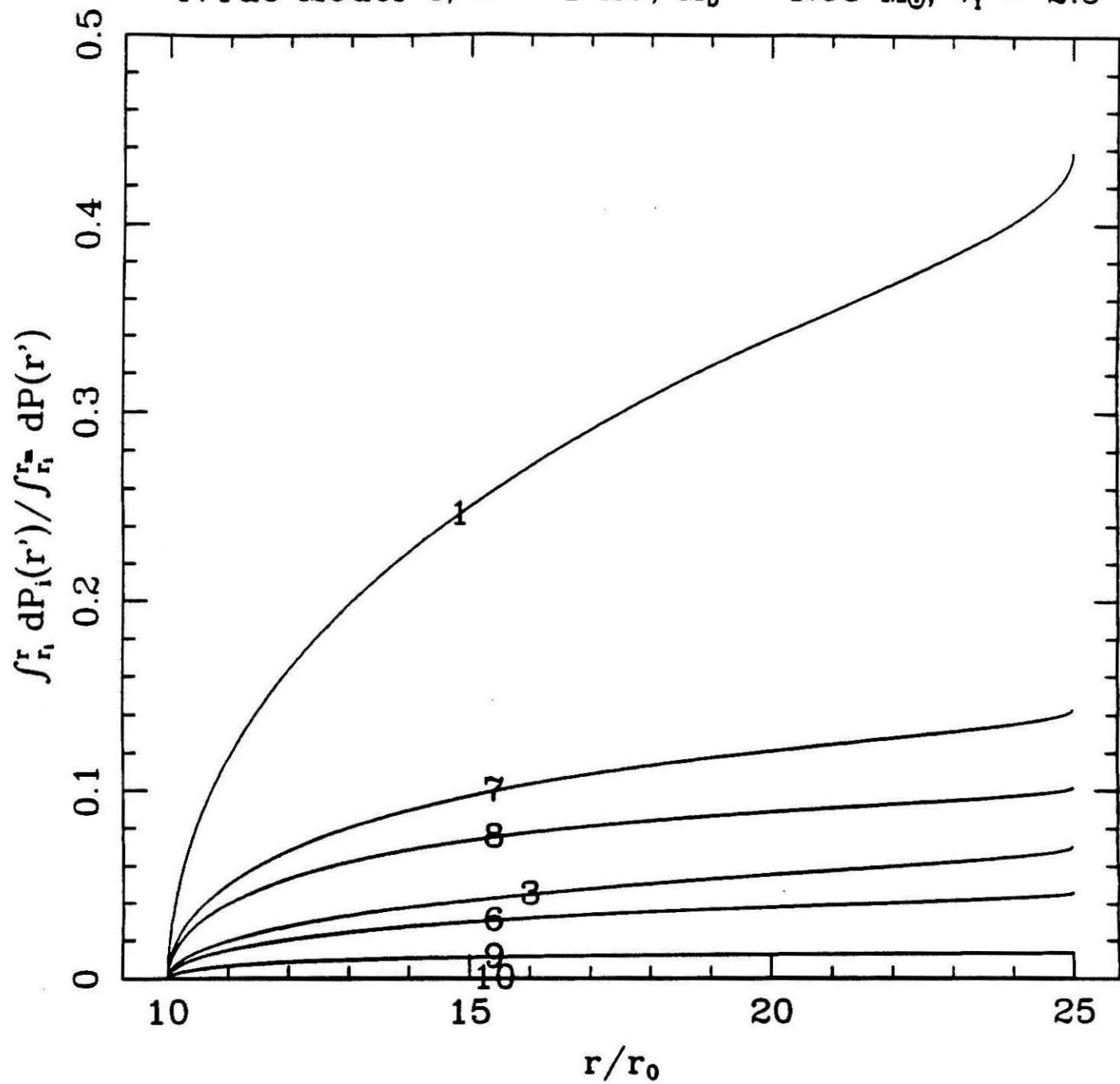
47Tuc Model 4, $a = 1$ AU, $M_b = 1.68 M_\odot$, $v_i = 2.5$ 

Figure 12

M15 Model 6, $a = 1$ AU, $M_b = 1.67 M_\odot$, $v_i = 3.0$

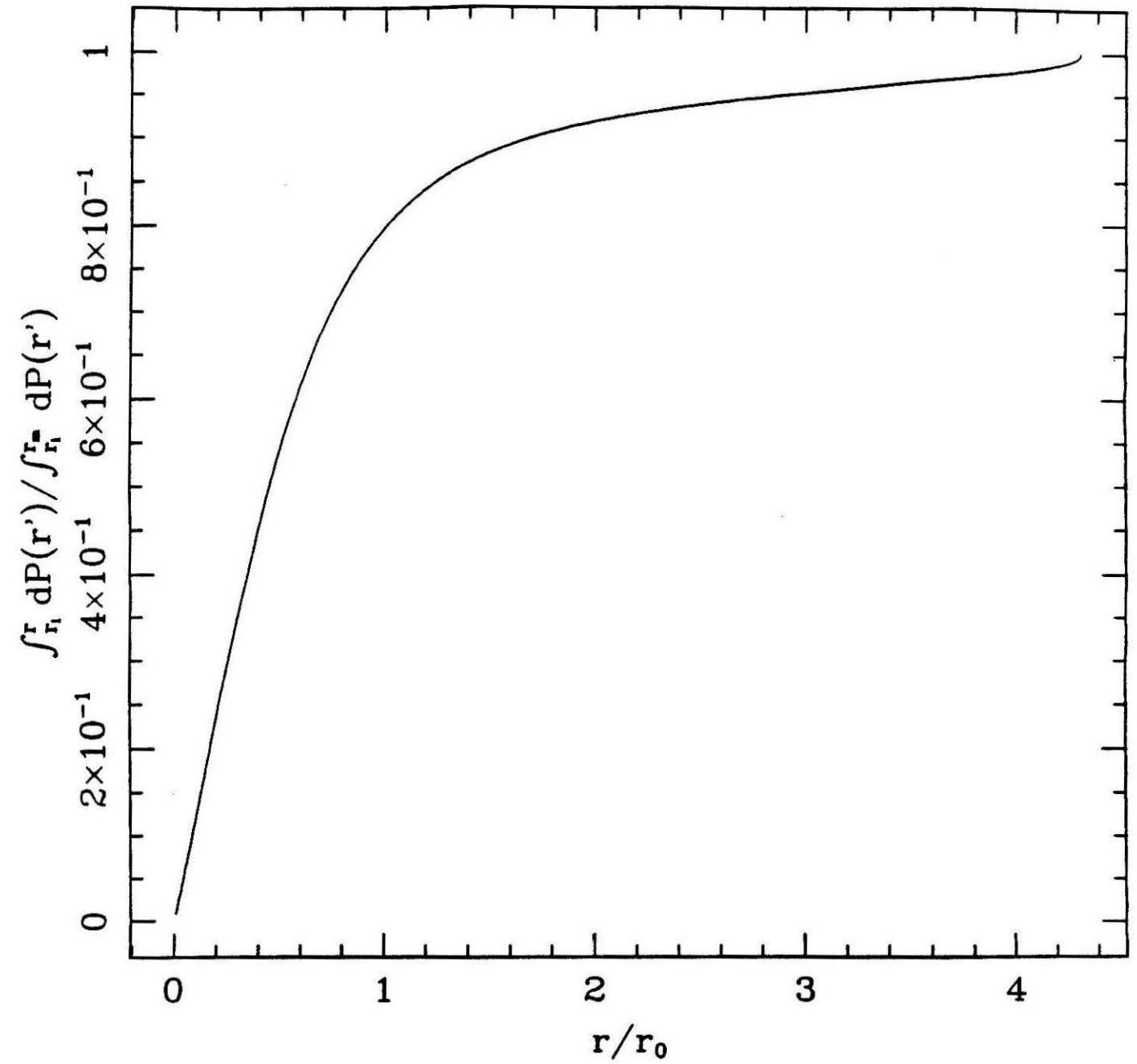


Figure 13

M15 Model 6, $a = 1$ AU, $M_b = 1.67 M_\odot$, $v_i = 3.0$

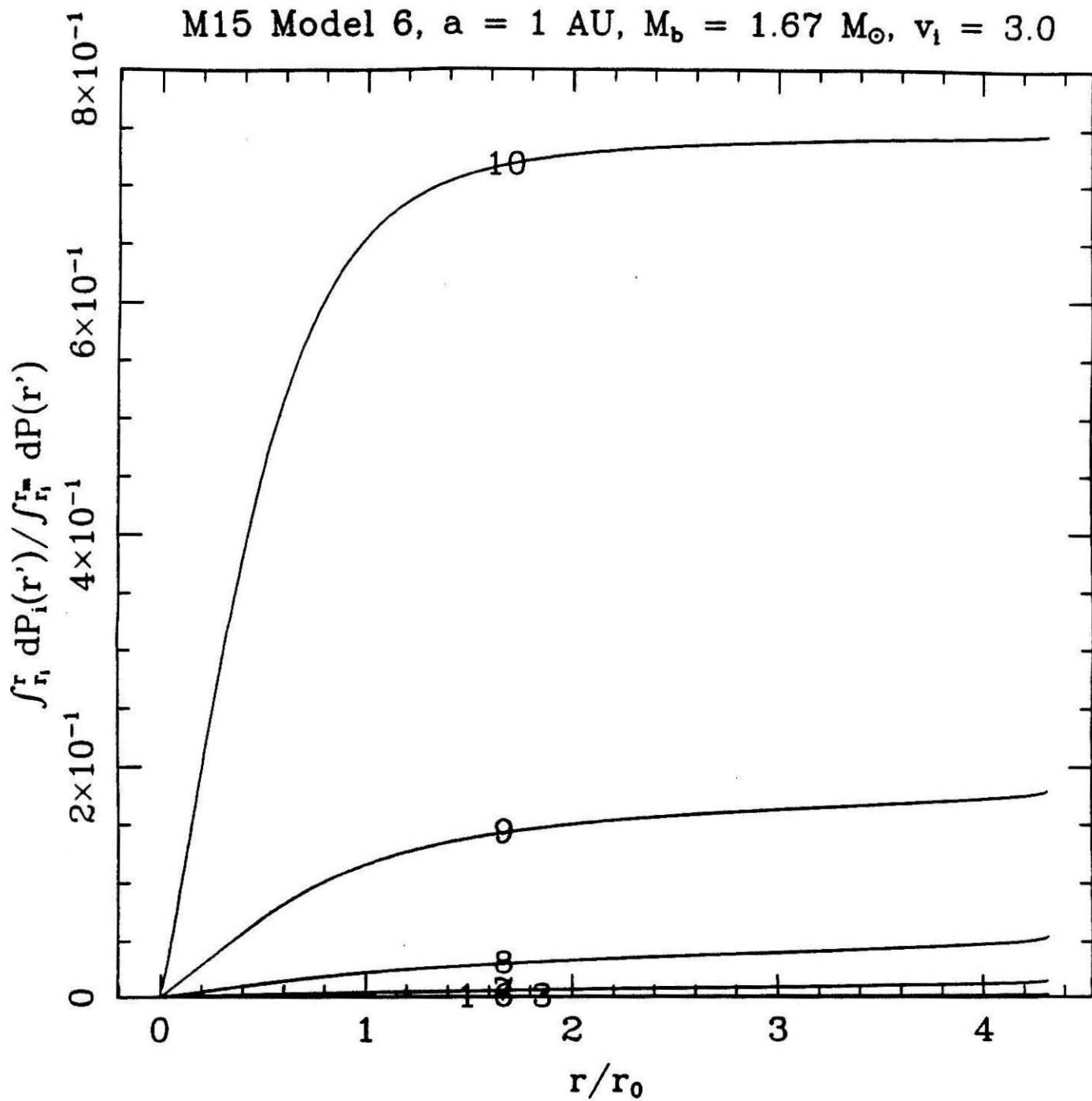


Figure 14

Initial radial distribution

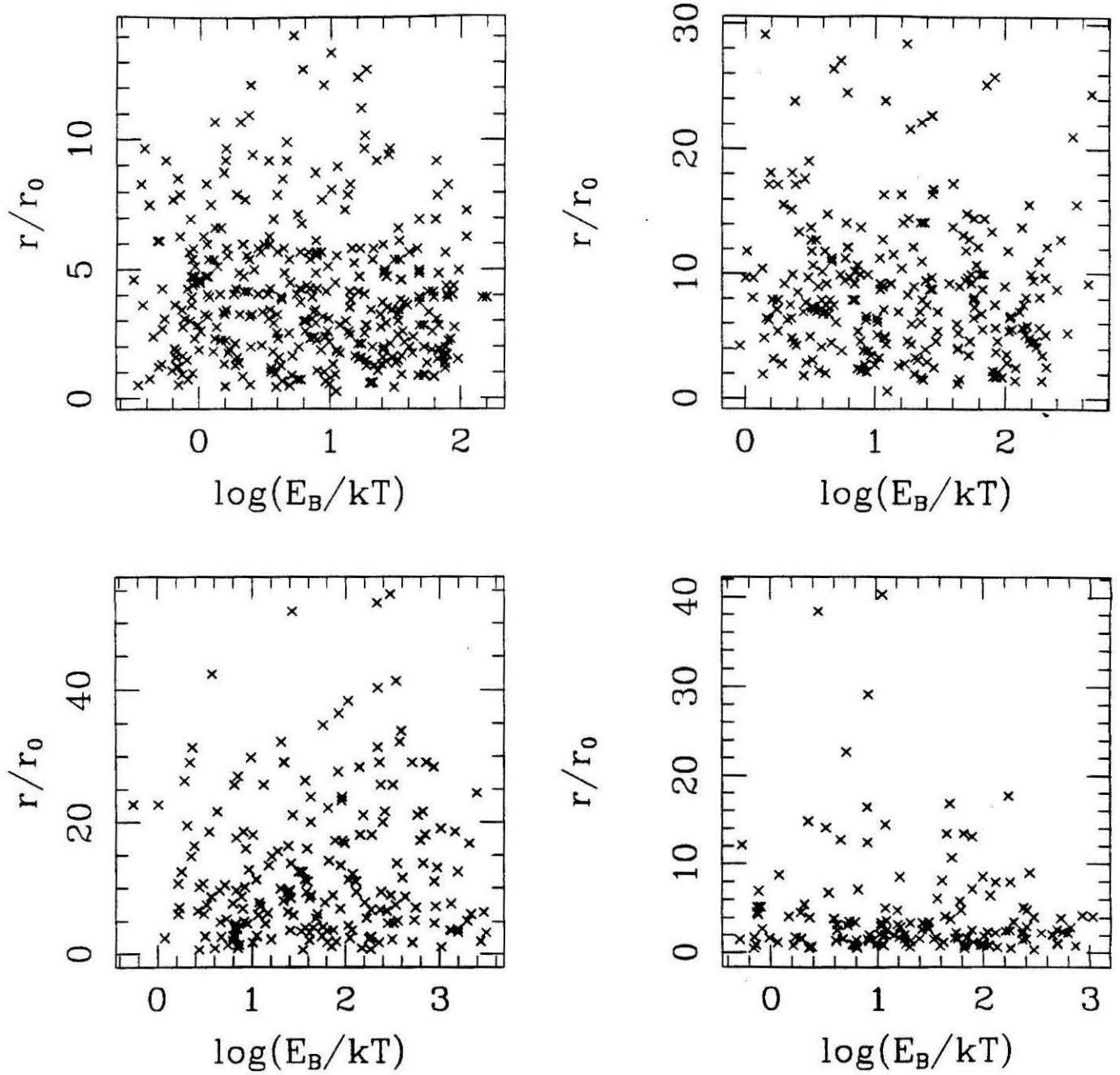


Figure 15a

Initial radial distribution

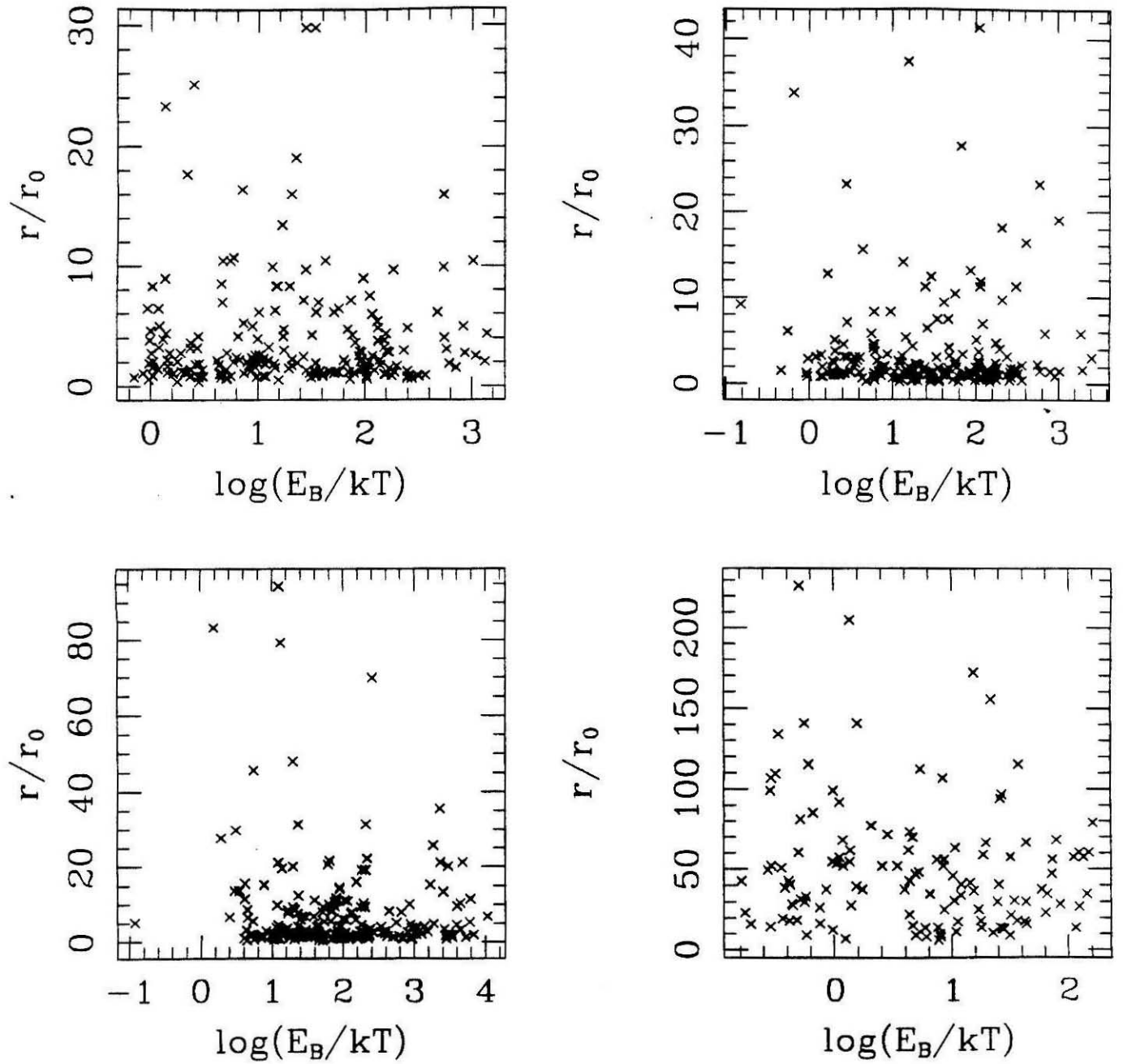


Figure 15b

Model 1, run 1.1.1

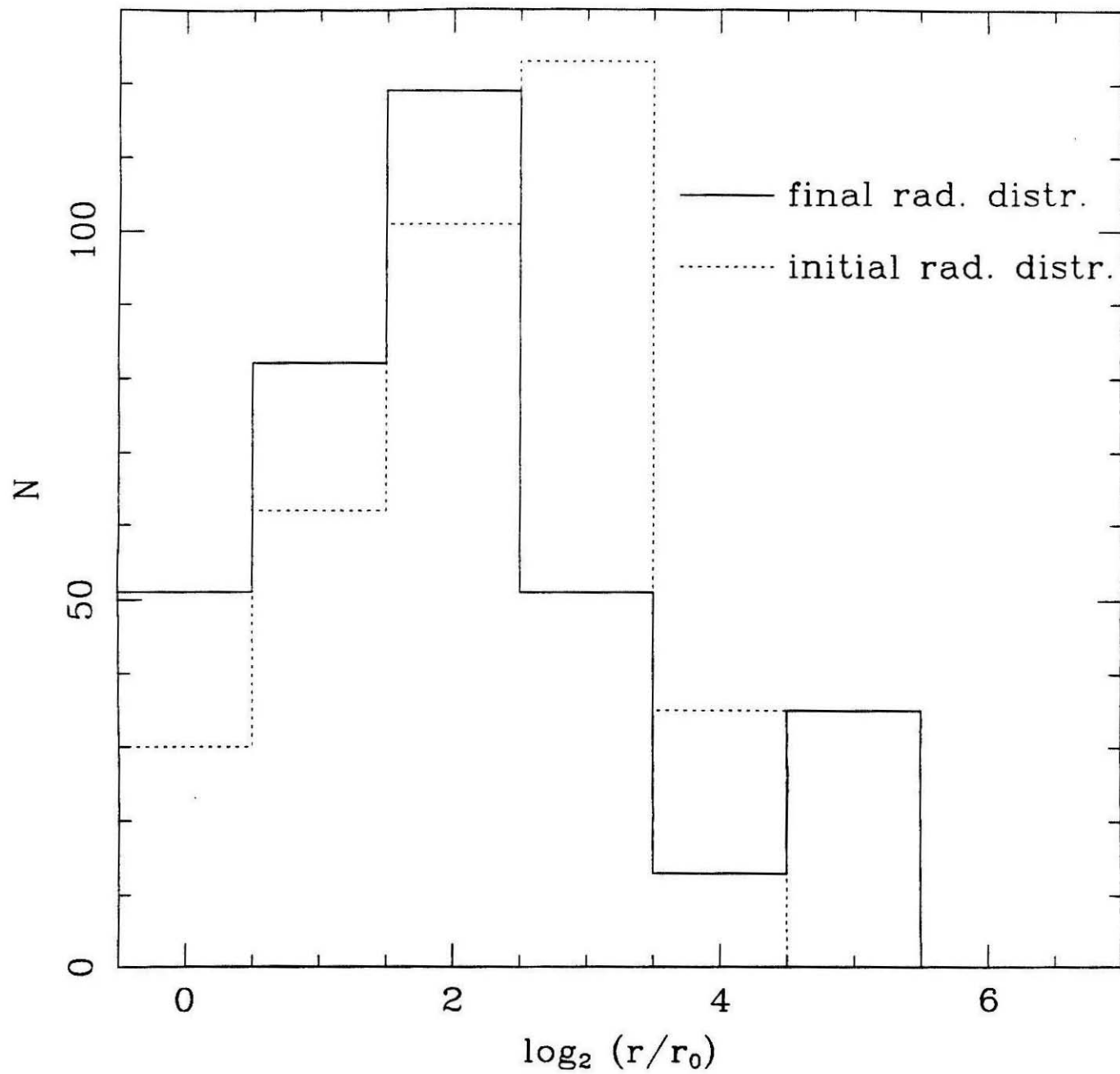


Figure 16a

Model 2, run 2.1.1

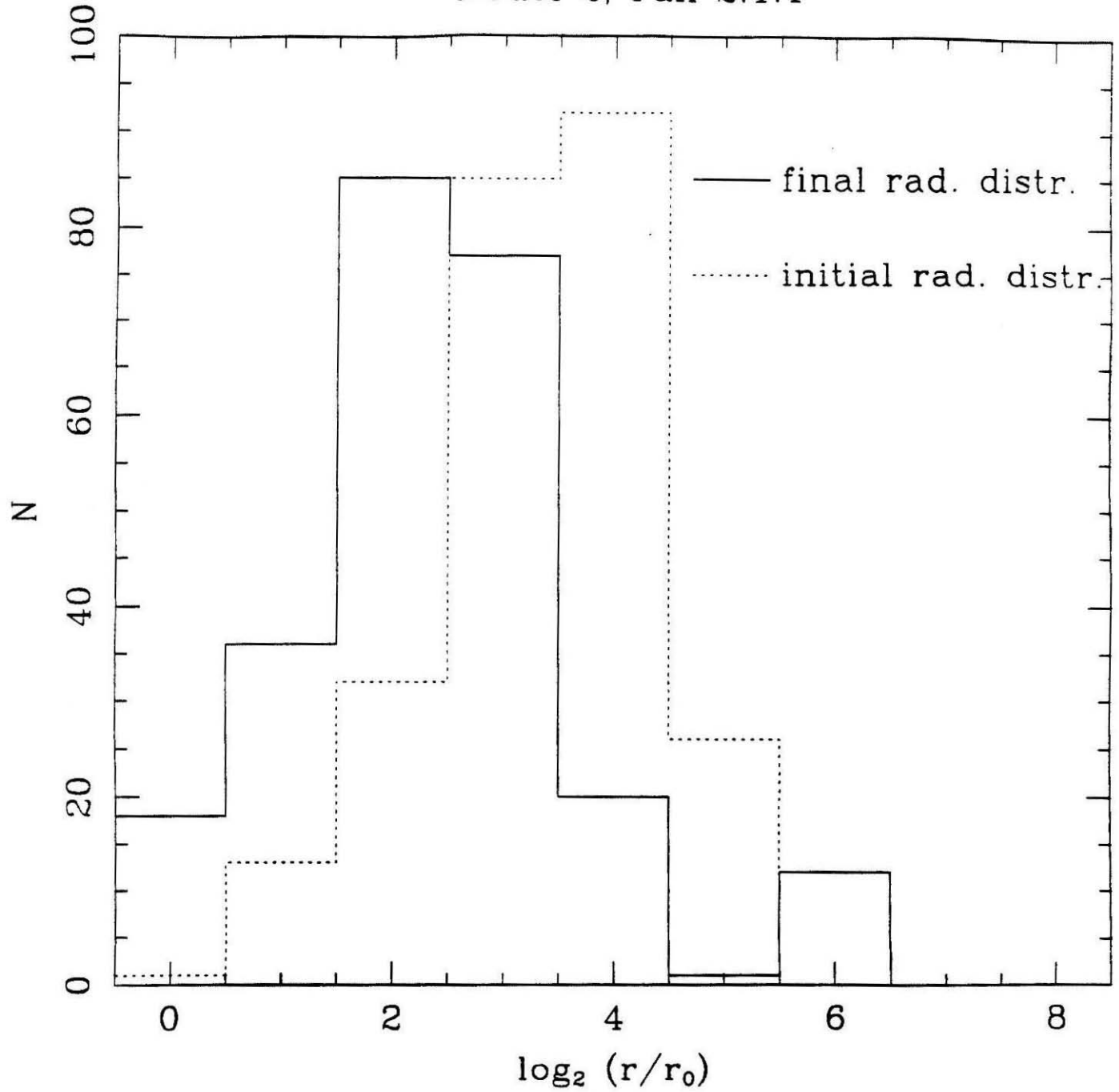


Figure 16b

Model 3, runs 3.3.1 and 3.4.1

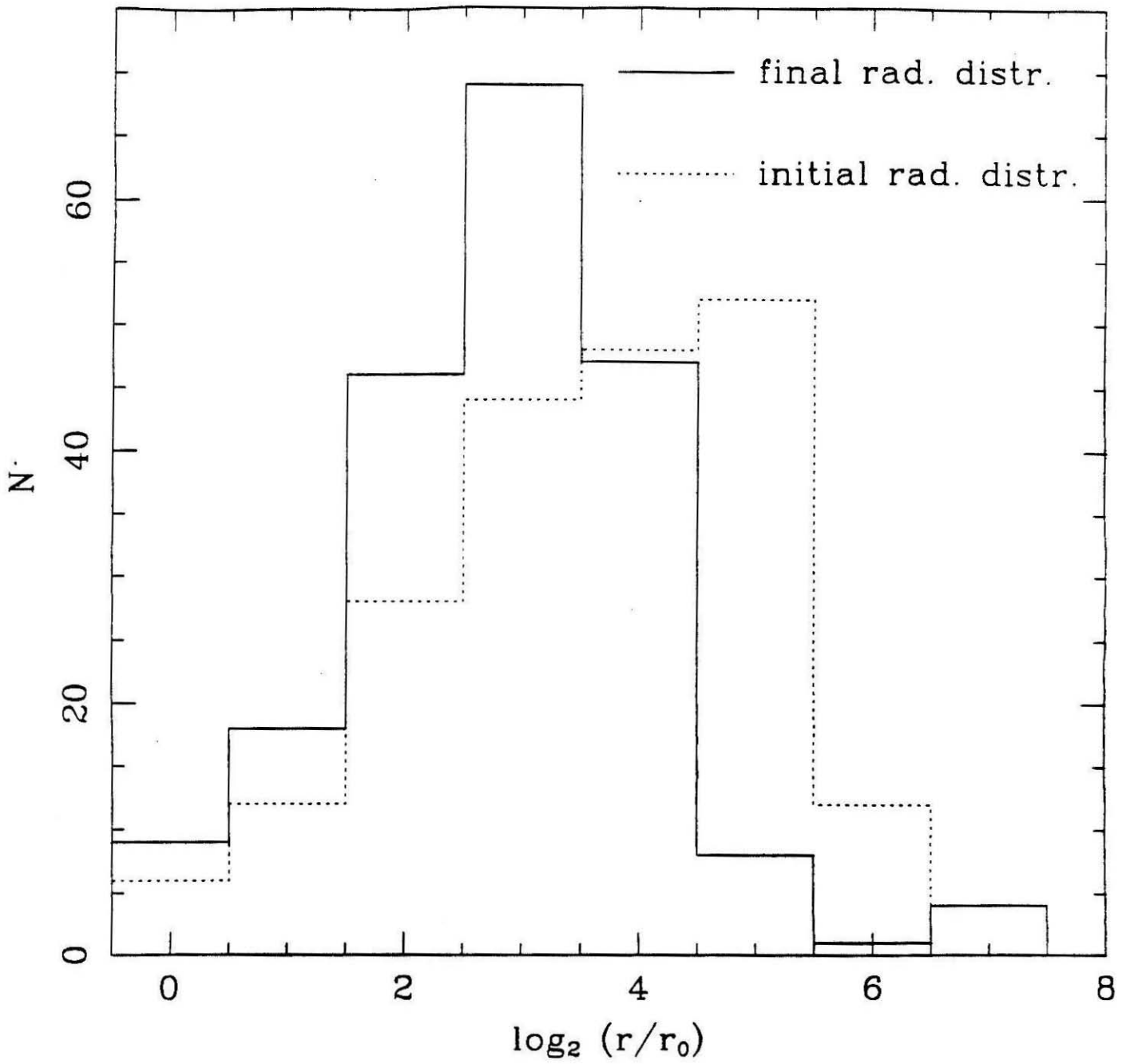


Figure 16c

Model 4, runs 4.2.1 and 4.2.2

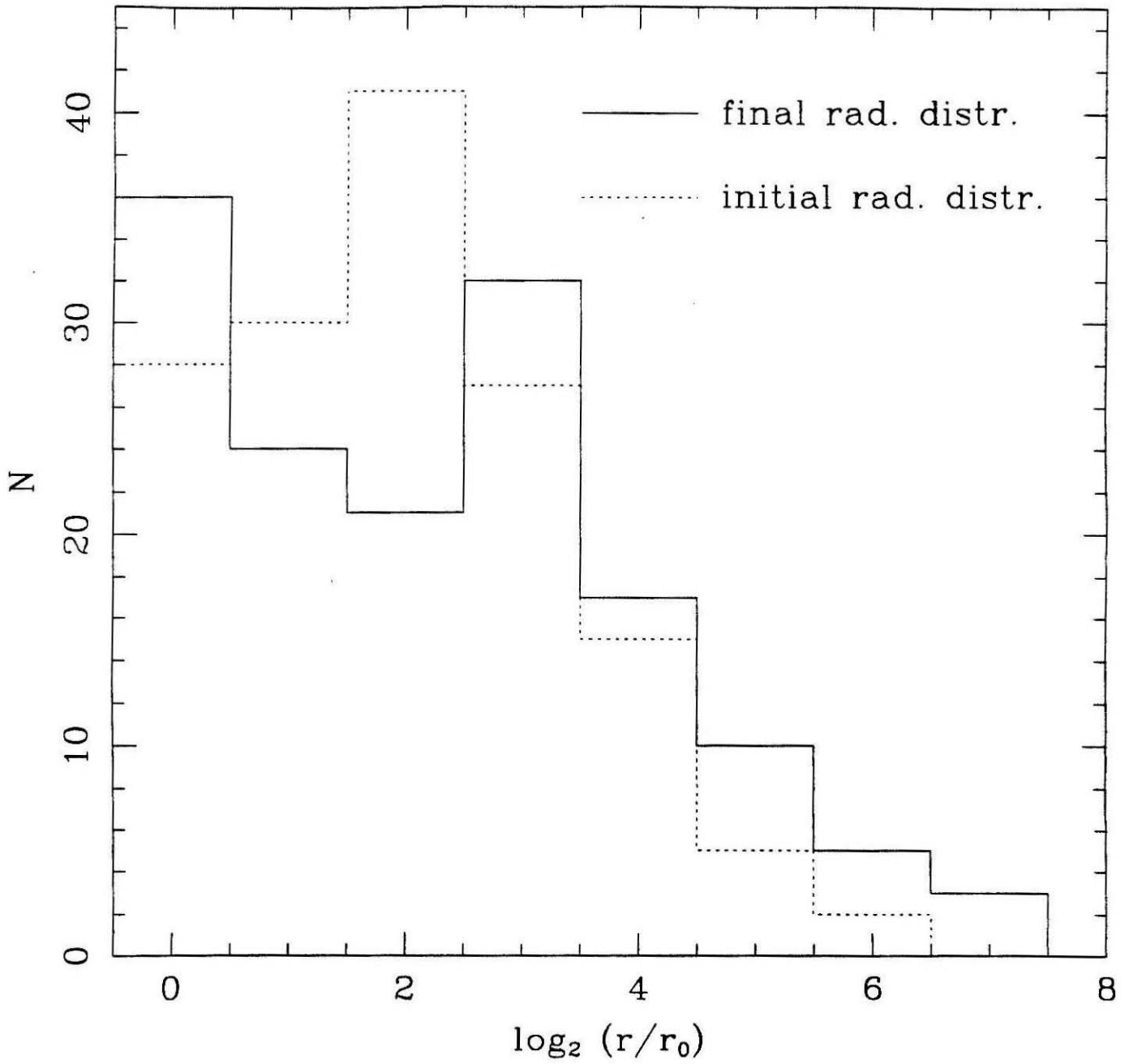


Figure 16d

Model 4, runs 4.3.1 and 4.3.2

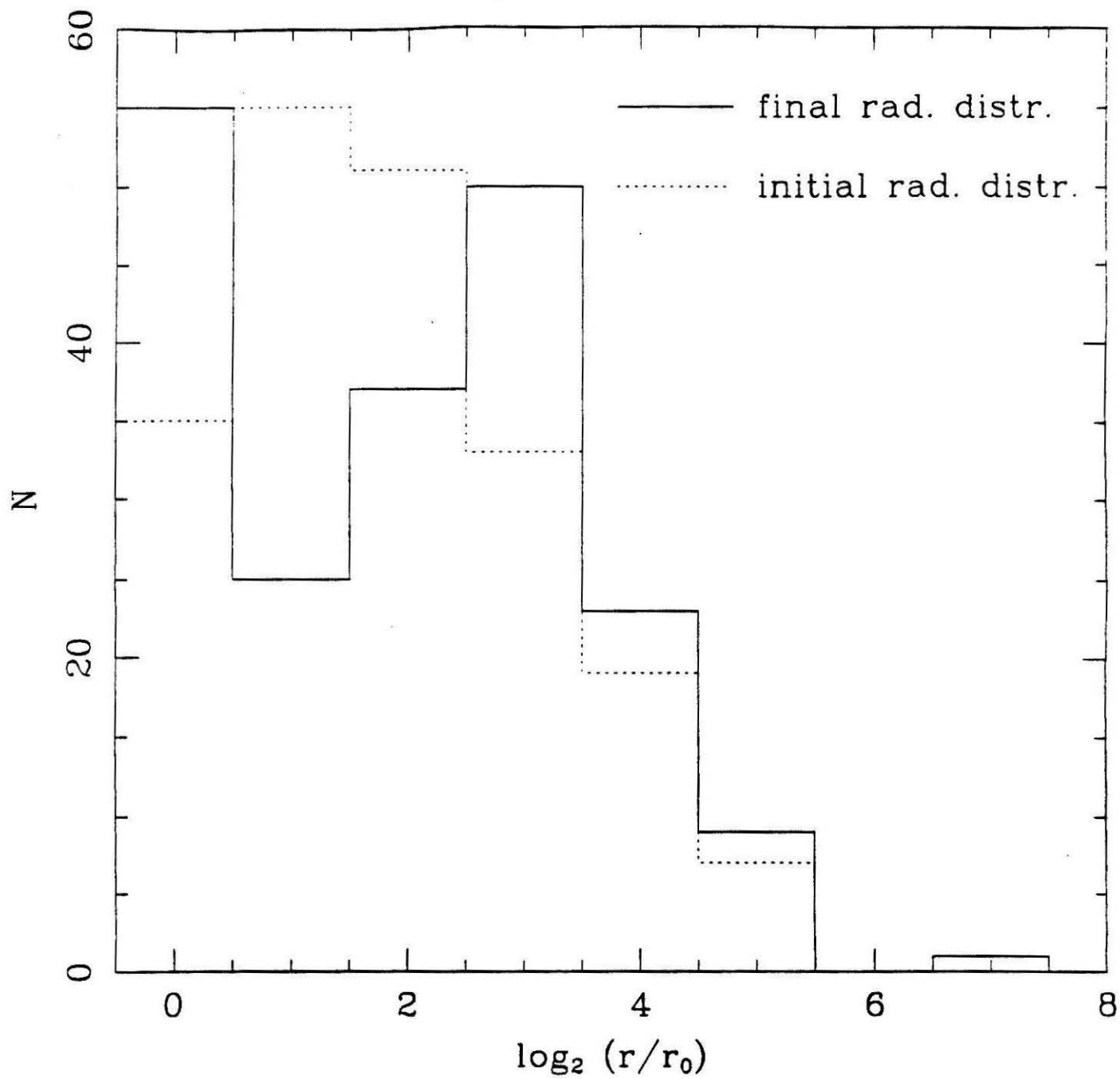


Figure 16e

Model 5, runs 5.1.1 and 5.2.1

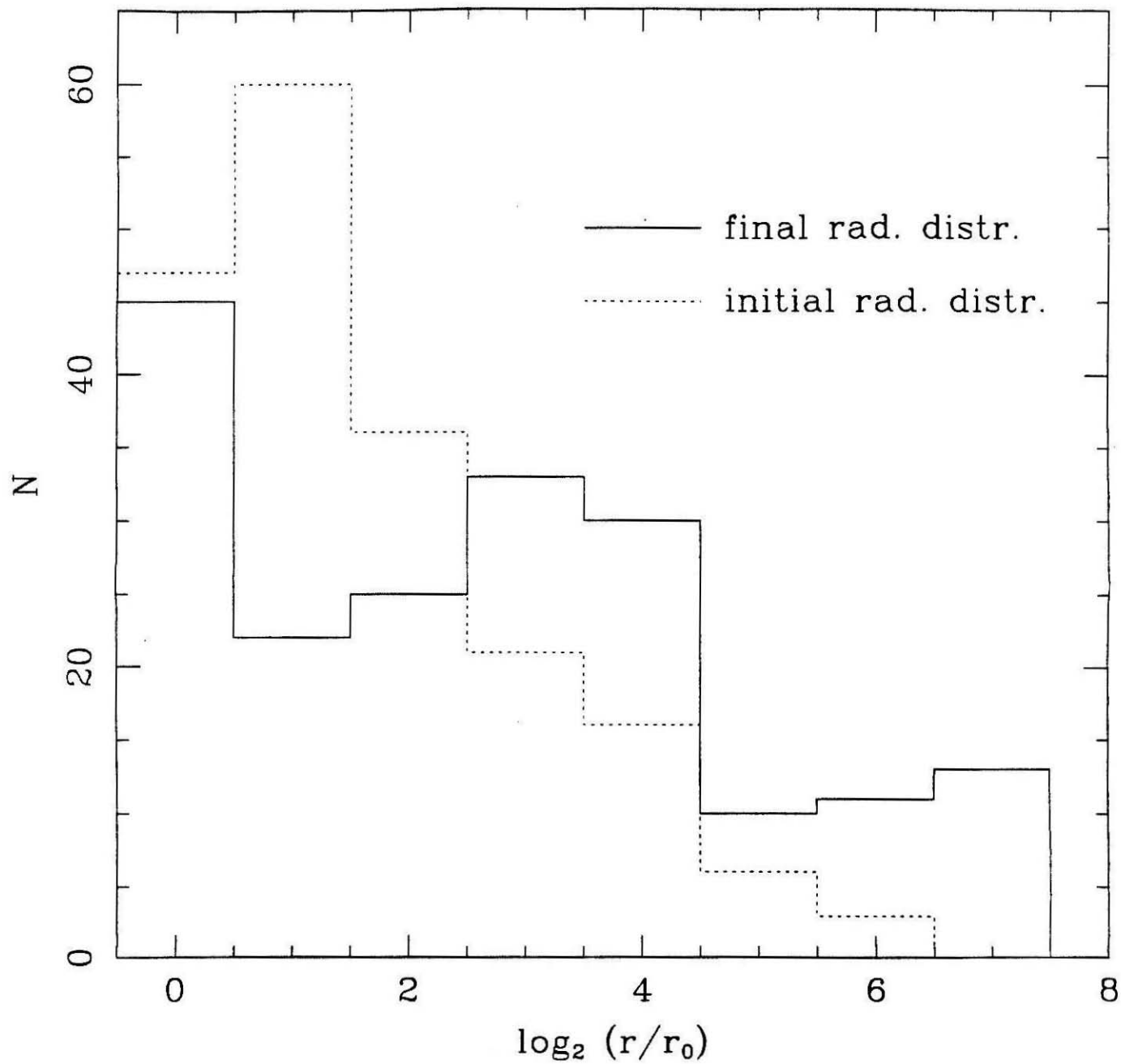


Figure 16f

Model 6, runs 6.1.1 and 6.1.2

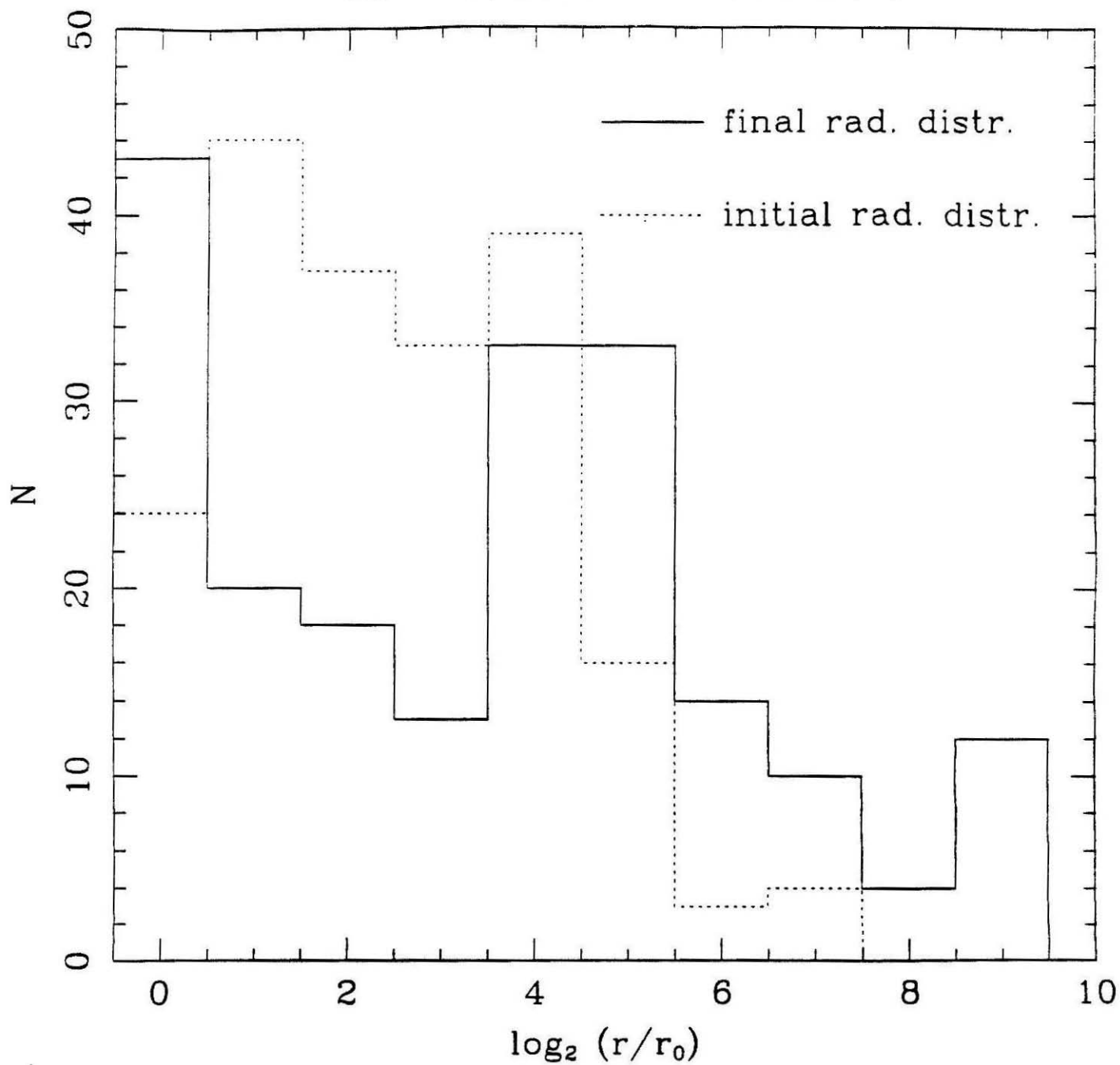


Figure 16g

Model 6, runs 6.2.1 and 6.2.2

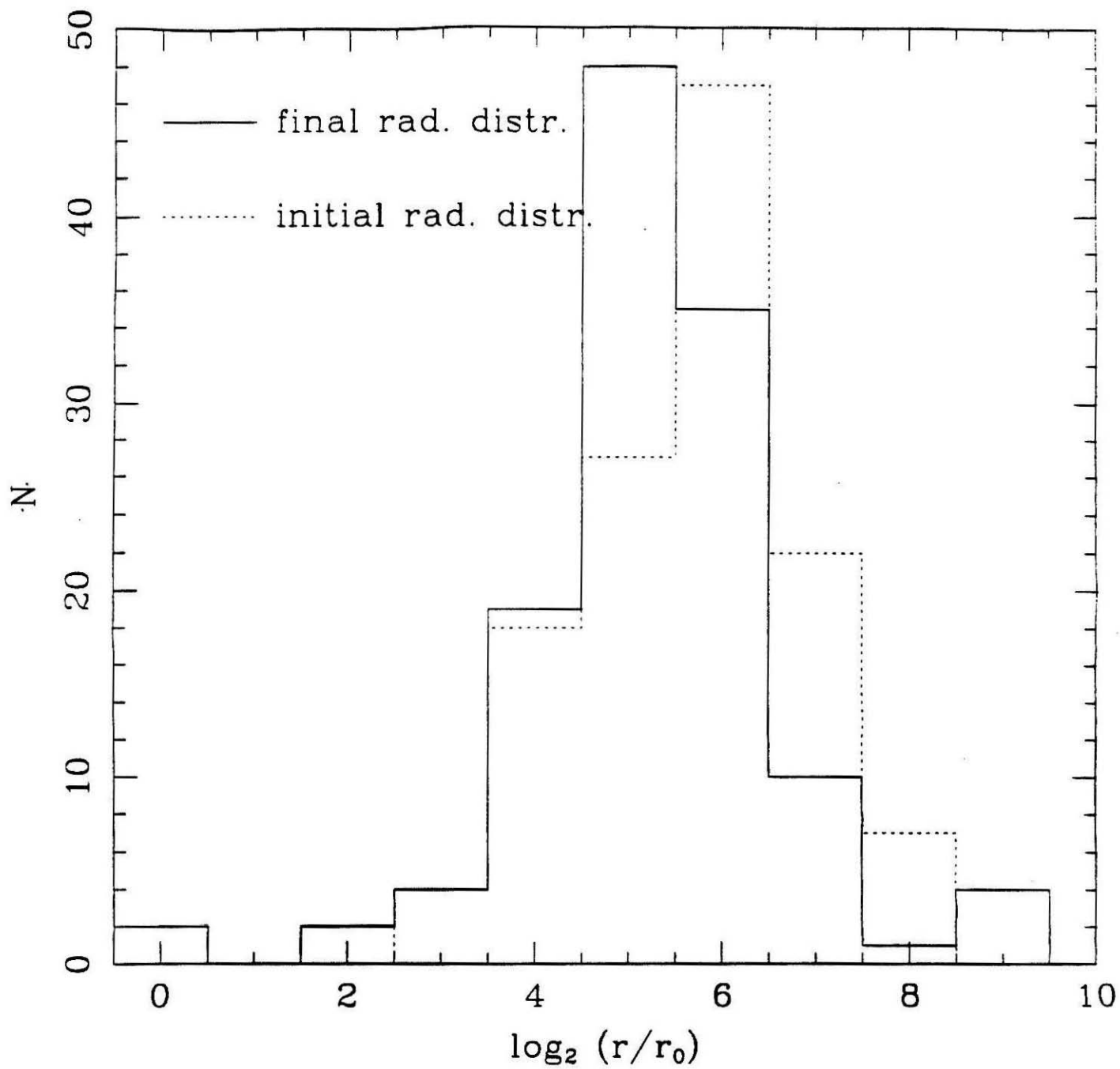


Figure 16h

Model 1, run 1.1.1, final distribution

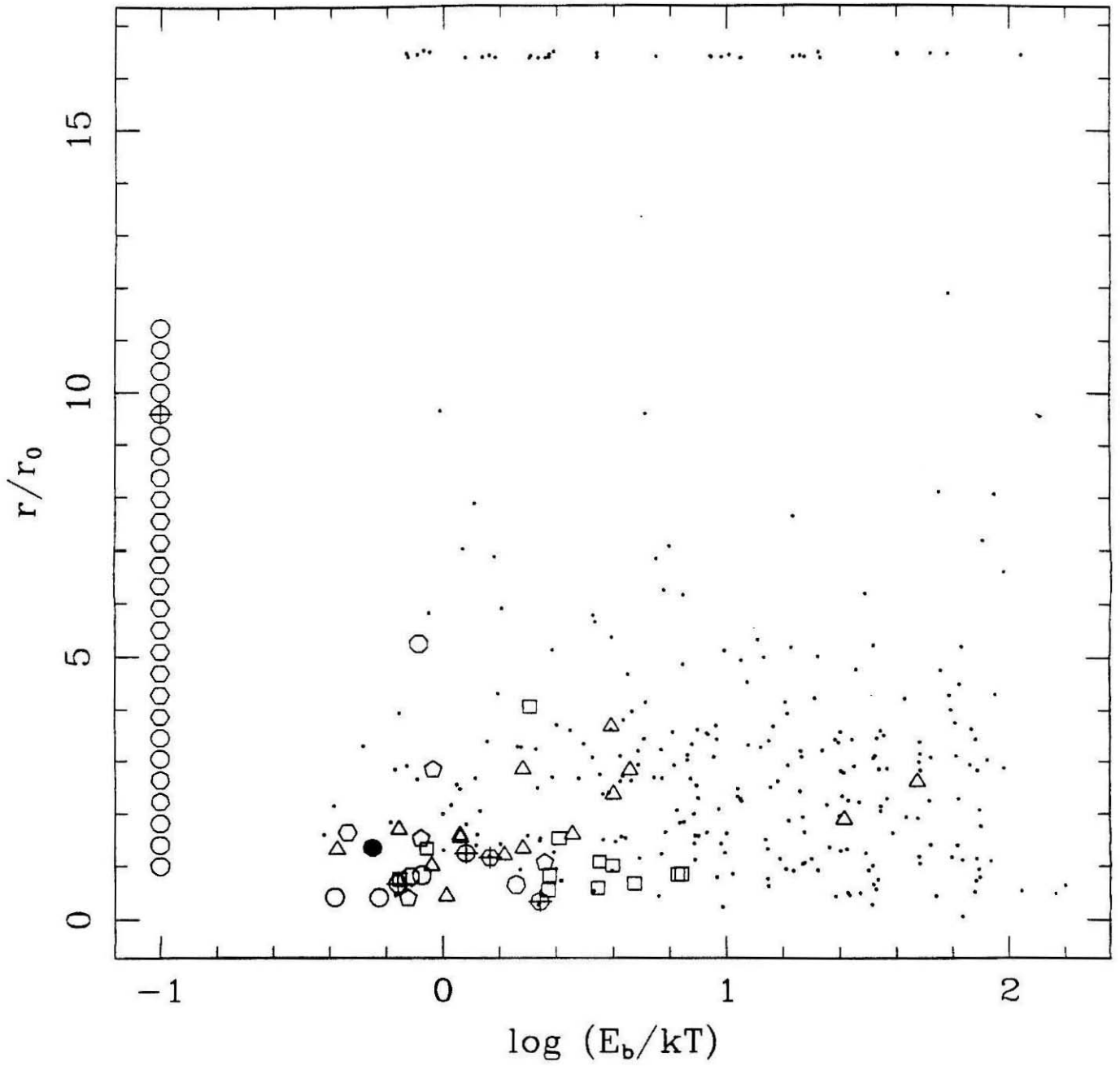


Figure 17a

Model 2, run 2.1.1, final distribution

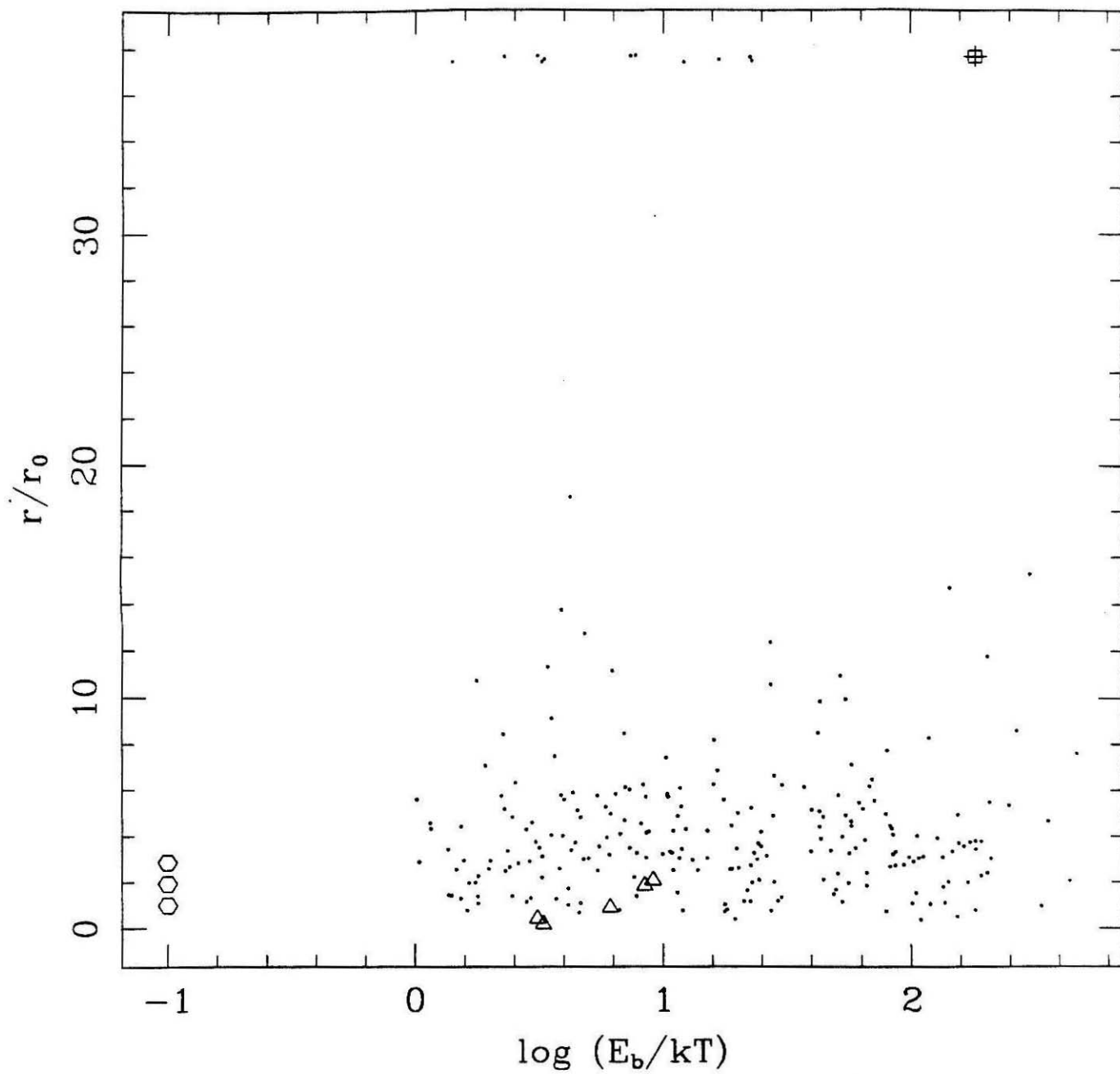


Figure 17b

Model 3, runs 3.3.1 and 3.4.1, final distribution

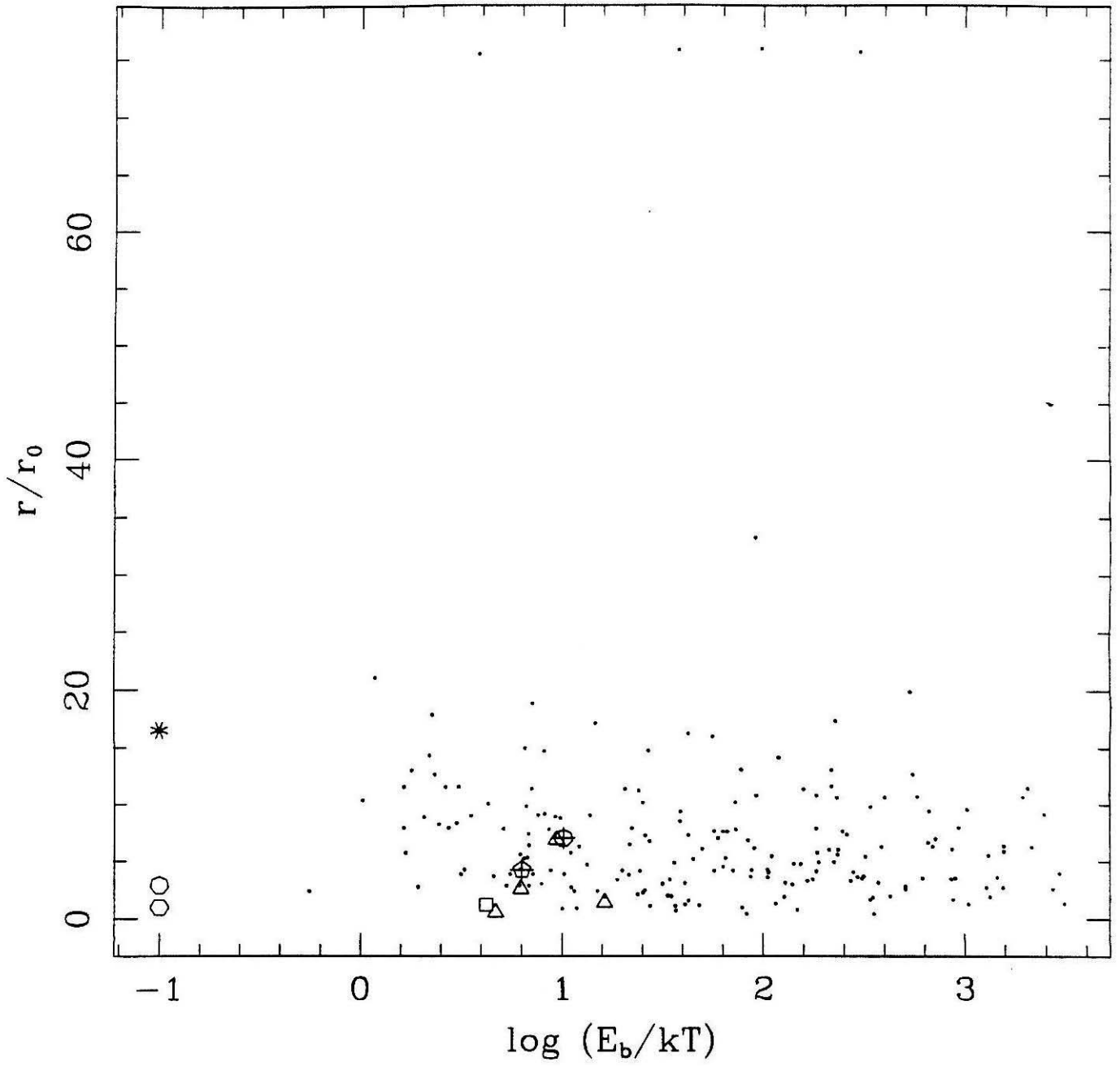


Figure 17c

Model 3, runs 3.3.1 and 3.4.1, final distribution, NS only

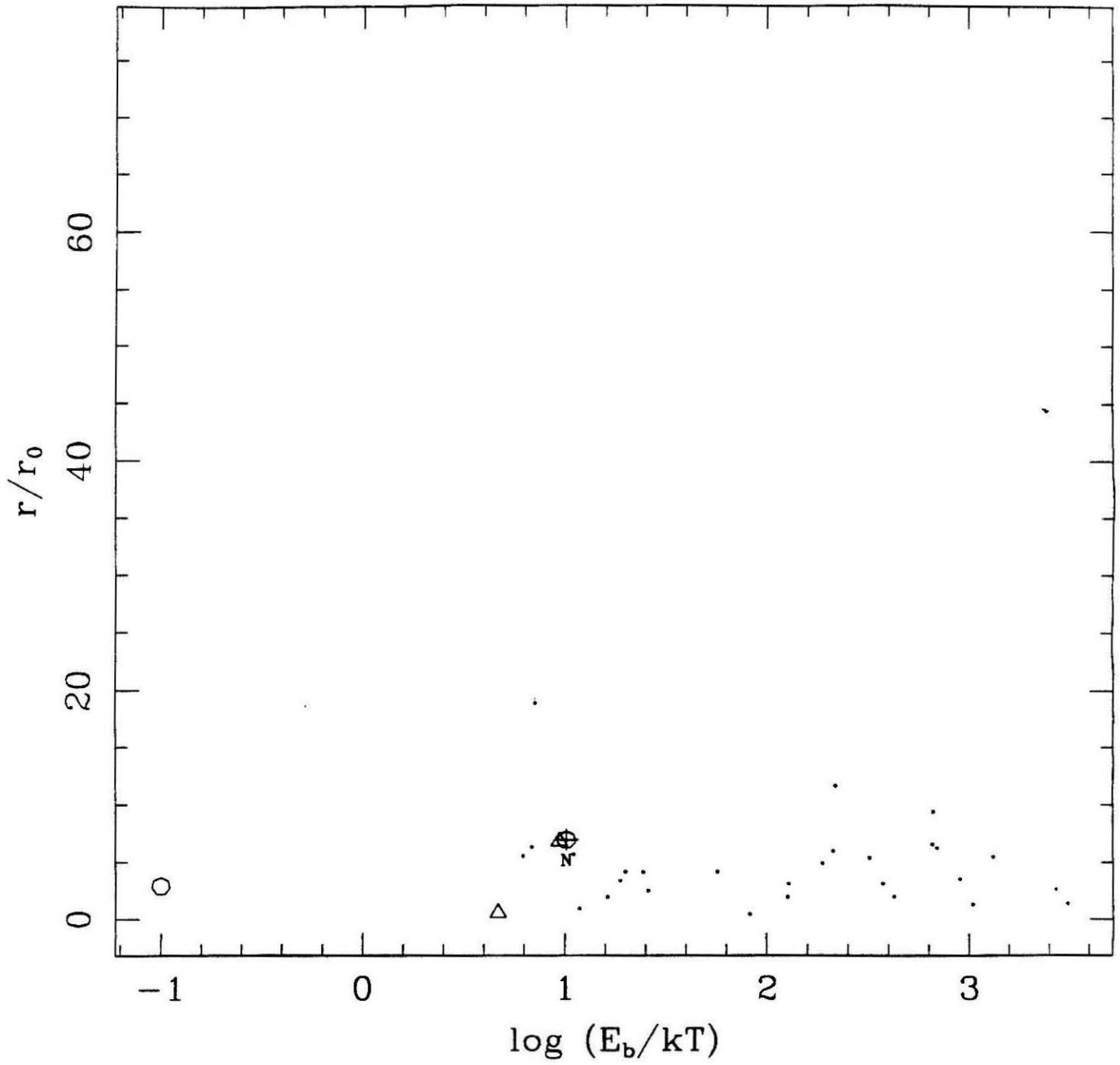


Figure 17d

Model 4, run 4.1.1, final distribution

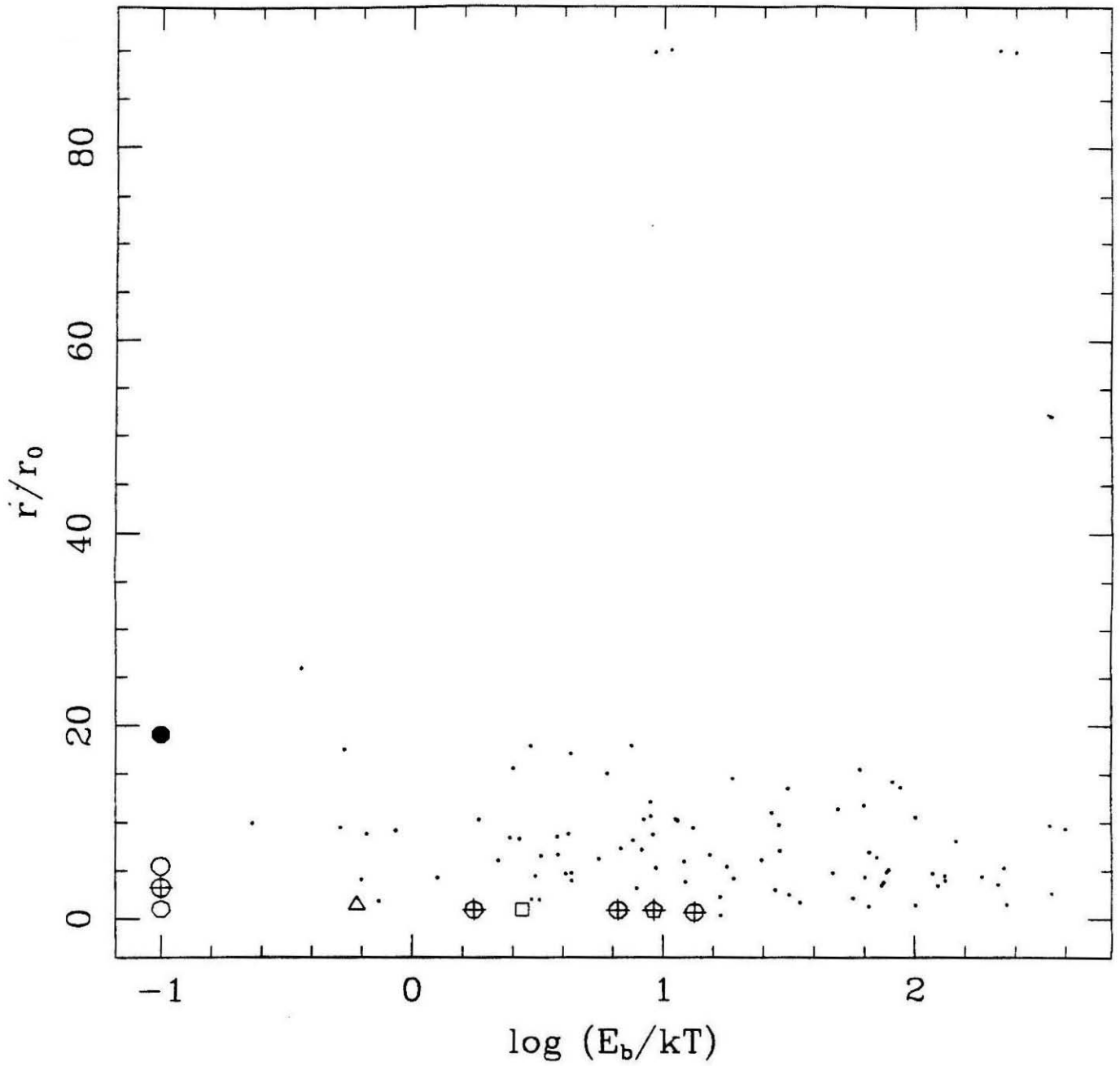


Figure 17e

Model 4, run 4.1.1, final distribution, NS only

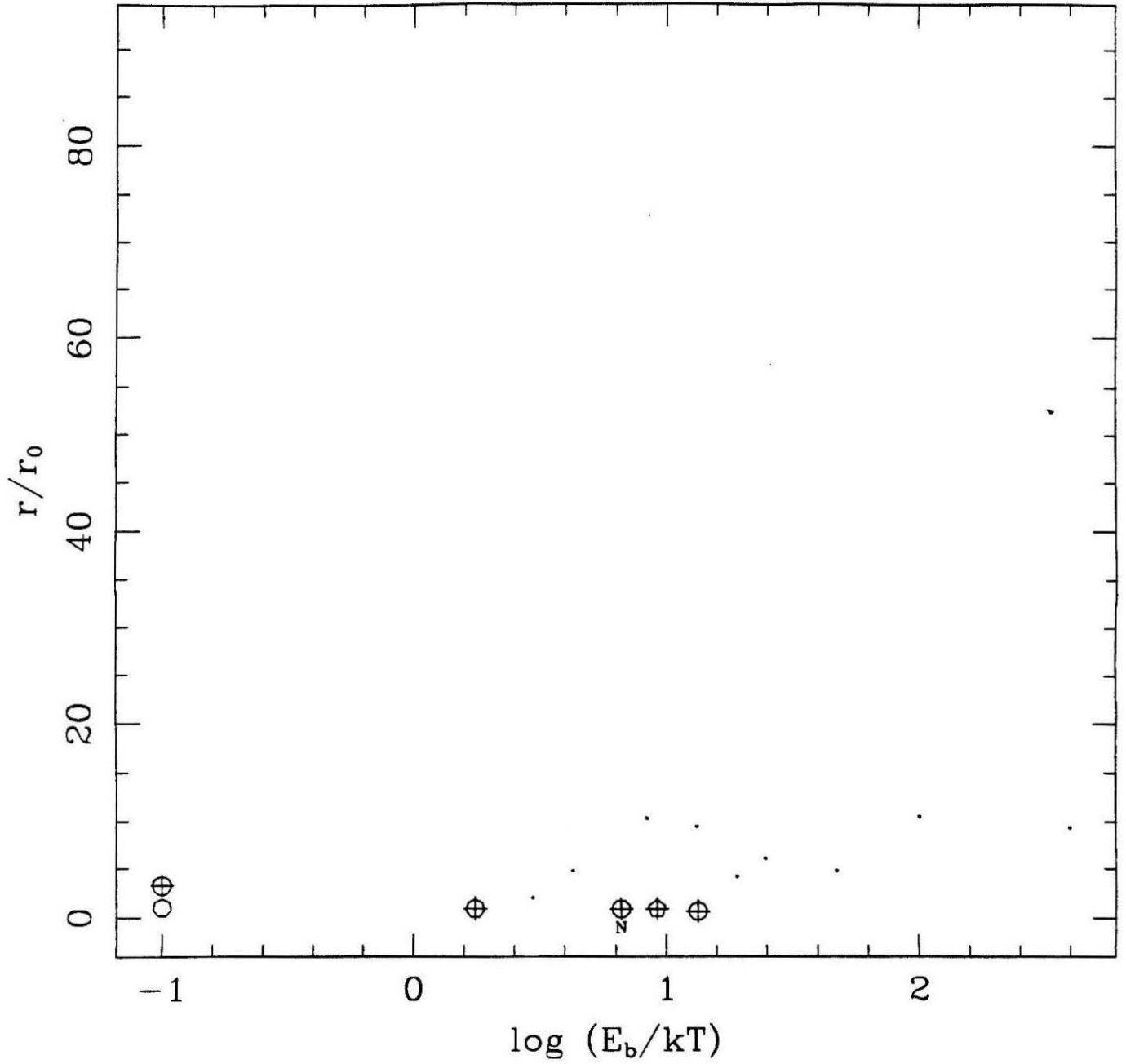


Figure 17f

Model 4, runs 4.2.1 and 4.2.2, final distribution

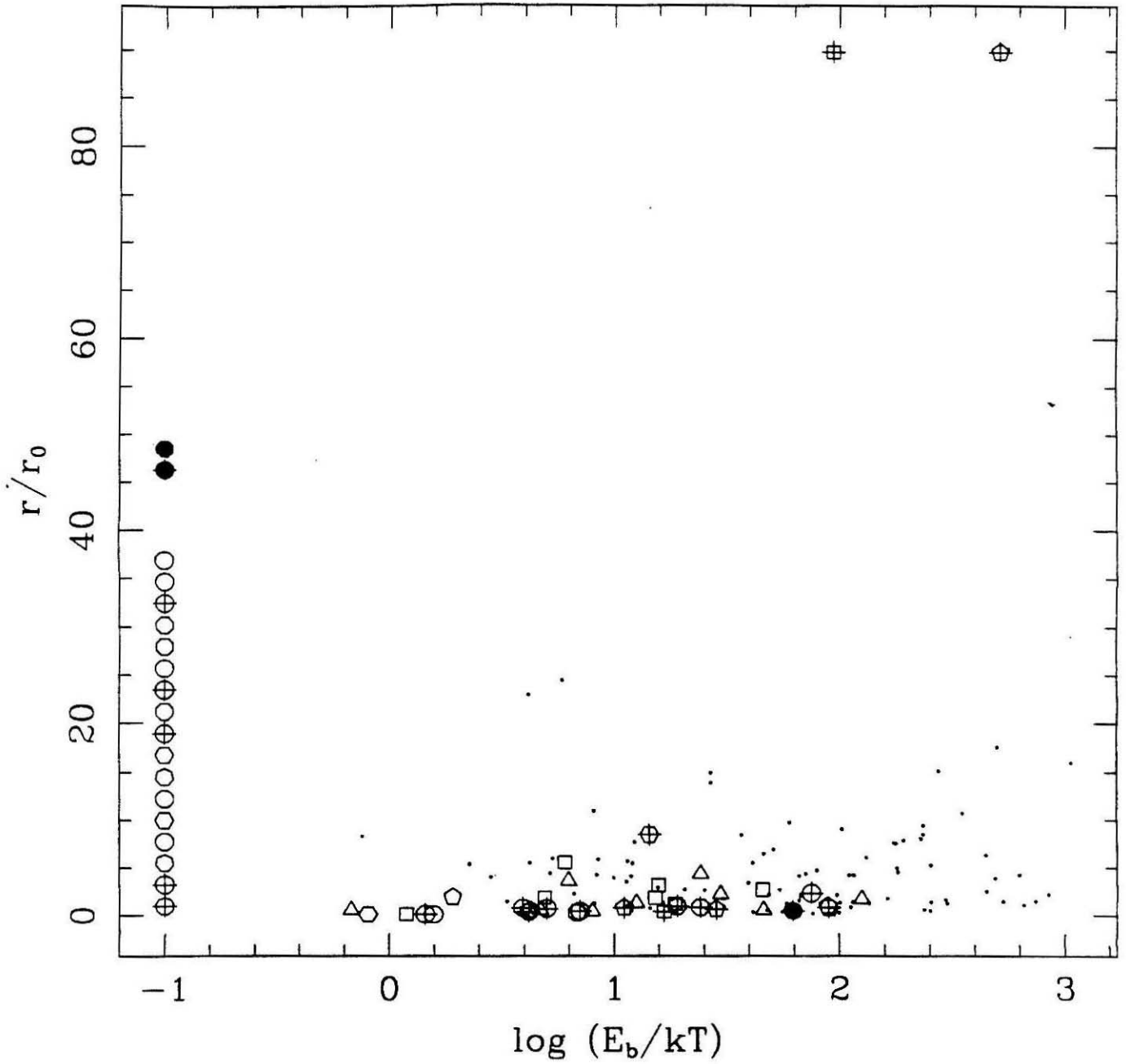


Figure 17g

Model 4, runs 4.2.1 and 4.2.2, final distribution, NS only

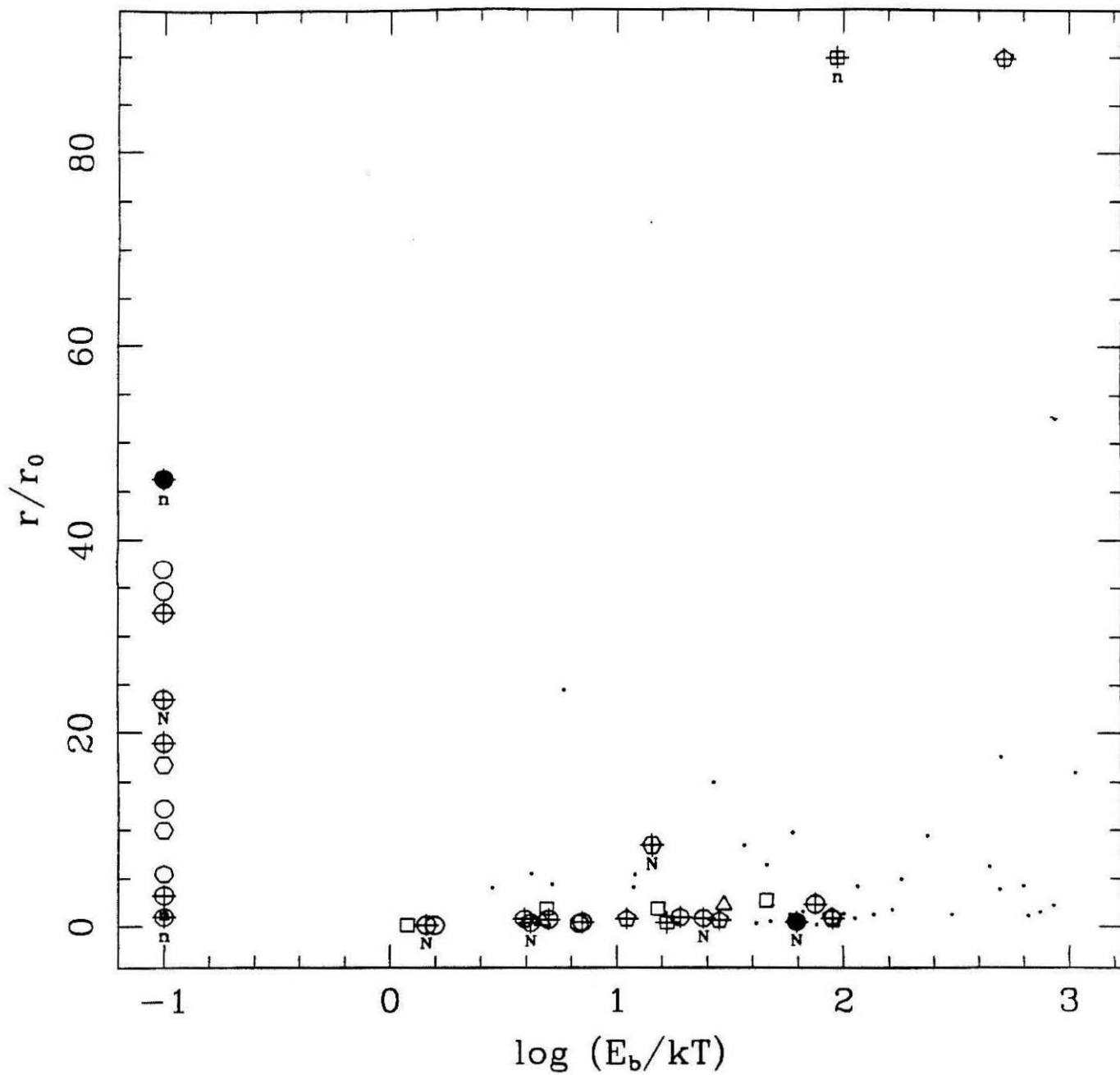


Figure 17h

Model 4, runs 4.3.1 and 4.3.2, final distribution

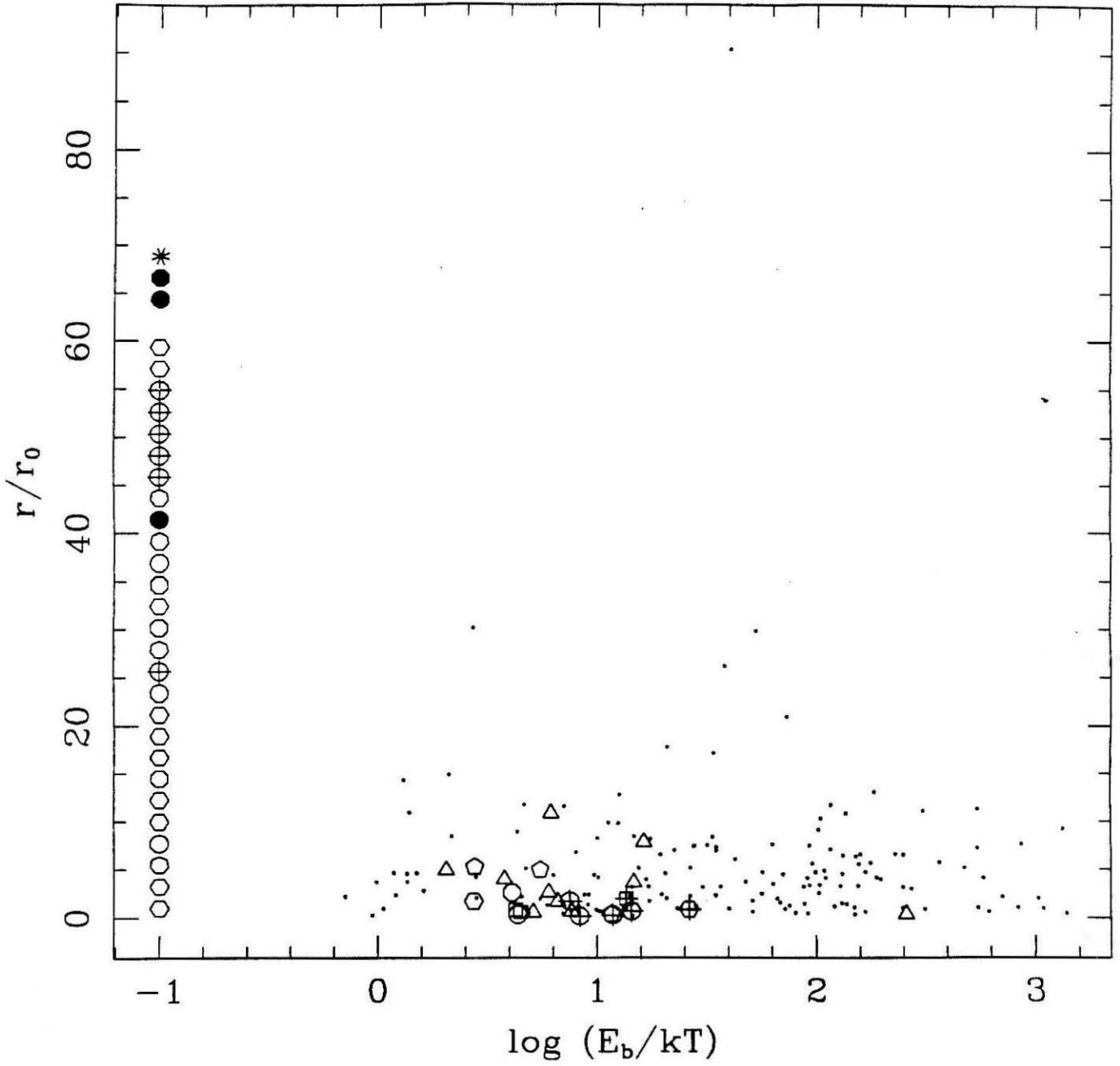


Figure 17i

Model 4, runs 4.3.1 and 4.3.2, final distribution, NS only

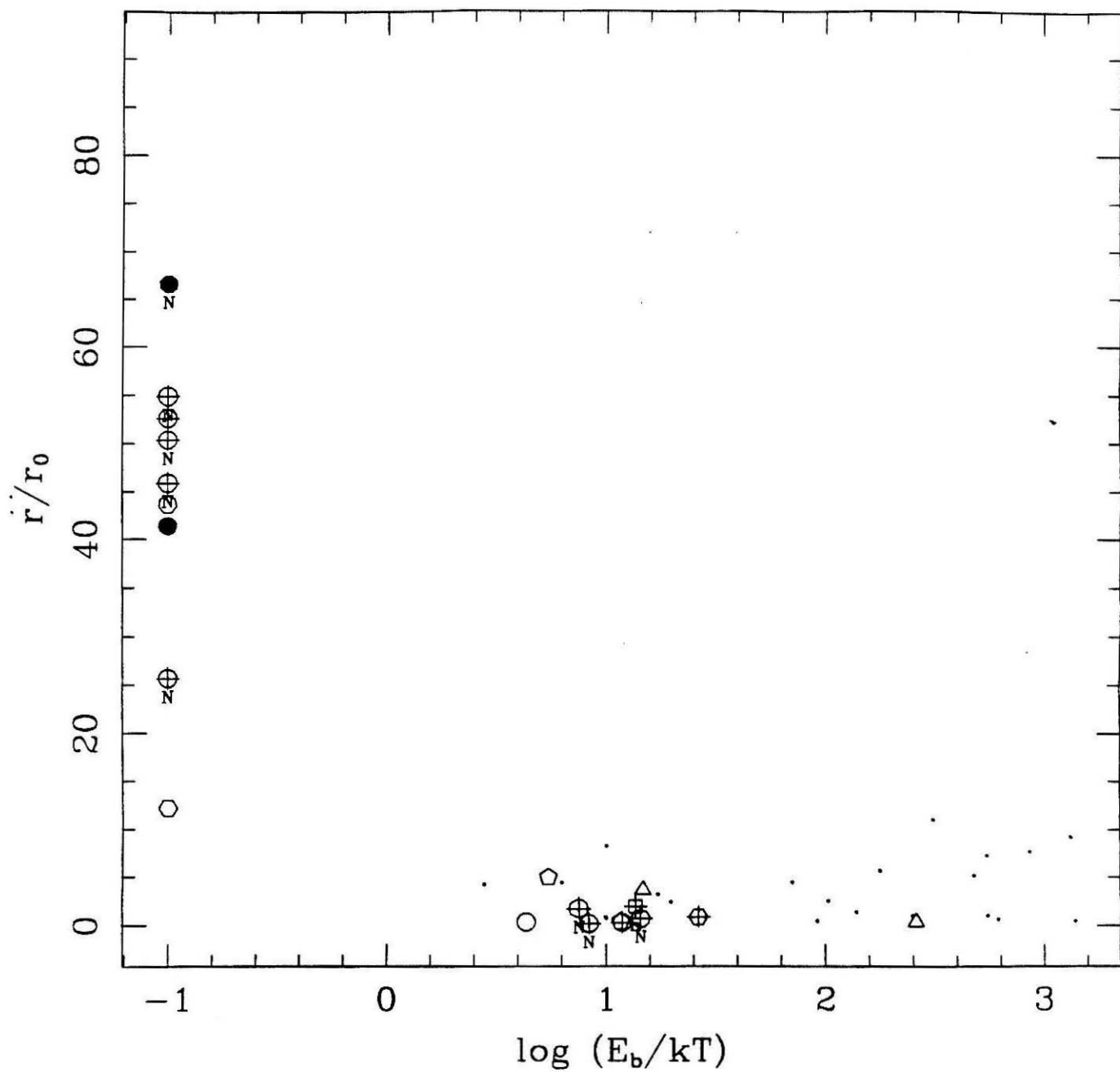


Figure 17j

Model 5, runs 5.1.1 and 5.2.1, final distribution

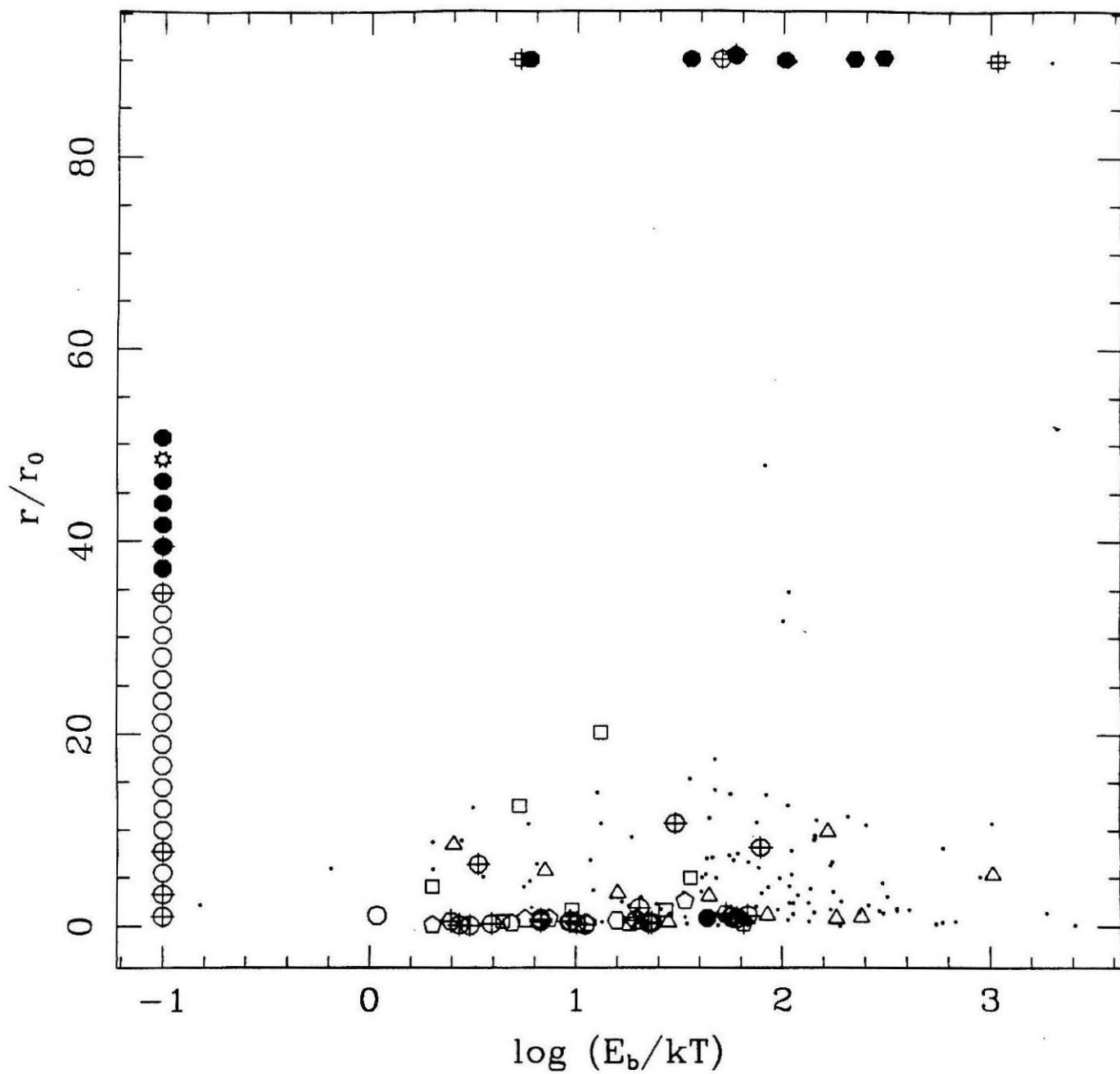


Figure 17k

Model 5, runs 5.1.1 and 5.2.1, final distribution, NS only

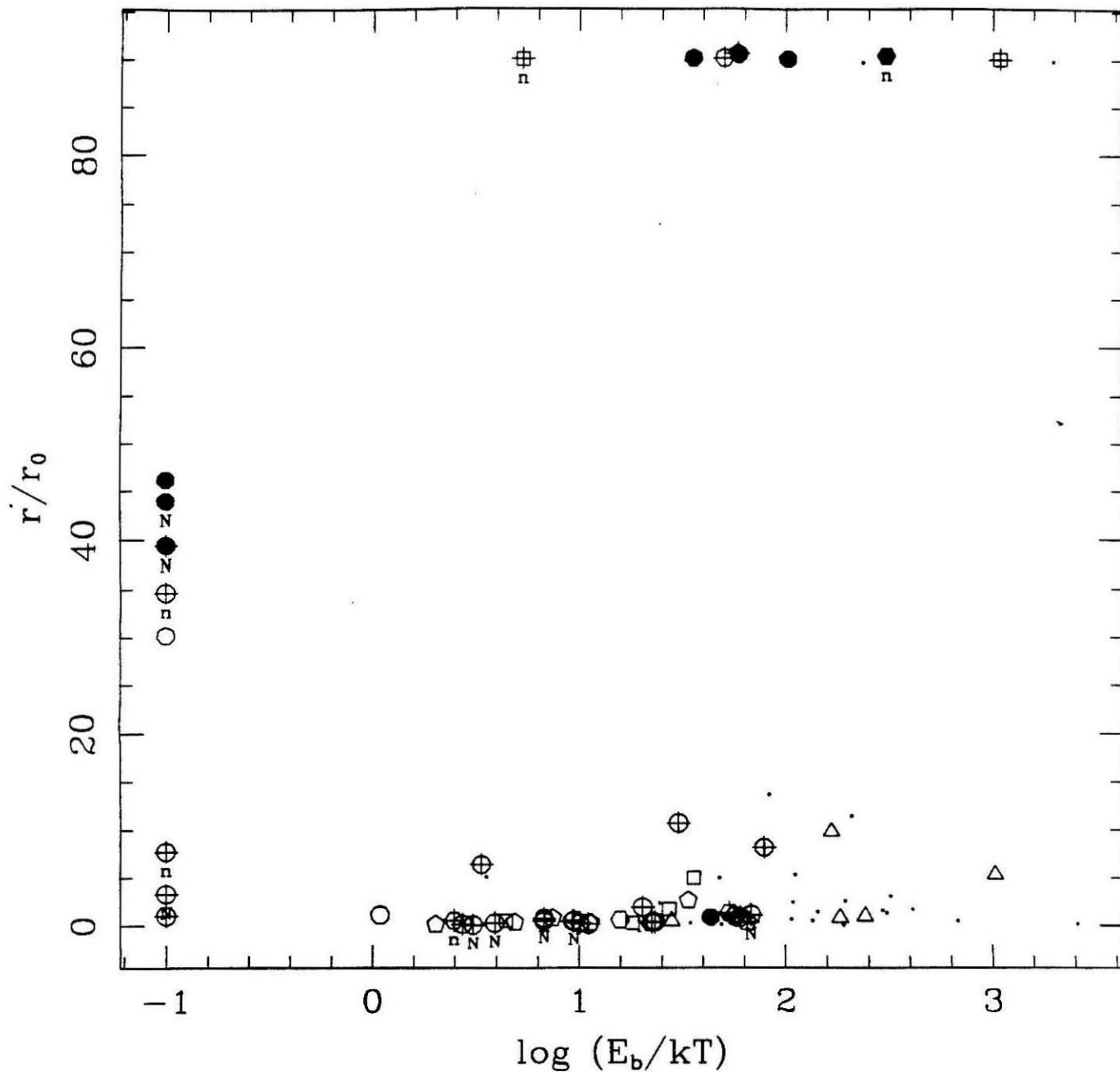


Figure 171

Model 6, run 6.1.1, final distribution, NS only

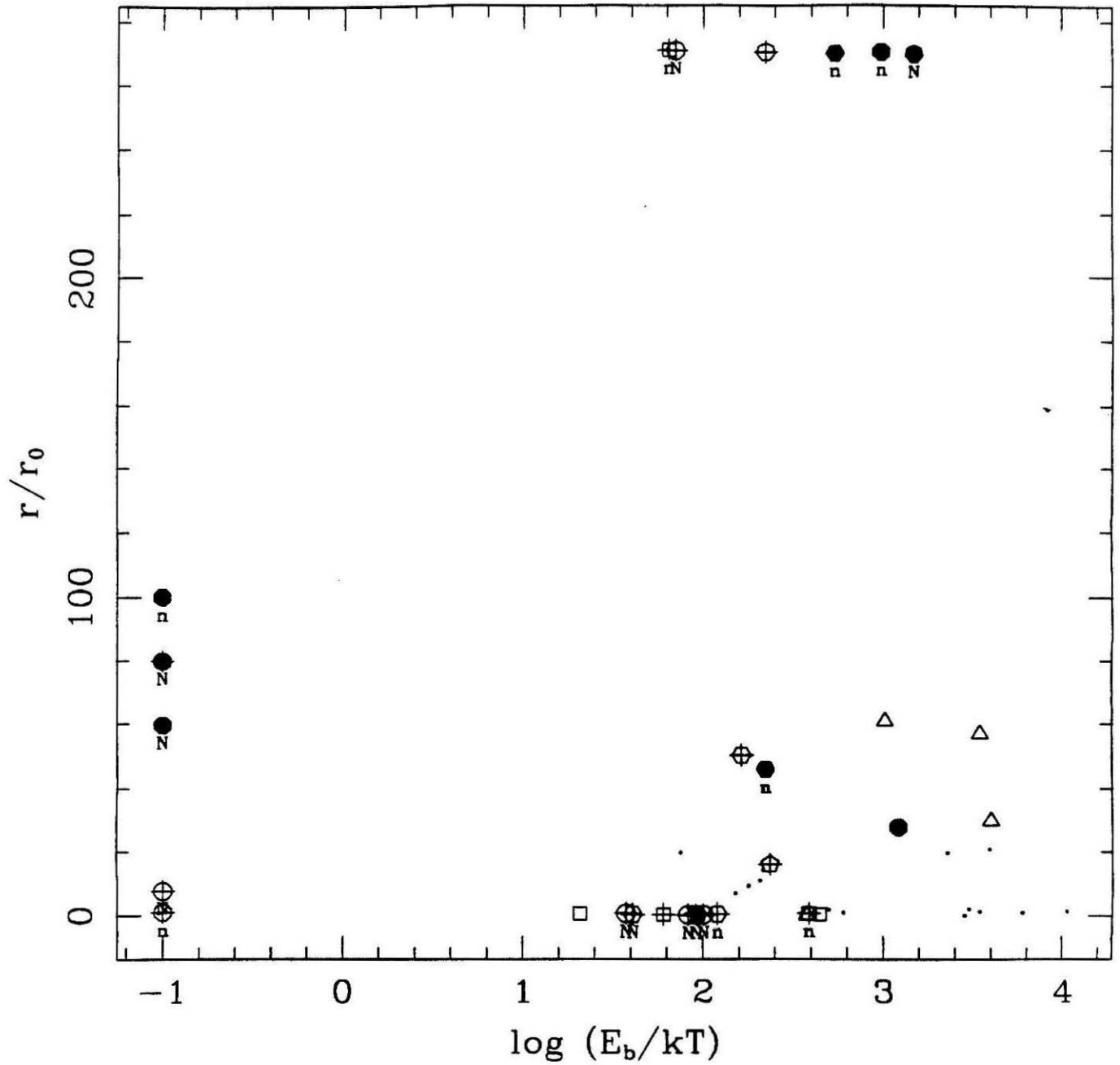


Figure 17n

Model 6, run 6.2.1, final distribution

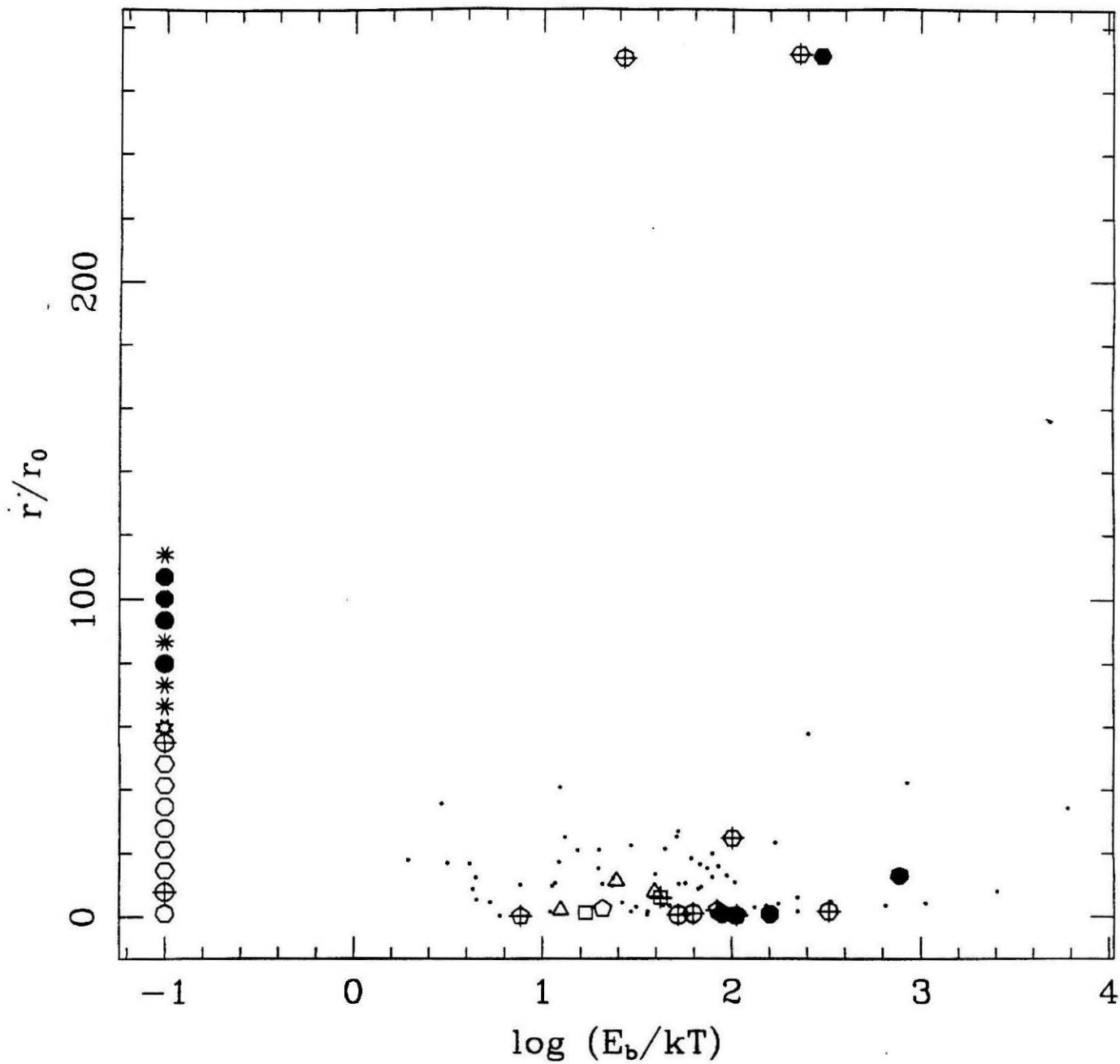


Figure 17o

Model 6, run 6.2.1, final distribution, NS only

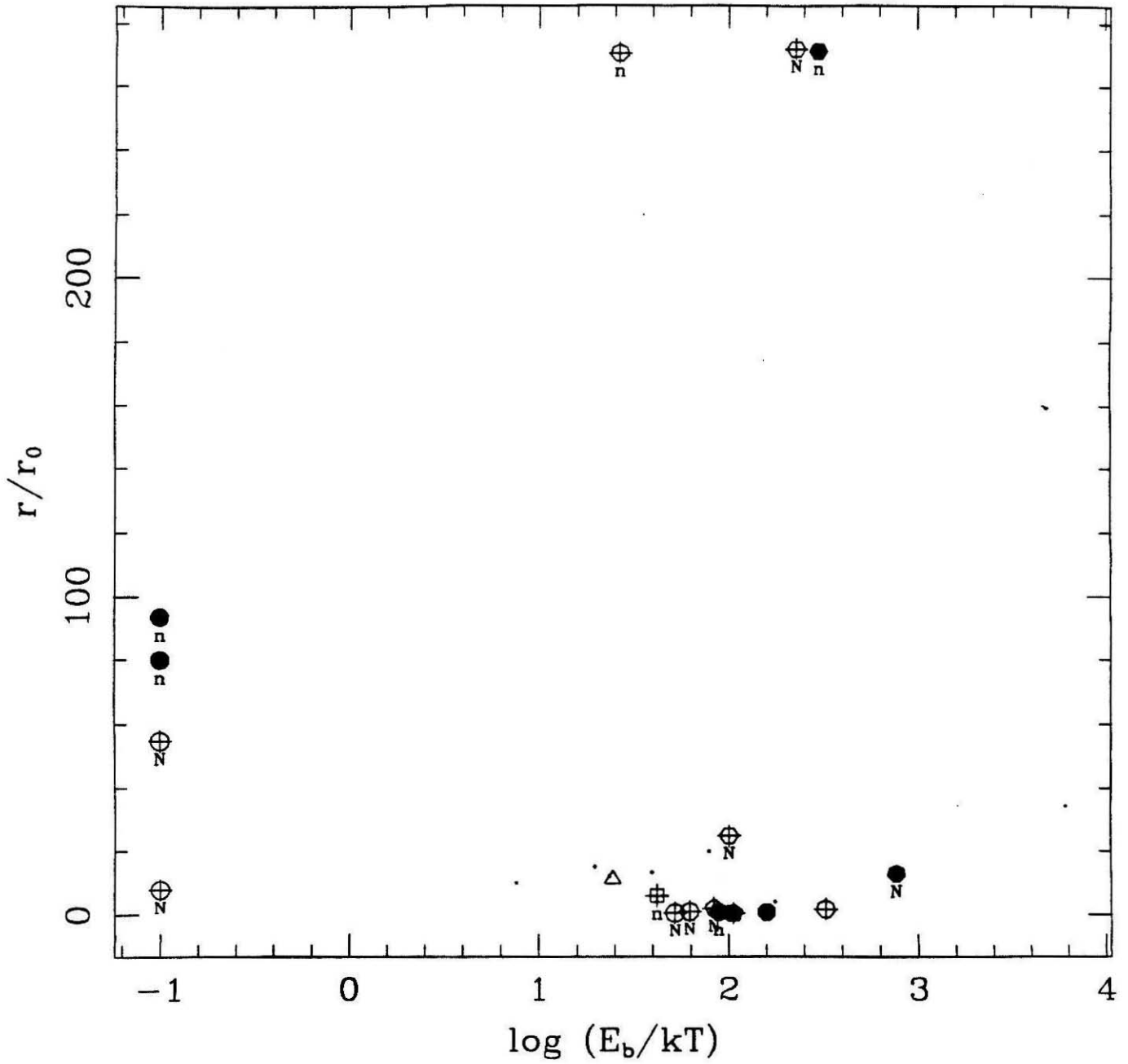


Figure 17p

The End